The behaviour of composite beam-to-column flush end plate connections using blind bolts

Author:
Waqas, Rumman

Publication Date:
2019

DOI:
https://doi.org/10.26190/unsworks/21346

License:
https://creativecommons.org/licenses/by-nc-nd/3.0/au/
Link to license to see what you are allowed to do with this resource.

Downloaded from http://hdl.handle.net/1959.4/63257 in https://unsworks.unsw.edu.au on 2024-05-05

The behaviour of composite beam-to-column flush end plate connections using blind bolts

Rumman Waqas

Thesis submitted in fulfilment of the requirement for the degree of

Doctor of Philosophy

School of Civil and Environmental Engineering
The University of New South Wales, Sydney, Australia

March, 2019

Thesis/Dissertation Sheet

Surname/Family Name	:	**WAQAS**
Given Name/s	:	**RUMMAN**
Abbreviation for degree as give in the University calendar	:	**PhD**
Faculty	:	**Engineering**
School	:	**Civil and Environmental Engineering**
Thesis Title	:	**The behaviour of composite beam-to-column flush end plate connections using blind bolts**

The numerous advantages achieved by using concrete-filled steel tubular (CFST) columns in multi-storey construction have been appreciated for decades. Tubular sections are more effective than open sections due to higher load carrying capacity, superior seismic capacity, improved ductility and fire resistance. However, the connections to CFST columns are complicated as they require access to the inside of the hollow steel tube. Complicated methods like welding were used to establish connections in the past which were not favourable due to several complications and the exorbitant cost involved. The recent development of the innovative blind bolting technique made it possible to connect beams to CFST columns economically without the need for access within the hollow section. However, the connections developed using this technique remain a concern for engineers due to lack of experience and poor guidelines specifically under cyclic loading. In order to achieve the numerous benefits associated with the use of these connections, it is imperative to investigate different structural components and their response under various loading scenarios.

Two sub-assemblages of cruciform composite beam-to-column joints connected using blind bolts were tested under static and cyclic loading. The test results were used to obtain the load-displacement characteristics of the connection, failure modes and strain development. The test results demonstrated sufficient stiffness and strength of the joints under both loading scenarios. Two finite element models were developed and validated with the experimental data that demonstrated accuracy and reliability. Parametric studies were performed to investigate the influence of various significant parameters on the behaviour of these connections.

Moreover, this thesis presents a useful in-plane structural analysis of low-rise blind-bolted composite frames with semi-rigid joints using ABAQUS software. Analytical models were used to predict the moment-rotation relationship of the composite joints that produced accurate results. Bending moment envelopes of the frames under various loading combination were determined. The analysis suggested that gravity loads governed the frame design and wind loads were found to be more critical in Australia as compared to the earthquake loads. The study provides useful understanding of the complex behaviour of these connections that can be effectively applied in engineering practice.

Declaration relating to disposition of project thesis/dissertation

I hereby grant to the University of New South Wales or its agents the right to archive and to make available my thesis or dissertation in whole or in part in the University libraries in all forms of media, now or here after known, subject to the provisions of the Copyright Act 1968. I retain all property rights, such as patent rights. I also retain the right to use in future works (such as articles or books) all or part of this thesis or dissertation.

I also authorise University Microfilms to use the 350 word abstract of my thesis in Dissertation Abstracts International (this is applicable to doctoral theses only).

…………………………………………………………… …………………………………….……………… ……….……………………..……..…

Signature Witness Signature Date

The University recognises that there may be exceptional circumstances requiring restrictions on copying or conditions on use. Requests for restriction for a period of up to 2 years must be made in writing. Requests for a longer period of restriction may be considered in exceptional circumstances and require the approval of the Dean of Graduate Research.

FOR OFFICE USE ONLY Date of completion of requirements for Award:

ORIGINALITY STATEMENT

'I hereby declare that this submission is my own work and to the best of my knowledge it contains no materials previously published or written by another person, or substantial proportions of material which have been accepted for the award of any other degree or diploma at UNSW or any other educational institution, except where due acknowledgement is made in the thesis. Any contribution made to the research by others, with whom I have worked at UNSW or elsewhere, is explicitly acknowledged in the thesis. I also declare that the intellectual content of this thesis is the product of my own work, except to the extent that assistance from others in the project's design and conception or in style, presentation and linguistic expression is acknowledged.'

Signed ……………………………………………………..........

Date ……………………………………………………..........

INCLUSION OF PUBLICATIONS STATEMENT

UNSW is supportive of candidates publishing their research results during their candidature as detailed in the UNSW Thesis Examination Procedure.

Publications can be used in their thesis in lieu of a Chapter if:

- The student contributed greater than 50% of the content in the publication and is the "primary author", ie. the student was responsible primarily for the planning, execution and preparation of the work for publication
- The student has approval to include the publication in their thesis in lieu of a Chapter from their supervisor and Postgraduate Coordinator.
- The publication is not subject to any obligations or contractual agreements with a third party that would constrain its inclusion in the thesis

Please indicate whether this thesis contains published material or not.

☐ *This thesis contains no publications, either published or submitted for publication*

☒ *Some of the work described in this thesis has been published and it has been documented in the relevant Chapters with acknowledgement*

☐ *This thesis has publications (either published or submitted for publication) incorporated into it in lieu of a chapter and the details are presented below*

CANDIDATE'S DECLARATION

I declare that:

- I have complied with the Thesis Examination Procedure
- where I have used a publication in lieu of a Chapter, the listed publication(s) below meet(s) the requirements to be included in the thesis.

Name	Signature	Date (dd/mm/yy)

COPYRIGHT STATEMENT

'I hereby grant the University of New South Wales or its agents the right to archive and to make available my thesis or dissertation in whole or part in the University libraries in all forms of media, now or here after known, subject to the provisions of the Copyright Act 1968. I retain all proprietary rights, such as patent rights. I also retain the right to use in future works (such as articles or books) all or part of this thesis or dissertation. I also authorise University Microfilms to use the 350 word abstract of my thesis in Dissertation Abstract International (this is applicable to doctoral theses only). I have either used no substantial portions of copyright material in my thesis or I have obtained permission to use copyright material; where permission has not been granted I have applied/will apply for a partial restriction of the digital copy of my thesis or dissertation.'

Signed ……………………………………………………………………

Date ……………………………………………………………………

AUTHENTICITY STATEMENT

'I certify that the Library deposit digital copy is a direct equivalent of the final officially approved version of my thesis. No emendation of content has occurred and if there are any minor variations in formatting, they are the result of the conversion to digital format.'

Signed ……………………………………………………………………

Date ……………………………………………………………………

ABSTRACT

The numerous advantages achieved by using concrete-filled steel tubular (CFST) columns in multi-storey construction have been appreciated for decades. Tubular sections are more effective than open sections due to higher load carrying capacity, superior seismic capacity, improved ductility and fire resistance. However, the connections to CFST columns are complicated as they require access to the inside of the hollow steel tube. Complicated methods like welding were used to establish connections in the past which were not favourable due to several complications and the exorbitant cost involved. The recent development of the innovative blind bolting technique made it possible to connect beams to CFST columns economically without the need for access within the hollow section. However, the connections developed using this technique remain a concern for engineers due to lack of experience and poor guidelines specifically under cyclic loading. In order to achieve the numerous benefits associated with the use of these connections, it is imperative to investigate different structural components and their response under various loading scenarios.

Two sub-assemblages of cruciform composite beam-to-column joints connected using blind bolts were tested under static and cyclic loading. The test results were used to obtain the load-displacement characteristics of the connection, failure modes and strain development. The test results demonstrated sufficient stiffness and strength of the joints under both loading scenarios. Two finite element models were developed and validated with the experimental data that demonstrated accuracy and reliability. Parametric

studies were performed to investigate the influence of various significant parameters on the behaviour of these connections.

Moreover, this thesis presents a useful in-plane structural analysis of low-rise blind-bolted composite frames with semi-rigid joints using ABAQUS software. Analytical models were used to predict the moment-rotation relationship of the composite joints that produced accurate results. Bending moment envelopes of the frames under various loading combination were determined. The analysis suggested that gravity loads governed the frame design and wind loads were found to be more critical in Australia as compared to the earthquake loads. The study provides useful understanding of the complex behaviour of these connections that can be effectively applied in engineering practice.

PREFACE

This thesis is submitted in partial fulfilment of the requirements for the degree of Doctor of Philosophy at The University of New South Wales (UNSW), Sydney, Australia. The work described herein was performed by the candidate in the School of Civil and Environmental Engineering, UNSW. The candidate was supervised by Professor Brian Uy during a period from August 2014 to March 2019.

The thesis has been supported by papers that have been published in internationally renowned journals and conferences. These papers are listed in the following:

Journal papers

Waqas, R., Uy, B., Thai, T., (2019), "Experimental and numerical behaviour of blind bolted flush endplate composite connections " *Journal of Constructional Steel Research*, 153: 179-195.

Waqas, R., Uy, B., Wang, J. and Thai, H.T., (2019), "In-plane structural analysis of blind-bolted composite frames with semi-rigid joints", *Steel and Composite Structures*, 31: 373-385.

Conference papers

Waqas, R., Uy, B. and Thai H.T., (2015), "Parametric studies on the behavior of beam-to-column flush end plate connections using blind bolts", *Proceedings of the 2015 World Congress on Advances in Structural Engineering and Mechanics (ASEM15)*, 25-29 August 2015, Incheon, Korea.

Waqas, R., Uy, B., Thai H.T., (2018), "Parametric studies of a composite connection subjected to static loading", *13th International Conference on Steel, Space and Composite Structures*, Perth, Australia, 31 January-2 February.

ACKNOWLEDGEMENTS

The research presented in this thesis would not have been completed without the contribution of a large number of people, and here I would like to take the opportunity to thank all of them.

Firstly, I would like to express sincerest appreciation and profound gratitude to my supervisor and mentor, Professor Brian Uy for his meticulous assistance, priceless advices and guidance throughout my PhD candidature and for assisting me to efficiently grow as a research scientist. It was his valuable comments and suggestions that helped me to produce a good quality work. Moreover, I am extremely grateful to my joint supervisor Professor Chongmin Song for his kindness, appreciation and encouragenment. I am also thankful to Dr. Huu-Tai Thai for his guidance and valuable suggestions regarding my work.

This research was financially supported by the Australian Research Council (ARC) Linkage grants (LP110200511) programme with industry partners Ajax Fasteners and Australian Tube Mills. I would like to express gratitude to the funding sponsors for their generous support. The technical assistance from Dr. Zhen-Tian Chang, Greg Worthing, Ronald Moncay, John Gilbert and Tony Macken in preparing and conducting experimental tests at the Randwick Heavy Structures Laboratory of UNSW is also gratefully acknowledged.

I would also like to thank all the staff members at the School of Civil and Environmental Engineering for their friendliness and technical support, especially Mrs. Patricia McLaughlin and Mr. Patrick Vuong. Additionally, I have a great honor to work with my colleagues and friends at the School of Civil and Environmental Engineering, UNSW especially Dr. Jia Wang, Dr. Sameera Pathirana, Dr. Dongxu Li, and Dr. Reza Ataei.

I owe a lot to my parents who gave me this remarkable confidence and energy, encouraged and helped me at every stage of my personal and academic life and longed to see this achievement come true. It was their prayers and encouragement that made me accomplish this long journey. I would like to thank my siblings, whose love, moral and emotional support are with me in whatever I pursue.

Nobody has been more important to me in the pursuit of this project than my loving and supportive husband, Muhammad Waqas Sattar and my three beautiful kids, Ibrahim, Mahnoor and Musa who endlessly supported me through thick and thin. Words cannot express how indebted I am to them for their unconditional love, countless sacrifices and assistance in every possible way just to make me accomplish this enduring and strenuous project. Without their patience and motivation, this research would not have commenced and completed. Hence, I would like to dedicate this thesis to my beloved husband and kids.

Above all, I owe it all to Allah Almighty for granting me the wisdom, health and strength to undertake this research task and to empower me to successfully achieve my dreams.

TABLE OF CONTENTS

LIST OF NOTATION

A_B	Cross-section area of blind bolt shank
A_{ce}	Cross-section area of concrete slab
A_o	Converted cross-section area of composite beam
A_s	Tensile stress area of bolts
$A_{s,r}$	Cross-section area of reinforcing steel
E	Young's Modulus
E_B	Design value of modulus of elasticity of blind bolts
E_s	Modulus of elasticity of structural steel (Design value)
E_{cm}	Modulus of elasticity of concrete (Design value)
$E_{s,r}$	Modulus of elasticity of reinforcing steel (Design value)
$(EI)_{eff}$	Effective flexural stiffness of composite columns
F	Strength of a component (Force)
F_{eq}	Earthquake actions
$F_{t,Rd}$	Tension resistance of bolts
$F_{t,wc,Rd}$	Column web in tension
$F_{t,fc,,Rd}$	Column flange in bending
$F_{t,,r, Rd}$	Tension resistance of bolts
$F_{t,,ep,Rd}$	End-plate in bending
$F_{t,wb,,Rd}$	Beam web in tension
$F_{v,Rd}$	Shear resistance of bolts
G	Dead loads
H_c	Height of inter-storey columns
I_b	Second moment of area of beam's section

I_c	Second moment of area of infilled concrete core
I_{sb}	Second moment of area of steel beam
L_B	Clear space of blind bolt shanks between bolt heads and nuts
L_E	Characteristic element length
L_b	Span of beams between columns
Mu	Ultimate moment
M_j	Moment capacity of beam-to-column joints
$M_{j,pc}$	Moment capacity of beam-to-column joints
N	Number of shear connectors distributed over hogging moment regions
N_{tf}	Nominal tensile capacity of bolts
P_u	Ultimate load
Q	Live loads
S_j	Stiffness of beam-to-column joints
$S_{j,ini}$	Initial stiffness of beam-to-column joints
$S_{j,pc}$	Strain-hardening stiffness of beam-to-column joints
V_f	Nominal shear capacity of bolts
W	Wind actions
b	Width
b_f	Flange width
b_{eff}	Effective width of concrete slab
$b_{eff,t,wb}$	Effective width of beam web
$b_{eff,t,wc}$	Effective width of column web
b_f	Flange width
b_0	Distance between centers of outstand shear connectors
d_s	Distance between longitudinal reinforcing bars in tension and centroid of beam's section
f'_c	Characteristic compressive strength of concrete

f_{ct} Tensile strength of concrete

f_t Tensile failure stress

f_{ub} Ultimate tensile strength of bolts

h Distance between centroid of beam flanges in tension and centroid of beam flanges in compression

h_r Distance between bolt-row r and the center of compression

h_s Distance between longitudinal reinforcing bars in tension and centroid of beam flanges in compression

k Stiffness

$k_{1,2..i}$ Stiffness of individual components which form the connection

k_{eff} Effective stiffness of the connection

k_{eq} Equivalent stiffness of the connection

k_0 Correction factor

k_e Calibration factor

k_b Stiffness coefficient for blind bolts

k_c Stiffness coefficient for column walls

k_{eff} Effective stiffness coefficient for basic components including end-plates, column walls and blind bolts

k_{ep} Stiffness coefficient for end-plates

k_{eq} Equivalent stiffness coefficient for beam-to-column joints

k_i Stiffness coefficient for basic components

k_{sc} Stiffness coefficient for shear connectors

k_{slip} Reduction factor of stiffness coefficient $k_{s,r}$

$k_{s,r}$ Stiffness coefficient for reinforcing bars

l_b Length of beams on hogging bending moment regions

t Thickness

t_p Thickness of end-plate

t_{wb} Thickness of beam web

t_{wc}	Thickness of column web
y	Distance to the centroid of the compression flange
z	Lever arm
z_{eq}	Equivalent lever arm
α	Thermal expansion coefficient
σ_c	uniaxially compressive stress
δ_b	Vertical deflection of beam
δ_x	Horizontal deflections of cantilever beam
δ_y	Yielding deflection
ε_c	Strain at peak of unconfined concrete
$\varepsilon_{c,pl}$	Concrete inelastic strain in compression
$\varepsilon_{t,pl}$	Concrete inelastic strain in tension
ε_{cc}	Strain at peak of confined concrete
ε_y, ε_u	Yield strain and ultimate strain respectively
v	Poisson's ratio
σ_y, σ_u	Yield stress and ultimate stress respectively
φ	Factor of initial stiffness
φ_j	Rotation capacity of the joint
ψ_L	Creep multiplier
ϕ_b	Beam rotation
ϕ_j	Rotational deformations of beam-to-column joints

Subscripts

b_m	Beam
b_f	Bottom flange
b_o	Blind bolt
b_w	Beam web (bottom region)
cc	Concrete in compression
ct	Concrete in tension
cs	Steel in compression
cw	Column web
ini	Initial
s	Concrete slab
sc	Shear connection
eff	effective
eq	Equivalent
ep	End plate
fb	Beam flange
r	Reinforcing bars
tf	Top flange
u	Ultimate
wb	Beam web
y	Yield
cw	Column web

LIST OF ABBREVIATIONS

AISC	American Institute of Steel Construction
Avg	Average
BF	Blind bolt fracture
BSCF	Bolted shear connector failure
CDP	Concrete damage plasticity
CFST	Concrete-filled Steel tubular
CHS	Circular hollow section
CM	Component Method
Exp	Experimental
EC3	Eurocode 3
EC4	Eurocode 4
FEM	Finite Element Method
FE	Finite element
FEPF	Flush end plate failure
FSC	Full shear connection
FEPF	Flush end plate fracture
LDS	Laser Displacement Sensor
LRFD	Load and Resistance Factor Design
LVDT	Linear Variable Deformation Transducer
Max	Maximum

mrad	milliradians
N.A	Neutral axis
N/A	Not available/ Not applicable
PEEQ	Equivalent plastic strain distribution
PSC	Partial shear connection
RBF	Reinforcing bar fracture
SHS	Square Hollow Section

LIST OF FIGURES

LIST OF TABLES

CHAPTER 1

INTRODUCTION

1.1. Introduction

This chapter presents an overview of the research work performed in this study and features its significance, advantages and contributions. Background knowledge is presented which highlights the grey areas that require further research and consideration. These issues are elaborated in Chapter 2 as part of the literature review. This thesis endeavours to comprehensively explore and investigate experimentally and numerically, the behaviour of typical beam-to-column flush endplate connections when subjected to static and cyclic loading conditions. Motivations of the research are discussed that identify the necessity of this research. Moreover, this thesis aims to investigate the behaviour and design of composite frames with beam-to-column blind bolted joints. The objectives and scope of this study, layout of the thesis and a brief description of each chapter in the thesis is presented in this chapter.

1.2. Background and motivation of research

Concrete and steel are the two most extensively used materials in the construction industry. However, the individual application of these materials is limited due to the fact that concrete is weak in resisting tensile stresses whereas steel is weak in resisting compressive stresses. As steel structural members are usually fabricated as thin plates, so they are prone to local buckling and fatigue. On the other hand, concrete structural members are relatively thick and buckle unlikely. Though, concrete is weak in tension and inclined to creep and shrink with the passage of time. When these two materials are combined together as a composite material, the advantages of both materials can be effectively utilized. This significantly increases the efficiency of the construction as the compressive strength of concrete infill and the ductility of steel hollow section tube is effectively utilized.

It has long been recognized that the CFST columns exhibits excellent benefits for both structural and constructional reasons. These columns have the capability to resist large axial compressive and flexural forces and demonstrate an improved stiffness, strength and fire resistance as documented comprehensively in publications by Uy and Liew (2003), Uy (2012), Li *et al*. (2012), Tizani *et al*. (2013a, 2013b), and Song *et al*. (2017). Han *et al*. (2008) stated that concrete-filled steel tubular (CFST) columns have many striking features and are being extensively used in construction due to their exceptional static and seismic resistant performance. Wu *et al.* (2005) suggested that the possibility of local buckling of the steel tube wall is reduced. The confined concrete provides an increased strength as compared with the unconfined concrete due to the enhanced material properties resulting from the confinement. Although the concrete-filled tubular column is a cost-effective form of composite steel-concrete construction, its use to date has been restricted due to the lack of design information on the beam-to-column connection and limited construction experience in Australia.

Composite bolted end plate joints have been increasingly used in multi-storey buildings, primarily due to simplicity of their assembly and fabrication. Fig. 1.1 represents a typical blind bolted flush end plate composite joint which is composed of universal steel beams connected to a concrete-filled steel tubular (CFST) column using flush end plates and blind bolts. These connections are not only economical but also very easy to fabricate as they allow the endplate to be shop welded and bolted to the CFST column on site.

The research conducted in the past focused on the use of I-beams connected to H-section steel columns. Open section columns were considered among the weakest components that led to premature failure. Therefore, the columns were supported with web stiffeners at the bottom flange of the beam. However, this method involved additional welding and formwork that resulted in a higher cost of fabrication. Some researchers also used concrete to encase H-section columns. However, this method involved additional formwork and reinforcements.

Prior to the 1994 Northridge and 1995 Kobe earthquake, rigid and fully welded connections were used in design. These drastic events led to severe brittle fractures of fully welded connections. As a result, the seismic design of moment resisting connections had to be updated to reduce structural damages. Therefore, increased research started to explore techniques to improve the seismic capacity of beam-to-column connections. Various researchers such as Silvana El-Debs (2004) and Wu et al. (2005) investigated connection alternatives to CFST column sections through the use of additional fittings, through-bolted connections or diaphragm plates. However, these methods were not considered feasible in construction practice as they involved extensive welding and high tolerance. Moreover, these methods were very costly and complicated. Welding to the steel tube induced large residual stresses and largely deformed the wall.

Bolted connections were the other extensively used method for joining structural steel members. Bolted connections had some benefits over welding such as being economical, lesser installation time, not requiring highly skilled labour, high performance under fluctuating stress, avoiding heating of steel members and eliminating the cracking of welds. However, tightening standard bolts required access to both sides of the member. This was not problematic when exposed members such as T-sections, H-sections, and I-sections were to be attached. However, problem raised when standard bolts were required to connect beams to steel hollow sectioned columns as there was no provision to the interior of the section to allow for fastening of the bolt. To address this issue, blind bolts were developed which did not require installation from both sides of the member. The bolt expanded and acted as a self-tightening gadget that allowed connecting steel beams to CFST columns from one side only. These bolts were efficient, economical and a rapid solution to the problem. Fig. 1.2 presents a one-side blind bolt and its installation process.

A considerable number of experimental and analytical studies were conducted on composite joints during the past three decades such as by Xiao *et al*. (1994 and 1996), Anderson and Najafi (1994), Li *et al*. (1996a, 1996b), Liew *et al*. (2000), Silva *et al*. (2001) and Liew *et al*. (2004a) etc. However, these studies involved the use of standard bolts as blind bolting technique was not developed at that time. Therefore, experimental studies particularly involving blind bolting technique to connect endplate composite joint to CFST columns are limited.

Whilst the behaviour of blind bolted endplate connections under static loading has been broadly studied, only a few studies have focused on the behaviour of these connections under cyclic loading such as Liew et al. (2004b), Xu et al. (2005), Wang et al. (2009), Tizani et al. (2014) and Tao et al. (2017). The current design of reinforced concrete and steel structures in Australia caters well for gravity loading, wind loading and seismic loading of a 1-in-500 years return period. There has been a lot of discussion regarding the need to design the structures for low probability-high consequence events such as 1-in-2500 years return period. Paulay and Priestley (1990) have defined it as a critical case for areas of low seismicity such as Australia and emphasized on the need to cater for this level of earthquake. As the probability factor has been improved from 1 in 500-event to a 1 in 2500-event for general structures, a new system of joints capable of handling such loads needs to be developed. Mirza and Uy (2011) performed full-scale tests on these connections for both static and cyclic loading scenarios. The test set up of their specimen is presented in Fig. 1.3. Their study demonstrated that the beam-to-column flush endplate connection demonstrated sufficient stiffness and strength for a 1-in-500 years return period. However, it required further improvements to withstand an earthquake of a 1-in-2500 years return period.

In conventional analysis and design of framed structures, the behaviour of beam-to-column connections was considered as either pinned or rigid in order to simplify the analysis and design procedure. However, experimental results indicated that the considered joints were of a semi-rigid and partial strength type whose behaviour lied in between the two extreme scenarios. Therefore, these simplified assumptions may be inaccurate and lead to the wrong interpretation of the structural behaviour of the framing components. The utilization of semi-rigid connections enables the adjustment of the design loads acting on the frame and enables the frame to be designed more efficiently. Therefore, the behaviour of such joints should be considered in the analysis and design of framed structures. Previous studies on the use of these connections in frames by Leon *et al*. (1987) and Ammerman and Leon (1990) demonstrated that the frames using semi rigid connections performed effectively as compared with the welded connections. These types of frames provide an excellent structural design for the low-rise buildings in Australia. The modern design codes such as EN 1993-1-8 (2010) and AISC-LRFD (1994) have formally recognized and accepted the consideration of semi-rigid behaviour in joints in order to reflect the actual situation (Thai *et al*., 2016a). Hence, the need arises to determine the key properties of the connection to be included in the frame analysis and design.

The behaviour of a joint is represented by its moment-rotation behaviour that depends on three key properties which are initial rotational stiffness, moment resistance and rotational capacity. These properties can be predicted using EN 1993-1-8 (2010) (for bare steel joint) and EN 1994-1-1 (2004) (for composite joint). However, characteristics of various components involved make it difficult to predict the structural performance reasonably well. Therefore, it requires re-planning of the structure on the basis of sub-model as well as global frame analysis.

Considerable progress has been made in recent years in order to develop an efficient and reliable analytical method to calculate the moment capacity and rotational stiffness of composite connections. Many models have been presented and mostly comprise of the parameters depending on the stiffness, strength or ductility for a given connection and shape parameters treated as curve fitting parameters (Lee and Moon, 2001). Therefore, the expressions prove to be accurate only for the particular type and limited range of data used in the regression analysis. Therefore, despite of the extensive research carried out to investigate the structural performance of composite frames with semi-rigid connections such as Xiao *et al*. (1996b), Liew *et al*. (2000), Hensman and Nethercot (2001), Zhao (2016) and Wang *et al*. (2018b), the moment rotation relationship of these innovative joints still appears to be limited.

As discussed above, the behaviour of these connections is extremely complicated and is affected by a number of factors. The lack of test results in literature particularly under cyclic loading impedes the formulation of design guidelines on these connections. Therefore, despite of the existing research on these connections, it is extremely necessary to further investigate their behaviour so that these structures can be effectively utilized in practice. Hence, comprehensive experimental, numerical and analytical studies were undertaken in this research to explore the behaviour of beam-to-column flush end plate connections with equal angles and blind bolts under static and cyclic loading conditions.

Overall, the study endeavours to deeply explore the behaviour of composite beam-to-CFST column joint sub-assemblies as well as frame structures. This contributes to a good understanding of these novel structures under various loading conditions. Moreover, it provides essential guidelines and useful information on the design of these beam-to-column composite connections and contributes to their development in engineering practice.

1.3. Objectives and scope of thesis

The primary objective of this thesis is to identify significant parameters that affect the load-displacement behaviour of the beam-to-column connections and to perform extensive parametric studies to deeply explore and provide an in-depth knowledge on the behaviour of these connections. The research work carried out in this thesis aims to investigate the issues which have been discussed above such that it provides further intuition and understanding on the issues specified. The work is mainly divided into experimental, numerical and analytical studies. The major objectives and scopes to be derived from the thesis are outlined as follows:

1. To undertake an experimental investigation on composite beam-to-column joints subjected to both static and cyclic loading scenarios

2. To extend the analysis on the beam-to-column flush end plate joints using finite element method. Three-dimensional models with geometrical and material nonlinearity considered will be built to simulate the experimental specimens.

3. To validate the numerical results with test outcomes to inspect the accuracy of finite element methods.

4. To investigate the load-displacement behaviour of typical beam-to-column flush end plate joints in terms of initial stiffness, ultimate strength and failure modes and to achieve a sound understanding of these connections with the help of parametric studies. Based on this, design requirements intend to be defined so as to provide specific recommendations for design engineers in practical situations.

5. To investigate the global behaviour of composite frames by using frame analysis. Two-dimensional finite element models will be built to simulate the behaviour of frame buildings under various loading conditions. Different design actions are to be incorporated into models including dead loads, live loads, wind actions and earthquake actions. Relevant results will be discussed so as to find out the extreme loading combination that imposed significant influence on the structures.

1.4. Research methodologies

The objectives of this research were achieved using the following steps:

1. Firstly, a comprehensive literature review was conducted to examine previous investigations in the relevant area and to further study the most beneficial aspects to be explored.

2. After that, full scale experimental investigation was performed to get the data of load-displacement behaviour under static and cyclic loading scenarios and to explore the respective failure modes.

3. Subsequently, 3D nonlinear finite element models were developed to simulate the experiments and most importantly, the finite element models were also validated against the test results.

4. Thereafter, parametric studies were performed to investigate the main geometrical, material and mechanical parameters that influence the behaviour of these innovative blind bolted beam-to-column connections under consideration.

5. Following that, moment-rotation models were developed using analytical approach. Finally frame models were developed using ABAQUS software (2014) that were subjected to gravity loads, critical loads of wind and moderate earthquake conditions in Australia.

1.5. Layout of thesis

The composition of the thesis is organised into seven main chapters, with the first and last chapters being INTRODUCTION and RECOMMENDATIONS FOR FURTHER RESEARCH respectively. Each chapter commences with an introduction to present an overview of the contents of that particular chapter. Meanwhile, a series of key findings and critical conclusions are summarized at the end of the chapter.

Chapter 1 commences with the introduction to the research, research background and motivation of research, the objectives and scope of the thesis, research methodology and layout of the thesis. A summary is also provided at the end of the chapter.

Chapter 2 presents a thorough review of the existing research work which has been published in the literatures and which is related to the area of interest in this thesis. This chapter not only includes the significant findings and results based on extensive experimental and analytical work but also the pertinent design rules and guidelines in international codes and standards. The literature review is essentially divided into a few major sections. The chapter commences with a brief introduction on various topics relevant to this research such as composite construction, lateral loads, earthquake prediction and return period. After that, the experimental studies on beam-to-column flush endplate connections under static and cyclic loading are presented. Subsequently, numerical studies on beam-to-column flush endplate connections are overviewed and finally analytical studies on beam-to-column joints are presented in section 3 followed by the prediction of moment-rotation relationship and the finally research work related to frame analysis is outlined.

Chapter 3 elaborates the experimental programme of two steel and composite beam-to-column flush end plate joints that involves the details of test specimens, material properties, test set-up, loading protocol and instrumentation arrangement. The load-displacement behaviour of these specimens is discussed in detail. General observations for each of specimens are described that include failure modes and strain development. Load-displacement relationships were discussed to inspect key findings.

Chapter 4 reports the three-dimensional non-linear finite element modelling of the composite beam-to-column joints, with concrete-filled columns connected to composite beams by blind bolts and flush end-plates. These joints were subjected to static and cyclic loading conditions that were similar as tests. Material nonlinearity was taken into account consisting of steel behaviour and concrete properties. Related modelling theories and techniques were reviewed. Numerical results validated with the experimental outcomes were finally discussed in terms of load versus displacement curves and failure modes. Parametric analysis incorporating various critical factors that affected the structural behaviour significantly was conducted. Based on the results of parametric analysis, design recommendations are presented to provide an insight into the design of beam-to-column flush end plate joints with blind bolts.

Chapter 5 describes the frame analysis regarding composite frames with beam-to-column bolted semi-rigid joints. Frames with different storeys and bays were analysed to investigate the flexural response under various extreme loading scenarios. The frames were subjected to dead loads, live loads, wind actions and earthquake actions. Both strength limit state and serviceability limit state were considered to investigate the frame performance.

Chapter 6 highlights the significant conclusions and findings obtained from the experimental study and finite element analysis of blind bolted sub-assemblies as well as from in-plane analysis of semi-continuous composite frames.

Chapter 7 presents the general comments and recommendations for further research and application of these connections in engineering practice.

1.6. Summary of chapter

This chapter has presented the research background together with motivations that revealed related grey areas highlighted. The objectives and scopes of each chapter in this thesis were summarised to focus the advanced and innovative feature of the research. The typical layout of the thesis was outlined as well. More precise description of the present studies of frames with beam-to-column joints is presented in the next chapter.

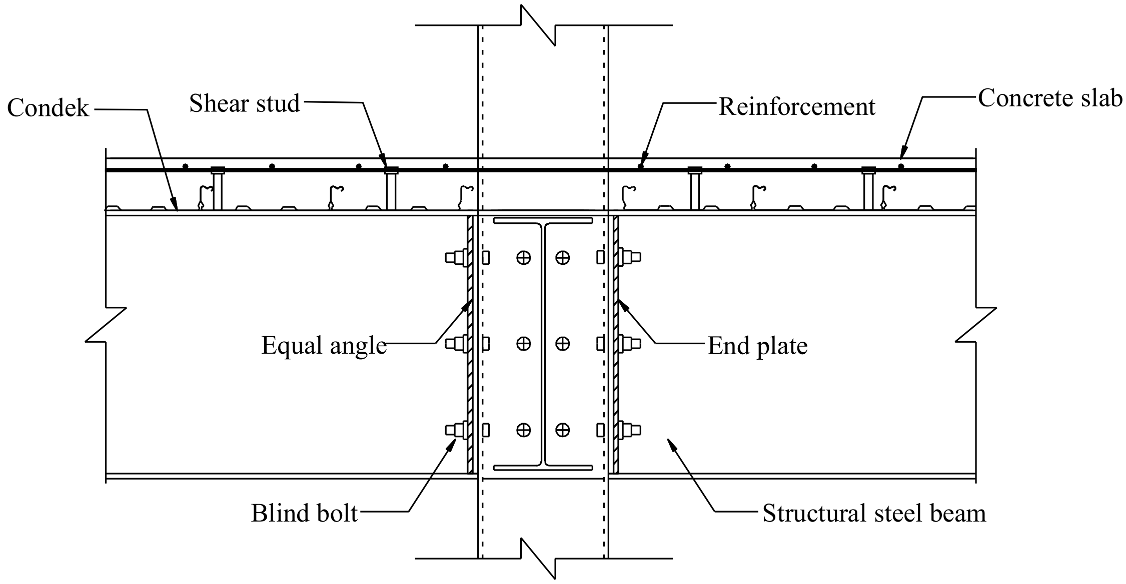

Fig. 1.1 – Typical layout of a flush endplate composite connection

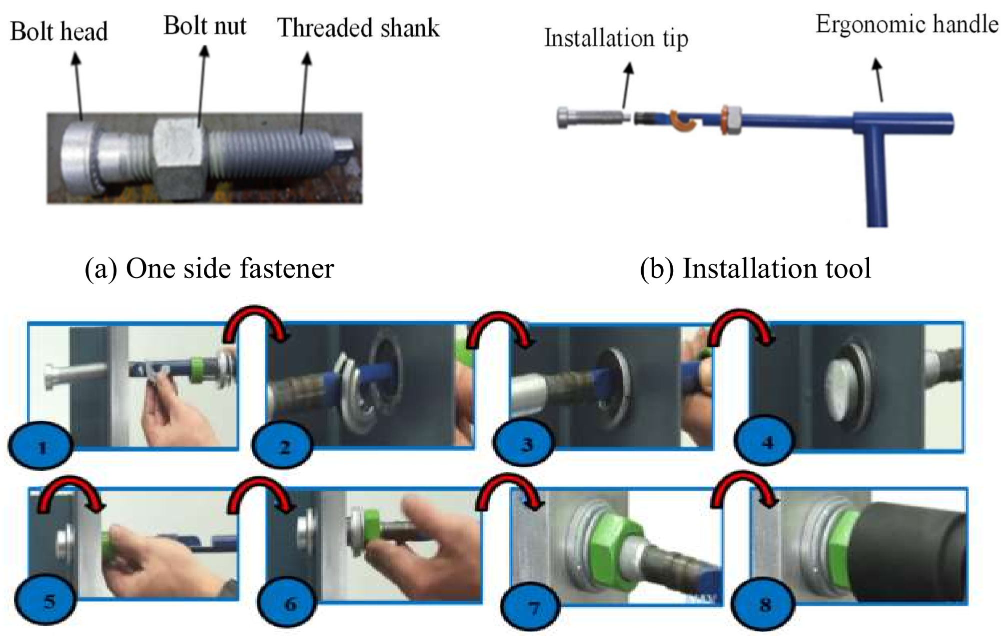

(c) Installation process

Fig. 1.2 –Ajax one-side blind bolt

Adapted from (www.ajaxfast.com.au)

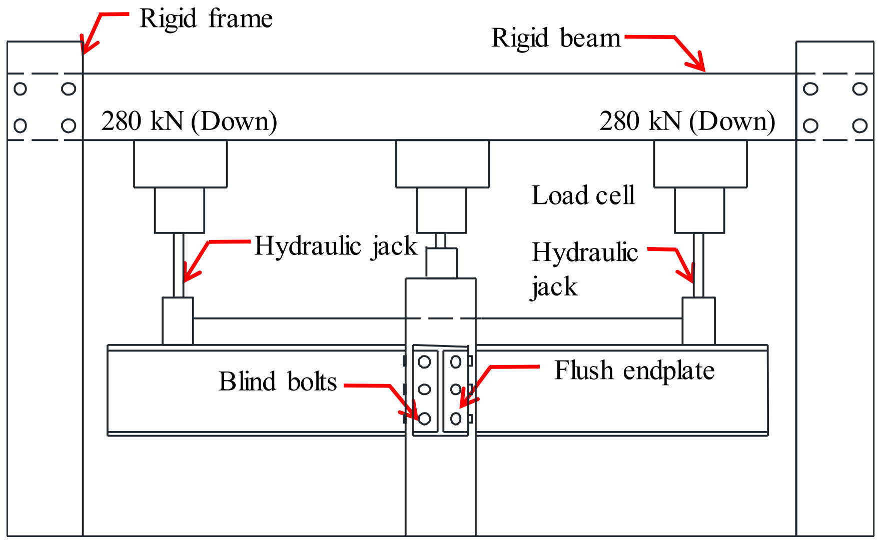

(a) Maximum load in compression

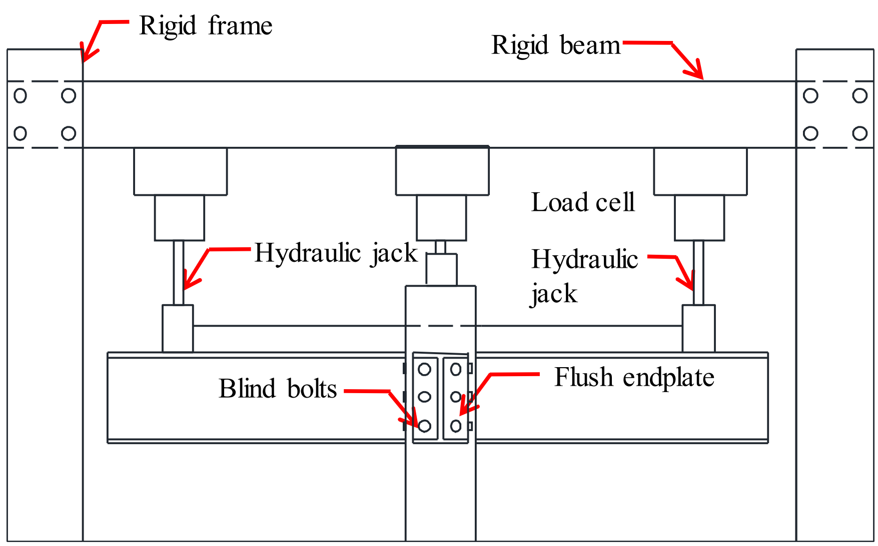

(b) Maximum load in tension

Fig. 1.3 – Loading set up of cyclic test on beam to column flush end plate joints (Mirza and Uy. 2011)

CHAPTER 2

LITERATURE REVIEW

2.1. Introduction

It is enormously important to comprehend the history of a particular field in order to improve the level of knowledge in that area. This could only be achieved by undertaking a comprehensive literature review. Therefore, this chapter aims to review the substantial findings and conclusions obtained from other researches in this area that helps to fill the missing gaps of knowledge and to get an insight into the importance and need for conducting the respective research work. Moreover, this chapter also highlights the shortcomings that exist in current literatures. This is the first step towards the achievement of the ultimate goal of this research.

The chapter instigates with brief information on earthquake loading, earthquake return period, composite steel-concrete construction, concrete filled steel tubular columns, flush endplates, blind bolts and shear connectors. Moreover, a wide range of literatures concerning beam-to-column behaviour involving experimental, numerical and analytical studies are overviewed. Furthermore, moment rotation models are briefly overviewed. Finally, the global behaviour of frames is summarised followed by a summary of the chapter.

2.2. Earthquake loading

An earthquake occurs as a consequence of sudden energy release in the earth's crust that develops seismic waves which leads to ground movement in any direction. Earthquakes are natural occurring catastrophes which are enormously devastating and are extremely problematic to manhood. The statistics of the twentieth century demonstrated a global average of 17,000 human beings killed each year as a consequence of earthquakes (Scawthorn 2003). Besides, they have a severe destructive impact on building structures which in some cases lead to failure. On the 2nd of December 1989, Newcastle in NSW, Australia experienced its largest earthquake that measured 5.6 on Richter scale. 13 people lost their lives, 35,000 homes, 147 schools, and 3,000 other structures collapsed in the region as shown in Fig. 2.1.

The earthquake in New Zealand, that took place on the 22nd of February 2011 shown in Fig 2.2 in Christchurch led to 185 human fatalities and severe structural damage to more than 3,000 buildings. Moreover, in Christchurch's main city 45% of the buildings were categorized as hazardous sites which were forbidden due to safety reasons (Beavan *et al*. 2011).

Whilst earthquakes worldwide predominantly occur along tectonic plate boundaries known as interpolate regions, destructive earthquakes do occur away from the plate boundaries which are known as intraplate earthquakes (Wilson and Lam, 2006). In the past 100 years, more than twenty earthquakes of 6 (M6) or superior magnitude occurred in continental Australia which is absolutely inside the Indo-Australasian plate. On average 2-3 earthquakes of M5 or greater magnitude occurring every year in Australia

(McCue *et al.*, 1995). The Meckering earthquake of M6.9, occurred in Western Australia in 1968, was the first earthquake to occur in Australia which produced noteworthy civil engineering damage. This event encouraged research to establish the first earthquake code AS2121 (1979) which was superseded by AS1170.4 (1993). The last standard added the seismic hazard map of Australia as stated by Gaull *et al.* (1990).

In intraplate regions that have low seismicity such as Australia, earthquakes occur as a consequence of reverse faults due to horizontal compression (Gibson and McCue, 2001). This results in a great reduction in stress with moderate attenuation which further leads to high frequency ground motion close to the earthquake and high accelerations. These frequencies finally result in high peak ground accelerations.

Chandler *et al*. (2001) stated that high frequency earthquakes produce lower ground motions whereas low frequency earthquakes produce higher ground motions. For example, an earthquake with M value 5 produces peak ground acceleration (PGA) of 3.9 m/s^2 while an earthquake with M value as 7 produces PGA of 2.6 m/s^2. This shows that acceleration is not critical to the earthquake, rather it is the drift demand of the structure. This phenomenon is also described in a study by Wilson and Lam (2006).

2.3. Earthquake return period

As illustrated by Gibson and McCue (2001), return period of an earthquake is an indicator of the size of an earthquake and depends upon a particular location. For instance, a 1-in-500 year's event in a high seismicity region indicates a huge earthquake. However, in a low seismicity region the same return period earthquake corresponds to a relatively small event. Current structures in Australia are designed with a 1-in-500-year event. It should be noted that a 1-in-500-year event is a low magnitude event and would hardly cause any damage to a properly designed structure. Instead, less frequently occurring earthquake having low frequency ground motions are more vulnerable.

In 1848 earthquake, centered in Marlborough, caused excessive damage to the brick and masonry construction in Wellington, and the city was rebuilt mainly in wood. However, it experienced relatively little damage in the 8.2 magnitude earthquake of 1855, which elevated the land 2-3 m. As compared to this, magnitude 6.3 Christchurch earthquake (2001) caused severe human fatalities and a great damage to buildings in the vicinity. The huge damage caused by several earthquakes in the region led to the discussion whether earthquakes should be designed for a low-probability-high-consequence event such as 2500-years return period, Mirza and Uy (2011, 2012). It has now been declared that according to the Australian standards, buildings in Australia should be designed for a higher return period such as that of a 1-in-2500 years earthquake event. Standards Australia (2004) has amplified the earthquake return period factor (k_p) for a 1-in-2500 years event by multiplying the site hazard factor by 1.8.

The use of 1-in-2500 years earthquake has also been encouraged by Lam and Chandler (2001) and Chan and Lam (2001) to apply in intraplate regions of low seismicity such as Australia, Hong Kong and Eastern USA. Recently, walker emphasized that multiple benefits would be achieved if higher return period calculations are incorporated in design. Human casualties will be reduced, increase in structural life and minimized economic and commercial impacts could be attained. Therefore, rigorous experimental studies need to be performed to explore how these composite connections will perform in the unlikely event of a high-consequence earthquake.

2.4. Composite steel-concrete construction

Infrastructure has been developing globally at a fast pace due to increased economic growth and globalization. To uphold structural integrity and improved performance it is mandatory to study various structural components and their response to loading. In particular, the use of composite structures has risen due to the benefits of enhanced performance resulting from the combine usage of concrete and steel. The development of composite structures dates back to the 19th century when in 1995. Hyogoken-Nanbu earthquake of magnitude 7.2 badly struck Kobe, Japan. It was the most severe earthquake and caused a huge damage to the county. The consequences of the earthquake led to the consideration of composite structures for large-sized structures as many reinforced concrete bridge piers and building columns experienced a huge damage (Wang *et al*. 2001).

Composite construction dominates the multi-storey building sector due to the strength and stiffness that can be achieved with minimum use of materials. By combining the concrete and steel material together, their strengths can be exploited to result in a highly efficient and lightweight design. Composite construction also offers benefit in accelerating the speed of construction. Depth reductions in floors can be achieved with benefits in terms of costs of services. Therefore, these structures have gained widespread popularity in the world particularly for bridge superstructures, industrial structure and multi-storey frames for over a century now.

In case of bridges, it provides the designer to take full advantage of the steel section in tension, by shifting the compressive force into the concrete slab in bending. With the development of high-performance steel and high-performance concrete, composite steel bridges have been designed to span longer and achieve what was impossible to achieve with ordinary materials and at a comparatively lesser expense. However, special attention should be given to predict the deflection for current and future composite structures (Nie & Cai 2003).

An economical structural system can be achieved by using composite floors and beams in frame structures as it eliminates the use of formwork and results in a reduction in the overall depth of the floor. This allows for an increase in the number of floors in a building. Furthermore, the use of composite columns and beams also allows the construction of buildings to a considerable height where bracing is not required. The local and global second-order effects are also reduced due to the increase in stiffness. Steel-concrete composite structures can deliver high performance in terms of energy dissipation and ductility. It also accomplishes reasonable performance in earthquake due to ductile design. Composite design offers high dissipation without affecting the strength of the structure. (Salvatore, Bursi, and Lucchesi 2005).

2.5. Concrete filled steel tubular columns

Steel hollow section columns have achieved extensive appreciation due to aesthetic appeal and structural proficiency in recent years. However, the complexity involved in design of the connections restricted the widespread applicability of these structures in practice. In the last two decades, welded connections were the most common method used to achieve connection between beams and columns. Although the brittle failure, associated heat, fabrication difficulty and high cost made it unattractive to designers. After extensive research on the semi-rigid method, blind bolts appeared to be the most recommended connectors in composite design under seismic loading.

There are two different types of composite columns such as concrete in-filled columns and concrete encased columns. In-filled columns involve steel section (square, circular or rectangular) filled with concrete and encased columns are steel sections enclosed in concrete as illustrated in Fig. 2.3. Concrete-encased steel composite columns are mostly used in seismic resistance structures. Concrete encasement suffers cracks under high flexural loading which leads to a decrease in the stiffness. Though, the steel core offers shear capacity and ductile resistance to the subsequent cycles of overloading (Shanmugam & Lakshmi 2001).

Concrete- Filled Steel Tubular Columns (CFST) such as Circular Hollow Sections (CHS) and Square Hollow Section (SHS) are increasingly used in buildings predominantly in bridge piers and high-rise buildings. Han, Wang and Zhao (2008) suggested that the CFST columns are preferable because of their excellent static and earthquake resistance properties. Furthermore, the key advantages of CFST columns include high energy absorption capacity, high ductility, increase in achievable strength, stiffness, good fire resistance, reduction in local buckling of the tube wall in comparison with reinforced concrete, elimination of formwork, reduction in reinforcing steel, and reduction in labour cost (Mirza and Uy 2011). The performance of CFST columns has become an attractive topic to many researches and studies aiming to investigate the behaviour on the frame of this type of construction.

2.6. Flush end plates

End plate moment connections consist of a steel plate that is shop-welded to the end of a steel beam that is then bolted to the connecting member using rows of high strength bolts. There are two types of endplates which are named as flush and extended. A flush end plate connection comprises of an endplate welded to the beam which does not extend beyond the outside of the flanges of the connecting beam while an extended end plate extends beyond the tension flange of the steel beam as shown in Fig. 2.4. The bolt rows are positioned within the flanges of the connecting beam. The flush end plate connections can be stiffened or unstiffened. The stiffened design has small plates (stiffeners) welded to the end plate and the beam web, on both sides of the web. These plates (stiffeners) can be placed between the bolt rows or outside the bolt rows. Flush end plate connections are normally used in frames subjected to light lateral loading or near inflection point of gable frames (Morris 1988).

Experiments by Wang *et al*. (2013) suggested that the thickness of the endplate is of a great importance, as it affects the stiffness and strength of the endplate joints to column. Flush end plate connections are an absolute choice for use in beam-to-column connections and are used in this study as well.

2.7. Blind bolts

Barnett *et al*. (2000) suggested that numerous blind bolting products have been explored over the years which include Huck fasteners, Flow drill and the Hollow bolt. However, the latter two types were limited to pinned connections only. Each type of fastener differs in the bolt components, resistance mechanism and method of installation. Yeoman (1998) stated that flow drilling is a specialized thermal drilling process that requires a distinct tool to create a hole and a separate tool to thread through the wall of the hollow section. The surrounding metal is locally displaced during the drilling process and the wall thickness is increased to accommodate the threads.

Unlike the flow drill process that needs separate tools for drilling and threading, the hollow bolts require only a conventional spanner or a torque wrench. Another option was to use blind bolts that require installation from one side only. These bolts are also used in the experimental and numerical phase of this study mainly due to easy installation, reduced labor requirement and being economical. It was concluded from an experimental study by Wang *et al*. (2016a) that the selection of correct size of blind bolts is an important consideration.

Broderick and Thomson (2002) suggested that a higher grade of bolt enhances the ductility of the joint and stripping of threads within bolts lead to brittle failure of the connection. Study by Loh *et al*. (2006) demonstrated that the blind bolts are probable to be used in composite joints as they exhibit marvelous capacity. Wang and Guo (2012) suggested that promising results could be achieved by strengthening of the blind bolt anchorage as it helped to reduce the pressure exerted by the blind bolts on tubular wall and improved the connection capacity.

Mourad *et al*. (1995) have investigated the experimental behaviour of the blind bolted extended end plate connections for HSS columns under cyclic loading, and analyzed the effect of the joint flexibility on the response of the type of frame. Owing to the many advantages associated with hollow section steel columns that include aesthetic appearance and economy in terms of material costs, the blind bolts were therefore used in this study for connecting steel beams to CFST columns.

Goldsworthy and Gardner (2006) proposed a T-stub connection that offered a simple and economical system to connect the beams and columns. The connection was composed of high strength bolt with an L-shaped extension entrenched in concrete. This connection permitted assembly from outside of the steel tubes. Experimental studies were performed to investigate the moment-resisting behaviour of the connections. The test results demonstrated dramatic improvements in stiffness and strength of the T-stub connection due to the addition of extensions. Moreover, the proposed connection exhibited enhancements in ductility of the beam-to-column joints.

Elghazouli *et al.* 2009), also examined the behaviour of blind-bolted-angled connections between tubular columns and beams under both monotonic and cyclic loading conditions. The most important finding was that grade of the bolt chosen and the distance between the bolt and the beam flange significantly affected the performance of the connection. Therefore, the grade of the bolt and the distance of the bolt from the flange must be carefully in the design of a composite connection in order to achieve fruitful outcomes.

Oktavianus *et al.* (2017) designed a new type of blind bolts in which the bolt shanks were prolonged and embedded into infilled concrete. Analytical models were established to predict the pull-out behaviour of the connections. The models involved all bolt components such as the bolt shank, embedded head, and washer bearing. In addition, finite element models were developed to calibrate the analytical models with the yield and ultimate strength, initial and secant stiffness of each component under consideration. The bolt diameter, size of circular hollow columns, embedded depth of bolt head and concrete strength were defined to determine the distinct behaviour of each component. The study concluded that the proposed method displayed a good agreement as compared with finite element models and experimental data when the behaviour of individual components or the global behaviour of combined components was considered.

The design herein makes use of 20 mm diameter AJAX Blind Bolts, which are capable of providing the desired connection strength according to manufacturer's specifications, whereby grade of the bolts, thickness of the flange and the distance between both the bolt and the flange are all considered during the design.

2.8. Shear connectors

One complication with composite construction in past was the longitudinal slip between the elements. This problem was resolved by an American engineer, who introduced headed stud shear connectors welded to the top flange of the steel beam to produce a strong shear connection. This helped to achieve composite action between the concrete slab and steel beam. These shear connectors have helped to get rid of the longitudinal slip (Uy and Liew 2003).

The performance of the shear connectors at the steel-concrete interface is extremely important as the action between steel and concrete relies on. The behaviour of shear connectors is examined by performing either the individual shear connector tests or standard push out tests. The connectors provide a medium to transfer the forces from concrete to steel and vice versa. They also support to prevent the vertical separation of steel and concrete. During these days, high-performance steel and concrete are used. Hence, more shear connectors are required to achieve a fully composite action. In some situations, a partial composite design is preferred when the top flange can only hold a limited number of shear connectors. A partial composite design will cause more slip at the interface between steel and concrete, resulting in more deflection with time. (Nie and Cai 2003).

Daniels and Fisher (1966 and 1967) performed experimental investigation on four two-span continuous beams to investigate the effects of using shear connectors in negative moment regions. Initially, all continuous beams were tested for fatigue under continuous stress ranges of service load levels, before being tested statically to failure. The authors observed that it was important to provide shear connectors in the negative moment regions of continuous beams. This was essential to avoid the additional force imposed on connectors in the positive moment regions which would result in premature failure.

Additionally, longitudinal reinforcement was found to be important to control the number and width of slab cracks and to improve interaction and flexural conformance. There was no indication of a decrease in strength in those sections where the slab was in tension since the shear connectors were observed to resist longitudinal shear forces as the tests advanced. The connectors were also found to have adequate strength to achieve the ultimate strength of the member.

2.9. Beam-to-column joints

The design of a connection is extremely critical from both structural and economical perspective. The connection serves as a medium for transfer of forces and moments from one member to another. The force transfer occurs between the components and the connection. Therefore, if these connections are not accurately designed, there is a likelihood of failure of the connection followed by failure of the structure. Establishment of a proper connection between a beam and column, especially under cyclic loading conditions is difficult to achieve due to a lack of both knowledge and guiding principles by most international codes (Elghazouli *et al.* 2009).

Beam-to-column connections are considered as one of the most important structural elements in a structural system as the proficiency and reliability of connections have a great influence on the structural components as well as the whole structure. The connection controls the amount of moment being transferred as well as provides stiffness to control the sway deflection. Therefore, the design of connection at the joint region is extremely important.

After Thessaloniki earthquake (1978), Halcyonides earthquake (1981), and Kalamata earthquake (1986), investigations revealed that beam-to-column connections are one of the most critical structural elements (Tsonos, 2000). Connections normally suffer shear and bond failures under earthquakes. Therefore, the successful performance of a structure relies on the design and fabrication of its connections.

Moreover, a successful connection design highly depends on the method by which a structure is analysed. A design approach was to establish rigid connections that allowed the joint to be fully continuous. These connections could be achieved by welding steel beams to steel columns and were capable to develop a considerable moment resistance. A fully rigid connection produces no rotation and makes beam's end moment fully transferable to the column. However, these connections were not preferred as they demonstrated a non-ductile behaviour and also due to the exorbitant cost involved in their fabrication. Nethercot (2001) also confirmed that it is extremely difficult to obtain sufficient ductility in rigid joints that is required for the re-distribution of moment and is mandatory for an effective plastic design approach.

Another option was to utilize simple or pinned connections. These highly flexible connections mainly transmitted vertical shear forces and delivered insignificant moment of resistance. Simple connection cannot resist rotation, for this reason the design must ensure that the connection moment is zero. Therefore, in order to meet the drift requirements, bracing the frames was essential. Additionally, large beam sections were required to withstand gravity loads. Therefore, this system was also un-economical and hence not feasible.

Moreover, the Simple method assumes beams to be simply supported. It indicates that beam-to-column connections should be sufficiently flexible to avoid the development of end fixity. All horizontal forces must be resisted. Research in the past demonstrates that most simple connections are capable of developing some amount of moment capacity. However, the simple method deliberately overlooks this effect.

Semi-rigid connection offers some resistance to rotation of the connected members and able to transfer force through the beam, column, and the connection itself. These characteristics make semi-rigid method a perfect connection design for seismic areas. The behaviour of joints fabricated with these connections is considered to be located between the two extremes of rigid and pinned connections. These connections are considered as semi-continuous and are capable to provide sufficient stiffness and moment capacity. Not only that these connections are very economical but they also allow an effective redistribution of moment according to the plastic design approach. Moreover, they also effectively control the service deflection. The beam design moment and most probably the size of the beam is reduced due to shifting fixing moment to the column, while the column size is increased. Fig. 2.5 presents the three types of connections considered in practice.

A considerable research on the use of these connections has been conducted in the past such as by Li *et al.* (1996a), Leon and Ammerman (1990), Liew *et al*. (2004a), Simoes *et al.* (2001), Loh *et al*. (2003), Mirza *et al*. (2010), Uy *et al*. (2012, 2017), Ataei *et al*. (2015) and Thai *et al*. (2017). The results demonstrated that the frames using semi rigid connections performed effectively as compared with the welded connection. These types of frames provide an excellent structural design for the low-rise buildings in Australia. Beam-to-column connection must fulfil some requirements irrespective of the type of fasteners used. They must be robust, ductile, provide a required degree of strain, and easy to manufacture and assemble. Additionally, connections should satisfy the equilibrium's requirements. A beam-to-column connection needs to transfer at least shear force as well as axial force, where bracing is used for stability. The connection must also expect to transmit moment when the frame provides stability itself (McGuire 1988).

In this thesis, the behaviour of composite joints under static and cyclic loading will be studied. A detailed study on the behaviour of these joints will contribute in developing an improved understanding of the response of the composite joint under earthquake loading and the critical components to consider for future designs.

2.10. Failure modes in a composite connection

Li, Nethercot and Choo (1996) highlighted twelve possible failure modes for a composite connection under bending. The prediction of these modes is developed on test results by (Xiao *et al*. 1994, Anderson *et al*. 1994, and Johnson *et al*. 1972, cited in Li, Nethercot, and Choo (1996). Failure modes of beam-to-column connection are:

- Yielding of the end plate in bending
- Fracture of the concrete reinforcement in tension;
- Fracture of the Blind Bolt in tension;
- Shear connectors failure
- Crushing failure of the concrete slab against the column face;
- Column flange yielding in bending;
- Yielding or buckling of the I-beam in shear or compression;
- Yielding or buckling of the column web in transverse compression;
- Yielding or buckling of the column web panel in shear.
- Failure of weld that connect end plate to the steel beam;

- Buckling or yielding of the I-beam lower flange in compression;
- Anchorage failure at the foundation support;

Normally the damage consisted of fractures of the bottom flange weld between the column and the girder flanges. However, there were examples where top flange fractured. By observing brittle fracture at the beam-to-column intersections, new connections approaches have been established to design the beams in such a way that the plastic hinges form away from the column face (Taranath 2005).

2.11. Experimental studies on beam-to-column connections using blind bolts

2.11.1. Static loading

Anderson and Najafi (1994) conducted an experimental investigation on the performance of five composite beam-to-column connections and one bare steel connection. Three main parameters were varied which are depth of the steel beam, reinforcement ratio and type of the end plate. It was found that an increase in the reinforcement and use of an extended end plate increased the moment resistance and rotation capacity. However, an increase in depth of the steel beam increased the initial stiffness but decreased the rotation capacity. Later, Brown and Anderson (2001) reported a series of tests to evaluate the structural performance in major axis endplate joints. The results concluded similar findings to the study by Anderson and Najafi (1994).

Liew *et al.* (2000) reported results obtained from a test series on six-composite beam-to-column joints with flush end-plates and blind bolts. The steel beam section and concrete slab was kept identical for all specimens. However, the differences between the specimen included different types of columns, varied reinforcement ratio, and presence of stiffeners in the column web. Moment rotation curves were obtained from the experiments and compared with those predicted analytically. The study concluded that the increase in reinforcement ratio significantly increased the initial stiffness of the connection while it had a very minor contribution to the increase in rotation capacity of the joint. Web stiffeners were recommended as they had a positive influence on the moment resistance and rotation capacity of the joint. Similarly, the use of fully encased columns enhanced the performance of the composite joint.

Da Silva *et al*. (2001) explored the flexural performance of interior and exterior joints under monotonic loading. The study focused to explore the contribution of concrete confinement in composite columns to the performance of the composite joint. Various loading conditions were applied to the interior joints, namely both symmetrical and asymmetrical loads were adopted to simulate hogging and sagging bending moments. Joints subjected to symmetrical loading demonstrated high initial stiffness and moment resistance, while reduced stiffness and strength exhibited by the joints subjected to asymmetrical loading since the deformations in column web panel governed the behaviour of the joint.

Liew *et al.* (2004) undertook an inspection on eight connections under positive moments. The specimen consisted of 120 mm deep slab with highly ductile 16 mm diameter bars of 1.12% reinforcement ratio. The study demonstrated that concrete encased columns produce 1.75 times more negative moment capacity as compared with a plain steel column. However, no obvious difference was observed when the positive moment section was tested. The modes of failure observed were fracture of the blind bolts and excessive endplate deformation. The connection capacity did not get affected due to unbalanced moments.

Loh *et al*. (2006a) carried out experimental studies on five bolted flush end plate joints in which they investigated the effect of partial shear connection on the composite beam-column joint by varying the number of shear connectors and reinforcement. The experimental results concluded that the shear connection ratio has a significant effect on the performance of the connection.

Wang *et al*. (2009a) extended a similar experimental investigation to explore the static behaviour and failure modes of beam-to-column joints with flush end-plates. The experimental set up is presented in Fig. 2.6. The study considered different types of columns and different thicknesses of flush end plates. All specimens were loaded symmetrically until failure. Experimental outcomes concluded that the beam-to-column joints with blind bolts and flush end-plates demonstrated satisfactory stiffness, strength and favourable ductility. Moreover, an increase in the thickness of end-plates improved the flexural behaviour in terms of stiffness and moment resistance, but reduced the rotational capacity to some amount.

Wang and Chen (2012) experimentally inspected the moment-rotation behaviour of steel beam to square CFST column joints. Two types of end-plates were considered which were flush end-plates and extended end-plates. Moreover, different blind bolts were used to tighten the joints. Test observations exhibited that the semi-rigid joints performed satisfactorily. A design recommendation was proposed to improve the structural performance of the joint by applying anchorage extensions of bolt shanks. Wang and Spencer (2013) also undertook a similar experimental investigation and reported similar findings. Furthermore, Wang and Guo (2012) conducted more experiments on blind bolted end-plate joints to CFST columns with thin walls, and summarized similar results.

Li *et al*. (2012) performed experiments on three composite beam-to-column joints with flush end-plates under fire conditions. The investigated parameters included temperature distribution, axial load resistance, failure modes and deflections of composite joints. Results recommended that initial stiffness and moment resistance are explicitly affected by the axial forces. Additionally, the reinforcement encased in concrete slabs experienced low temperature which produced a high moment resistance. Semi-rigid connections enabled the beams to increase the bearing capacity.

Furthermore, Ataei *et al*. (2015 and 2016a) performed an extensive experimental investigation that involved beam-to-column tests with deconstructable structural systems that possessed the novelty of precast concrete slabs associated with low CO_2 emissions, high strength steel and blind bolting. A general description of their test specimen and experimental set up is presented in Fig. 2.7.

Wang *et al*. (2017a) attempted an experimental investigation on the seismic behaviour of blind bolted composite frames with semi rigid connections. Two specimens with two spans and single layered blind bolted composite frames were subjected to low cyclic loading conditions. The main criteria considered were the effect of end plate type and type of loading. The composite structures were analyzed in terms of strength and stiffness degradation, failure modes, energy dissipation and ductility. Some simplified models to calculate the initial stiffness and moment capacity were also suggested. The study concluded that composite beam-to-column frames fabricated with semi rigid joints and blind bolts performed satisfactory in terms of ductility, energy dissipation capacity and exhibited large hysterics loops. The test set up of the composite frame tested by Wang *et al*. (2017a) is presented in Fig. 2.8.

Thai *et al*. (2017) performed an investigation to experimentally investigate the structural behaviour of composite joints with different shapes of CFST columns and different types of endplates. Four full-scale sub assemblages of cruciform joints were tested under static loading conditions. Square and circular CFST columns and flush and extended end plates were considered. Structural performance was investigated in terms of initial stiffness, moment capacity and rotational capacity. From the results, it was found that the beam-to-column joints possessed high ductility and behaved in a semi-rigid manner. A key finding of the test was that the use of square column instead of circular and extended end plate instead of flush end plate considerably enhanced the initial stiffness and moment resistance of the tested connections. There were 15% to 22.6% enhancements in moment capacity and initial stiffness when square CFST column and extended end plate were used respectively. In particular, the study demonstrated that use of both extended end plates and circular columns enhanced the strength of these connections.

2.11.2. Cyclic loading

The existing design philosophies used to verify that structures can withstand large seismic loads much bigger than their elastic limits, have very comprehensive mathematical and engineering groundings. Recent seismic events in the surroundings have shown that while the present design method is sound, there are still many problems which need additional investigation and study, specifically in the area of connections. It is the beam to column connection that delivers a structure with its lateral stiffness, and likewise it is these connections that play a significant role in building safety during a seismic event. These connections must either be sufficiently strong to form a hinge in the connection beam element, or experience yield themselves while upholding their shear transfer capability and capacity to produce the essential bending capacity. This must be continued over many cycles of reversible loading, and must not affect the load carrying capacity of the column. Consequently, these connections need a design procedure that integrates a strength hierarchy in all of its components and methodology to ensure yielding at pre-ordained locations to shield others that are more critical (Wang *et al.* 2009b).

Bursi and Gramola (2000) emphasized on the absence of any European background regarding the design of composite structures particularly in seismic areas. Research focused on the connection between the columns and the beam and generally assumed to be rigid and full strength under lateral loads due to earthquakes, as most international codes show lack of experimental data for a partial shear connection. However, the contribution of the slab and its behaviour was considered a complex phenomenon which required further research.

Bernuzzi *et al.* (1996) conducted several tests on flush end plate connections to determine the connection behaviour under cyclic reversal loading conditions. It was observed that the bolts excessively elongated and got separated from the endplate. The author assumed that the design moment under reversal of loading was the same as the maximum negative moment due to gravity loading in the connection zone. It was also found that maximum moment reversal was approximately 25% to 25% of the moment due to gravity loading.

Liew *et al*. (2004) performed experimental studies on composite joints subjected to cyclic loading. Eight sets of cruciform beam-to-column joints were designed in which one side of the composite beam was exposed to hogging bending moments, and the other was exposed to sagging bending moments. Different types of end-plates such as flush end-plates with or without haunch, and extended end-plates, were selected to study the moment-rotation behaviour. The experimental results recommended that the strength of panel zone mainly goverened the behaviour of composite joints under unbalanced moments. Flush end-plates with haunch or extended end-plates can improve the initial stiffness and moment capacity. Moreover, the moment-rotation performance was also evaluated using the analytical method proposed by Liew *et al*. (2004b). Individual stiffness and moment resistance were calibrated by means of the component method and were compared with test results. It was observed that design codes overvalued the initial stiffness of composite joints when subjected to hogging bending moments.

Xu (2005) focused on the reinforcement ratio in the slab and its influence on beam-to-column joints, under controlled cyclic loading conditions. The investigation focused on three different finite Element models with the same steel connection components, a steel composite connection with 0.94% longitudinal reinforcement ratio and a composite connection with 1.68% longitudinal reinforcement ratio. Results indicated that the concrete slab had a significant effect on the mechanical behaviour of composite joints, when compared to pure steel joints. The increase of concrete slab reinforcement ratio can improve and increase the moment capacity and stiffness. As a result, the concrete slab must therefore be considered in current and future designs of composite beam-to-column connections subjected to earthquake loads.

Vasdravellis *et al*. (2009) investigated four specimens, each representing a full-scale one-storey moment-resisting frames. The concrete slabs were connected to steel beams with the help of shear connectors in order to achieve the composite action. All specimens were subjected to cyclic loading under displacement-controlled conditions. The results of the experiment highlight that a full shear connection is not always the best option, as it led to a brittle failure of the welded beam-to-column connection. Moreover, the concrete slab had a significant effect on the mechanical behaviour of composite joints, when compared to pure steel joints. As a result, the concrete slab must therefore be considered in current and future designs of composite beam-to-column connections subjected to earthquake loads. The authors also suggested that an increase in the reinforcement ratio can improve and increase the moment capacity and stiffness of the joint.

Wang *et al*. (2009b) experimentally inspected the seismic behaviour of internal beam-to-column joints with flush end-plates and the external beam-to-column joints with extended end-plates in another study by Wang *et al*. (2013). Both experimental programme involved circular and square CFST columns. Test results showed that both types of joints exhibited excellent hysteresis performance in terms of moment-rotation response and energy dissipation. Moreover, the seismic behaviour of an innovative form of composite joints was also discussed by Wang *et al*. (2016a). The results demonstrated that the semi-rigid joints possessed adequate ductility and energy dissipation.

Nogueiro *et al*. (2009) initially collected a large test results data from documented literatures for connections subjected to cyclic loading. After that, an improved moment-rotation model was developed to accurately estimate the structural performance of the joint. Later, numerical analysis was conducted to explore the hysteresis response with six-degree-of-freedom spring elements. Numerical results were validated with specific experimental outcomes in terms of energy dissipation and strength. Moreover, hysteresis model parameters for composite beam-to-column joints were proposed. It can be stated that the beam-to-column joints fulfilled the demand of seismic design.

Zhao *et al*. (2010) developed a simplified analytical approach to predict the behaviour of composite beam-to-column joints. Shell elements were selected to develop concrete slabs while nonlinear beam elements were selected to simulate steel beams. Interactions between concrete slabs and steel beams was developed using spring elements. The composite joints were developed as a panel zone to represent shear-moment interaction. The authenticated method was found to accurately simulate the behaviour of the composite connection.

Braconi *et al.* (2010) performed successive experiments to inspect the seismic behaviour of beam-to-column partial-strength joints. Specimens were fabricated using different types of connections, different arrangement of end-plates, column web panel zones, steel and concrete strength to evaluate the corresponding moment-rotation response. The analysis focused on both the local and global behaviour of the joints that mainly targeted the stiffness degradation, ductility and energy dissipation. The test results demonstrated that an increase in concrete strength was damaging to the flexural performance of composite joints.

Mirza and Uy (2011) reported a study to investigate the behaviour of composite beam-to-column joints with flush end-plates under low-probability and high-consequence loading. The study explored the load-displacement behaviour of the flush end plate composite joints when subjected to static and cyclic loading. In addition, three-dimensional finite element models were established to compare with the test results. Parametric analysis was performed to evaluate the effects of changes in axial loading level, shear connector spacing, reinforcement spacing and slab depth. It was found that the composite beam-to-column joints are capable to withstand an earthquake of 1-in-1500 years return period. The load-displacement behaviour for both loading cases was quite similar. Design recommendations were made which are helpful for the design of these joints in engineering practice.

Tizani *et al.* (2014) investigated the structural performance and reliability of the innovative blind bolted joints targeting to enhance the strength and stiffness of the connectors. Experimental studies were performed to assess the hysteresis performance under cyclic loading. The analysis considered strength of bolts, tubular column wall thickness, cyclic amplitudes and compressive strength of concrete. The joints were inspected in terms of stiffness, strength, rotation capacity and energy dissipation. The results exhibited that an appropriate thickness of column wall and concrete strength influenced the seismic performance of structures. Moreover, the beam-to-column joints offered appropriate energy dissipation capacity and sufficient ductility for use in seismic design.

Tao *et al*. (2017) experimentally investigates the cyclic behaviour of ten composite end plate joints consisting of square and circular CFST columns. Lateral cyclic loads were applied with horizontal displacements imposed the top of CFST column. The main parameters investigated were axial load level, type of column cross-section and cross-sectional configuration of steel beam. The study of initial stiffness demonstrated that the reinforcement ratio has a significant impact on both types of joints.

2.12. Analytical studies on beam-to-column connections using blind bolts

Considerable progress has been made in recent years in order to develop an efficient and reliable analytical method to calculate the moment capacity and rotational stiffness of composite connections. Many models have been presented and mostly comprise of the parameters depending on the stiffness, strength or ductility for a given connection and shape parameters treated as a curve fitting parameter (Lee and Moon, 2002). Therefore, the expressions prove to be accurate only for the particular type and limited range of data used in the regression analysis.

Xiao *et al.* (1996) developed a comprehensive mathematical model to predict the behaviour of various types of endplate connections. The model was validated against available test results obtained from the data base developed by the authors. Parametric studies were performed to inspect the balance between the beam strength and connection for a wide range of factors. The authors suggested designing the composite joints as partial strength and moment resisting connections.

Li *et al*. (1996b) proposed a comprehensive approach to predict the moment capacity of composite joints with flush end-plates under non-symmetrical moments and varying shear/moment ratios. For each loading scenario, bearing capacities of individual components were calculated using component method. The analytical model was validated with the experimental results and was found capable to accurately estimate the ultimate moment resistance. It was also observed that shear resistance in the panel zone had substantial effects on the effective reinforcing force and a compressive force in beam flanges. Li *et al*. (1996b) and Liew *et al*. (2004 a) outlined the principles involved in calculation of the positive moment capacity of a connection. The forces involved are mainly the compressive force of the concrete bearing on the column flange and the tensile resistance provided by the bottom row of bolts in tension. The authors emphasize that the panel zone resistance should be carefully monitored to ensure that the column is able to bear additional force induced at the web by the concrete slab. This is not an issue when CFST columns are used as the strength of steel is considerably high due to the presence of concrete infill.

Ahmed and Nethercot (1996) proposed a cohesive method to predict the initial stiffness and rotational capacity of major axis flush endplate composite connection. The proposed method for initial stiffness calculation was based on a force-transfer mechanism that considered the individual behaviour of all components of the connection. Likewise, the calculation of rotation capacity was based on a simple procedure. These methods when used in combination with the moment capacity and failure mode prediction methods presented by the authors earlier helped to achieve a complete representation of the key design properties of composite flush end plate connections.

Da Silva *et al*. (2001) assessed the moment-rotation response of end-plate beam-to-column composite joints under monotonic loading by means of experimental and analytical approaches. The component method from Eurocodes 3 and 4 was utilized to investigate the strength of essential individuals that were thought to make significant contribution to the overall structural performance. The components were simulated with spring elements to represent stiffness and resistance before assembling them to evaluate the global behaviour. The analytical model demonstrated a reasonably good agreement with experimental results.

Moreover, Abolmaali *et al*. (2005) used Ramberg-Osgood and Three Parameter Power model to develop equations to predict the moment-rotation (M-Ø) behaviour of flush endplate connections with one row of bolts between tension and compression flanges. The comparison of finite element models with test results demonstrated a good agreement. Thai and Uy (2016b) predicted the initial stiffness and moment capacity of blind bolted flush endplate composite joints with hollow and CFST column using regression analysis. The analytical models were based on the component method outlined in EN 1993-1-8 (2010) and EN 1994-1-1 (2004). Their analytical model developed for joints with CFST columns will also be used in the present study to calculate the stiffness of various components of the blind bolted flush endplate composite joint in Chapter 5.

Loh *et al*. (2006b) presented an algorithm of a simple iterative program that successfully simulates the behaviour of beam-to-column flush endplate connections under hogging moment. The study discussed methods for the calculation of moments, stiffness and rotation from various authors. The authors presented a method to investigate the reduced moment capacity of a partial shear connection. The results from the analytical model demonstrated close agreement to the experimental results of Loh *et al*. (2006a) in terms of structural performance. Systematic parametric studies were undertaken using the properly calibrated analytical model. The paper highlighted innovative and simplified modelling of semi-rigid flush end plate joints within hogging moment regions.

Thai and Uy (2016b) extended the application of the design rules mentioned in EN 1994-1-1 (2005) to determine the mechanical properties of a blind bolted flush endplate composite joint with hollow and CFST column using regression analysis. The resistance and stiffness of a new component named 'column face in bending' was calculated using the Gomes and Neves (1996) model. The analytical model developed was validated against the experimental results by Loh *et al.* (2006b). The empirical equations resulted in accurate and reliable predictions of the test results. The components of the analytical model are identified in Fig. 2.9 and the spring model developed for joints with CFST columns is presented in Fig. 2.10. The analytical model can accurately predict the behaviour of the composite blind bolted joints. However, further study was recommended to improve the capability of the proposed model to predict the moment rotation behaviour due to omission of the effects of local buckling of steel beam and formation of cracks in the concrete slab in the proposed model. Their analytical model developed for joints with CFST columns will also be used in the present study to calculate the stiffness of various components of the blind bolted flush end plate composite joint in Chapter 5.

2.13. Numerical studies on beam-to-column connections using blind bolts

Full scale tests can be used to obtain the most reliable behaviour of composite beam-to-column flush end plate connections. However, they are expensive and time consuming which makes it very hard to examine the effect of parameters on the behaviour of the composite connection. Many researchers have reported work on numerical simulation of composite beams and joints using finite element modelling technique such as Kim *et al*. (1999), Bursi *et al*. (2005), Mirza and Uy (2011, 2012), Ataei and Bradford (2014), and Thai *et al.* (2015) etc.

Wang (2010) developed two-dimensional finite element models to investigate the structural performance of composite joints with semi rigid connections. The ultimate moment resistance was calculated by considering nonlinearity of material and geometrical properties. Both models were validated with the associated test results and it was concluded that the three-dimensional models were accurate and could be adopted to accurately predict the moment-rotation relationships. Moreover, extensive parametric studies were undertaken. The study mainly focused on the effects of using shear connectors and tensile reinforcing bars on the overall flexural behaviour. It was proposed that composite joints with a large depth of end-plates should be designed to have a full shear connection. Reinforcement ratio was observed to significantly influence the design of these connections. Moreover, in order to avoid non-ductile deformations, ductile shear connectors are required for semi-rigid joints designed as partial shear strength connection.

Ataei and Bradford (2014) simulated a semi rigid flush endplate joint in hogging bending moment. They considered a partial shear connection. They validated the finite element model with the experimental data to perform parametric studies. They suggested that the modelling technique could be easily applied to model the connection and resulted in quick and reliable solutions. Moreover, Ataei *et al.* (2016b) performed rigorous finite element analysis of high strength steel semi rigid composite joints. The study explored the structural behaviour of an innovative beam-to-column semi rigid connection with deconstructable post-installed friction grip shear connectors. Finite element models were validated with a previous study by Ataei *et al.* (2015) and used to perform an extensive parametric study on parameters like reinforcement ratio, concrete slab thickness, degree of shear connection, number of bolted shear connectors, flush end plates thicknesses, various sizes of steel beam and different sizes of bolt. The finite element model accurately predicted the behaviour of the composite joint.

Hassan *et al.* (2014) prepared three-dimensional finite element models to investigate the behaviour of beam-to-CFST column flush end plate connections. The finite element simulations are verified with test data. Parametric studies of different types of blind bolts and different types of binding bars are performed. Mesh sensitivity analysis was conducted to explore element sensitivity. It was concluded that C3D8R elements were more sensitive in modelling of steel beam to CFST column joints and C3D8I, C3D20 and C3D20R gave more precise results as compared with C3D8R. However, the computational time was much higher for later as compared to C3D8R. However, to optimize the computational time and obtain accurate results, C3D8I elements were recommended. The finite element model is presented in Fig. 2.11. The modelling of hollow and Ajax blind bolts was also considered in this study and a simplified model was presented. It was observed that the load capacity of hollow bolts is greater than AJAX one side bolts. Steel tube separation was observed when using AJAX blind bolts. However, binding bars can be used to minimize this effect. The use of binding bars increases the load capacity of the joint but decreases the outward deformation of CFST column.

Kataoka and EI Debs (2014) performed parametric studies on composite beam-to-column joints. Parameters considered in the analysis involved diameter of blind bolt, reinforcement ratio and spacing of shear connector. Computational results proposed that all parameters were far associated with each other such as a single variation did not seem to have a noteworthy effect on the global performance of the connection.

Thai and Uy (2015) developed a comprehensive three-dimensional finite element model to explore the performance of blind endplate connection under monotonic loading. All components of the connection such as composite columns, composite beam, composite slab, reinforcement, shear stud, endplate was separately modelled using shell, solid and truss elements. The numerical model considered nonlinearity of material properties and geometrical configurations. In addition, analytical models were proposed on the basis of the component method. Through the comparison between both models and experimental outcomes, they found numerical models had a promising agreement with reality while analytical methodology underestimated ultimate moment resistance to some extent. Parametric studies indicated that the behaviour of composite joints was mainly dominated by concrete slabs and reinforcements.

2.14. Prediction of moment-rotation relationship

In order to determine the behaviour of a joint in global analysis of a structure, it is mandatory to consider the mathematical representation of the moment rotation curve. This can be achieved by using various relationships and precision levels. Fig. 2.12 represents different mathematical models to represent moment rotation relationship which are linear, bi-linear, tri-linear and non-linear (Diaz *et al*. 2011). The curve can either be represented using parameters like stiffness that have a physical meaning or by regression analysis which is based on no physical meaning. These types of formulations are termed as "curve fitting formulations". A brief review of moment rotation models by various researchers is presented as follows.

Yee and Melchers (1986) proposed a mathematical model to predict the moment-rotation behaviour of bolted-extended endplate connections. The model was based on the deformation characteristics of the connection elements and the possible failure modes. The moment-rotation curve consisted of four parameters which were related to the initial stiffness, strain-hardening stiffness and moment capacity. The initial stiffness and moment capacity can be calculated using component method, whereas the strain-hardening stiffness was observed to be associated with the initial stiffness. The proposed moment-rotation curve demonstrated a good agreement when validated with the existing test results.

Lee and Moon (2002) proposed a two-parameter log model to demonstrate the moment-rotation behaviour of semi-rigid joints. The proposed model could be applied to almost all connection types to accurately predict the moment rotation behaviour by changing shape parameters α and η. Since the shape parameters had no physical meaning, a semi-analytical approach was derived using statistical regression analysis which focused on the initial stiffness and plastic stiffness for both double web angle and top and seat connection respectively. The analytical model was used to predict the response of semi-rigid joints with angles and validated with the experimental results. The proposed approach demonstrated to estimate the structural behaviour of the joints with high accuracy and can be effectively utilized to perform frame analysis.

Abolmaali *et al*. (2005) developed an approach to effectively evaluate the moment-rotation response of flush end-plate joints. Finite element models were developed considering nonlinearity of material and geometrical properties. A range of test results from available literatures were accumulated to compare with the numerical models. The moment-rotation data were developed and curve fitted to Ramberg-Osgood and Three-Parameter Power model to calculate relevant variables. After that, regression analysis was applied to analyze the structural behaviour. The results demosntrated that both equations were able to accurately estimate the moment rotation model. However, the Three-Parameter Power model was found to be more progressive as compared to the other approach.

Diaz *et al.* (2011) reviewed three major areas of steel joint research which are methods of analysis of semi-rigid joints, prediction methods for the mechanical behaviour of joints and mathematical representation of the moment rotation models. Analytical, empirical, numerical, experimental and mechanical models are used to determine the mechanical behaviour of a joint. The mechanical behaviour of a joint must be modelled when semi-rigid frames are analyzed. Any moment rotation curve can be used, depending on the type of structural analysis required. Mathematical representation of different types of moment rotation curves were presented by the authors. A brief discussion on advantages, disadvantages and characteristics of each model were overviewed.

2.15. Frame analysis

The behaviour of a joint is represented by its moment-rotation behaviour that depends on three key properties which are initial rotational stiffness, moment resistance and rotational capacity. These properties can be predicted using EN 1993-1-8 (2010) (for bare steel joint) and EN 1994-1-1 (2004) (for composite joint). However, characteristics of various components involved make it difficult to predict the structural performance reasonably well. Therefore, it requires re-planning of the structure on the basis of sub-model as well as global frame analysis.

Considerable progress has been made in recent years in order to develop an efficient and reliable analytical method to calculate the moment capacity and rotational stiffness of composite connections. Many models have been presented and mostly comprise of the parameters depending on the stiffness, strength or ductility for a given connection and shape parameters treated as a curve fitting parameter (Lee and Moon, 2001). Therefore, the expressions prove to be accurate only for the particular type and limited range of data used in the regression analysis. A brief overview of the literature associated with frame analysis is presented as follows.

Li *et al*. (1996), experimentally investigated a pair of full-scale, two span, one-bay, two storey composite frames and compared the results with tests on isolated composite connections. The study explored the influence of semi-rigid and partial strength connections on the pattern of moment in a composite frame at various levels of loading until failure was achieved. It also presented complete test histories to be used for the validation of analytical and numerical model. The failure modes reported were local failure of columns, local buckling of steel beam compression flanges next to the columns and crushing of concrete slab adjacent to columns when significant un-symmetrical moments were applied.

Wang and Li (2017a) experimental study is based on two full-scale semi-rigid composite frames. Each is a one-and-half storey frame of two bays, which were designed based on international standards (BS5950 1990) and (GB50017 2003). The steel beams were connected to the flanges of H-shaped column by means of flush end plates and two rows of M22 Grade 10.9 bolts. A concrete slab of 140 mm thickness was supported by the longitudinally placed steel sheets with shear connecters welded-through to provide a composite action. Both frames were subjected to vertical static loads. The static loading provided simple experimental procedures, where the first frame was subjected to symmetrical downward loads, while the other frame was subjected to non-symmetrical downward loads. Results obtained from experiments indicated no sign of shear connector's failure, as there was very small shear slip, therefore proving that composite steel-concrete beams work even in full shear connection. Both specimens showed failure patterns of the cracks in the slabs. This static loading provided significant results, while maintain a relatively simple procedure in terms of loading and monitoring.

Lam *et al*. (2008) presented an overview of the research into seismic activity in Australia and ground motion modeling that gave rise to a new response spectrum model for Australia which is featured in the new standard for seismic actions. The study included the prediction of displacement demand for intraplate regions of small to moderate magnitude of earthquakes. A practical representation of the response spectrum model was also presented. The utilization of the response spectrum model for site-specific applications which permit the effects of soil resonance have been demonstrated by the case-study of a lifeline facility in Australia.

Wang *et al*. (2009c) reported the mechanism of composite frames consisting of steel beams connected to CFST columns. A comprehensive analysis was performed that considered axial stress distribution in concrete, stress in concrete along the column height and the connection zone. Numerical models were developed and validated with the experimental data in terms of reliability and flexibility. The authors described the five different stages corresponding to the incremental lateral load (P) versus lateral displacement (Δ) curves of a typical CFST frame which are presented in Fig. 2.13. Parametric studies were performed that investigated the effect of various axial load levels and stiffness ratio of beam-to-column joints. Simplified and efficient hysteric lateral load versus lateral displacement models were proposed that can be applied to the dynamic analysis of similar composite frames.

Nie *et al*. (2011) established finite element models to inspect the global behaviour of frames in which fibered beam elements were used to replicate steel beams and columns whilst concrete slabs were modelled with layered shell elements and beam-to-column joints were modelled with spring elements respectively. The results from FEM were validated with the experimental results. The suggested model demonstrated that the slab space composite effect and beam-column semi-rigidity were the two critical parameters that significantly affected the behaviour of the frame. It concluded that the finite element method included combined elastic-plastic analysis exhibited high precision. This model can be useful to a wide variety of frames to be analysed in construction practice.

Pokharel *et al.* (2014) reported a displacement-based assessment of moment resisting frames with blind bolted connections. The framing system included CFST columns, universal beam sections composite with concrete slab and blind bolted connections. A force-based design approach was used that considered life safety in a 500 years design period earthquake event. A capacity spectrum approach was used to evaluate the actual performance at different earthquake levels such as 500 year and 2500-years return period. Non-linear push over analysis were also performed and two different methods were presented to improve ductility of the connections and to improve the over- all displacement capacity of the buildings.

Thai *et al*. (2016a) presented an accurate numerical model to evaluate the system reliability of steel frames with semi-rigid joints. Due to computational efficiency of the plastic hinge model, it was used to predict the ultimate strength of the frame. The non-linear behaviour of the frame was captured using "Three parameter power model". Moreover, Monte Carlo simulation technique was used to determine the possibility of failure and system reliability index. Two frames were exposed to combined gravity and wind loads. The reliability of the system was examined in strength limit state and serviceability limit state based on random variables including random loadings, material and geometrical properties and semi-rigid connections. The study concluded that the semi-rigid connections significantly influenced the reliability of the frames.

Yao *et al*. (2009) proposed a practical design method for a typical five storey building frame that comprised of composite columns, beams and semi rigid connections. The effect of soil type, column base fixity and rigidity of the connection were focused. The main objective of the study was to explore probability of the frame in terms of strength and drift demands when exposed to lateral wind and earthquake actions for low to medium rise buildings in Australia.

Wang *et al*. (2018a) explored the behaviour of demountable composite beam-to-column joints using semi-rigid connections. The authors presented a new approach for the development of moment rotation relationship of the joint that was verified with the test results from another study by Wang *et al*. (2018b). The proposed model was able to predict the moment-rotation relationship accurately. The prediction was then applied to the frame analysis and the performance of demountable composite frames under gravity and lateral loads was explored. This method was used in combination with the method specified in EN 1993-1-8 (2010) and EN 1994-1-1 (2004) to calculate the moment capacity of the blind bolted end-plate composite joint considered in this study.

2.16. Present research and the research gaps

As discussed above, concrete filled steel tubular (CFST) columns offer significant benefits in multi-storey buildings together with the use of innovative blind bolting technique for beam to CFST column connections. However, due to lack of knowledge and understanding of the behaviour of these connections under static and cyclic loads, availability of reliable and appropriate design guidelines has been a problem for structural engineers. Overall, a detailed investigation into the structural behaviour of composite beam-to-column flush end plate connections with blind bolts based on experimental and numerical studies is desirable. This thesis therefore addresses this problem based on full scale tests of two sub-assemblies of composite beam-to-column connections using blind bolts under static and cyclic loading, development of FE models of the tested connections and validation using the load displacement profiles and failure modes, parametric study using the validated FE model to evaluate the effects of a range of important parameters and finally in-plane structural analysis of blind bolted composite frames with semi-rigid connections to investigate the flexural response of these frames under gravity and lateral loads of wind and earthquake actions in Australia.

This study was a part of an on-going research on the composite joints previously tested by Mirza and Uy (2011). However, the beam-to-column connection proposed in this study was unique and different from the connection tested by Mirza and Uy (2011) as it included equal angle plates on all four sides of the CFST column. This was equivalent to an increase in the thickness of the CFST column which was thought to enhance the strength of the connection. The addition of equal angles between flush endplates and CFST column made it different from the typical beam-to-column connections studied in the past as they have not been used in any study on these connections previously. Moreover, the composite slab and steel beams were attached using a full shear connection unlike the studies on similar connections by Mirza and Uy (2011) that used a partial shear connection. Furthermore, frame analysis for this type of connection has not been performed earlier. Thus, the beam-to-column connection studied in this research is different from the connections developed in previous researches.

Accurate numerical models were developed using finite element method (FEM) that replicated the experimental results efficiently. The FEM was thought to be extremely useful as it saved a lot of time and money that would otherwise be spent on further investigations, if experimental work was to be performed. Little research has focused to investigate the performance of this type of construction in a frame environment, particularly when it comes to theoretical investigation by an accurate and reliable analytical model. Design engineers avoid detailed modelling of composite joints in frames due to complicated geometrical modelling, deficient guidelines, high computational cost and complex interaction behaviour between joints and other structural components (Jeyarajan and Liew, 2016). The perceived complexity and accuracy of the existing techniques highlights that there is a considerable scope for improvement in this area. Consequently, a lack of reliable information on the moment rotation characteristics of the connection is a hurdle in the widespread application of blind bolted composite frames in engineering practice. Therefore, the behaviour of these connections was further explored in a frame environment. These frames were subjected to lateral loads that replicated a range of typical wind and earthquake actions on low-rise semi continuous composite frames in Australia. Moment rotation models were predicted using the guidelines from the relevant Australian standards and Eurocodes. The predicted moment rotation models were then used to investigate the flexural behaviour of the composite blind bolted frame under strength and serviceability limit state requirements.

The results from this study are expected to be helpful in understanding the complicated behaviour of these composite beam-to-column connections under various loading conditions and also for the design of composite frames developed using these connections in engineering practice.

2.17. Summary of chapter

This chapter presents an understanding of the rich background information on the topic and details of a wide range of associated studies undertaken by other researchers which helps to fill the gaps of missing information. The chapter commences with an introduction, followed by a brief discussion on earthquakes and return period of an earthquake. Subsequently, general information on composite construction, beam to column joints, concrete filled steel tubular columns, end plates, blind bolts, failure modes in a composite construction is presented. Finally, research summarizes extensive experimental studies and analytical studies related to the topic of this research. Additionally, analytical models that predict the moment-rotation relationship of beam-to-column joints theoretically are outlined. Eventually, frame analysis is introduced to provide an insight into the global behaviour of composite frames.

Fig. 2.1 – Newcastle Earthquake 28th Dec 1989 (abc.net.com)

Fig. 2.2 – A building in Christchurch Earthquake on 22nd Feb, 2011 (Britannica.com)

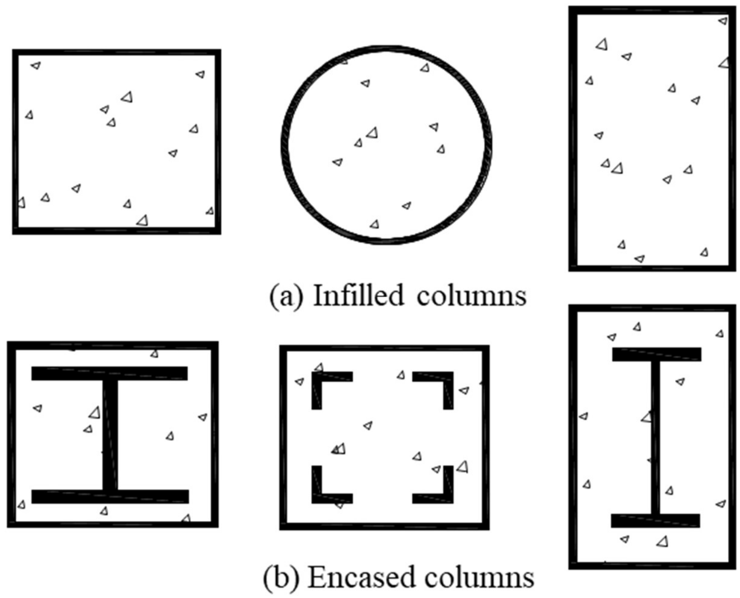

Fig. 2.3 – Types of Composite Columns

(a) In-Filled Columns, (b) Encased Columns

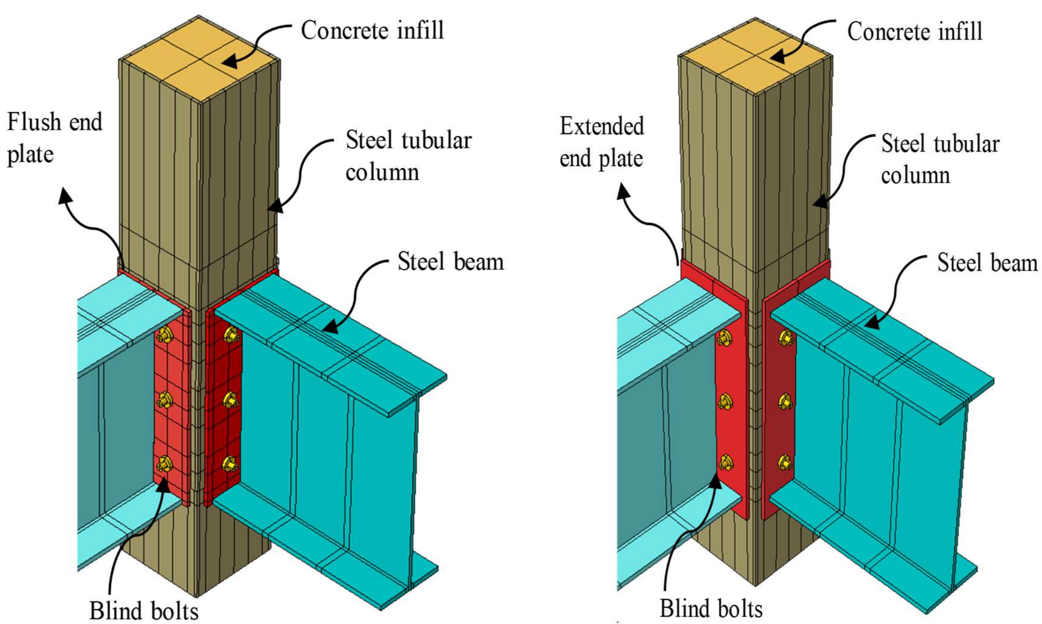

Fig. 2.4 – Beam-to-column joint with flush and extended end plates

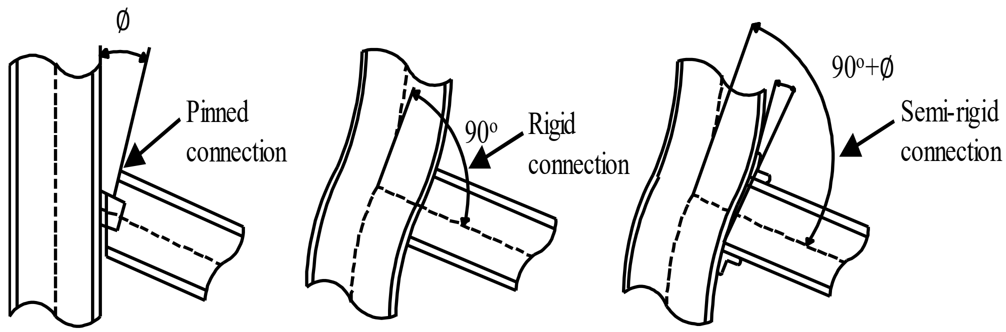

Fig. 2.5 – Classification of connections

(Diaz *et al*. 2011a)

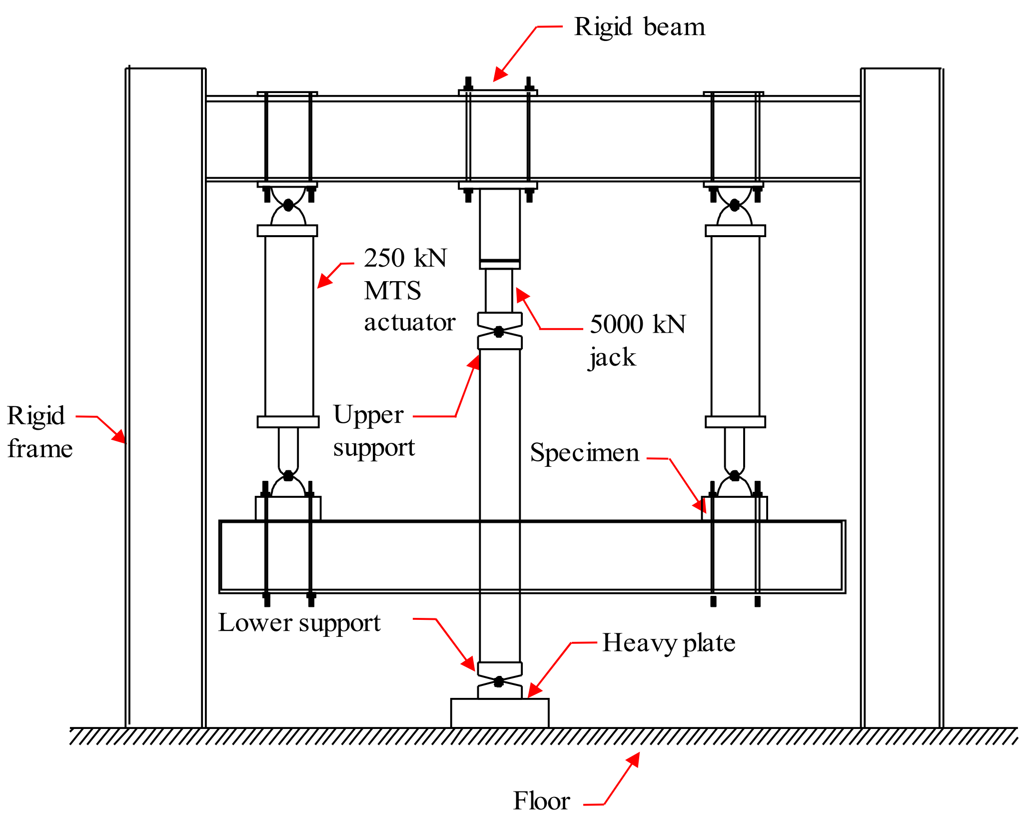

Fig. 2.6 – Experimental set-up of a composite joint subjected to static loading

(Wang *et al.* 2009a)

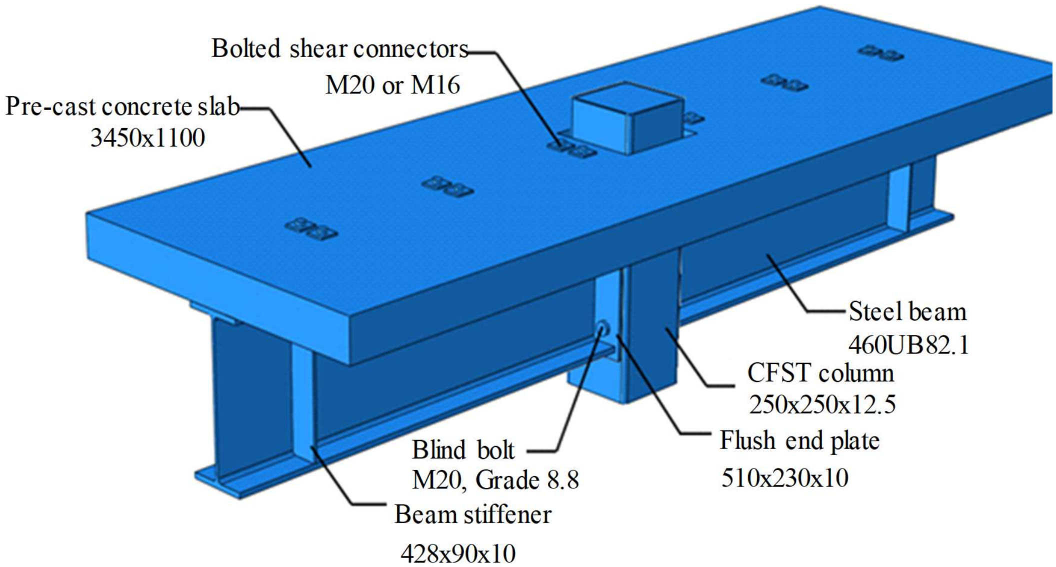

(a) General description

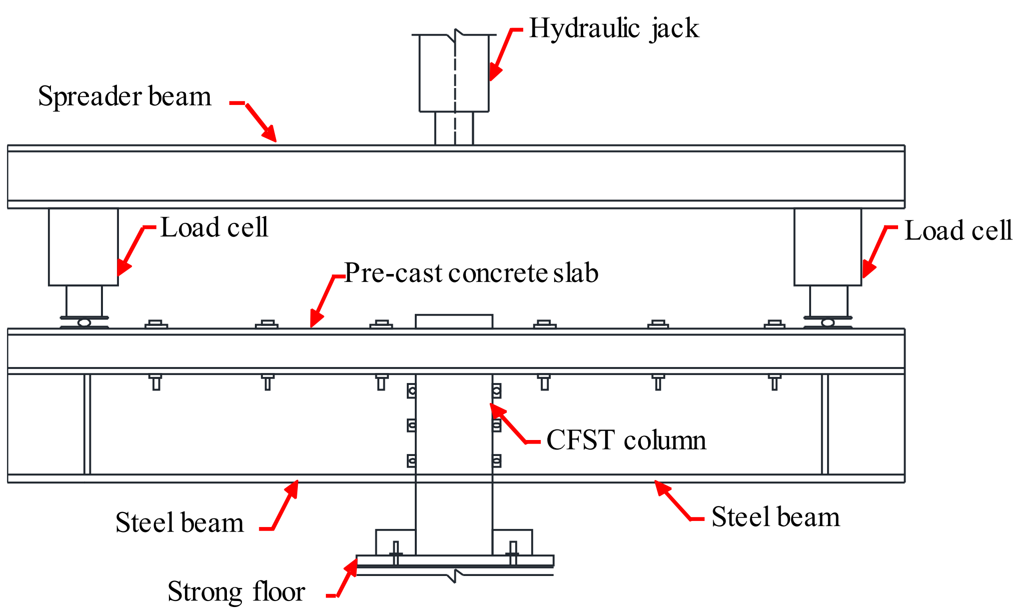

(b) Experimental set up

Fig. 2.7 – Descrition and test set-up of a blind bolted end plate CFST joint

(Ataei *et al*. 2016)

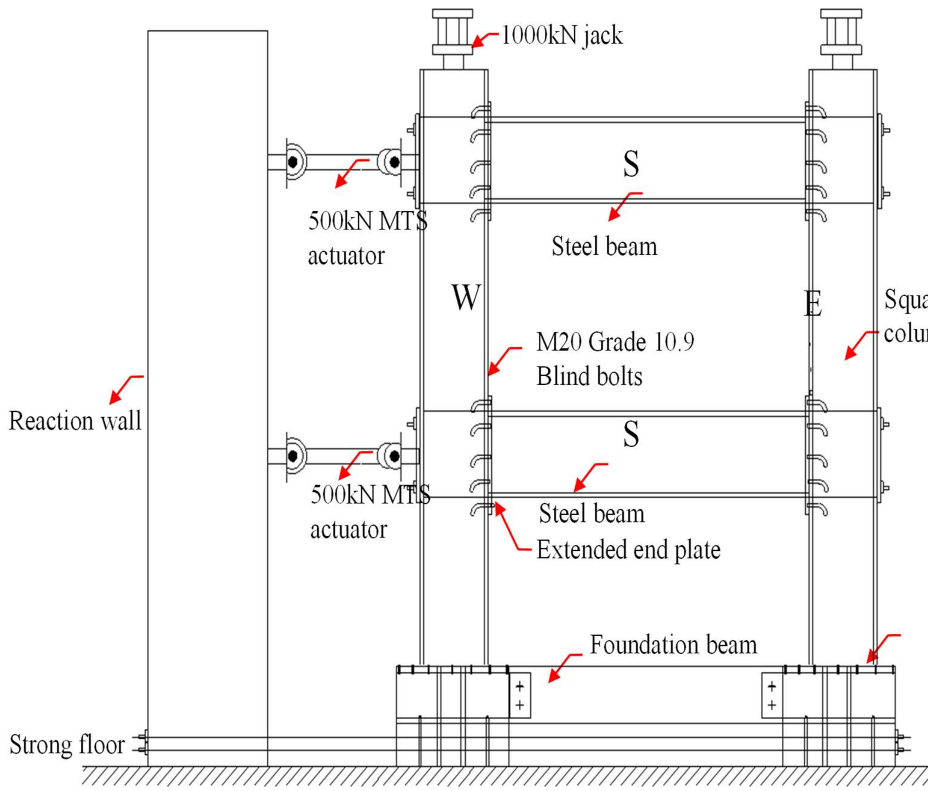

Fig. 2.8 – Testing of a blind bolted end plate CFST frame

(Wang *et al.* 2017)

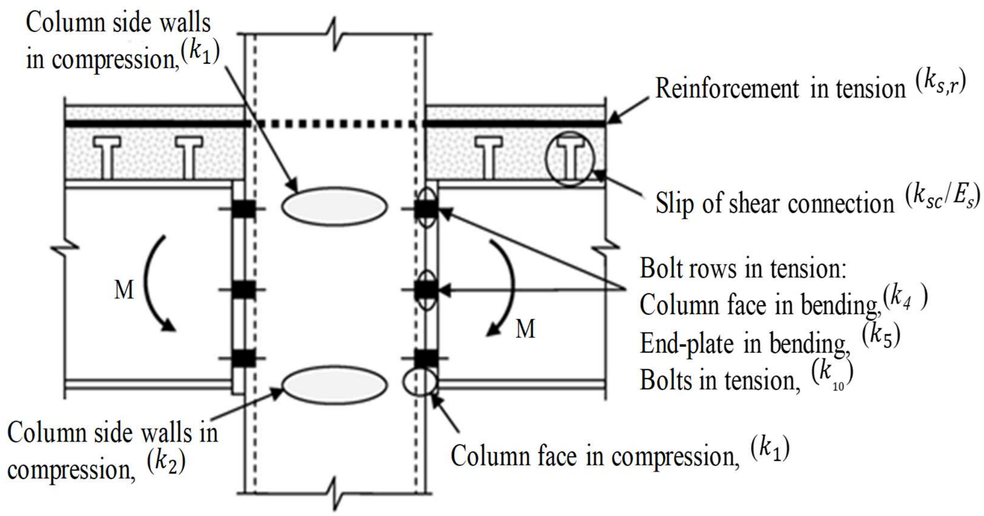

Fig. 2.9 – Identification of components of the composite joint

(Thai and Uy, 2016b)

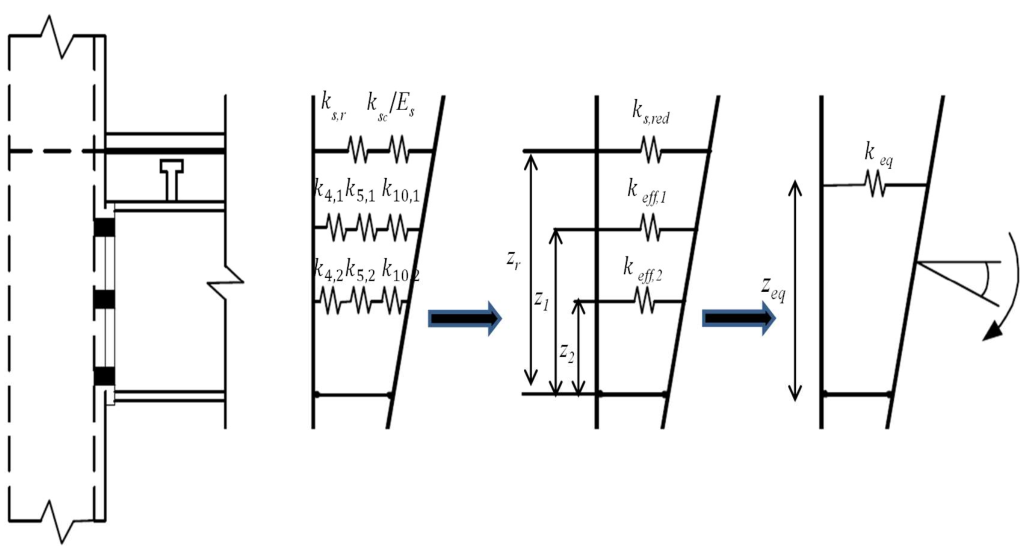

Fig. 2.10 – Spring model for joints with CFST columns

(Thai and Uy, 2016b)

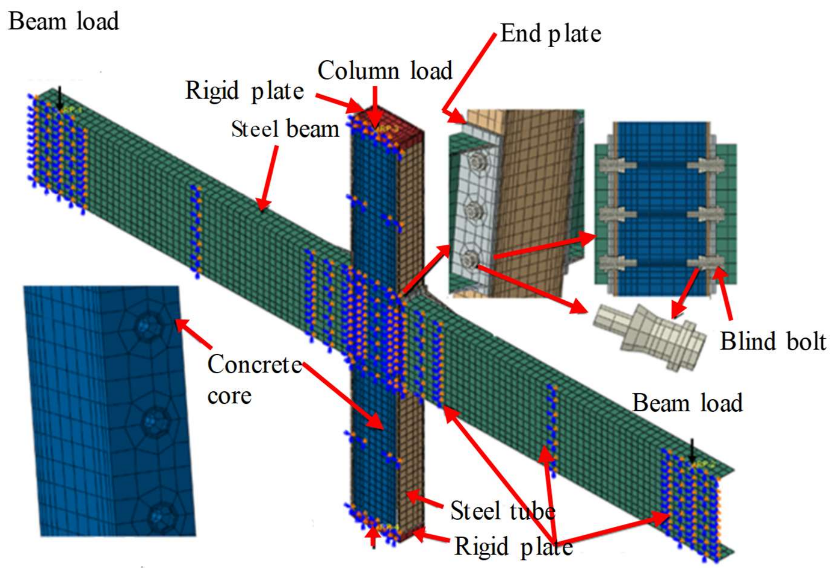

Fig. 2.11 – Finite element model of blind bolted endplate connection to CFST column in bending

(Hassan *et al*. 2014)

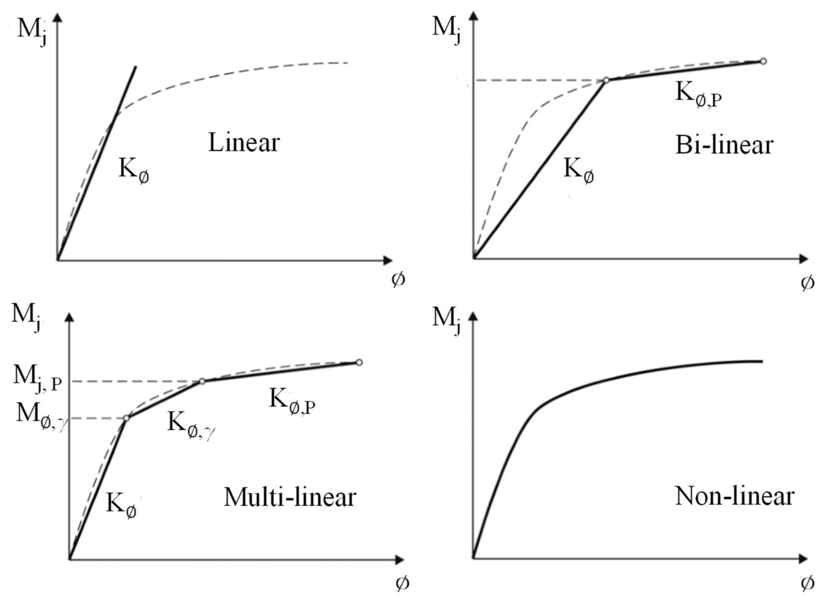

Fig. 2.12 – Mathematical representation of moment rotation model

(Diaz *et al*. 2011)

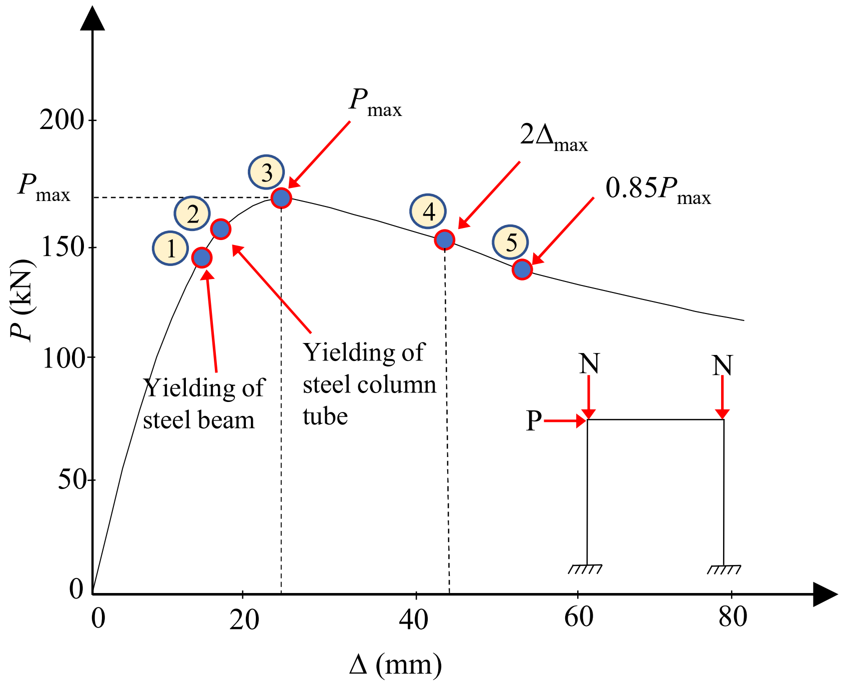

Fig. 2.13 – Lateral load versus displacement curves of a typical composite frame (Wang *et al.* 2009)

CHAPTER 3

EXPERIMENTAL BEHAVIOUR OF COMPOSITE BEAM-TO-COLUMN FLUSH ENDPLATE JOINTS

3.1. Introduction

The need for further study on the behaviour of beam-to-column flush endplate joints using the innovative blind bolts has been identified from the background literature presented in Chapter 2. In order to achieve the research objectives presented in Chapter 1, an experimental programme was conducted that consisted of two specimens under hogging moment designed with full shear connection. Both specimens were fabricated in a cruciform arrangement that represented the internal region of a composite frame. The purpose of this study was to investigate the load-displacement behaviour of these connections under static as well as cyclic loading.

In the beginning of this chapter, the experimental programme is outlined which includes the description of the test specimen, specimen fabrication, material properties, instrumentation, test set up and loading procedure. Secondly, the load-displacement relationships of the specimens, structural response, failure modes, ultimate capacity of the joint and load versus strain response of reinforcement and steel beam web and flanges are discussed in detail. Finally, a summary of the work presented in this chapter is outlined at the end.

3.2. Design of beam-to-column joints

3.2.1. General description

The experiments were based on an economical design of two geometrically identical specimens, Specimen 1 (S-1) and specimen 2 (S-2) with full shear connection, tested under different loading conditions. S-1 is tested under static loading whilst S-2 is tested under cyclic loading conditions. Each specimen consisted of four 610UB101 Grade 300 universal steel beams connected to a 300x300x10 mm Grade 350 square hollow section (SHS) column in a cruciform arrangement as shown in Fig. 3.1. A 1600 mm wide, 3868 mm long and 120 mm deep reinforced concrete slab was connected to the four universal beams by means of 16 headed stud shear connectors. The testing rig at "The Heavy Structures Laboratory" at UNSW could not accommodate a slab with width greater than 1600 mm. Therefore, the width of the concrete slab was determined as 1600 mm due to the space limitations of the yellow testing frame. The geometrical dimensions of all components of the specimen are presented in Table 3.1. Each specimen consisted of the concrete filled steel tubular (CFST) column connected to the steel beams through the innovative blind-bolting technique, where a total of 24 blind bolts were used in each specimen. 150x150x12 mm equal angles were welded to the steel tubular column on each side as illustrated in Fig. 3.2. The equal angles were placed on the sides of the CFST column with the help of an extremely simple welding procedure which was only meant to hold the equal angles in position so that they could be easily fixed on the marked position with the help of blind bolts. Therefore, these welds were not at all complicated and did not play any role in the structural behaviour of the beam-to-column joint. Infact, the endplate and equal angles were connected to the CFST column with the help of blind bolts. Six shear studs were placed on each of the primary beams placed at a distance of 200 mm away from the steel tubular column at a spacing of 300 mm. On the secondary beams, two shear studs were placed at a distance of 200 mm away from the steel tubular column with a spacing of 200 mm. Endplates were welded to the steel beams and attached on all four sides of the CFST column with the help of blind bolts. The detailed dimensions of flush endplates are provided in Fig. 3.1(d). N12 steel bars were used for tensile reinforcement of the slab. Profiled steel sheeting of 1 mm thickness was used for the concrete decking.

The sub-assemblies represented the internal hogging moment regions of a typical composite frame. Hogging moment generally occurs in composite structures. The beam represents a part of a continuous frame which implies that there will be hogging moment at the ends of the beam and sagging moments in the middle. For a composite frame exposed to uniformly distributed loads and 9000 mm beam lengths, the hogging moment region took up around 15%-20% of the whole length. And thus, a beam length of 1695 mm in this study was feasible for both specimens under hogging moments. The selected configuration was designed to provide adequate capacity, improve the strength and stiffness of the beam-to-column joint as compared to previous studies and to eliminate the failure of the connection as discussed in Chapter 1.

3.2.2. Specimen fabrication

The specimen preparation is illustrated in Fig. 3.3. The specimens were fabricated in two parts starting from steel components assembling to concrete casting. Firstly, holes were drilled in each endplate to accommodate the blind bolts. The endplates were then welded to the steel beams. Equal angles were welded to the steel tubular column on all sides. The universal steel beams were then welded to the 12 mm thick flush end-plates and bolted to the square hollow section (SHS) column by means of six M20 (Grade 8.8) blind bolts on each side. 10 mm thick fillet welds were used between the steel beam and the flush end-plates. According to the recommendations of bolt manual, a torque of 370 Nm was adopted for tightening of the blind bolts.

Plywood formwork was constructed for both the concrete slab and the profiled steel sheeting as shown in Fig 3.3(a). The steel decking was then cut and positioned in formwork as shown in Fig 3.3(b). Temporary formwork was also used for stability of the specimens during pouring of concrete. Each beam accommodated six headed stud shear connectors. According to AS2327.1 (Standards Australia, 2003), the longitudinal spacing of shear connectors shall not be greater than four times the depth of concrete slabs or 600 mm, whichever was the lesser and shall be greater than five times the diameter of the bolt shank. Therefore, the shear connectors were equally spaced in a straight line at 300 c/c on the primary beams. Six shear connectors on the primary beams were considered to be sufficient to provide resistance to the slip between the concrete slab and steel beam that can also be confirmed from the test results. On the other hand, two shear connectors were placed on the secondary beams which were equally spaced at 200 mm c/c. These studs were installed by a qualified stud fabricator using a welding gun directly on to the profiled steel sheeting at marked points on top of the flange of the beam as shown in Fig 3.3 (b). All welded studs were then tested to ensure that the welding process was performed successfully.

Reinforcement mesh was positioned into place and strain gauged prior to the pouring of concrete as shown in Fig 3.3 (c). Eight 12 mm diameter steel rebars were placed in the longitudinal direction for the tensile reinforcement of the slab whereas nineteen 12 mm diameter rebars were placed in the transverse direction. A standard mix of normal weight concrete was ordered from a local supplier with a specified compressive strength of 40 Mpa at 28 days. Finally, pouring of concrete was performed as shown in Fig 3.3 (d). After the surface of fresh concrete had been prepared, the surfaces were covered with jute cloth and cured under wet conditions.

3.3. Material properties

All materials vary significantly in their composition, properties and performance. It is extremely important to have a sound knowledge of the important properties of the materials used in the experiments as failure of these materials in service conditions may result in extensive damage to the structures and human life. Therefore, material properties of all the materials used in the experiments were obtained by carrying out standard tests following guidelines from the relevant Australian standards.

3.3.1. Steel coupon test

Standard tensile tests were conducted to determine the mechanical properties of structural steel material. These tests were performed on coupons cut from the flange and web of the steel beams, endplates, equal angles, blind bolts and reinforcing bars as shown in Figs. 3.4. The procedure for calculating and testing of all steel samples followed the guidelines of AS 1391-2007. The preparation of coupons and testing of steel material is shown in Fig. 3.5 and illustrated in Table 3.2.

All tensile coupons were tested using a computer controlled universal testing machine. The machine had a loading rate of 20 mm/min that was progressed until the failure occurred. Load was applied to the complete length of the coupons that included the grip length and the transition between the gripped and parallel length. The Young's modulus, yield strength, ultimate tensile strength and the percentage elongation rate can be determined from the uniaxial stress-strain tests which are presented in Table 3.3.

3.3.1.1 *Reinforcing steel bars*

The N12 normal ductility reinforcing steel bars with Grade 500 (f_{sy}= 500 Mpa) and a nominal diameter of 12 mm were used as the longitudinal reinforcement in the concrete slabs. These bars were the major structural component that sustained tensile stresses. In order to calculate the mechanical properties, three samples of the reinforcement were cut for the coupon tests which were performed in accordance with AS1302 (1991) as shown in Fig. 3.6. Fig. 3.7 presents the stress-strain relationships of various steel materials obtained from the uniaxial tension tests. It can be observed that the stress-strain curve of the reinforcement exhibited a distinguishable yield plateau. Therefore, the yield stress for these bars was considered as 0.2% of the proof stress.

3.3.1.2 *High strength steel bolts*

The tensile tests on blind bolts were performed in accordance with the Australian Standard AS4291.1 (2000) in order to determine the mechanical properties such as yield stress, tensile strength and the stress-strain relationship as shown in Fig. 3.8. The bolts were machined according to the guidelines in the standards and their cross-section in the middle was reduced. The uniaxial tension test results for M20 grade 8.8 blind bolts are presented in Table 3.3.

3.3.1.3 *Profiled steel sheeting*

The stress-strain relationship of profiled sheeting was difficult to obtain due to their size being too small to be tested in the machine. Therefore, their strength was referred to the study presented by Tao *et al*. (2013) respectively which is summarised in Table 3.3. It was satisfactory to use these results as the thickness of profiled steel sheeting was similar to the study reported herein.

The profile sheeting used in the joint tests did not contribute to the stiffness and moment capacity of the joint as it was discontinuous over the joint and acted as a formwork only. Therefore, it did not have any contribution to the strength of the composite connection.

3.3.1.4 *Flush endplates*

The procedure for the preparation and testing of the mechanical characteristics of flush endplates followed the recommendations from Australian Standard AS1391 (2007). Three coupons each were cut from the flanges and webs of the steel beams. The stress-strain relationship of end plates is presented in Fig. 3.7. The tensile test results for the endplates in terms of yield stress, ultimate tensile strength, percentage elongation and Young's modulus are presented in Table 3.3.

3.3.2. Concrete test

3.3.2.1 *Slump test*

Slump test is a popular test which is performed in the laboratory or the construction site to determine the consistency of freshly prepared concrete. A slump cone was filled with layers of fresh concrete as specified in the Australian Standard AS 1012.3.1 (2014). Immediately after the fresh concrete was prepared, the surface of the mould was properly cleaned and set free from any set concrete. The internal surface was moistened with a damp cloth and placed on a carefully levelled surface. Each layer was properly tamped before the next layer was poured into the slump cone as shown is Fig. 3.9. The mould was lifted carefully and the slump was measured as the difference in the height of the mould and the average height of the top surface. After that, various cylinders were filled with the fresh concrete for performing compressive strength and splitting cylinder test as shown in Fig. 3.10.

3.3.2.2 *Concrete cylinder test*

Standard cylinder compression test was performed to determine the compressive strength of concrete according to AS 1012.9 (Standards Australia, 2014a). As the concrete strength varied with the number of days passed, the tests were conducted at 7, 14, 28 and 42 days to track the changed compressive strength as shown in Fig. 3.11**.** These tests were performed using a 500 kN. Instron testing machine with a loading rate of 365 kN/min. Two samples were tested on each testing day before each test. The key characteristics obtained from the tests are outlined in Table 3.4.

3.3.2.3 *Splitting tensile strength test*

Splitting test which is also known as 'Brazil' test was performed to determine the indirect tensile strength of concrete cylinders according to AS 1012.10 (Standards Australia, 2014b). A concrete cylinder was positioned on a clamp in the testing jig where the central axis of cylinder and that clamp overlapped. After that, the concrete cylinder was placed in the testing machine and compressed until failure which occurred in the form of tension splitting along the longitudinal direction of the cylinders. The results were recorded and presented in Table 3.5. The stress-strain curve for concrete cylinders tested on 28 days was plotted in Fig. 3.12**.** Based on these tests, the average values of compressive strength and indirect tensile strength of concrete at 28 days were 52.8 MPa and 4.6 MPa, respectively.

3.4. Test set-up and loading protocol

3.4.1. Test set-up

Fig. 3.13 shows a general arrangement of the set up in the loading frame. The joint specimens were tested in the Heavy Structure Laboratory at the University of New South Wales. The specimen was positioned in the testing frame and during the whole test a nominal compressive load was applied continuously at the top of the CFST column with the help of a hydraulic jack which was mounted to a rigid beam. The beam ends were supported using a roller and pinned bearing at 1.6 m away from the column surface. A nominal vertical load was applied at the top of CFST column using a hydraulic actuator which was mounted at the top of the testing frame. Moment at the connection can be easily determined by multiplying the lever arm with the reaction force. Two more hydraulic jacks with 500 kN capacity each were used to apply monotonic and cyclic loads at both ends of the beam segments to simulate the hogging moment condition. The vertical loads were applied using displacement control method. The loading position was 1695 mm away from the column center. In order to keep the tip loads vertical to the ground, the surface of support and actuator were lubricated to avoid horizontal reactions.

3.4.2. Specimen loading

3.4.2.1 *Specimen 1, S-1*

At the commencement of the test, a small load in the elastic range of approximately 10-20% of the ultimate load capacity of the specimen was applied. This load was only applied to inspect the test set up, instrumentation and loading system. The specimen was unloaded after all checks were made. After this, the load was progressively increased at a constant rate of 0.3 mm/min on the primary beam ends using the two hydraulic jacks positioned at North and South ends of the specimen until the specimen achieved failure and could not sustain any load further applied on it.

3.4.2.2 *Specimen 2, S-2*

Similar to the static loading test performed on specimen 1, S-1, specimen 2, S-2 was pre-loaded up to 10% of the ultimate capacity to make sure that all the instruments and hydraulic jacks responded well to the logger and also to ensure that all the jacks had the same contact with the concrete slab. The specimen was unloaded and all the readings on the instruments were set back to zero. And finally, the test was started. There was a constant nominal load of 250 kN load on the middle hydraulic jack. This load was only applied to keep the CFST column in place when it is subjected to compression and tension loads during the experiment. Due to the limitations at the laboratory, 250 kN was the maximum magnitude of load that could be applied at the top of CFST column and is equivalent to 2.7% of the column capacity. The vertical load was applied in displacement control mode and the loading rate was set about 0.3 mm/min in the linear elastic range which was later increased to 1 mm/min in the in-elastic range towards the ultimate load. At each load step, a complete set of readings including the hydraulic jack force and reaction due to applied load were continuously fed into the data logger and acquisition system and the readings from LVDTs, strain gauges and inclinometers were recorded.

The cyclic loading protocol proposed by AISC (2005) was adopted for S-2 to explore the hysteretic response of the specimen as shown in Fig. 3.14. Earthquakes are not critical in Australia. Infact, compression is more critical as compared to tension. Therefore, there are no strict requirements regarding earthquake loading. The connections do not have to be considered for moment reversal. This has also been suggested previously by Nethercot and Hensman (1999), Loh (2004) and Wang et al. (2017). Following on the findings from a previous study by Maenpaa (2007) for a 2500-year's return period scenario, only 30% of load reversal occurred in the worst scenario in Australia. Therefore, only 30 % of the load was applied in tension as illustrated in Fig. 3.15.

Deflection was controlled by the magnitude of measured load at the beam ends according to the percentage of load in every cycle as mentioned in the loading protocol. Cyclic loads were applied that imposed the hogging and sagging moment to the joints. The load history consisted of total nine stages with proportional increments of yielding deflection (δy) corresponding to the yielding load 0.8 Pu, where Pu represents the ultimate load. The yielding deflection δy and the ultimate load Pu were determined from the test results of specimen, S-1. Both specimens S-1 and S-2 were loaded up to failure.

3.5. Instrumentation

Various measurement devices were employed to record the relevant parameters that are useful to understand the behaviour of the system. These instruments were strain gauges, LVDT's and inclinometers as shown in Fig. 3.16. The location of these instruments is illustrated in Figs. 3.17 - 3.20.

3.5.1. Strain gauges

In order to depict the strain profile in steel materials, strain gauges were installed on the reinforcement and steel beam web and flanges where high levels of stresses were expected. For the composite joint specimens, a total of twenty-eight strain gauges were used. In general, twelve strain gauges were placed on the reinforcing bars as shown in Fig. 3.17 and eighteen were placed on the web and flanges of the steel beam as shown in Fig. 3.18. Strain gauges were placed mainly on the regions closer to the connection as the regions closer to the supports were thought to be subjected to mostly linearly elastic behaviour as the stress levels were relatively lower as shown in Fig. 3.19.

3.5.2. Linear variable displacement transducers (LVDT)

Each specimen was equipped with eleven linear variable displacement transducers (LVDTs) which were installed at various locations on the specimen. Two LVDTs (LVDT-2 and LVDT-3) were mounted at both ends of the cantilever beams to measure the relative slip between the concrete slab and steel beam. The vertical end deflection of the beam was recorded by LVDT-8 and LVDT-9 as shown in Fig. 3.20. Two LVDT's, by LVDT-5 and LVDT-6 were mounted on endplates to measure the transverse deformation of endplates and the rest were placed at midpoint, quarter span and end of the steel beam to measure total mid-span deflection of the beam.

3.5.3. Inclinometers

Two inclinometers were mounted on the two ends of the steel beam to measure the rotation of the steel beams. Third inclinometer was placed at the center of the web close to the face of the column and fourth one on the column at the center of the face of the column to measure the rotation of the steel column as shown in Fig. 3.20. The layout of instrumentations for both specimens was basically identical.

In order to record the rotation of the joint, the relative horizontal displacement of the end-plate between the point near the top beam flange and the point close to the bottom beam flange could be measured. Though, it was hard to achieve due to limited space. Alternatively, it was determined in terms of the rotation of the beam, which was calculated as the vertical deflection (δ_b) divided by the distance (L_b) from the location of the LVDT to the surface of the end-plate as shown in Eq. (3.1).

$$\varphi_b = \frac{\delta_b}{L_b} \tag{3.1}$$

The supposition is satisfactory since the bottom flanges of steel beams were supposed to remain straight throughout the tests which is also confirmed from the test results as the bending in the steel beam was insignificant to influence the precision of the joint rotation. Furthermore, the calculated rotation could be measured by the inclinometers mounted on the steel beams.

3.6. Experimental results and discussion

3.6.1. General observations

3.6.1.1 *Static loading experiment S-1*

During the experiment, when the load reached 110 kN, a few barely visible cracks started to appear along the side of the slab towards the East of the specimen as shown in Fig. 3.21(a). These cracks were fairly tiny and not remarkable cracks. As the applied load progressed up to 140 kN, fine cracks were observed on the edge of the slab on the West side of the specimen as well. At a loading level of 165 kN, detachment of the profiled steel decking from concrete slab was observed which was specifically prominent on all corners of the slab as shown in Fig. 3.21 (b). At an applied load level of 272 kN, two fairly visible cracks and several small cracks were evident through the width of the slab and much more separation of the bond between the profiled steel decking and slab was observed. Cracking in shear was also observed on both the North and South sides of the specimen. As load kept on increasing gradually, several fine cracks kept on appearing especially around the mid span of the slab and along the edges close to the connection region as shown in Fig. 3.21 (c). Finally, at the load level of 352 kN, remarkable cracking of concrete slab was observed that became the reason for the failure of the specimen as shown in as shown in Fig. 3.21 (d). The load-displacement relationship for S-1 obtained from the experiment is shown in Fig. 3.22.

3.6.1.2 *Cyclic loading experiment S-2*

When the specimen had been placed in the loading frame and all the instruments had been connected, a nominal load of 250 kN was applied to the center of the column of the specimen. This load was 2.5% of the column capacity and was maintained constant throughout the test. Cyclic loading was applied at the two beam ends using two hydraulic actuators of 500 kN capacity each in compression and 250 kN capacity each in tension. Extremely fine cracks began to appear across the width of the slab around 104 kN in the fourteenth cycle as shown in Fig. 3.23 (a). The debonding between metal decking and concrete slab was quite evident as shown in Fig. 3.23 (b). The cracks started to become more prominent and widespread across the slab in the area close to the connection region after 200 kN in the twentieth cycle. The number of cracks kept on increasing with the increase in applied load as shown in Fig. 3.23 (c).

After 80% of the cyclic load in compression had been applied, the specimen was loaded monotonically up to failure in compression. The value of ultimate load was 352 kN. Finally, there was a huge noise due to cracking of the concrete slab and a sudden drop of load at 352 kN indicating failure of the specimen as shown in Fig. 3.23 (d). The load displacement relationship for S-2 is presented in Fig. 3.24.

3.6.2. Failure modes

The failure modes for both static and cyclic loading cases were very similar as shown in Figs. 3.25-3.27. The test results in terms of critical parameters such as the ultimate load, maximum displacement, initial rotational stiffness ($S_{j,ini}$) and the ultimate bending moment (M_u) are presented in Table 3.6. The initial stiffness is related to the elastic behaviour of the connection. Therefore, its value was determined by using a tangent to the Moment-rotation curve at the very initial stage when the curve is fairly linear. The slope of any two values selected in the truly linear range of loading represents the initial stiffness. ie. 10 kN or 20 kN. Moreover, the calculation of initial stiffness using the analytical method is provided in Appendix A of the thesis.

In both cases, cracks initiated around the column surface and propagated towards the edges of the concrete slab following an inclined pattern. The formation of cracks was traced during the loading process. Cracking of the concrete slab occurred prior to the failure of the connection. In S-1 and S-2, approximately 30 mm wide cracks across the mid span were observed from the edge of the column spreading transversely towards the edge of the concrete slab as shown in Fig. 3.25.

The failure of both specimens occurred due to the yielding of reinforcement embedded in the concrete slab. Broken rebars were clearly visible from the wide-open crack for S-2 while S-1 was further knocked down to confirm the failure of rebar which is shown in Fig. 3.26. No failure in blind bolts or beam web or flange was observed. According to the results obtained from LSCT-1 and LSCT-2, no relative slip was detected at the interface between the concrete slab and the steel beam flange. No local buckling of the steel beams was found close to the compressive regions during the experiment.

It was observed that all the composite joints experienced large rotations which satisfied the requirements of ductility design. These rotations occurred due to the noteworthy deflections of the end-plate in tension. The deformation of the top region of endplate at the bolt row close to the concrete slab occurred almost 11 mm on both sides as shown in Fig. 3.27. However, the part of endplate at the bolt row farthest from the concrete slab remained perfectly intact. The measurements from the LVDT's demonstrated that no interface slip occurred between the concrete slab and steel beam. This was expected as both tested joints were designed to have a full shear connection.

3.6.3. Classification of the joints

Moreover, EC3 and EC4 classified the bolted joints by stiffness or strength. A joint should be categorized as semi-rigid if the initial stiffness for an unbracing frame lies between 0.5 EI_b/L_b and k_bEI_b/L_b which is demonstrated by the following Eq. (18).

$$k_{\mathrm{b}} EI_{\mathrm{b}} / L_{\mathrm{b}} \geq S_{\mathrm{j,ini}} \geq 0.5 EI_{\mathrm{b}} / L_{\mathrm{b}} \tag{3.2}$$

where I_b is the second moment of inertia of the steel beam and L_b is the length of the steel beam. L_b is selected as 9000 mm in this study and the value of k_b is 25 for unbracing frames. The contribution of the concrete slab to the second moment of area can be considered by transferring the concrete slab into the steel beam.

The specimen S-1 and S-2 were designed as semi-rigid and full-strength joints. According to Eurocode, EN-1993-1-8 (2010) the joints can be classified by their stiffness or strength. A joint which does not meet the criteria for a rigid joint or nominally pinned joint is classified as a semi-rigid joint. Similarly, a joint can be considered as full-strength if the design moment resistance of that joint is greater than the design plastic moment resistance of a beam. Also, if the design moment resistance is less than 25% of the design plastic moment resistance, the joint can be regarded as a pinned connection according to the joint classification by strength.

3.6.4. Moment-Rotation relationship

The moment rotation relationship of S-1 and S-2 is presented in Figs. 3.28 and 3.29 respectively. Moments at the connection can be obtained by multiplying the load applied at the support with the lever arm (length of the primary beam from the center of the support to the face of the steel tubular column). The rotation of the connection was obtained from the difference between the rotation of the steel tubular column and the steel beam measured by the corresponding inclinometers. The ultimate rotation capacity of the connection can be defined as the rotation corresponding to the ultimate moment capacity of the connection.

According to EN 1994-1-1, a beam-to-column composite joint should be able to withstand a minimum rotation of 30 mrad that is considered sufficient for the plastic analysis and earthquake design. From the test results, it was observed that both specimens were able to sustain satisfactory deformations at peak load as they failed in a ductile manner.

3.6.5. Strain development

The load versus strain relationship for steel beam and reinforcement are plotted in Figs. 3.30-3.32. The yield strains were calculated using relevant material test data from coupon samples and were plotted against the strain profile curves. The strain gauge readings show that rebars R-3, R-4, R-7, R-8 and R-9 embedded in the concrete exceeded the yield strain obtained from the tensile test results as shown in Fig. 3.30. The load transfer occurred from rebars to the tension part of the column as the yielding of rebars occurred first, followed by cracking of the concrete slab and bending of the endplate. The results from strain gauges R-10, R-11 and R-12 have been omitted because these strain gauges got damaged during the test.

Fig. 3.31(a) shows the top and bottom flange strains of the steel beam for S-1. The top flange displays tension as it shows positive strain values, whereas the bottom flange displays compression as it shows negative strain values. Based on the tensile test results presented in Table 3.3 earlier, it was observed that strains in the top and bottom flange were much lower than the yield strains. Fig. 3.32 shows some portions of the web experiencing tensile strain while some portions experiencing compressive strain. No yielding of steel beam web or flanges occurred as indicated in Figs. 3.31 and 3.32.

Inclined crack patterns in the concrete slab were observed. Liew *et al*. (2000) states that more flexible connections and less effective shear studs lead to almost straight cracks running transversely across the slab, whereas stiffer connections increase the shear lag which is reflected in the inclined pattern of the cracks. No damage appeared on the blind bolts, shear studs or steel column wall.

Further comparisons against the static tests of Mirza and Uy (2011) and Thai *et al.* (2017) were made and comparably excellent agreement in terms of load deflection response as shown in Fig. 3.33. The failure modes were also quite similar as reported by the authors. The test results show considerably improved stiffness and strength as compared to previous studies by Mirza and Uy (2011). No failure of blind bolts or shear studs was observed as in previous studies and also blind bolts performed very well for both loading scenarios which demonstrates improvement in the connection's performance.

3.7. Summary of chapter

This chapter describes the testing of two composite beam-to-column flush endplate joint sub-assemblies in order to investigate their structural performance. Monotonic loading and cyclic loading programme were designed to explore the static and seismic behaviour of beam-to-column joints. Accordingly, some main conclusions are herein drawn.

The cyclic loading had insignificant effects on the stiffness and ultimate load achieved by the composite connection. The repeated loading increased the beam deflection and strains in the reinforcement and steel beam in every upcoming cycle, however it had negligible effects on the performance of the connection.

The semi-rigid beam-to-column bolted joints exhibit high ductility under the monotonic loading where the rotational capacity corresponding to the moment capacity exceeds 30 mrad. Therefore, they are sufficient to be used for the plastic analysis and seismic design. The cyclic loading test further exhibits the good hysteresis performance of the construction.

The shear studs embedded in the concrete slab did not exhibit any degradation in the concrete strength. The reinforcing bars were completely yielded and were able to transfer the tensile forces. The reinforcement had a substantial impact on the behaviour of the connection in terms of stiffness, strength and ductility.

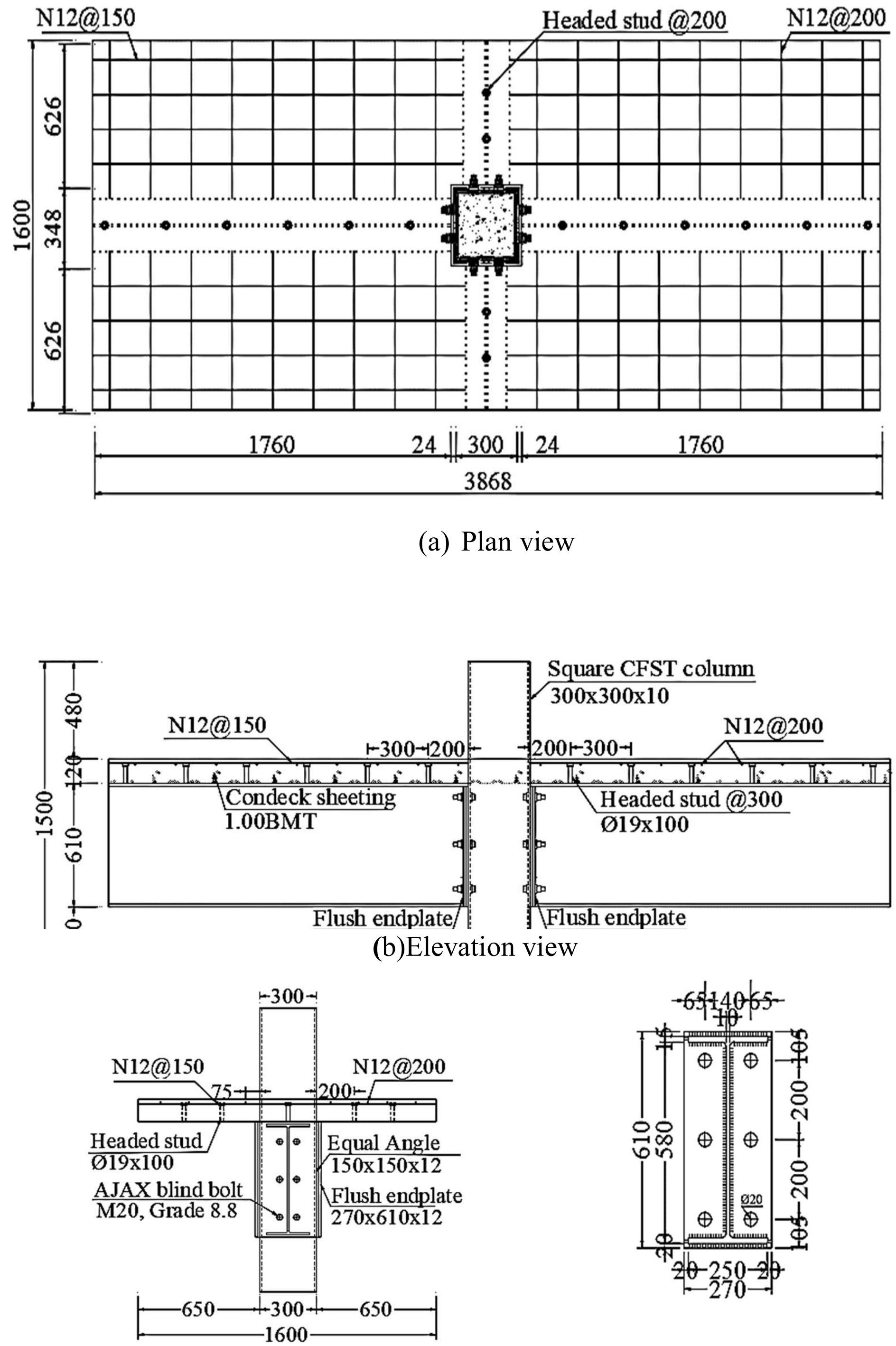

(a) Plan view

(b)Elevation view

(c) Transverse view

(d) Flush endplate

Fig. 3.1 – Detailed geometry of specimen S-1 and S-2

(Units: mm)

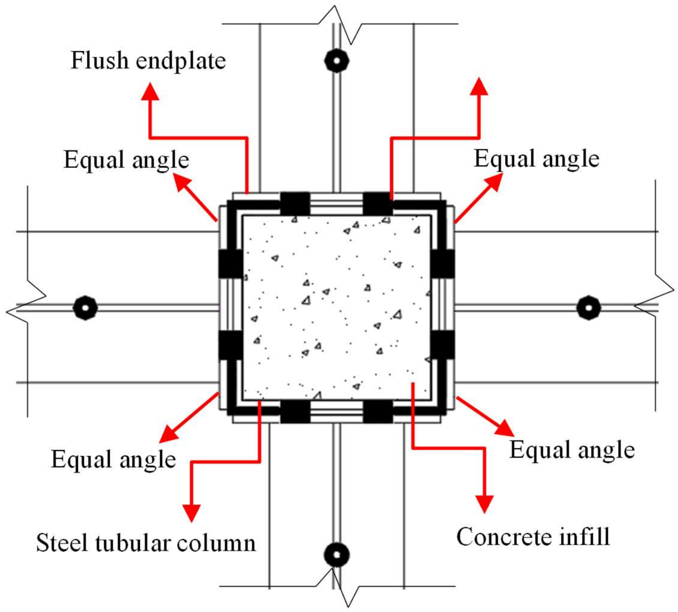

(a) Plan view

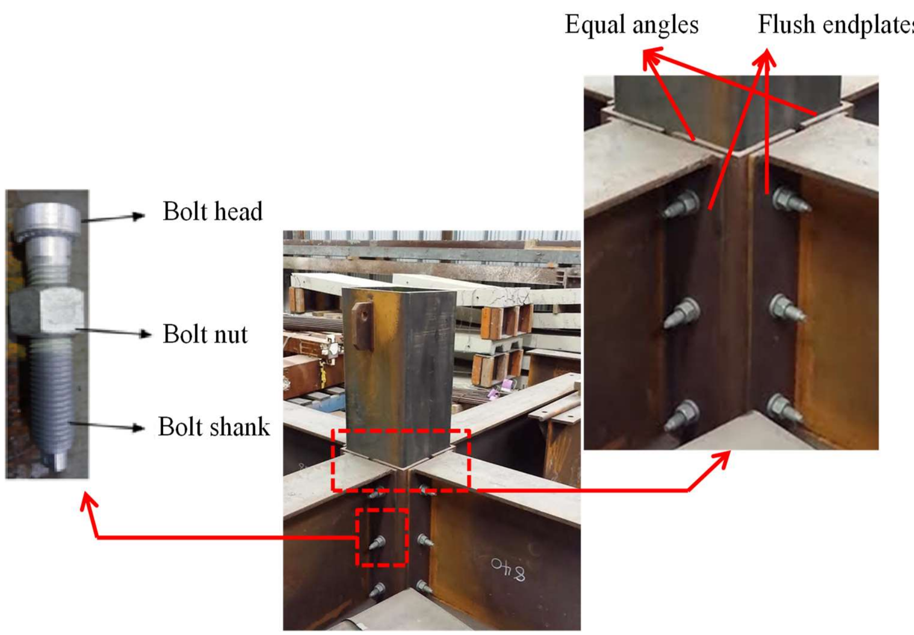

(b) Detailed view

Fig. 3.2 – Proposed composite connection with the addition of equal angle sections

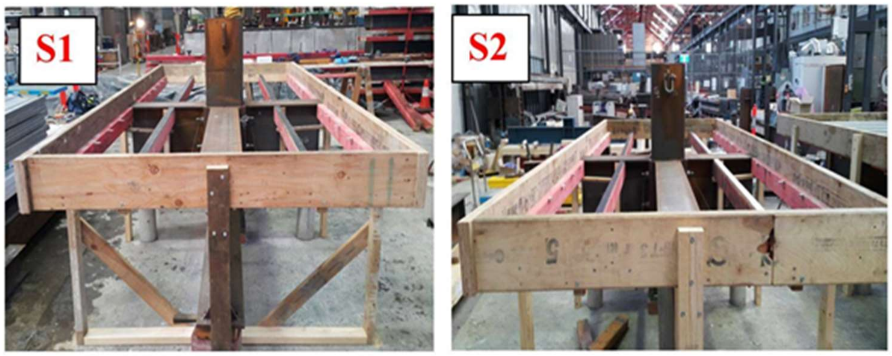

(a) S-1 and S-2 formwork

(b) Welding of shear connectors

(c) Laying of reinforcement mesh

(d) Concrete casting

Fig. 3.3 – Specimen preparation

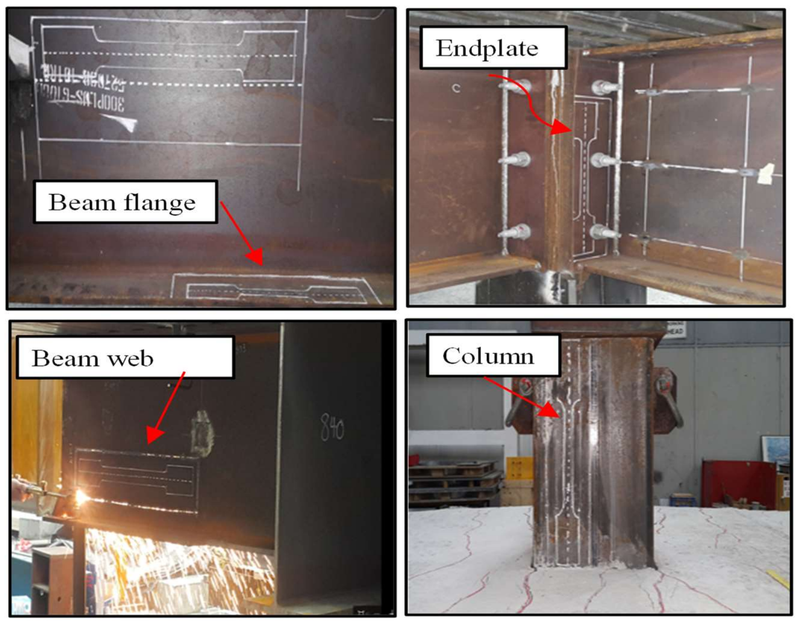

Fig. 3.4 – Drawing for coupons cuttings

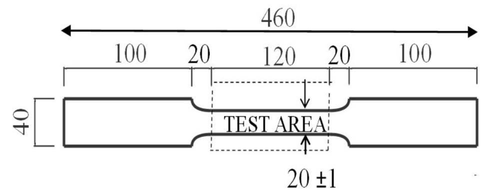

Beam Flanges (F1, F2, F3)

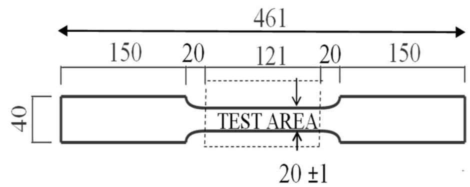

Beam web (W1, W2, W3)

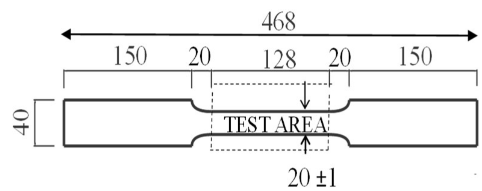

Endplates (EP1, EP2, EP3)

468

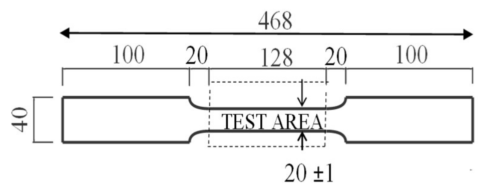

Equal angles (EA1, EA2, EA3, EA4

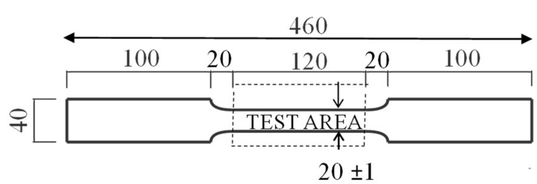

Steel column (C1, C2, C3)

Fig. 3.5 – Material test samples drawings according to AS 1391-2007

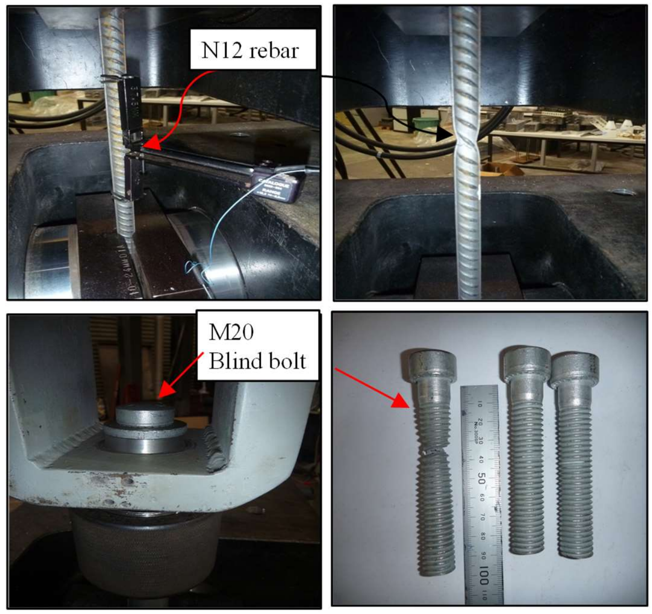

Fig. 3.6 – Tensile testing of reinforcement and blind bolts

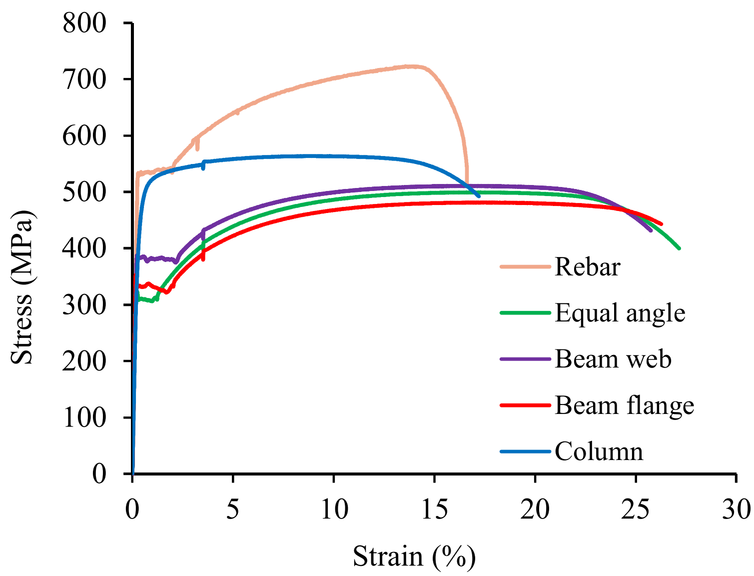

Fig. 3.7 – Stress-strain relationship of various steel materials

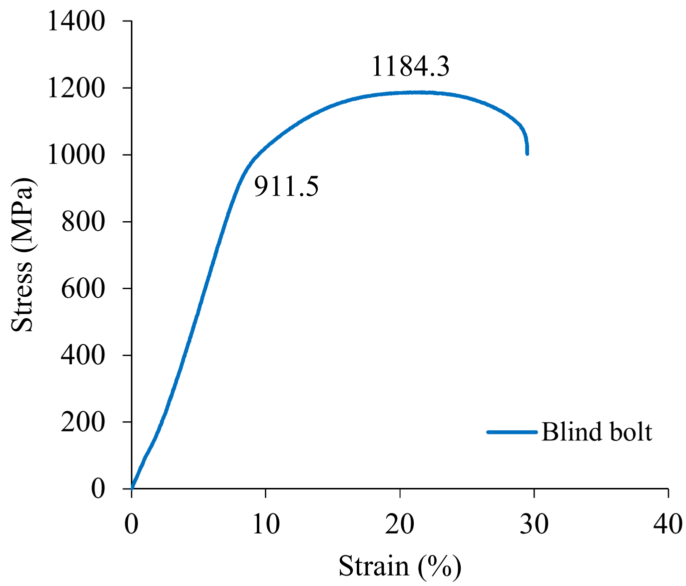

Fig. 3.8 – Stress-strain relationships of blind-bolt

Fig. 3.9 – Slump test

Fig. 3.10 – Concrete cylinders prepared for material tests at different days

Fig. 3.11– Testing of compressive strength test of concrete

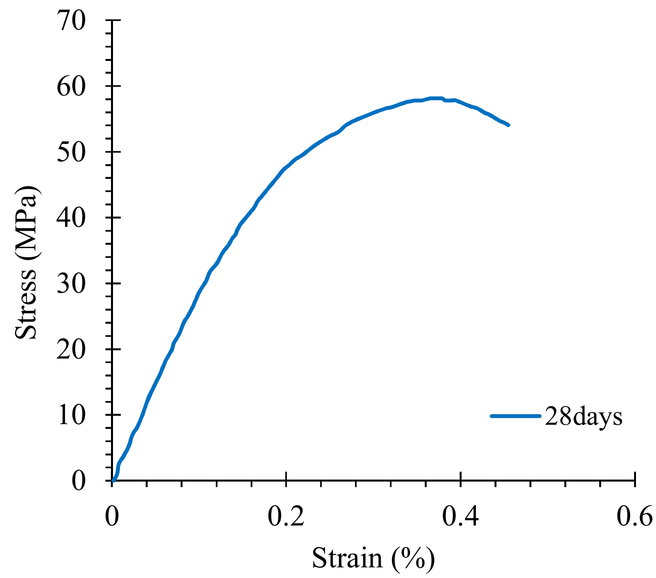

Fig. 3.12 – Stress-strain relationship of concrete at 28 days

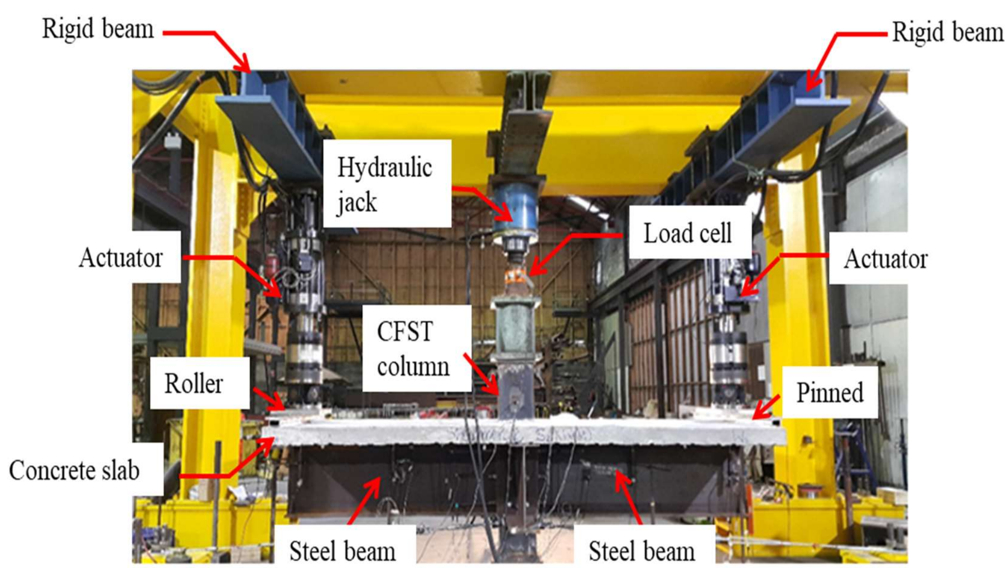

Fig. 3.13 – Schematic of test set-up

(Units: mm)

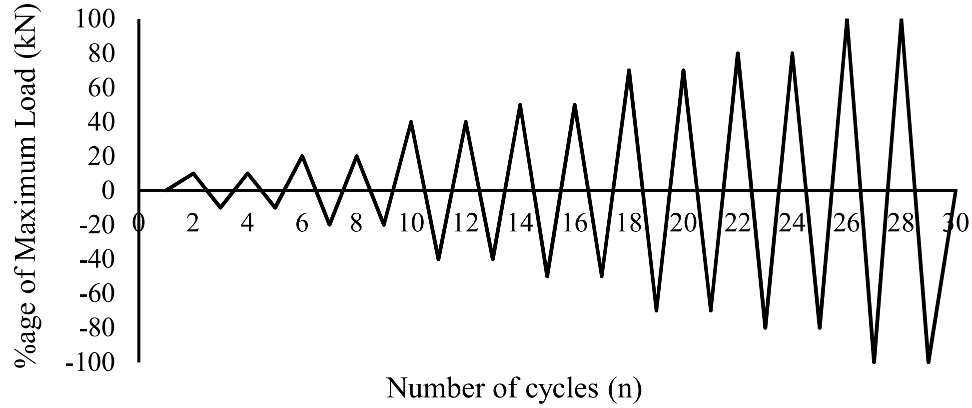

Fig. 3.14 – Cyclic loading protocol

(AISC, 2005)

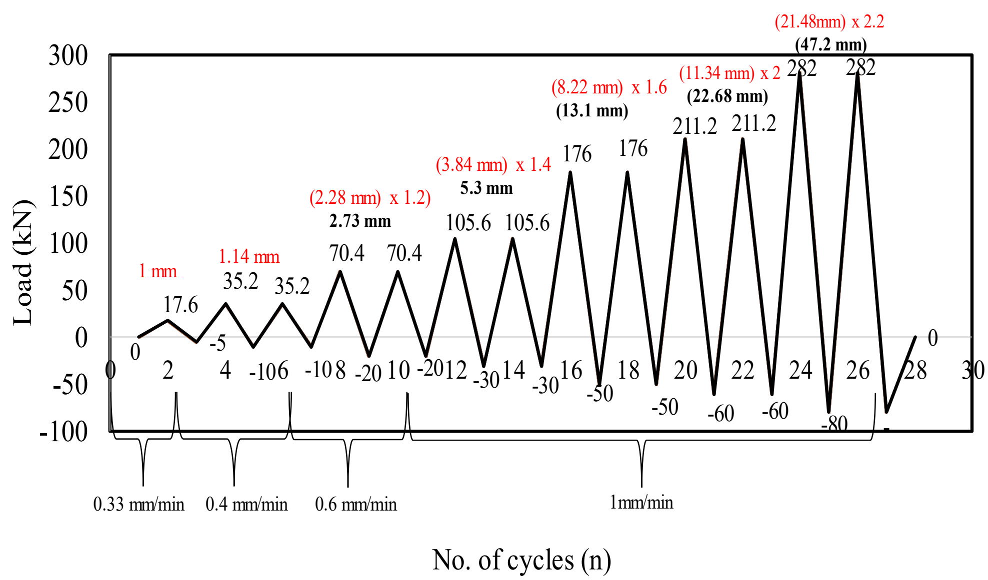

Fig. 3.15 – Planned loading protocol for S-2 according to AISC (2005)

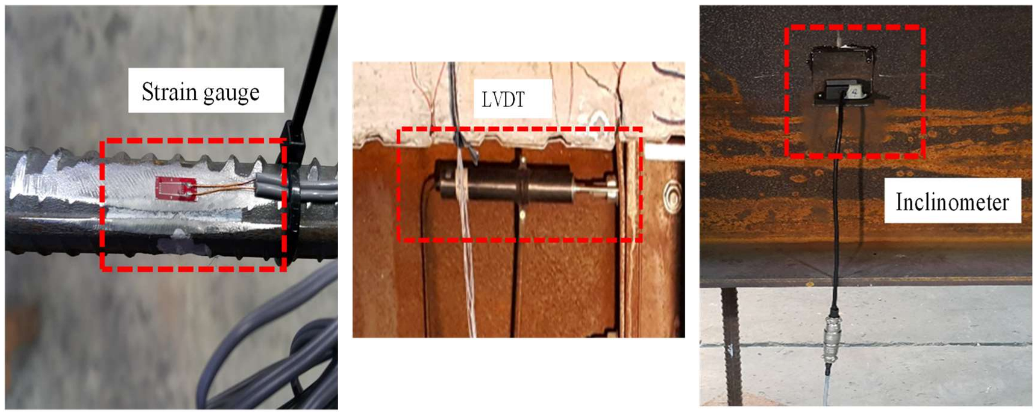

Fig. 3.16 – Instrumentation

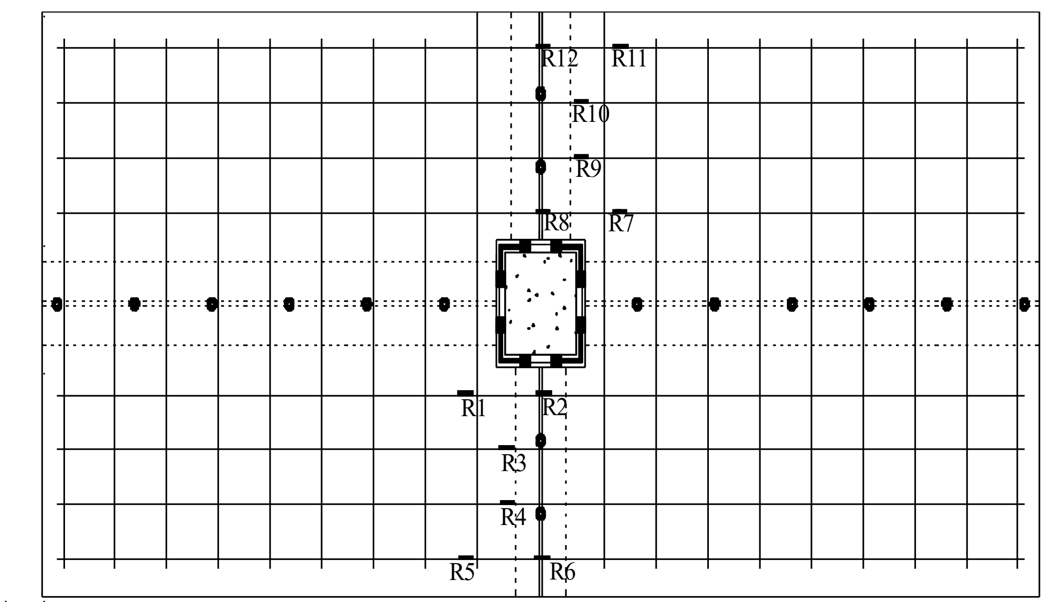

Fig. 3.17 – Strain gauges on reinforcement in embedded in concrete slab

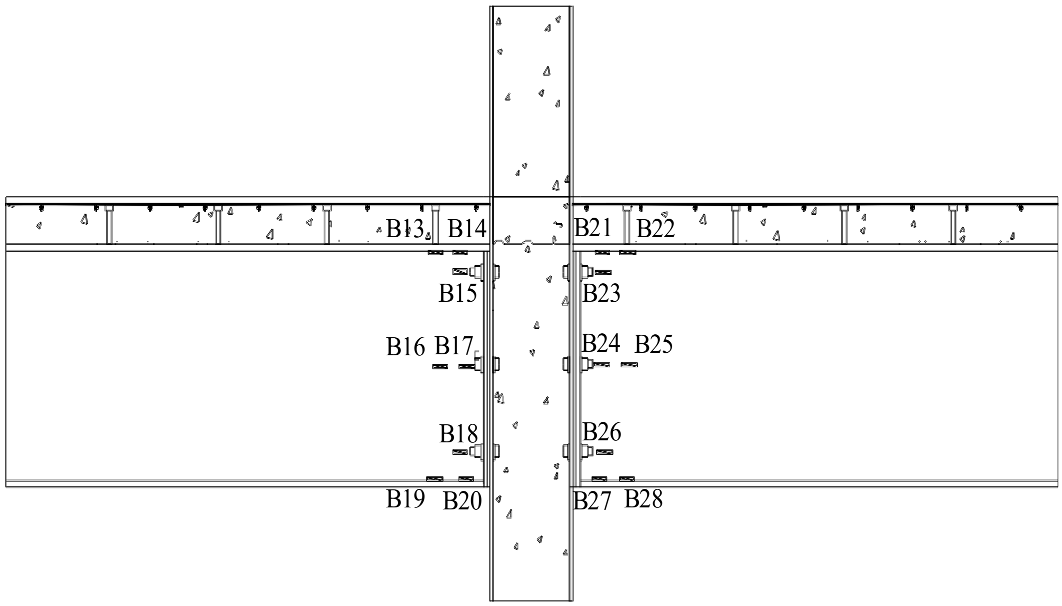

Fig. 3.18– Strain gauges on steel beam web and flanges

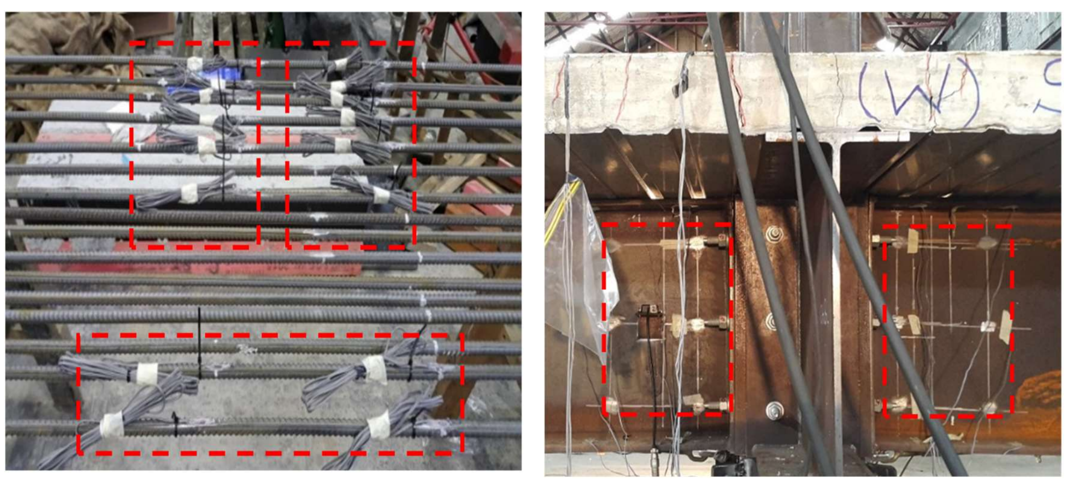

Fig. 3.19 – Strain gauges on reinforcement, steel beam web and flanges

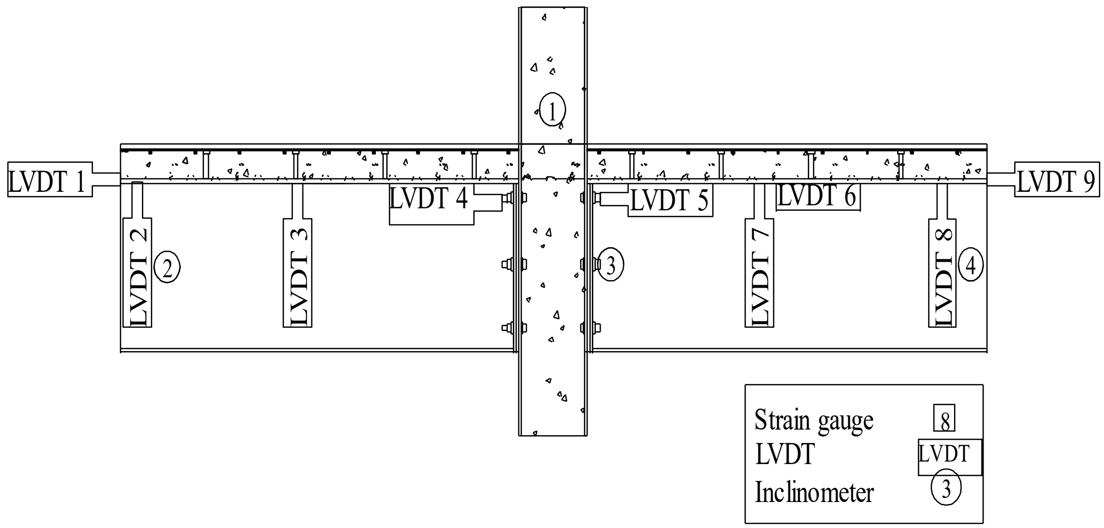

(a) Instrumentation plan

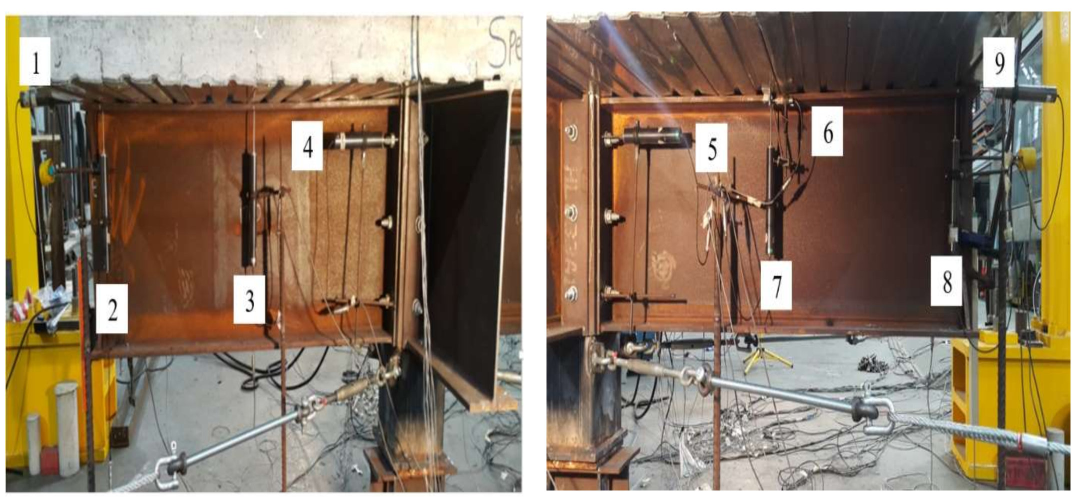

(b) Instruments mounted on primary beams

Fig. 3.20 – Installation of LVDT's and inclinometers

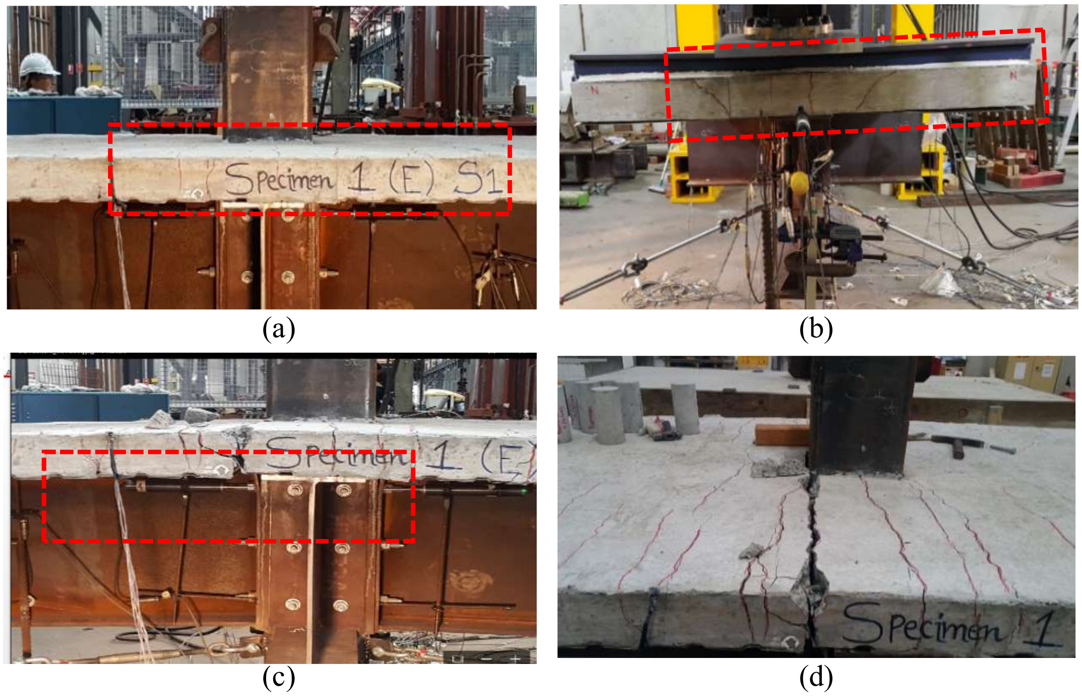

Fig. 3.21 – Propagation of cracks, S-1

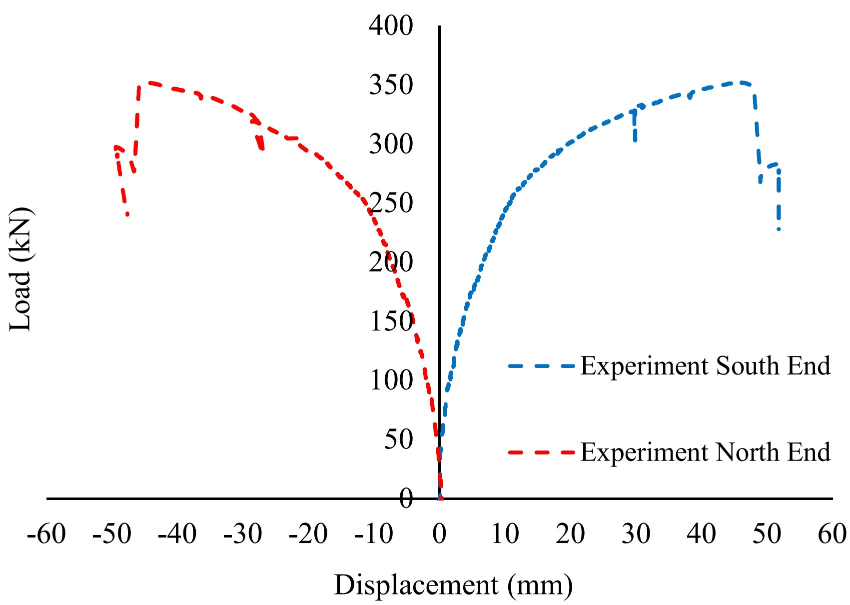

Fig. 3.22 – Load-displacement curve of specimen, S-1

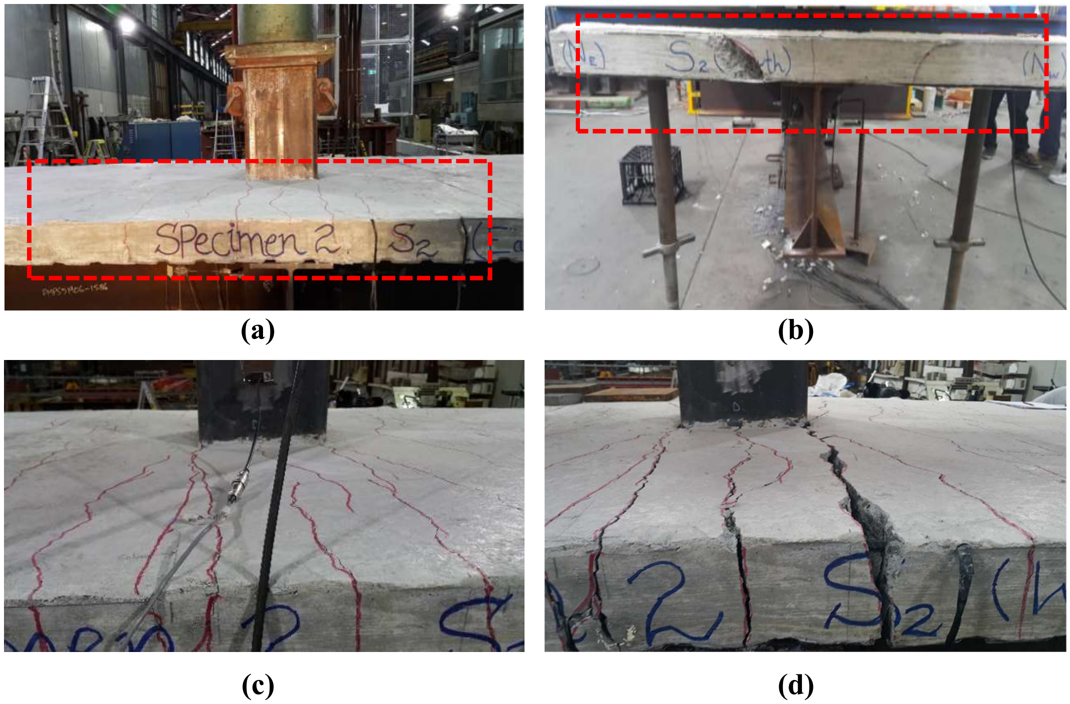

Fig. 3.23 – Propagation of cracks, S-2

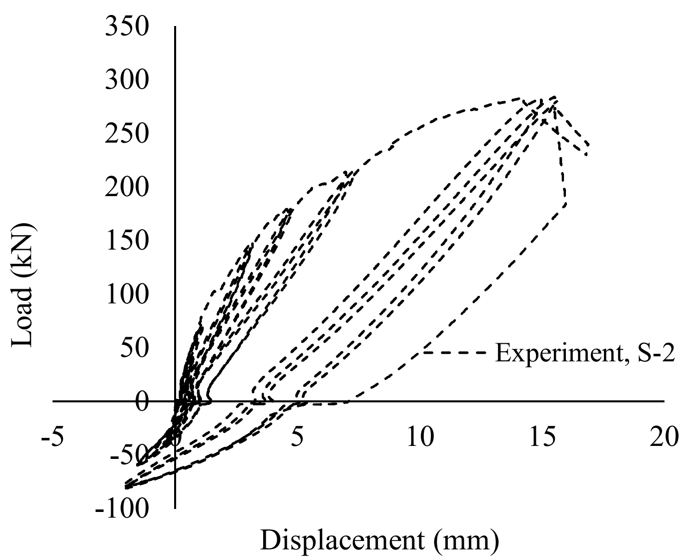

Fig. 3.24 – Load-displacement curves of specimen, S-2

Fig. 3.25 – Cracking of concrete slab, S-1 and S-2

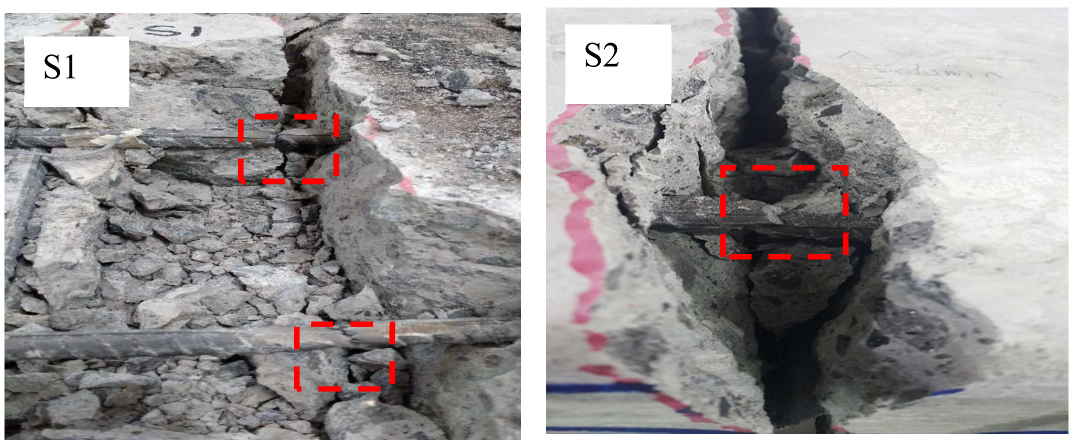

Fig. 3.26 – Reinforcement fracture

Fig. 3.27 – End-plate deformations

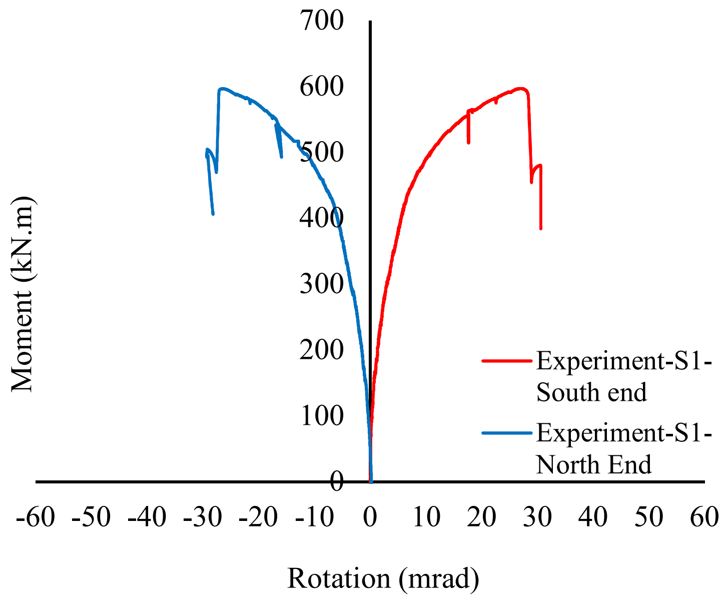

Fig. 3.28 – Moment-rotation relationship of S-1

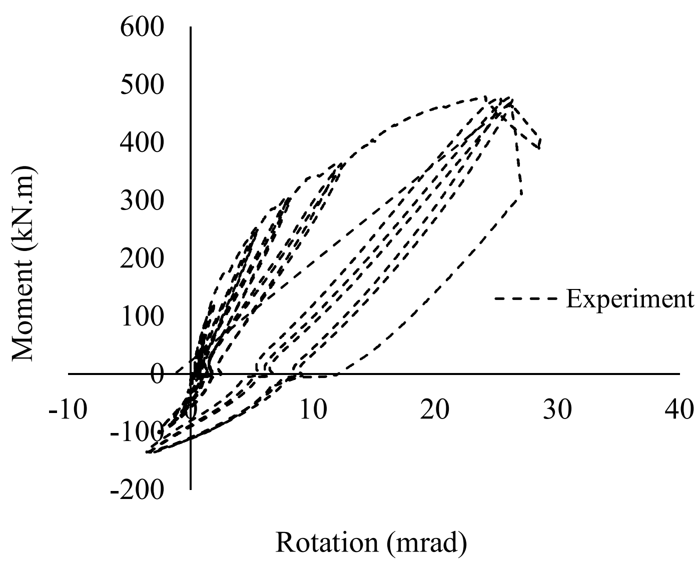

Fig. 3.29 – Moment-rotation relationship of S-2

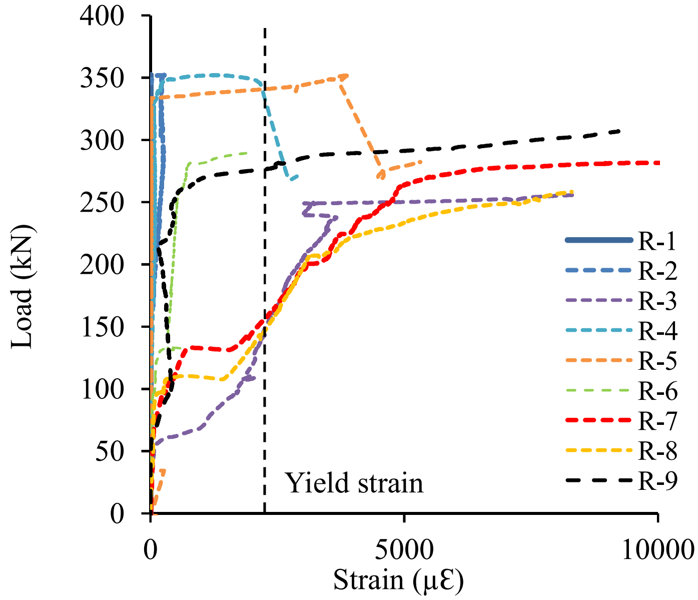

(a) S-1

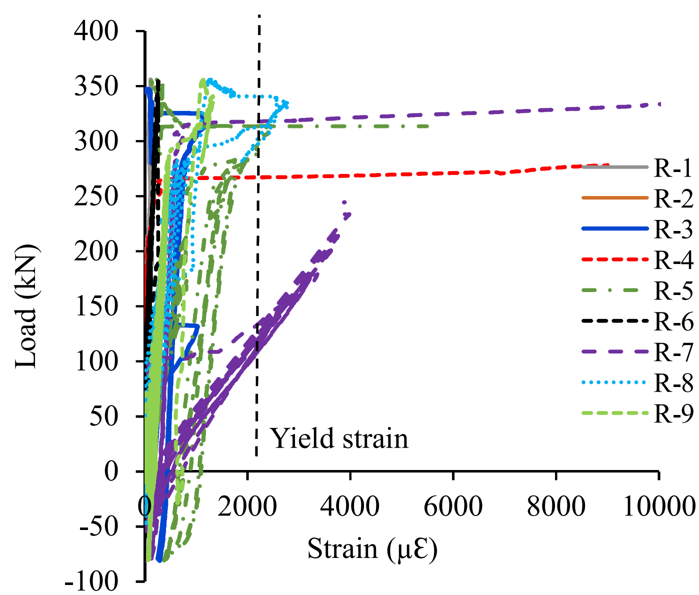

(b) S-2

Fig. 3.30 – Load-strain response for reinforcement

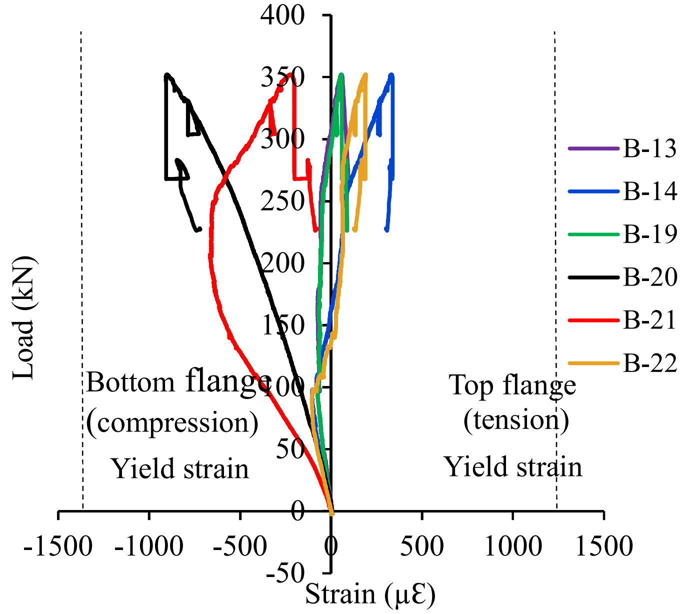

(a) S-1

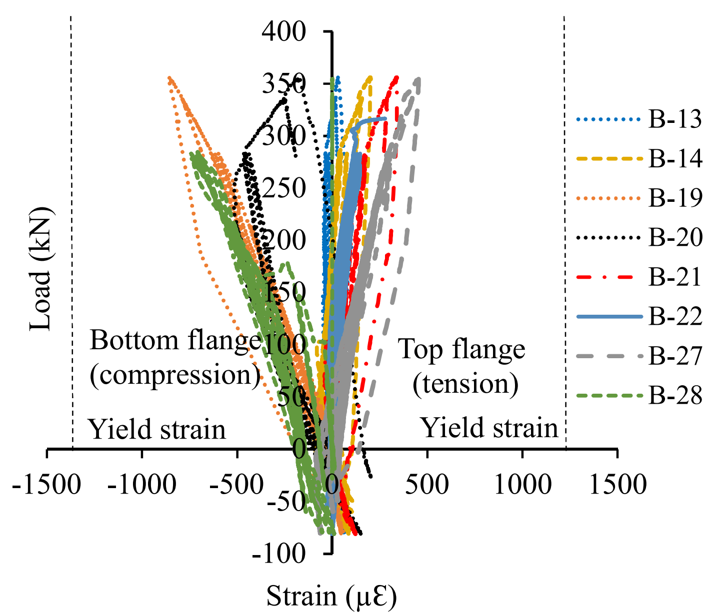

(b) S-2

Fig. 3.31 – Load-strain response for steel beam flanges

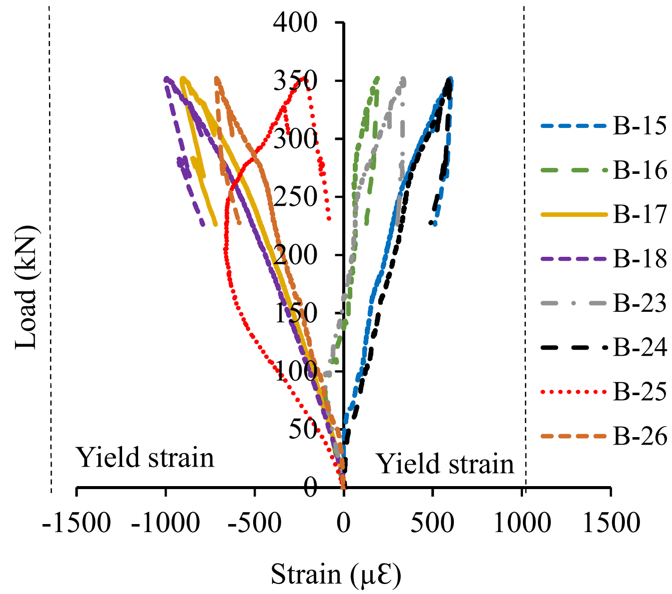

(a) S-1

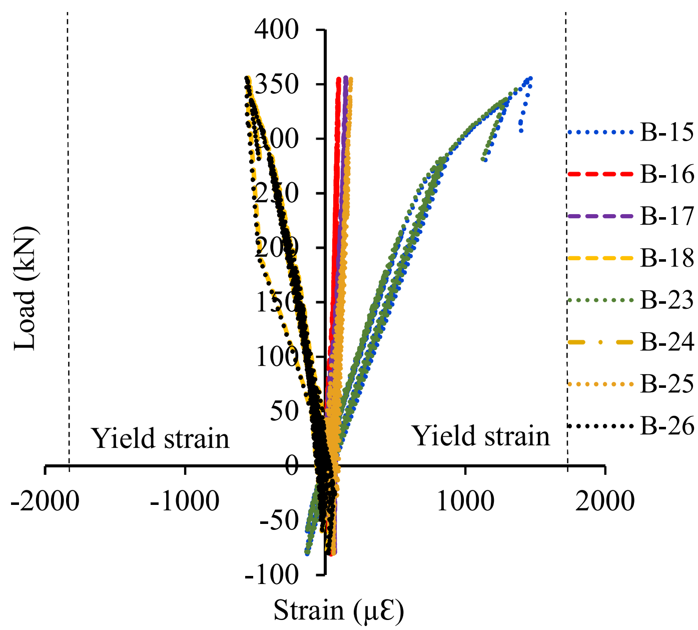

(b) S-2

Fig. 3.32 – Load-strain response for steel beam web

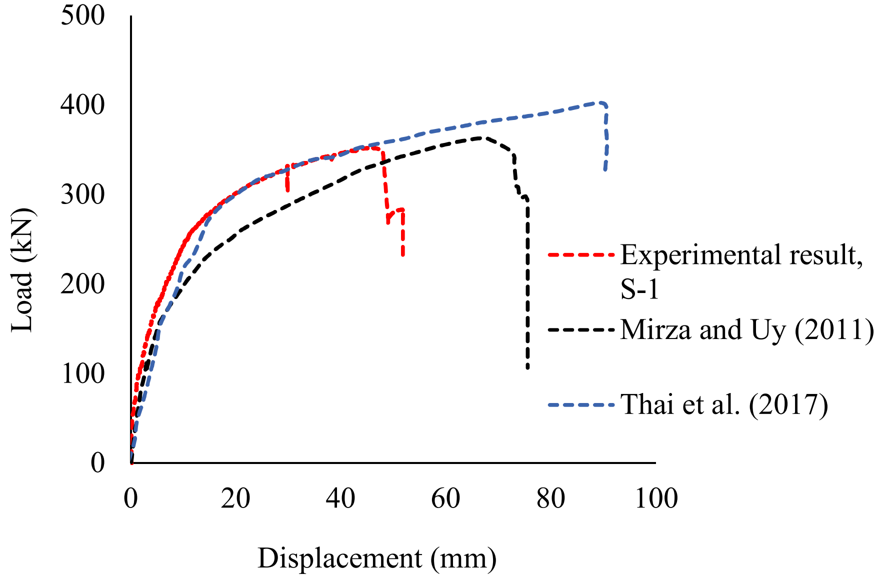

Fig. 3.33 – Load-displacement curves of S-1

Table 3.1 – Details of specimen S-1 and S-2

No.	Member	Dimensions (mm)
1	Steel column	SHS 300 x 300 x 10 mm
2	Concrete slab	3868 x 1600 x 120 mm
3	Endplates	270 x 610 x 12 mm
4	Equal angles	150 x 150 x 12 mm
5	Ajax blind bolts	M20 AJAX Grade 8 .8
6	Headed shear studs	19 x 100 mm
7	Primary steel beam	610UB101 x 1760 mm
8	Secondary steel beam	610UB101 x 626 mm
9	Longitudinal reinforcing	8 N12
10	Transverse reinforcing bars	19 N12

Table 3.2 – Details of coupons for material tests

Member	No.	Thickness (t) mm	Max. variation	Gauge length (L_o)	Parallel length (L_c)	Total length (L_t)	Transition radius	Max grip length
Flange F1, F2, F3	3	14.8	0.1	100	140	480	20	150
Endplate EP1, EP2, EP3	3	12	0.1	88	128	468	20	150
Equal angle EA1, EA2, EA3, EA4	4	12	0.1	88	128	468	20	150
Web W1, W2, W3	3	10.2	0.1	81	121	461	20	150
Column C1, C2, C3	3	10	0.1	80	120	460	20	150

Table 3.3 – Material properties for steel

Structural steel	Yield stress (MPa)	Ultimate stress (MPa)	Elongation at fracture
Steel beam web	380	508	27
Steel beam flange	325	483	30
Steel column	485	552	28
Flush endplate	367	499	23
Reinforcing bar	530	640	15
M20 blind bolt	820	966	30

Table 3.4 – Cylinder compression test results

Age	Sample	Height (mm)	Diameter (mm)	Max. Load (kN)	Compressive strength (N/mm^2)	Avg. strength
7 days						
	1	200	100	220.32	37.87	37.715
	2	200	100	217.67	37.56	
14 days						
	3	200	100	328.98	45.79	45.235
	4	200	100	334.43	44.68	
28 days						
	5	200	100	415.41	52.79	52.835
	6	200	100	415.29	52.88	
42 days						
	7	200	100	449.186	57.08	57.1
	8	200	100	449.215	57.12	

Table 3.5 – Splitting tensile test results

Age	Sample	Height (mm)	Diameter (mm)	Max. Load (kN)	Tensile strength (N/mm^2)	Avg. strength
7 days						
	1	200	100	95.2	3.04	3.05
	2	200	100	99.1	3.06	
14 days						
	3	200	100	154.1	3.78	3.78
	4	200	100	153.5	3.79	
28 days						
	5	200	100	186.1	4.15	4.16
	6	200	100	174.9	4.17	
42 days						
	7	200	100	203	4.55	4.56
	8	200	100	209	4.58	

Table 3.6 – Test results

Specimen	Max. load (kN)	Deflection at max. load (mm)	Max. moment (kNm)	Rotation at max. moment (mrad)	Initial stiffness (kNm/mrad)	Failure mode
S-1	352	52.7	594.88	28.89	99.74	1,2,3
S-2	356	59.9	601.64	32.1	99.25	1,2,3

Failure mode: 1-cracking of concrete slab, 2- Bending of endplate, 3-Reinforcement bar fracture

CHAPTER 4

FINITE ELEMENT MODELLING OF BEAM-TO-COLUMN COMPOSITE JOINTS

4.1. Introduction

Full scale tests can be used to obtain the most reliable behaviour of composite beam-to-column joints. However, performing full-scale tests using real specimen is a laborious and expensive process. Consequently, numerical analysis of real structures has gained extensive popularity in recent years as substantial outcomes can be achieved in a significantly lower time and expenditure. Considerable research has focused on the use of computational techniques for composite structures such as Han *et al*. (2007), Tahmasebinia *et al*. (2012; 2013), Zona and Ranzi (2011), Erkmen and Bradford (2009), Kataoka *et al*. (2014), Thai *et al*. (2015).

The numerical modelling has more advantages as compared to the experimental investigations. The preparation of specimen and execution of loading set up is not required and can be used to accurately investigate complex structures in a significantly reduced time and material cost. This approach has become an essential part of investigating structural behaviour as it has eliminated the limitations in research due to lack of experiments. Due to the numerous benefits associated with using numerical modelling, it is adopted in this study to simulate the testing specimens.

The recent advancements in high-speed computer technology have led to the development of highly sophisticated and user-friendly three-dimensional finite element analysis packages such as ABAQUS and ANSYS. These softwares can be used to precisely replicate the experiments and to obtain reliable outcomes. Henceforth, this Chapter elaborates on the procedure and technique followed to develop the three-dimensional finite element model using ABAQUS software (2014). The implemented constitutive laws for the materials, boundary conditions and element types for all components of the composite joints are elucidated. Both geometrical and material non-linearities as well as nonlinearity of the contacts/interfaces were considered in the analysis. Moreover, the finite element models were validated with the test results presented in Chapter 3. Additionally, failure modes of the composite joints were compared with the experimental results and discussed in detail. Finally, extensive parametric studies were performed which provide an in-depth knowledge on the behaviour of these connections under static and cyclic loading conditions.

4.2. General description of the finite element model

ABAQUS is an advanced non-linear finite element analysis software that can be used for different types of investigations such as stress, heat transfer, fluid flow etc. It is generally used all over the world for structural and civil engineering applications. The software package contains three essential products namely ABAQUS/Standard, ABAQUS/Explicit and ABAQUS/CAE.

ABAQUS/Standard offers solution expertise perfect for static and low-speed dynamic events where extremely accurate stress resolutions are highly critical. Hence, ABAQUS/Standard was used in this study for the replication of static and cyclic behaviour of beam-to-column flush end plate connections. The program comprises of a wide range of options concerning element types, material behaviour, graphical user interfaces, solution controls, and an efficient post-processor to facilitate quick and reliable results.

Two main models were created in this study to perform finite element analysis. Both models were geometrically identical and possessed the same configuration as the experimental specimen, S-1 and S-2 discussed in Chapter 3. In order to accurately replicate the behaviour of beam-to-column joints, an accurate modelling of main components of the specimens is required. The components of the model included concrete slab, steel beam sections, CFST column, concrete infill, reinforcing bars, profiled sheeting, blind bolts, shear connectors, interface between steel and concrete material and beam to column connection detail.

Moreover, a suitable selection of element type, mesh size, loading and boundary conditions are some other factors that are important to achieve accurate simulation. Similar to the tests, one model was subjected to static loading while the other model was subjected to cyclic loading conditions. A general layout of FE model is presented in Fig. 4.1 and the geometrical dimensions of all components are presented in Table 4.1.

4.3. Modelling procedure

The modelling procedure can be essentially divided into the following main steps.

i. Three-dimensional modelling and execution
ii. Analysis procedure and control
iii. Output analysis

- Step-1 included the developments of all parts of the of the finite element model. In addition, material properties were assigned to the created parts. The created parts were then assembled and meshing of parts was also performed in this step.

- Step-2 involved defining of the analysis type to be used. It also involved the development of contacts, constraints, interactions, boundary conditions and loading.

- Step-3 was associated with the analysis process and outputs of the analysis. In this study, the results were obtained in terms of load-displacement characteristics of the beam-to-column connection. The initial stiffness, ultimate load capacity, stress distribution and failure modes were analysed.

4.4. Element type and meshing

The selection of type and size of elements have a significant effect on the precision and accuracy of the finite element analysis results. Therefore, proper selection of element type and size is one of the most important concerns in the FE analysis. Over-all, well-shaped elements with moderate aspect ratio and mild distortion are preferred. A finer mesh also enhances the accuracy of the results. However, a finer mesh results in a longer analysis time and a higher computation cost. Therefore, a reasonable mesh size is desired which is computationally cost effective and also provides accurate results. Additional effort such as partitioning of the surfaces is required in order to achieve a well-shaped mesh. The slave surface must contain more seeds as compared to the master surface in order to accurately simulate the surface-to-surface contact between two surfaces.

In order to achieve a more realistic representation, three-dimensional eight node elements (C3D8R) were used for steel column, structural steel beam, concrete slab, equal angles, end plate, blind bolts, and shear connectors as shown in Fig. 4.2. These elements were selected due to high accuracy and their ability to effectively capture stress concentration. They possessed 8-node linear brick, reduced integration with hourglass control. They were found to yield more accurate results and minimized the complications associated with shear locking which were encountered when other elements such as C3D8I were used. Hence, the rate of convergence was improved due to the use of eight nodes and three translational degrees of freedom.

For modelling the profiled steel sheeting, a four-node shell element (S4R) was used as shown in Fig. 4.3. This element was particularly selected to model the profiled metal sheeting because it was found to be the most suitable element type for thin-walled steel structures. A three-dimensional two-node truss element (T3D2) was used for the reinforcing steel. All (C3D8R), (S4R) and (T3D2) used reduced integration, therefore the total running time was reduced. The mesh configuration used for each element was selected after conducting an extensive mesh sensitivity analysis beforehand. Figs. 4.4 and 4.5 presents the various element types used and meshing of various parts.

4.5. Material properties and constituent material models

Accurate inputs of the material properties are one of the most important necessities for any numerical analysis to obtain accurate results. Generally, empirical constitutive laws are used to express the stress-strain characteristics of materials. The precision of the analysis is reliant on these laws that represent the mechanical behaviour. Therefore, the material properties of all components of the finite element models were obtained from material property tests. These standard tests and the material test results are discussed in detail in Chapter 3. The composite structure investigated in this thesis is a steel-concrete structure. Therefore, this chapter will discuss the material properties of steel and concrete.

4.5.1. Concrete material behaviour

The concrete slab and concrete infill were modelled using the concrete damage plasticity (CDP) model available in ABAQUS. This is a continuum, plasticity-based and damage model for concrete. It considers the degradation of the elastic stiffness stimulated by plastic straining in tension and in compression. This model assumes tensile cracking and compressive crushing of the concrete material as the two main failure mechanisms. The elastic modulus (E_c), poisson's ratio (γ_c), flow potential eccentricity (e) yield surface (k_c), the ratio of initial uniaxially compressive yield stress to initial uniaxially compressive yield stress (f_{bo}/f_c') and yield surface parameters of the CDP model were defined using the default values given ABAQUS user manual (2014). According to the recommendations by ACI (2005), poisson's ratio was taken as 0.2 and the elastic modulus of concrete was calculated from E_c=3320 $f_c'^{\,0.5}$ +6900, where f_c' is in MPa. The viscosity parameter was taken as 0.001 while the flow potential was taken as 0.1. As suggested by Aslani *et al*. (2015), the dilation angle ψ was taken as 40°, while f_{bo}/f_c' and k_c were considered as $1.5\left(f_c'\right)^{-0.075}$ and 5.5/ [5+2(f_c') 0.075].

The compressive and tensile behaviour of the CDP model were defined separately in terms of plasticity and damage parameters. The compressive and tensile damage for concrete slab was specified using two damage parameters d_c and d_t respectively. These damage parameters are expressed as $d_c = 1 - \sigma_c / f_c'$ and $d_t = 1 - \sigma_t / f_t'$.

For unconfined concrete, the model presented by Carreira and Chu (1985) was used to describe the elastic-plastic behaviour of the compression region of the concrete as shown in Fig. 4.6. The model is expressed by the following Eqs. (4.1) and (4.2), and compression is assumed to be linearly elastic up to 0.4 f_c' .

$$\sigma_c = \frac{f_c'\gamma\left(\varepsilon_c/\varepsilon_c'\right)}{\left[\gamma - 1 + \left(\varepsilon_c/\varepsilon_c'\right)^{\gamma}\right]} \tag{4.1}$$

$$\gamma = \left[\frac{f_c'}{32.4}\right] + 1.55 \tag{4.2}$$

Where, $\varepsilon_c' = 0.002$, f_c' is the characteristic uniaxial compressive strength of concrete, σ_c is the uniaxial compressive stress and ε_c is the uniaxial strain of the concrete. For tensile behaviour, concrete is assumed to be linear until uniaxial tensile stress is reached. This uniaxial tensile stress of concrete is determined as 0.56 $(f'_c)^{0.5}$. Beyond this failure stress, the tensile stress linearly reduces to zero with respect to strain.

To simulate the unconfined concrete behaviour under cyclic loading, material constitutive laws were used for damage mechanics as discussed by Li *et al*. (2017). In this analysis, the unilateral damage law with two damage variables (d_c and d_t) is included to describe the concrete behaviour. The concrete damage in compression and tension is designated as d_c and d_t, respectively. Fig. 4.7 presents the behaviour of confined concrete in cyclic loading. In the beginning, the concrete acts linearly up to a tensile failure stress f_t. Beyond this stress, the concrete behaviour is defined by a post failure stress-strain relationship modelled by "Tension Damage" (Ali *et al*. (2013) and Thai and Uy (2015). During the transition of load from tension to compression, the elastic stiffness of concrete is degraded as the unloading response starts to decline. Similarly, the CDP model is used when the loading is reversed from compression to tension. The concrete elastic stiffness degradation can be characterised by the tension damage variable d_t and compression damage variable d_c as shown in Eqs. (4.3) and (4.4)

$$E_t = (1 - d_t) E_0 \tag{4.3}$$

$$E_c = (1 - d_c) E_c E_0 \tag{4.4}$$

The concrete damage variables are determined using Eqs. (4.5) and (4.6) as

$$d_c = 1 - \frac{\sigma_c / E_0}{\varepsilon_{c,pl}\left(1/b_c - 1\right) + \sigma_c / E_0} \tag{4.5}$$

$$d_t = 1 - \frac{\sigma_t / E_0}{\varepsilon_{t,pl}\left(1/b_t - 1\right) + \sigma_t / E_0} \tag{4.6}$$

where b_c and b_t were taken as 0.7 and 0.1 as recommended by Birtel and Mark (2006). $\varepsilon_{c,pl}$ and $\varepsilon_{t,pl}$ are the equivalent plastic strains. $\varepsilon_{c,in}$ and $\varepsilon_{t,ck}$ represent the concrete inelastic strain in compression and concrete cracking strain in tension respectively. Their values can be calculated from Eqs. (4.7) and (4.8).

$$\varepsilon_{c,in} = \varepsilon_c - \sigma_c / E_0 \tag{4.7}$$

$$\varepsilon_{t,in} = \varepsilon_t - \sigma_t / E_0 \tag{4.8}$$

The compressive and tensile stiffness recovery was determined using w_c and w_t. This analysis is based on the assumption that concrete can regain full stiffness recovery without damage.

For confined concrete, the model presented by Tao *et al*. (2013) was used which is presented in Fig. 4.8. The tensile behaviour is supposed to rise linearly up to concrete cracking at the tensile strength and then decreases to zero with the tension stiffening effect as reported by Thai *et al*. (2015). A fracture energy criterion was used in this study. The brittle behaviour of concrete is represented by a stress-displacement curve rather than a stress-strain relationship. Compressive damage was ignored in the analysis as the failure mode detected in the experiment was cracking of the concrete slab in tension rather than crushing of the concrete in compression.

4.5.2. Steel material behaviour

The stress-strain relationships of various steel materials used in the FE models were defined using the material property records obtained from the standard tests presented in Table 3.3 in Chapter 3. These steel materials show initial elastic behaviour up to their yield points. The area underneath the linear curve characterizes the elastic region, while the slope describes the Young's Modulus. The curve typically decreases beyond the yield point. As the deformation continues, the stress increases and the cross-sectional area reduces until it reaches the ultimate strength. A neck is formed after the rupture point where the local cross-sectional area decreases rapidly. These three individual parts of the stress-strain curves of these steel materials can be represented using three distinct lines to be conveniently used in ABAQUS.

In addition, the piecewise linear strategy was also found to be adequate to characterize the stress-strain relationships of steel material. Mirza and Uy (2011) effectively accomplished extensive finite element studies using this method. Loh *et al*. (2006) generalized the stress-strain curves for steel beam section, reinforced steel and profiled sheeting as shown in Figs. 4.9-4.11. These curves are accurate enough to represent the stress-strain relationship and can be used in the absence of stress-strain data. Table 4.2 illustrates the different values of stress-stain for steel materials.

4.6. Analysis procedure

There are two different solution strategies in ABAQUS which are known as the explicit and implicit solver. The comparison between the two types has been performed by Van der Vegete and Makino (2004) and Thai *et al*. (2015). The investigation recommended the use of explicit method to simulate bolted connections as it helps to overcome the difficulties associated with numerical convergence. Based on these recommendations, initially the explicit solver was used in this study to simulate the behaviour of blind bolted joints. However, it was not feasible due to the excessively long time taken for the cyclic analysis to complete. Therefore, implicit technique was adopted finally as it took a significantly smaller time to finish the analysis. Fig. 4.12 presents a comparison of load-displacement behaviour of the beam-to-column joint under static loading condition using both analysis techniques.

Moreover, ABAQUS/Standard allows a wide range of linear and nonlinear engineering simulations to be performed proficiently, precisely, and reliably. There is no limitation regarding the size of the time increment that can be used for most analysis in ABAQUS/Standard. Furthermore, the flexibility achieved by this integration permits ABAQUS/Standard to be used in areas that are compatible to an implicit solution technique, such as static, low-speed dynamic, or steady-state transport analysis.

4.7. Element contact

ABAQUS uses a Master-Slave strategy to develop contact between different surfaces in an interacting pair. Master represents the larger and stiffer surface while slave represents the smaller and weaker surface. Moreover, surfaces with a coarser mesh should also be selected as a master surface. Generally, surface to surface contact, tie constraint and embedded constraint were the three main contact types used in this analysis.

4.7.1. Surface to surface contact

Surface to surface contact was used between parts that demonstrated relative slip at their interfaces with small sliding option. For example, between the bolt shank and steel tubular column hole, bolt head and column hole, end plate and bolt shank, equal angle and blind bolt shank, CFST column and end plate, column and concrete slab, steel column and concrete etc.

According to Abaqus (2004), surfaces with a finer mesh and higher ductility were selected to be the slave surfaces, and those with rougher mesh were selected as the master surfaces. Accordingly, profiled steel sheeting was selected as slave surfaces, while concrete slabs were selected as the master surfaces. The surfaces selected as master and slave to create contact between various parts of the FE models are illustrated in Fig. 4.13**.** Table 4.3 summarises the details of contact surfaces defined in the models.

4.7.2. Tie constraint

The 'TIE' option was used for connecting components that were reasonably fixed to each other such as the shear studs to the bottom of the steel beam because these two components were welded together and the test results did not show any separation between these two components. Moreover, tie contact was used for contact between steel beam and end plate, top flange of steel beam and bottom of shear connectors.

No relative slips between profiled steel sheeting and concrete slabs were detected from the experimental observations. Therefore, tie-constraint was used to develop contact between the concrete slab and profiled metal sheeting. Tie-constraint allowed nodes on slave surfaces and master surfaces to share the same motion. This constraint simplified the numerical analysis due to numerous benefits. One advantage was that the degrees of freedom of nodes on slave surface were no longer considered during analysis. Moreover, the contact status of nodes on slave surface was not required to be checked to decrease the calculation time.

4.7.3. Embedded constraint

Lastly, the embedded constraint option was used to develop the contact between reinforcing bars and concrete slab. The reinforcement was embedded into the slab, with the slab being the host region and the bars being an embedded region. This technique connects these two different components and prevents slip between them. Using this technique, a perfect bond between embedded elements and host elements was achieved. This bond restrains the translational degree of freedom of the embedded nodes and prevents slip between the reinforcing bars and concrete. The details of contact between blind bolt, steel column, flush endplates and equal angles are detailed in Fig. 4.14.

4.8. Loading and boundary conditions

In FE modelling, accurate demonstrations of the boundary conditions have an important role in the precision of the model results and a small difference in boundary conditions can significantly affect the results. In this model, simply supported boundary conditions were applied. All boundary conditions were consistent with experiments aiming to achieve highly accurate results. This model consisted of three types of loadings which were pretension in the bolt, axial load on the column and loading on the primary beam ends which were applied in three different steps. Fig 4.15 provides a basic idea of the loading and boundary conditions for this model. Pretension force was applied in the first step. Axial load was applied in the second step and displacement control was applied in the last step. A nominal compressive load was applied vertically at the centre of the column using a reference point tied to the top surface of the column. In addition, load was applied 100 mm away from the edge of the concrete slab to simulate the vertical load applied at both ends. The load applied was calculated as the total reaction acting on the reference point. Theoretically, the boundary conditions were achieved by resisting translation in longitudinal directions, that is u_x=0 shown in Fig. 4.15. Additionally, rotations were restrained in y-y, z-z directions as well. All translations in orthogonal directions were constrained at the bottom of CFST columns in order to prevent rigid body motion and zero pivots, namely $u_x=u_y=u_z=0$.

4.9. Contact interactions

Contact interaction are extremely critical to the beam-to-column joints as the flexural resistance of structures is dependent on the cooperation of all individuals in which forces are transmitted by the contact. When two components are brought in contact with each other, normal pressure and frictional shear force is developed at the interface. Therefore, the contact analysis is performed to determine the most accurate contacting region and the corresponding stress in models. The surface-to-surface contact with a coefficient of friction of 0.25 was adopted to simulate the interaction between two adjacent precast concrete blocks in the tangential direction. In addition, a hard contact property was used in the direction normal to the interface plane. The model assumes "Hard" and "Penalty" options by default. The mechanical surface interaction models assume that the contacting surfaces transfer shear forces and normal forces through the interfaces. There is a relationship between these two force components which is termed as friction. As a result, frictional behaviour should be found considering shear forces in the models by defining friction coefficient. The normal and tangential behaviour between these contact surfaces was defined using the "Hard" and "Penalty" options respectively. The value used for the friction coefficient was 0.3. The "Master" and "Slave" surfaces of these interactions were appropriately defined by taking the mesh density and the material strength of each component into consideration.

4.10. Pretension in the bolts

The technical guides of blind bolts specify to provide pretension as obligatory to avoid relative movement of the connected members. There are two methods to provide the pretension force in Abaqus. One option is to apply bolt load to the cross-section of the bolt along its axis as a concentrated force. This option can only be applied in Abaqus/Standard. The second option is to simulate pretension by means of temperature, which can be adopted in Abaqus/Standard as well as Abaqus/Explicit. This method was used to apply pretension in this study as well.

As blind bolts are tightened with enough pretension in practice, the same effect was achieved by applying a negative temperature to the shank of the blind bolt, which ultimately led to shrinkage of the bolt. Since this technique was an estimated approach to achieve pretension, the precise value of temperature was obtained by trial and error. Similar approaches were adopted by Tanlak *et al*. (2011), Egan *et al*. (2012) and Thai *et al.* (2015).

Coefficient of thermal contraction was also applied to the bolt material. A step was created from the predefined field option and was applied before the actual load step. After that, a reference temperature was allocated to the bolt shank in a step made before the load step by using the predefined field option. The increase in temperature induces the shrinkage of the bolt shank in the through-thickness direction and as a result produces the anticipated bolt pre-stress.

4.11. Results and validation

The desired outputs such as loads and deflections values and stress and strain distribution of the parts can be obtained using a variety of output variables present in ABAQUS/Standard. However, these variables can be retrieved only in the visualization module of ABAQUS/CAE (Abaqus/Viewer). Some examples of output variables available in ABAQUS/STANDARD include nodal variables, whole element variables, surface and section variable and element centroidal variables. These output variables can be obtained as either field or history outputs.

Two FE models developed in this study were verified against the experimental results. From Fig. 4.16, it can be observed that the FE model for S-1 accurately predicts the initial stiffness, ultimate load capacity and overall behaviour of the connection. The FE model also predicts the actual failure modes of the respective test specimens as shown in Figs. 4.18-4.20. Fig. 4.17 demonstrates that the FEM for S-2 accurately predicts the critical parameters like initial stiffness, peak loads at every cycle in compression and tension, ultimate load and failure modes very well. However, the overall stiffness in this case is not very well predicted. The reason for this discrepancy might be due to using tie constraints to define the contact between the bolt head and infill concrete. As cyclic analysis takes a very long time to complete as compared to the static analysis, therefore, the reason for using embedded constraint instead of surface to surface constraint was only to simplify the model in order to save computational time. In addition, this study focused on the global moment rotation behaviour of the connection and not the local crack in the concrete slab which makes it satisfactory for the validation. It was therefore suggested that these models were suitable to be adopted for parametric studies to study the effect of certain key parameters on the load versus displacement behaviour of connections.

Fig. 4.21 presents the equivalent plastic strain distribution of concrete slab (PEEQ). It is observed that plastic behaviour occurred mostly around the loading regions and near the periphery of steel tubular column. Moreover, the maximum deflection for both of the beam-to-column joints was found from the respective experimental results. The deflection at the ultimate load of each test specimen was considered as the maximum displacement of the corresponding beam-to-column connection model.

Fig. 4.22 presents the comparison between test results and FE results in terms of load capacity, deflection, moment capacity and initial stiffness. The details of these comparisons are presented in Table 4.5. Overall, the numerical models were capable of predicting the static and cyclic response of the tested specimen accurately. The comparison between results from experiments and finite element analysis for load versus displacement behaviour demonstrated a very low value of error. It is therefore suggested that these models are suitable to be adopted for parametric studies to study the effect of certain key parameters on the load versus displacement behaviour of these connections.

4.12. Parametric studies

The finite element models were used to perform parametric studies on various material related and geometrical parameters which helped to investigate their influence on the structural behaviour of the composite connection under different loading scenarios. The material related parameters selected for study under static loading conditions were axial load on column, pretension force in the bolts, compressive strength of concrete, different grades of blind bolts, effect of steel strength as shown in Table 4.6. These parameters were selected due to their importance in the connection’s resistance and due the reason that they could improve the performance of the connection without making changes to the thickness or sizes of steel column or steel beam.

Similarly, the geometrical parameters selected for study under both static and cyclic loading conditions were thickness of flush end plates, thickness of equal angles, reinforcement ratio, shear connection ratio and thickness of concrete slab. The details of these parameters are presented in Table 4.7. These parameters were selected due to their significance in contribution to the improvement in the strength and performance of connections. These parameters are discussed in detail as follows.

4.12.1. Parametric studies for S-1 under static loading

4.12.1.1 *Pretension force in the blind bolts*

In order to study the behaviour of different pretension loads on the behaviour of the composite beam-to-column connection a range of various pretension loads was selected which are 25%, 50%, 75%, 100% and 150% of the minimum pretension load. The results presented in Fig. 4.23(a) demonstrate that pretension loads did not affect the initial stiffness of the composite connection regardless of the different percentages. However, they created a small change in the ultimate load capacity of the connection. The increment in load capacity is around 10% for 150% value of pretension load. However, the load capacity increased only 7%, 6%, 5% and 8% for 100%, 75%, 50% and 20% value of minimum pretension loads.

4.12.1.2 **Compressive strength of concrete (fc')**

Fig. 4.23(b) presents the effects of various compressive strengths of concrete on the behaviour of the connection. The results demonstrate that the initial stiffness did not change with the increase in the compressive strength of concrete. However, increase in the value of ultimate load was observed with the increase in the compressive strength of concrete.

4.12.1.3 *Effect of steel grade (fsy)*

There are different grades of steel and each grade encompasses different properties. These properties can be chemical composition, physical or environmental. All steel is composed of iron and carbon. It is the quantity of carbon and supplementary alloys that determine the properties of each grade. Parametric studies were performed on three different grades of structural steel which were Grade 250, Grade 350 and Grade 450. It can be seen from Fig. 4.23(c) that increase in grade of steel did not considerably improve the ductility of the connection.

4.12.1.4 *Effect of different diameters of blind bolts*

The diameter of bolts is selected according to the thickness of the end plate used in design. According to EC-4 (2004), the thickness of end plate must be smaller than 60% of the bolt diameter. The effect of using diameters M26, M24, M20 and M16 in the connection region was investigated. The load deflection response for these joints was modelled and the results are presented in Fig. 4.23(d). The results show that there is no change in initial stiffness with the increase or decrease in bolt diameter. However, the ultimate load capacity of the composite connection increases with the increase in diameter of blind bolts. However above M20 there appears negligible change in strength and ductility of the composite connection.

4.12.1.5 *Effect of different grades of blind bolts*

Ajax blind bolts come in sizes M16, M20 grade 8.8 products. Special orders have to be placed for higher grades such as Class 10.9 and 12.9 with clamping lengths of 5 mm to 120 mm. Class 10.9 of bolts have almost 40% greater clamping load as compared to class 8.8.

As we have used Ajax one side blind bolts in this study. These bolts are available in class 8.8 and 10.9 in Australian market. Therefore, parametric study was performed using these two classes to investigate their effect on the connection behaviour. The results are presented in Fig. 4.23(e) which show that the grade of bolt had no effect on the initial stiffness of the connection. However, ultimate strength seems to increase slightly with higher grades.

4.12.1.6 *Effect of different axial loads on the column*

The finite element modelling results for axial load of 0.2 *Pu*, 0.4 *Pu* and 0.6 *Pu* shown in Fig. 4.23(f) demonstrates a slight reduction in load capacity of the composite connection with an axial load of 0.6 *Pu*.

The load capacity is reduced by 8% only which is quite minimal. There is negligible change in both stiffness and load capacity of the composite joint for any value of axial load. For example, only 8% decrease in the load capacity of the joint is observed when 60% of ultimate axial capacity of the column is applied.

4.12.1.7 *Effect of flush endplate thickness*

Five different thicknesses were selected which are available in the market easily. These were 8 mm, 10 mm, 12 mm, 16 mm and 20 mm. Fig. 4.24(a) shows that an increase in the thickness of the flush end plates to 12 mm, 16 mm and 20 mm improves the initial stiffness and ultimate strength of the connection to 12%, 15% and 7%. The endplate with 8 mm and 10 mm thickness reduces the initial stiffness and strength up to 13 and 7%. For an 8 mm thickness endplate, the mode of failure was the fracture of the endplate whereas, for an increased thickness of endplate such as 10 mm to 20 mm, the mode of failure was fracture of the reinforcement. Further increase in the thickness of flush end plate led to the fracture of blind bolt as shown in Fig. 4.25. It can be concluded that the thickness of flush end plate should not be too small so that fracture of the endplate can be avoided.

On the other hand, the thickness of the flush end plate should not be very large so that the failure of blind bolt can be avoided. The finite element analysis results demonstrate that the configurations with t_{ep}/d_b (thickness of endplate to diameter of bolt ratio) below 0.6 mm experienced failure of the flush endplate whereas, above 0.6 mm suffered blind bolt failure. Therefore, in order to achieve ductile behaviour of the composite joint the t_{ep}/d_b ratio should be kept 0.6 mm, 60% of bolt diameter which is also mentioned in EC3 (2005) and EC4 (1992). Another observation was that using an endplate thicker than the steel tubular column leads to the bending of the flange of steel tubular column as in the case of 16 mm and 20 mm thick flush endplates.

4.12.1.8 *Effect of equal angles thickness*

In this study, equal angles were proposed as a possibility to improve the connection's behaviour in terms of strength. Therefore, parametric studies on various thicknesses of equal angles were performed to explore their effect on the behaviour of these connections. The thicknesses considered in FE models were 8 mm, 10 mm, 12 mm, 16 mm and 19 mm as shown in Fig. 4.26 respectively. The results presented in Fig. 4.27(a) show an increase in ultimate strength of 8% when the thickness of equal angles is increased from 12 mm to 16 mm. When the thickness of the equal angle is increased further to 19 mm, the value of ultimate load increases by 4% only. The ultimate strength decreases to 13 and 8 % for 8 and 10 mm thick equal angle.

The increase in thickness of equal angles has a negligible effect on the initial stiffness of the connection. It can be concluded that the use of equal angles on the side of steel tubular column does not make a significant contribution towards improving the stiffness and ultimate strength of the connection.

4.12.1.9 *Effect of reinforcement ratio*

Four different reinforcement ratios (RR) were considered which were 8 N12 (0.5%), 8 N16 (0.83%), 8 N24 (1.88%) and 8 N28 (2.5%). These ratios were calculated based on the tensile reinforcing area versus total slab cross sectional area. Fig. 4.28(a) shows that a very low value of reinforcement ratio results in limited strength and ductility. An increase in reinforcement ratios increases the initial stiffness, load capacity and ductility of the connection for 0.5% and 0.83%. However, for 1.88% and 2.5%, there is a slight increase in initial stiffness only. By using N16, N24 and N28 rebars, there is an 11%, 27% and 8% increase in ultimate load capacity of the connection. Moreover, an increase in reinforcement ratio limited the ductility and rotation capacity of the joint for 1.88% and 2.5% due to sudden failure of shear studs. Therefore, reinforcement should be very carefully designed as a greater number of reinforcements will not always be beneficial for the improvement of the connection's performance.

4.12.1.10 *Effect of shear connection ratio*

Four different degrees of shear connection were considered which are 35%, 50%, 100% and 140%. The first two values represent partial shear connection, whereas the second two represent full shear connection. The respective load-displacement behaviour of S-1 with these ratios is plotted in Fig. 4.29(a). It can be observed that the initial stiffness of the connection increases gradually with an increase in shear connection ratio from 35% to 100%. However, there is a slight increase in ductility and ultimate load capacity for 100% and 140% full shear.

A partial shear connection ratio of 35% shows limited strength and ductility. In this case the mode of failure is fracture of the shear studs as shown in Fig. 4.30. The ultimate load capacity reduces to 36% and 15 % with 35 % and 50 % shear connection ratios. The model with 35% shear connection ratio demonstrated significant slip between the composite slab and steel beam. There was no slip at all in the case of 100% and 140% shear connection ratio. However, greater number of shear connection ratio led to limited rotation capacity and ductility of the joint.

4.12.1.11 *Effect of concrete slab depth*

In this study four different slab depths were selected which are 120 mm, 150 mm, 200 mm and 250 mm. Fig. 4.31(a) shows that an increase in the depth of the concrete slab significantly increases the stiffness and strength of the connection. An increase of slab thickness of 150 mm, 200 mm and 250 mm causes a 17%, 24% and 35 % increase in load capacity. However, failure of connection was observed at a comparatively lower value of deflection when the thickness of the slab was increased respectively from 120 mm to 250 mm.

4.12.2. Parametric studies for S-2 under cyclic loading

4.12.2.1 *Effect of various thicknesses of end plates*

Fig. 4.24(b) shows that an increase in the thickness of flush endplates gradually improves the initial stiffness and significantly improves the ultimate strength of the connection. For t_{ep}/d_b ratio below 0.6, the mode of failure observed was yielding of endplate, whereas for t_{ep}/d_b ratio above 0.6, the mode of failure changed to yielding of rebar and deformation of blind bolts. For a decrease in the thickness of endplate from 8 to 10 mm, the corresponding reduction in stiffness and strength is 27 and 10 %, respectively. While an increase of 12 mm, 16 mm and 20 mm thickness causes 13%, 11% and 7% increase in initial stiffness and ultimate strength of the connection. The results show that an optimum value of flush endplates should be adopted in order to maximise the performance of these connections.

4.12.2.2 *Effect of various thicknesses of equal angles*

Fig. 4.27(b) exhibits the load versus deflection relationship of S-2 with different thicknesses of equal angles. It shows that an increase in the thickness of equal angle does not have a significant effect on the initial stiffness of the connection but slightly improves the ultimate strength. For an increase in thickness of 8 mm, 10 mm, 12 mm, 14 mm, 16 mm and 19 mm, the increase in ultimate load is about 26%, 21%, 13%, 11%, 7% and 4 % only. The results demonstrate the use of equal angles is not quite beneficial to improve the behaviour of the connection. Therefore, some other technique should be adopted.

4.12.2.3 *Effect of reinforcement ratio*

Four different reinforcement ratios were considered which were 8 N12 (0.5%), 8 N16 (0.83%), 8 N24 (1.88%) and 8 N28 (2.5%). Fig. 4.28(b) shows that an increase in the area of reinforcement enhances the initial stiffness and load capacity of the connection. The results show that after a certain limit, further increase in reinforcement was not much beneficial to the improvement of the connection's performance. A very low reinforcement ratio causes limited strength and ductility.

4.12.2.4 *Effect of shear connection ratio*

Four different degrees of shear connection ratio were considered which are 35%, 50%, 100% and 140%. The results are presented in Fig. 4.29(b) which show that a decrease in shear connection ratio leads to a reduction in load capacity and ductility. A degree of shear connection of 35% and 50% causes 27% and 15% decrease in the load capacity. It was also observed that lower values of shear connection ratio cause an increase in deflection. The mode of failure for 35% shear connection ratio was fracture of shear studs. It can be concluded that the shear connection ratio should at least be 50% to avoid fracture of shear studs before reinforcing bar failure.

4.12.2.5 *Effect of various thicknesses of concrete slab*

Fig. 4.31(b) shows the load versus deflection curves for S-2 with different thicknesses of concrete slab. The results show that an increase in slab thickness causes an increase in the load capacity. The initial stiffness did not change very significantly. However, the ductility increases by 3%, 7% and 10 % for 150 mm, 200 mm and 250 mm depths of concrete slab, respectively. It is observed that cracking of concrete is reduced by using a greater thickness of concrete slab and can withstand greater ultimate loads under seismic conditions. The ultimate load capacity that the concrete slab can bear is increased to 10%, 16% and 21% when a concrete slab thickness of 150 mm, 200 mm and 250 mm are used. Failure of shear connectors was observed when 250 mm thick concrete slab was used.

4.13. Summary of the chapter

Computer-based numerical simulation techniques are largely used now a days to analyse real structures in virtual modelling environments. This thesis utilised ABAQUS simulation program to simulate the load-displacement behaviour of composite beams-to-CFST column joints with blind bolts.

This chapter discussed the modelling procedure using ABAQUS in detail. The significance of appropriate selection of element types and appropriate mesh sizes was clearly emphasised. The material properties and element types used for all components of the composite beam-to-column joints were described in detail. Moreover, details of the complicated contact interaction between different components were explicitly illustrated in this chapter. The boundary conditions applied on the finite element models were described and details of the loading procedure was also provided.

The finite element models developed in this research demonstrated a reasonably good agreement with the test results. The initial stiffness, ultimate strength and failure modes of the beam-to-column connection for static and cyclic loading scenarios are predicted accurately. The numerical results were validated with the experimental outcomes to validate the reliability of FEM. Extensive parametric studies on various parameters were performed which help to identify the critical components that had significant effects on the load-displacement behaviour of the joints.

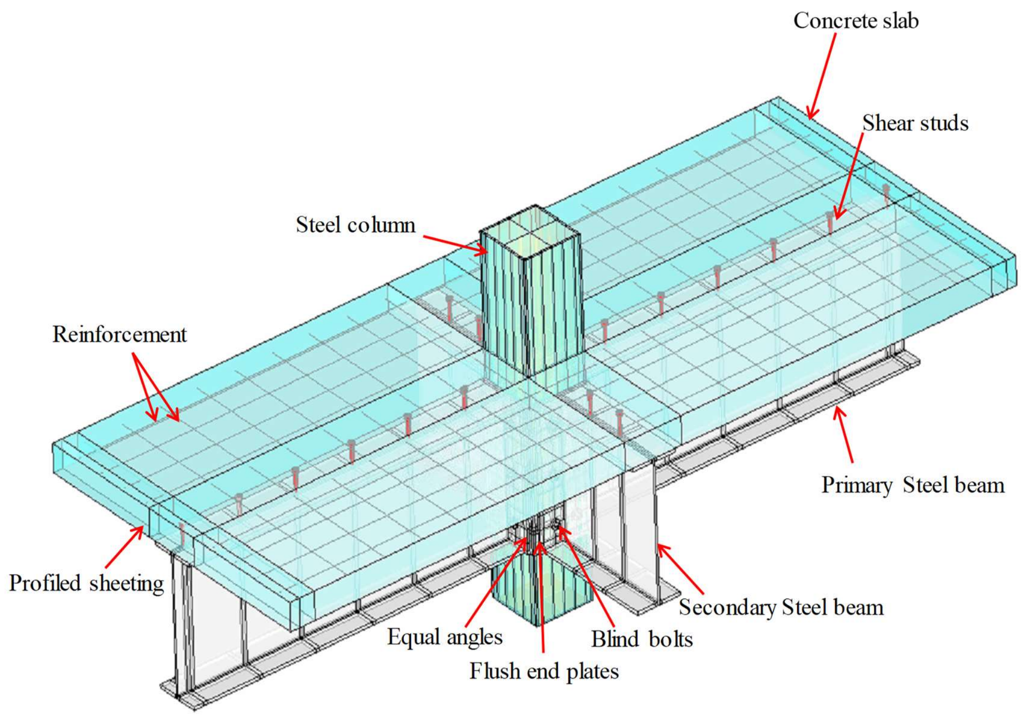

Fig. 4.1 – FE model

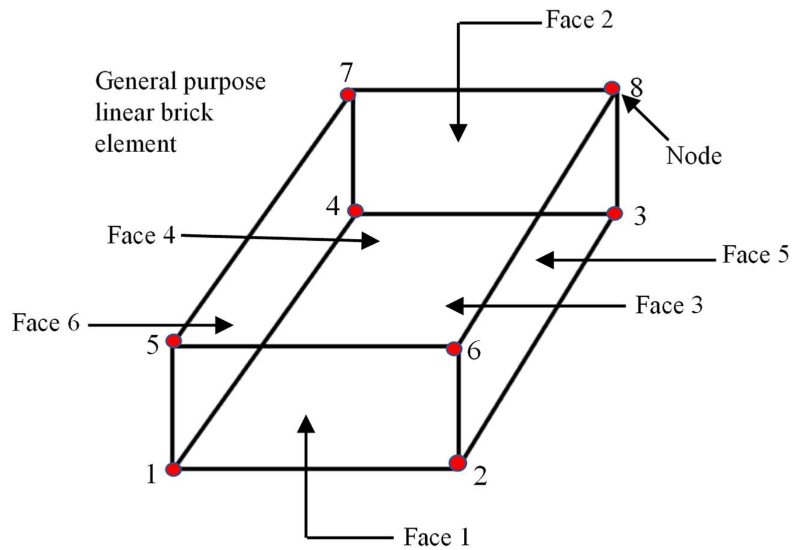

Fig. 4.2 – Three dimensional solid elements (C3D8R)

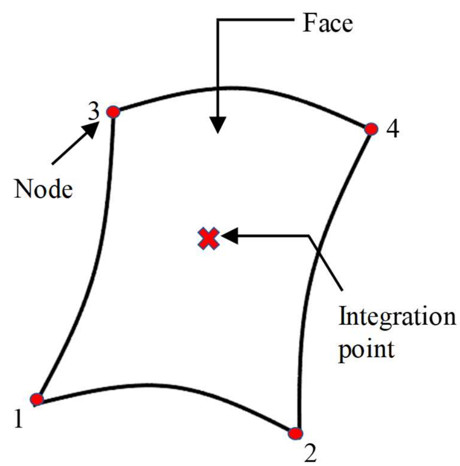

Fig. 4.3 – Shell element (S4R)

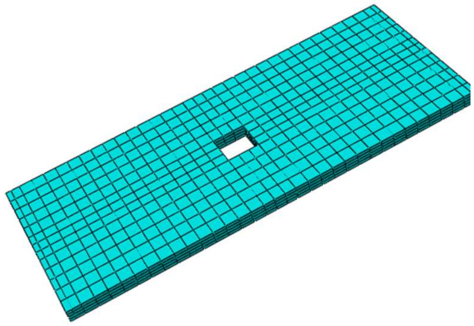

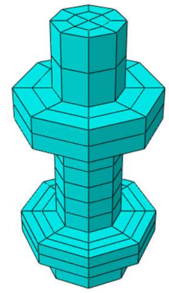

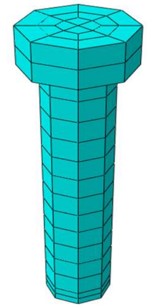

(a) Concrete slab (C3D8R) (b) Ajax bolt (C3D8R) (c) Shear connector (C3D8R)

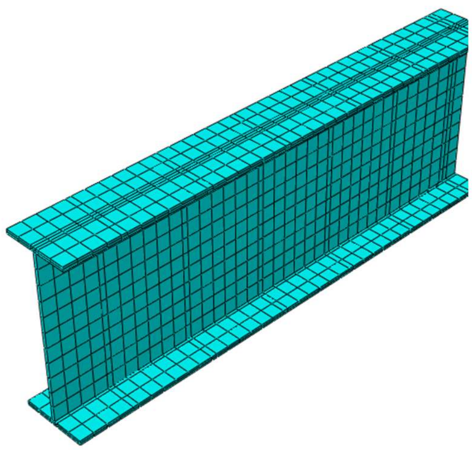

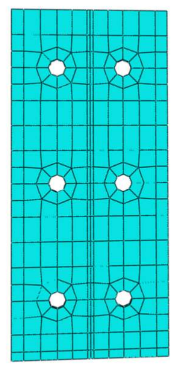

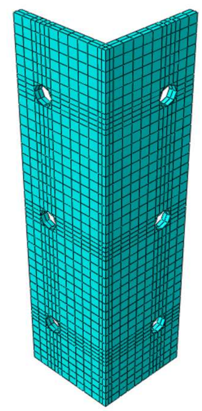

(d) Primary beam (C3D8R) (e) Flush end plate (C3D8R) (f) Equal angle (C3D8R)

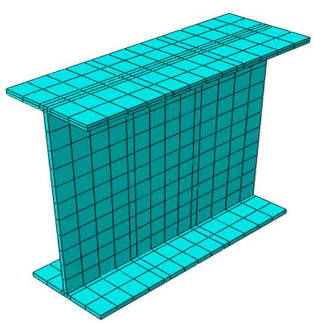

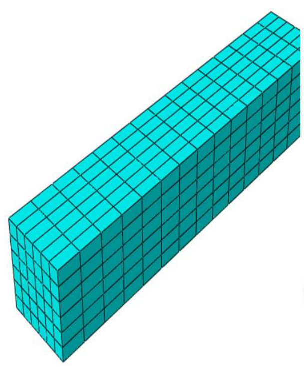

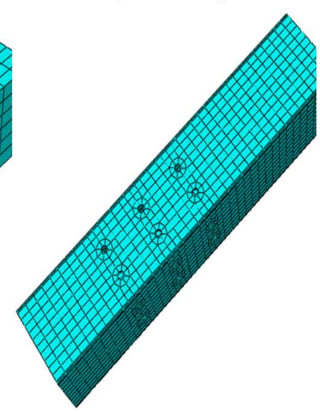

(g) Secondary beam (C3D8R) (h) In-filled concrete core (C3D8R) (i) CFST column (C3D8R)

Fig. 4.4 – Element types and meshing of various parts

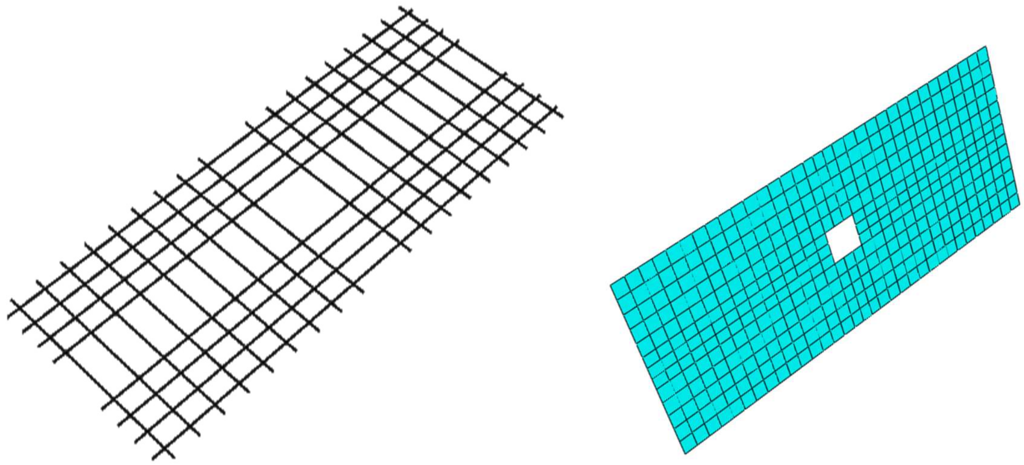

(a) Reinforcement (T3D2)

(b) Profiled sheeting (S4R)

Fig. 4.5 – Element types and meshing of truss and shell elements

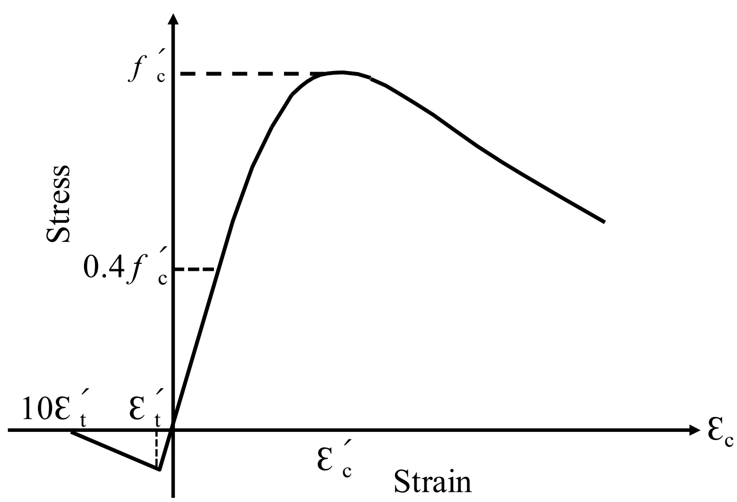

Fig. 4.6 – Stress-strain relationship of unconfined concrete under static loading

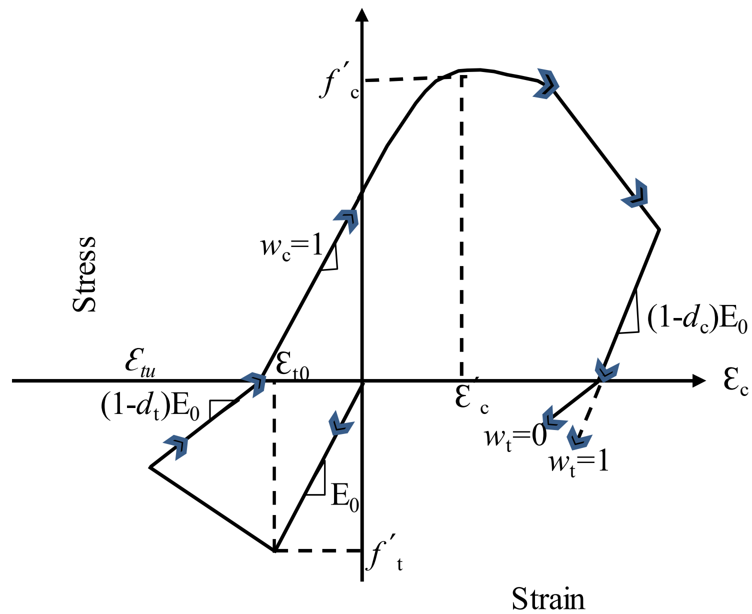

Fig. 4.7 – Stress-strain relationship of unconfined concrete under cyclic loading

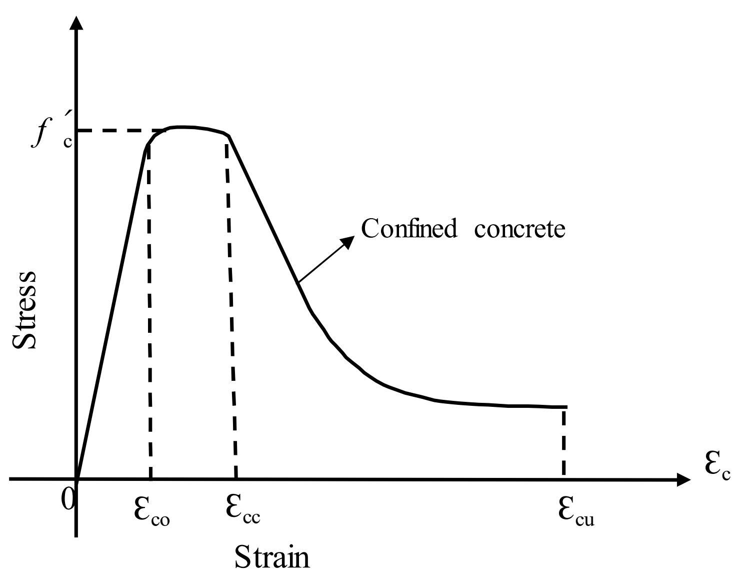

Fig. 4.8 – Stress-strain relationship of confined concrete

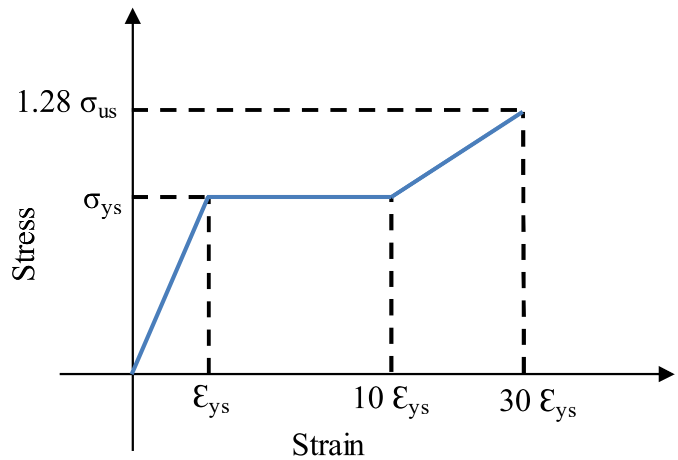

Fig. 4.9 – Stress-strain relationship of structural steel

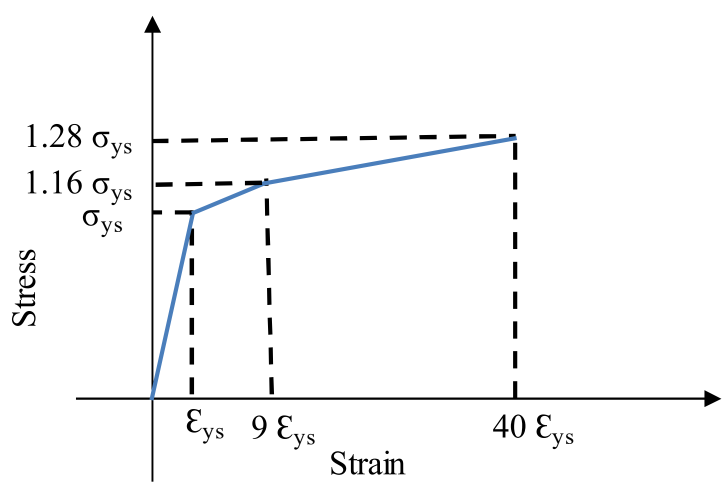

Fig. 4.10 – Stress-strain relationship of reinforcing steel

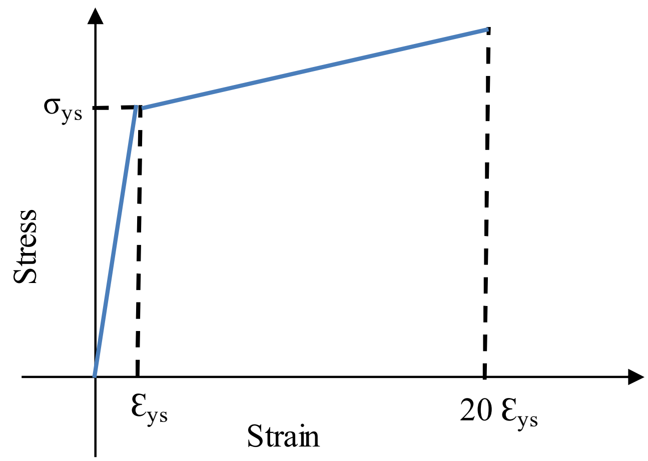

Fig. 4.11 – Stress-strain relationship of profiled steel sheeting

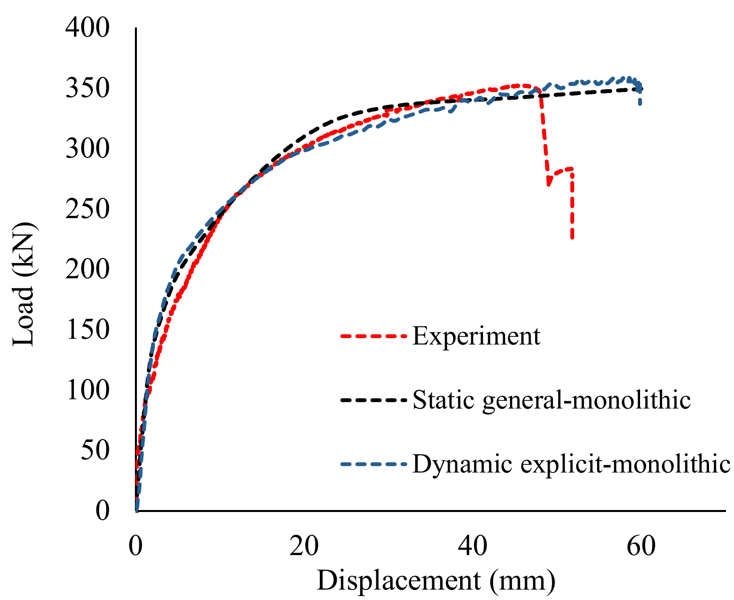

Fig. 4.12 – Load displacement results for S-1 using different analysis methods

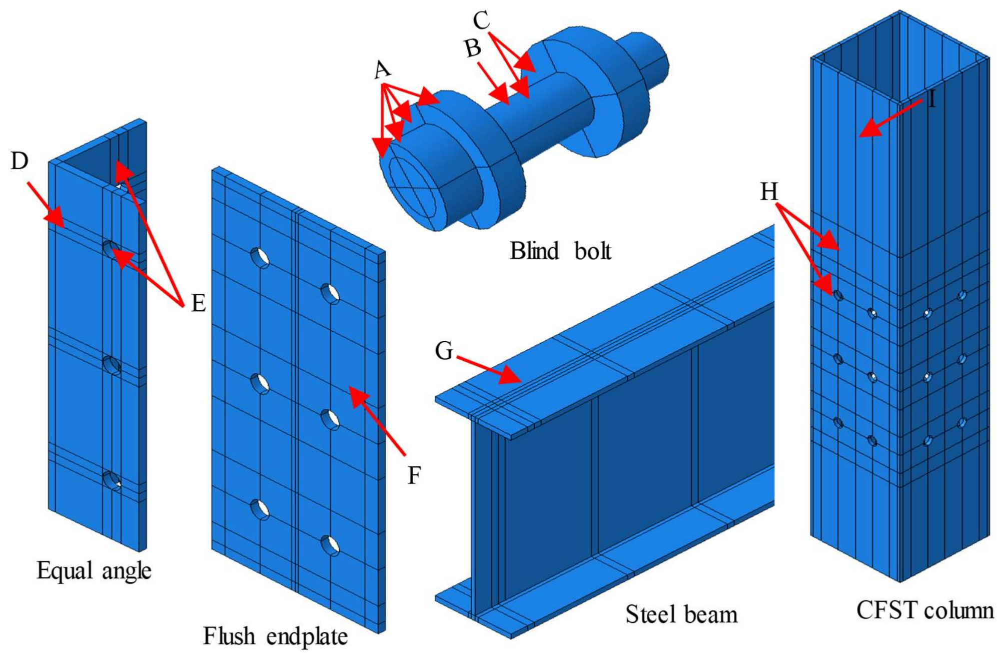

Fig. 4.13 – Contact interactions

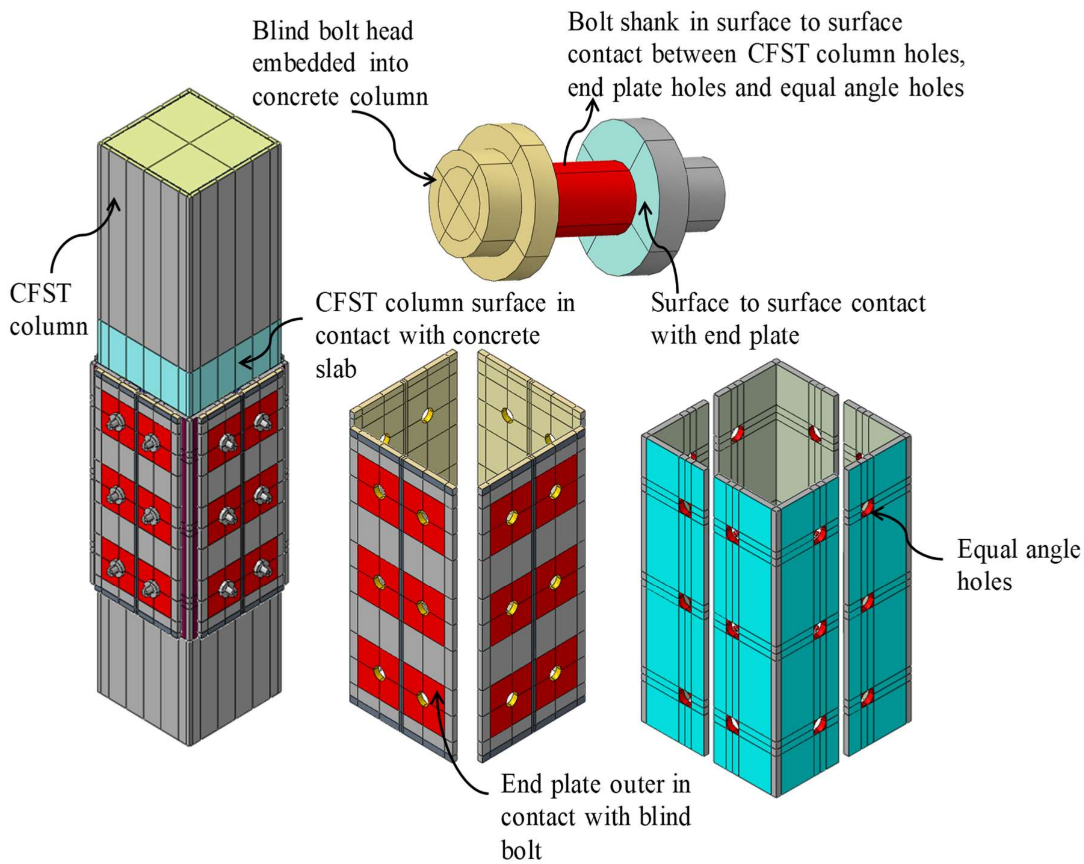

Fig. 4.14 – Contact between blind bolt, steel column, flush endplates and equal angles

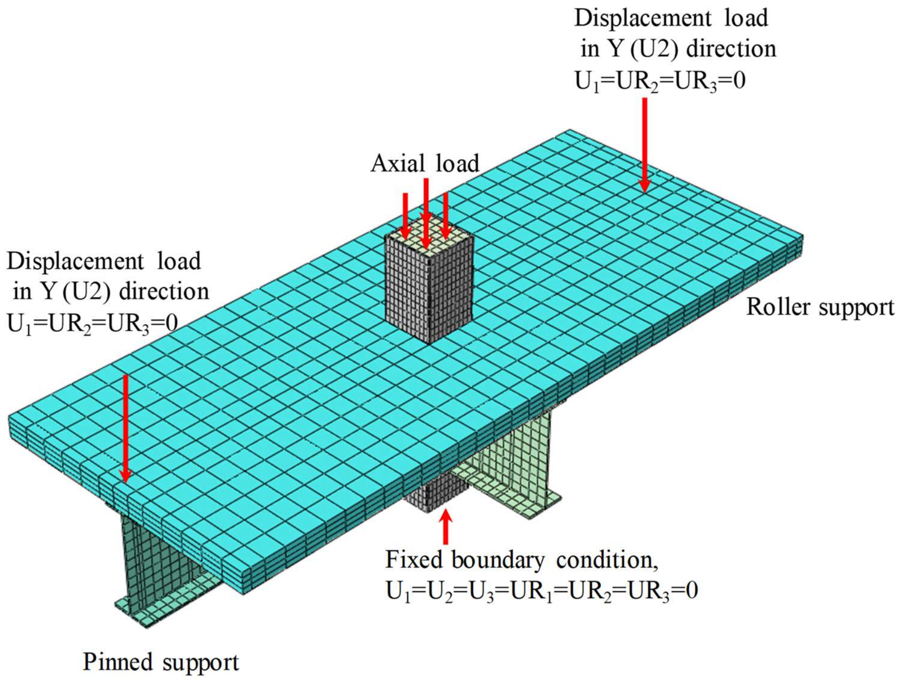

Fig. 4.15 – Loading and boundary conditions

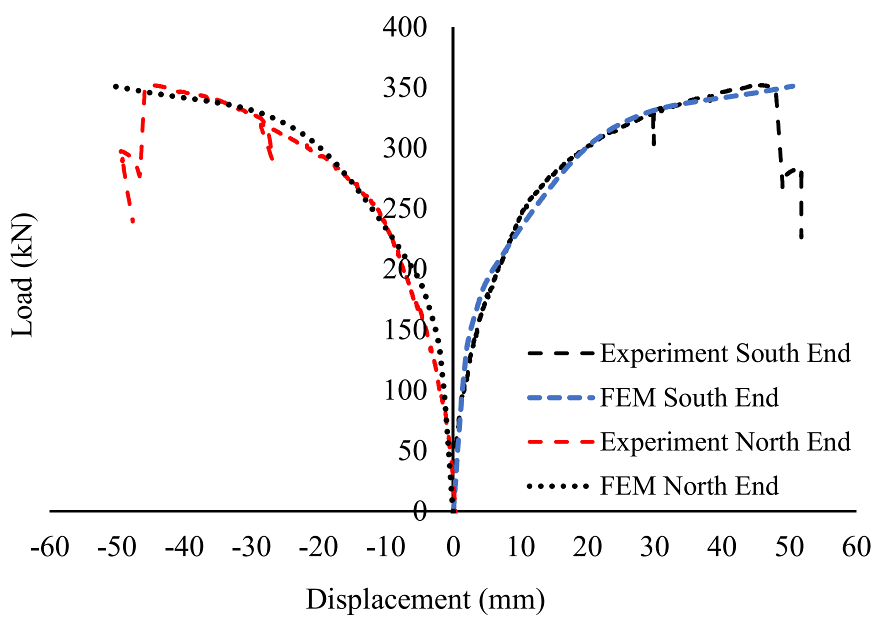

Fig. 4.16 – Comparison of load-displacement relationship of S-1 under static loading

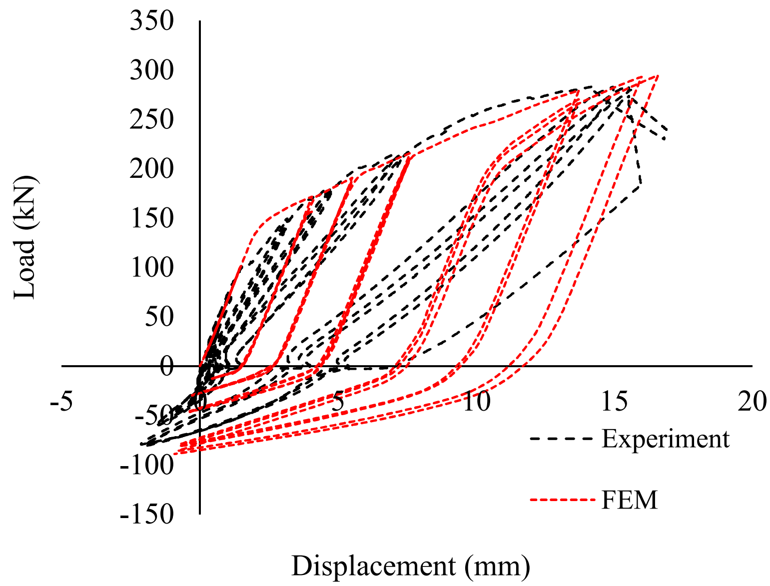

Fig. 4.17 – Comparison of load-displacement relationship of S-2 under cyclic loading

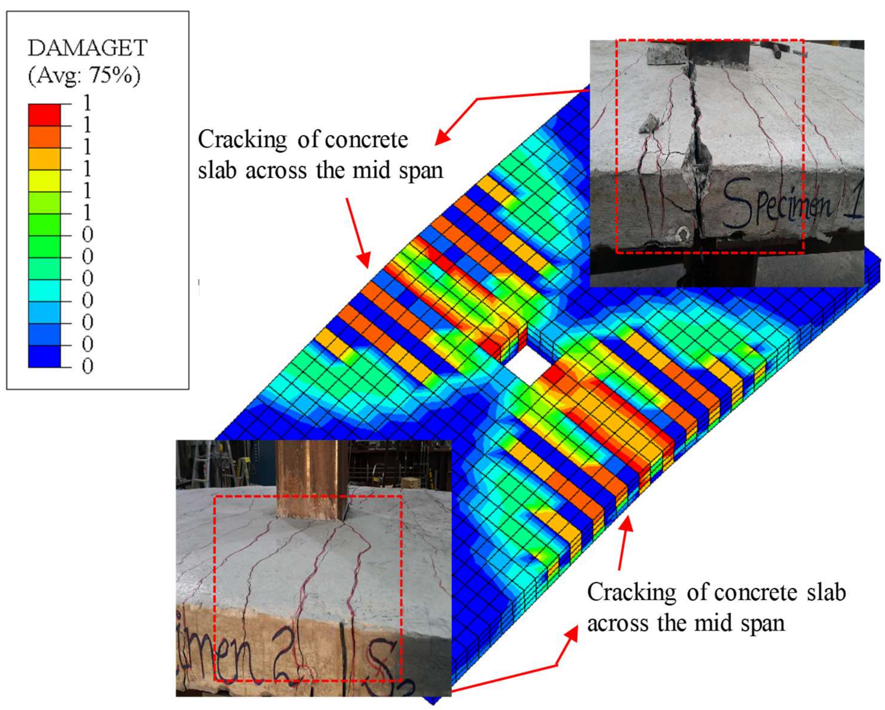

Fig. 4.18 – Cracking of concrete slab, Experiment versus FE model

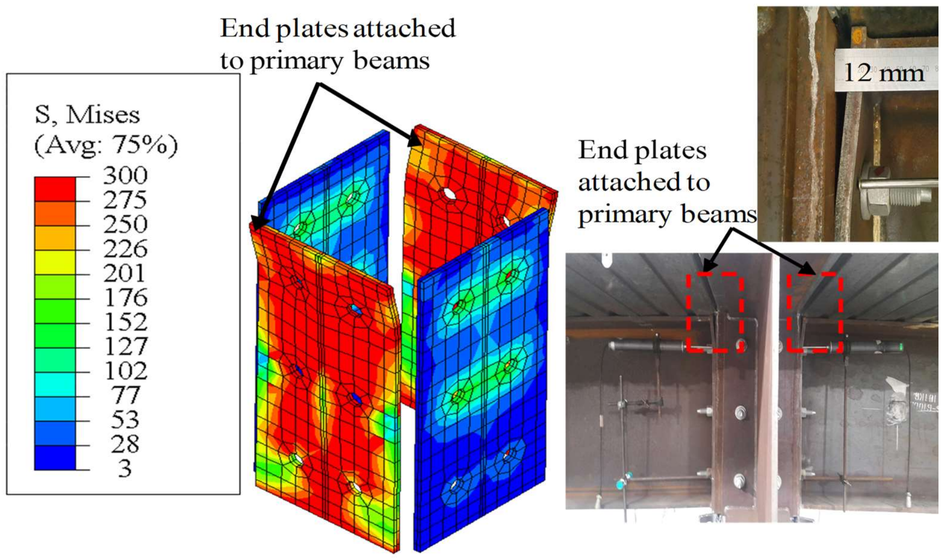

Fig. 4.19 – Bending of top of flush endplate, Experiment versus FE model

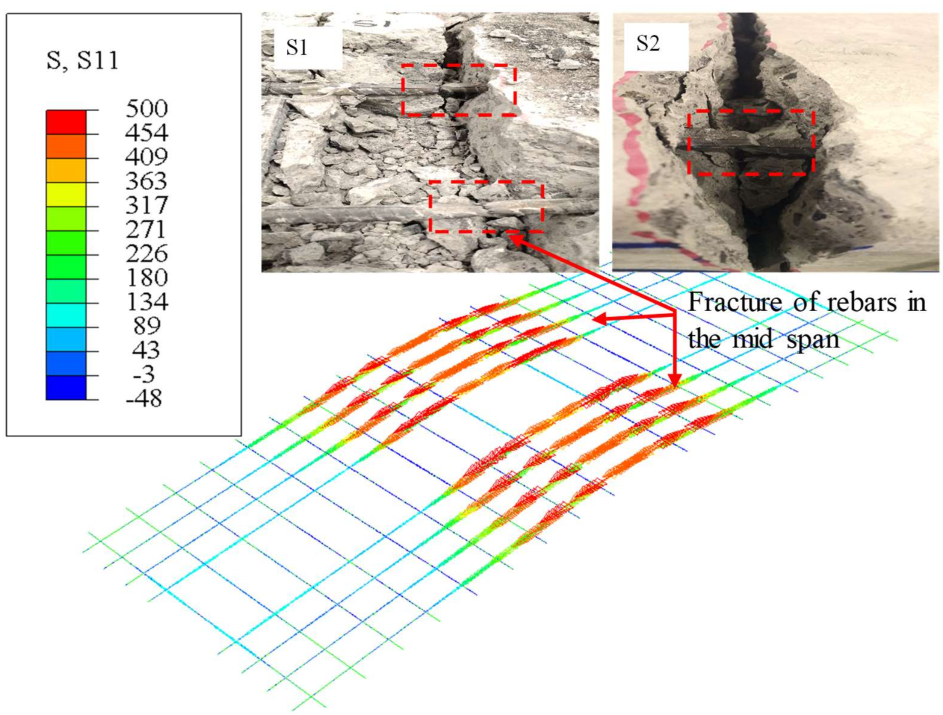

Fig. 4.20 – Failure mode of rebars for S-1 and S-2, Experiment versus FE model

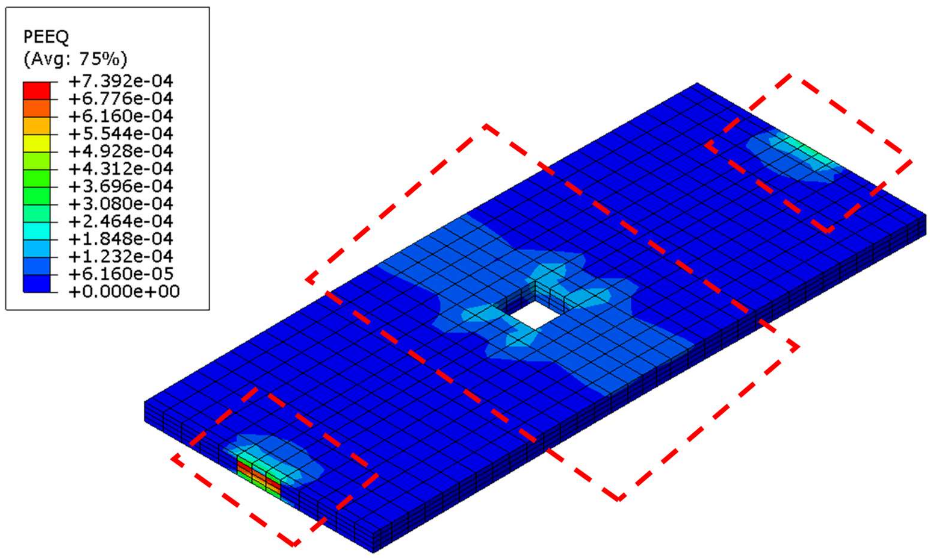

(a) S-1

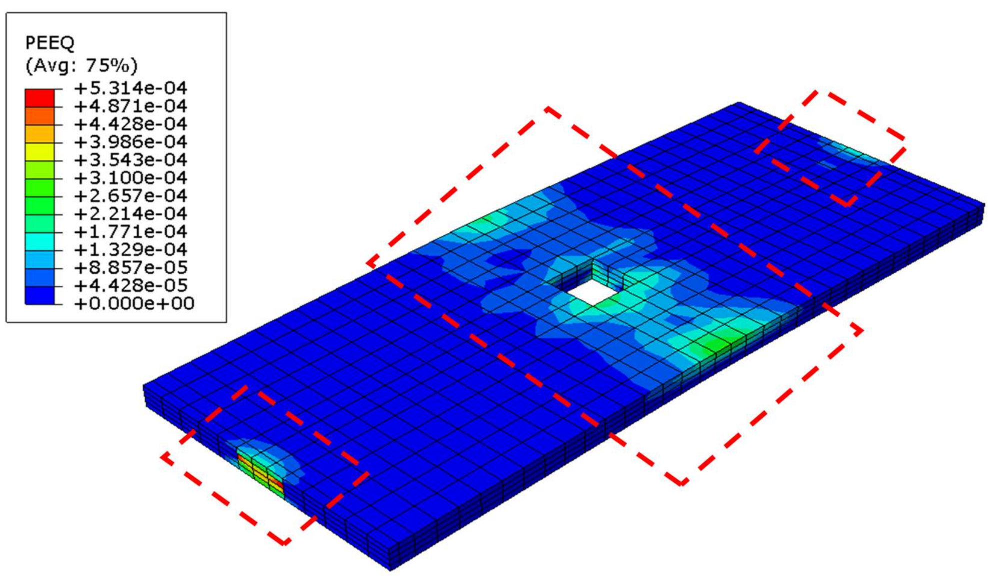

(b) S-2

Fig. 4.21 – Stress propagation in slab

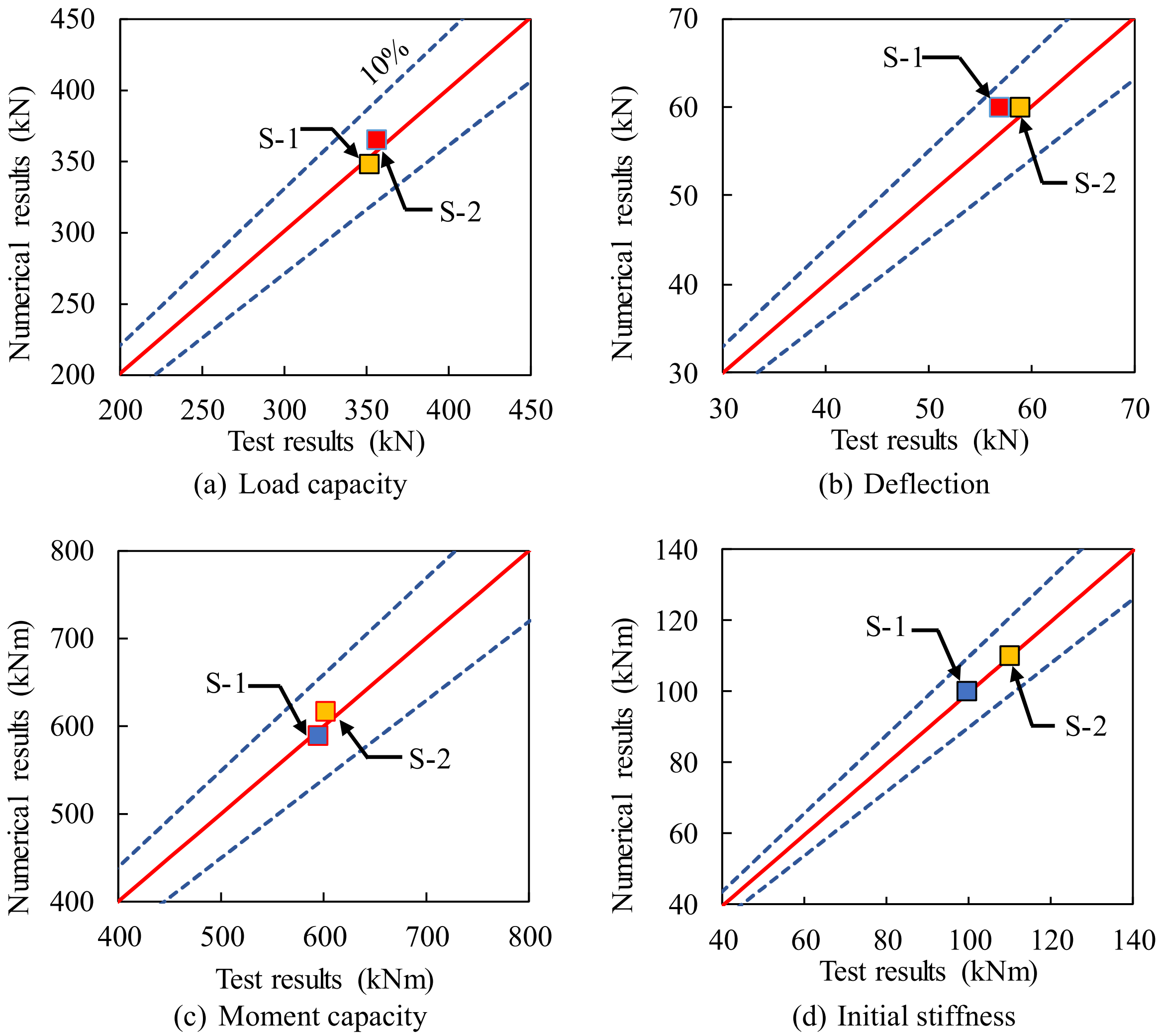

Fig. 4.22 – Comparison between test and numerical results

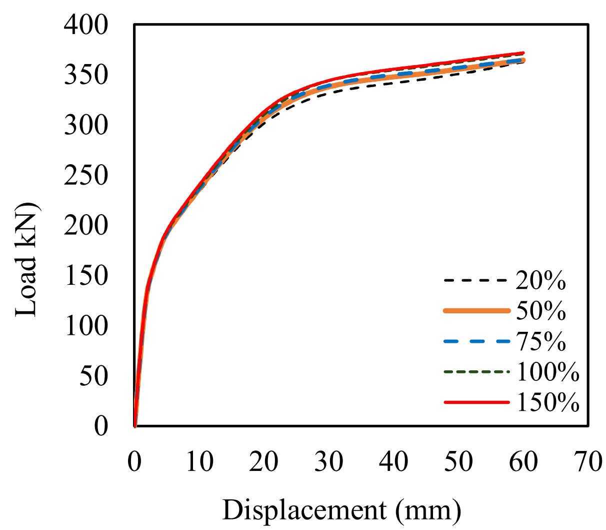

(a) Effect of different pretension force

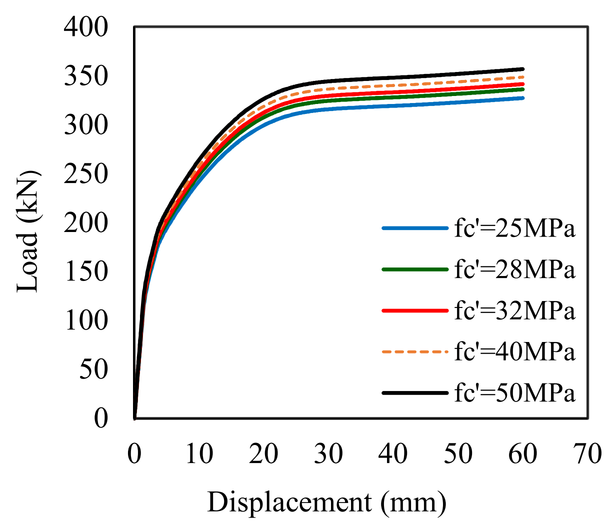

(b) Effect of different compressive strengths of concrete

Fig. 4.23 (a, b) – Parametric studies on various material related parameters

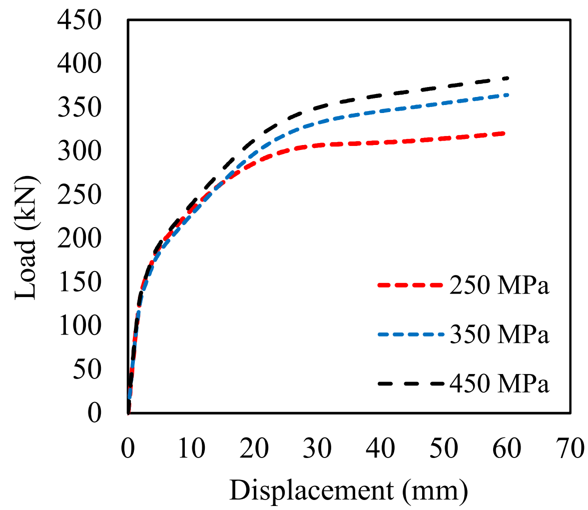

(c) Effect of different grades of steel

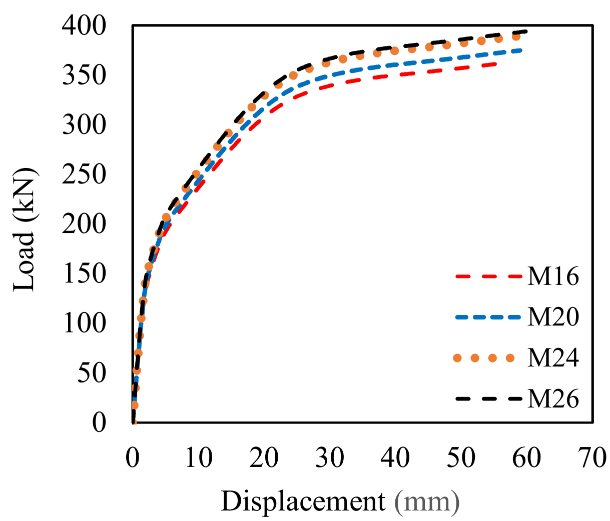

(d) Effect of different diameters of blind bolts

Fig. 4.23(c, d) – Parametric studies on various material related parameters

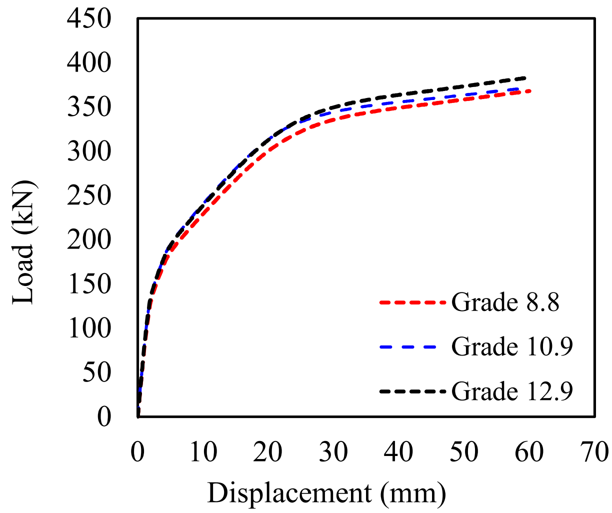

(e) – Effect of different grades of blind bolts

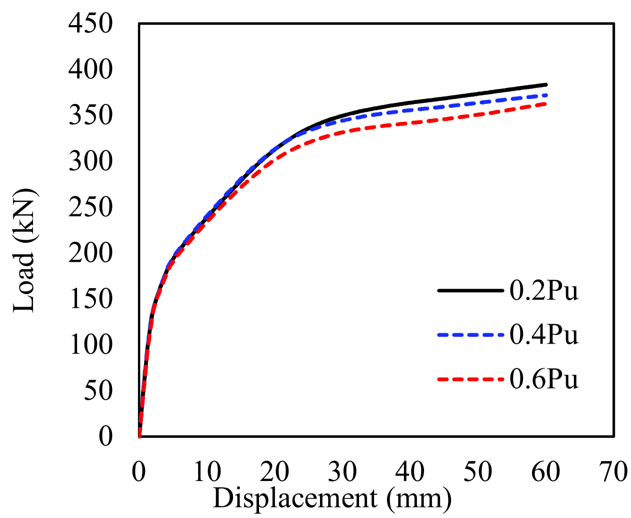

(f) – Effect of axial load on CFST column

Fig. 4.23(e, f) – Parametric studies on various material related parameters

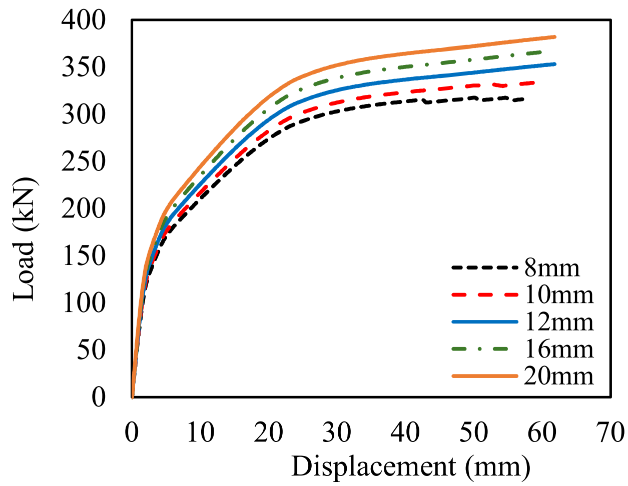

(a) – Static loading

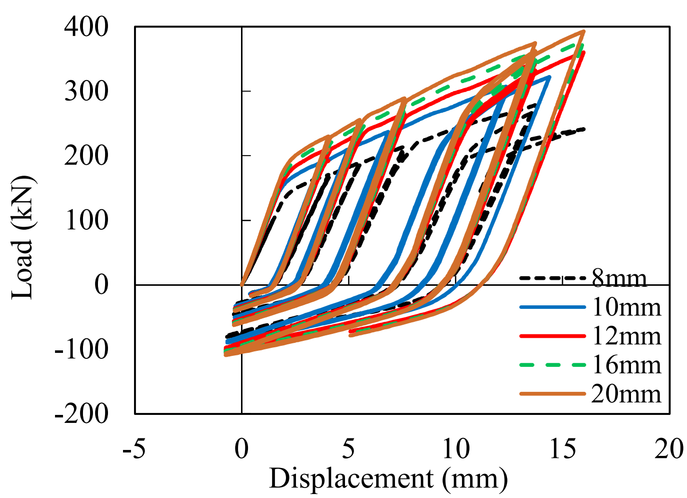

x

(b) Cyclic loading

Fig. 4.24 – Effect of the thickness of flush end plates

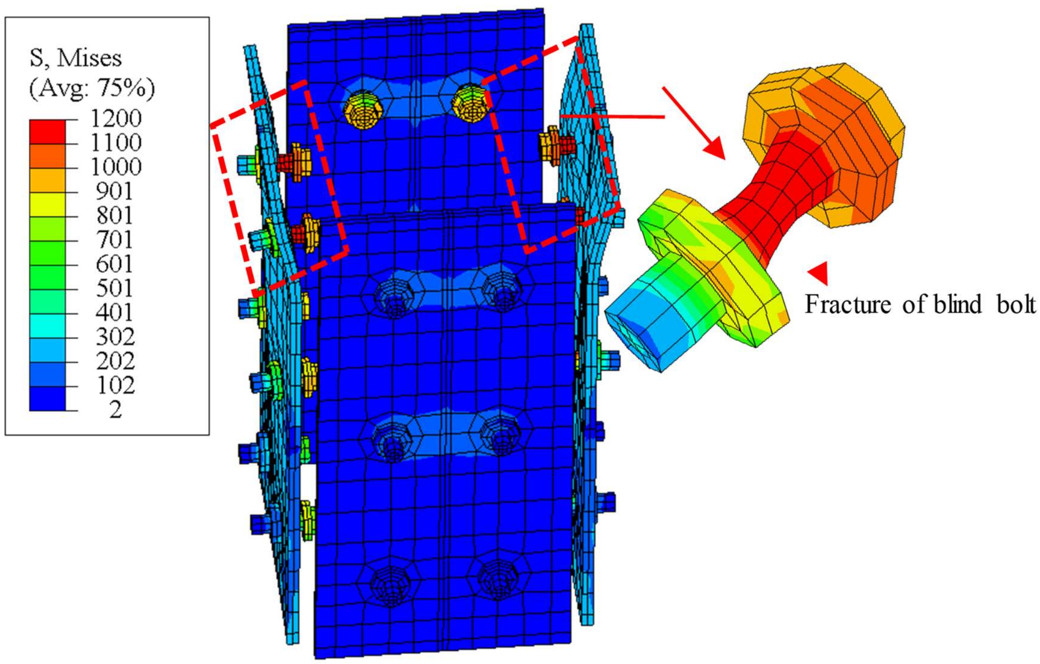

Fig. 4.25 – Failure of blind bolts connected to the primary beams in top row

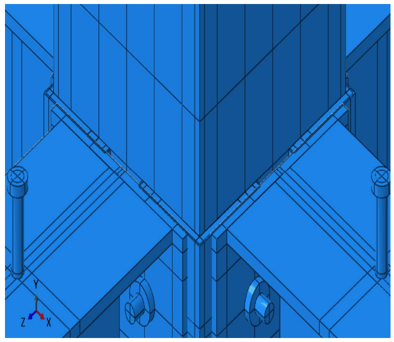

(a) t=8 mm

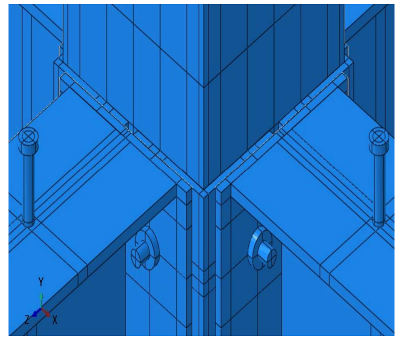

(b) t=10 mm

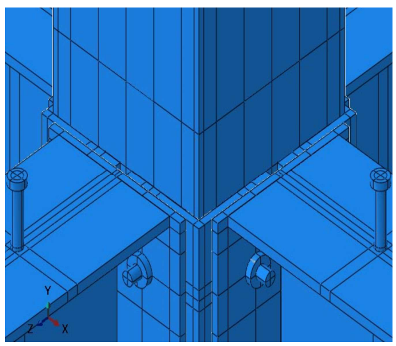

(c) t=12 mm

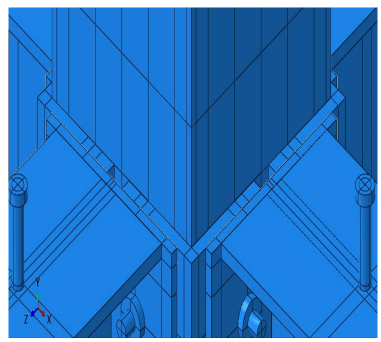

(d) t=16 mm

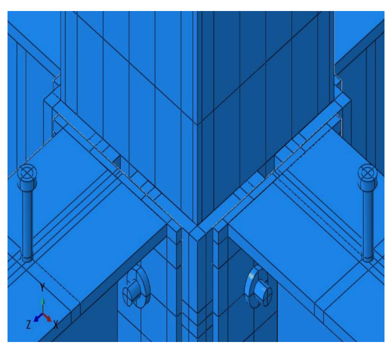

(e) t=19 mm

Fig. 4.26 – FE models with different thicknesses of equal angles

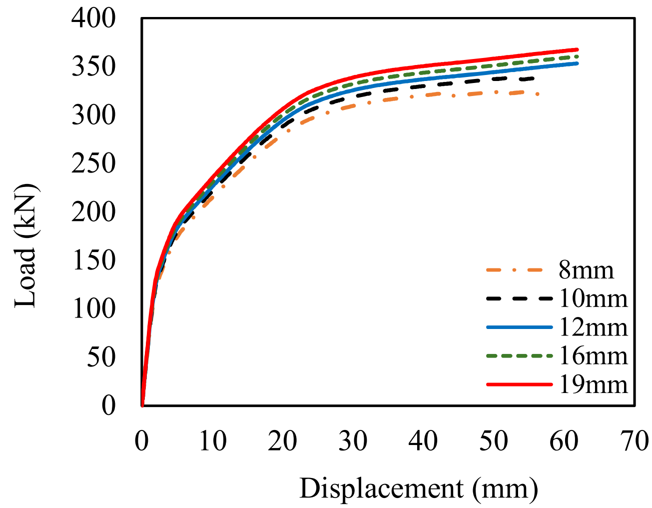

(a) Static loading

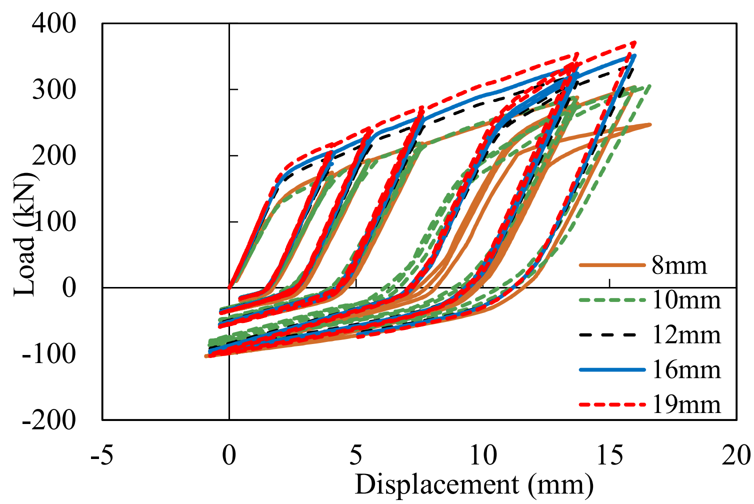

(b) Cyclic loading

Fig. 4.27 – Effect of the thickness of equal angles

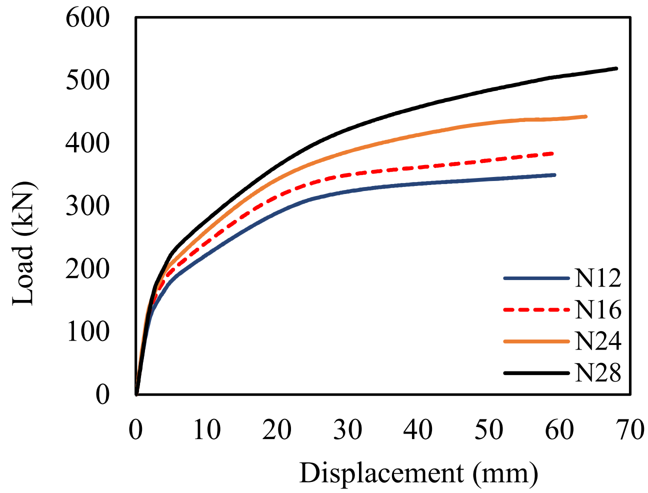

(a) Static loading

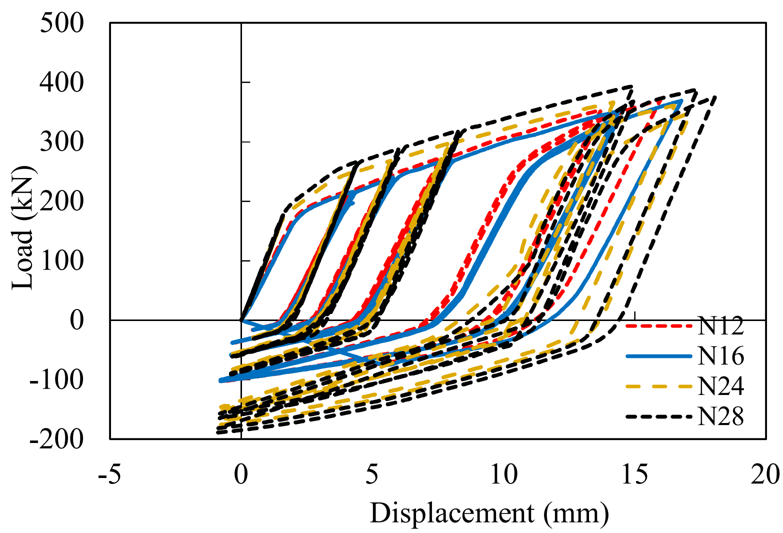

(b) Cyclic loading

Fig. 4.28 – Effect of different reinforcement ratios

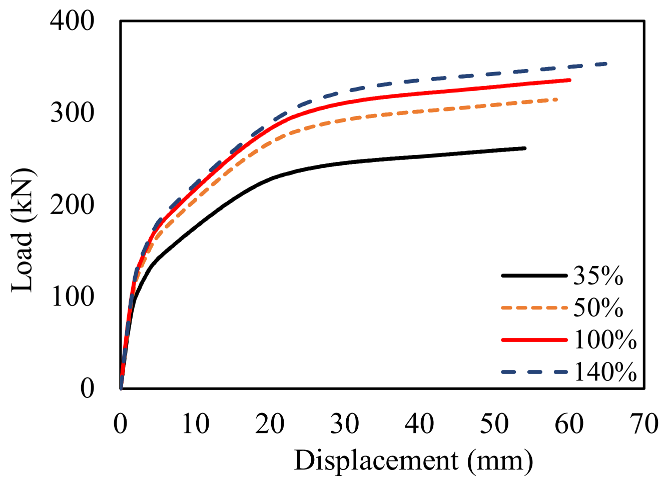

(a) Static loading

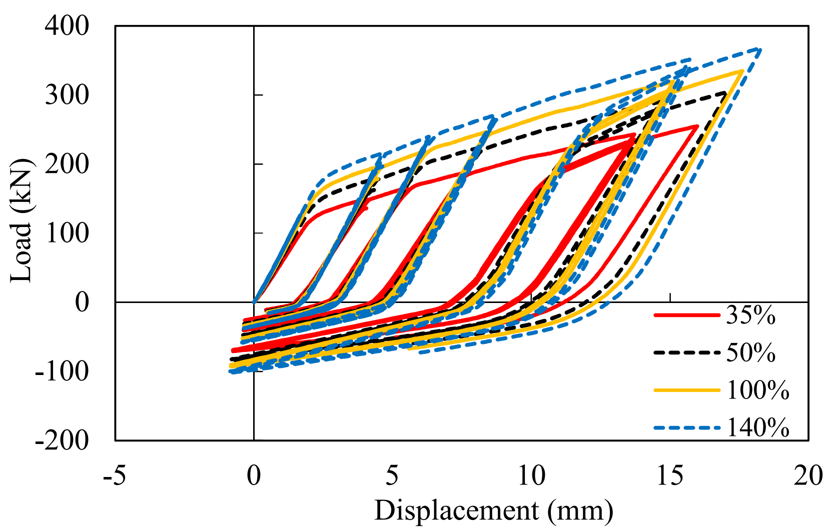

(b) Cyclic loading

Fig. 4.29 – Effect of shear connection ratio

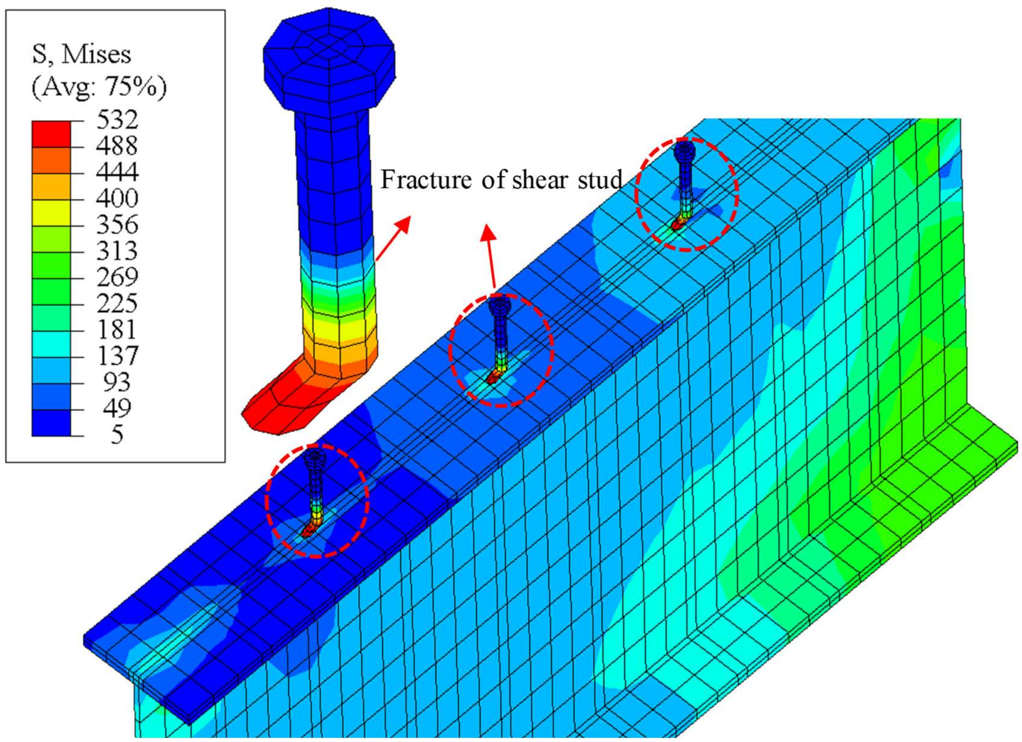

Fig. 4.30 – Failure of shear studs attached on primary beams

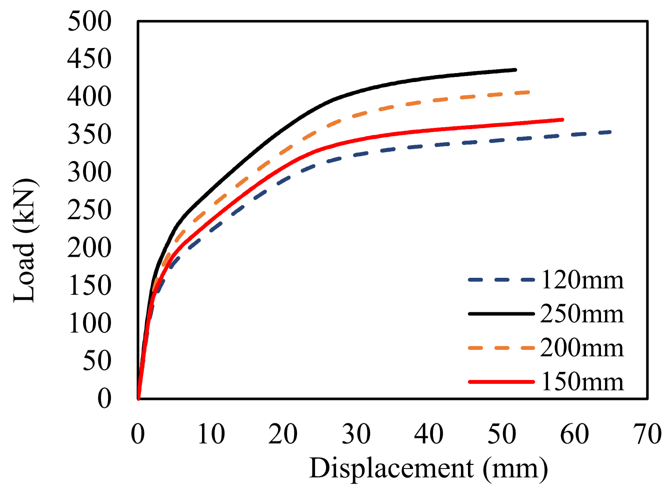

(a) Static loading

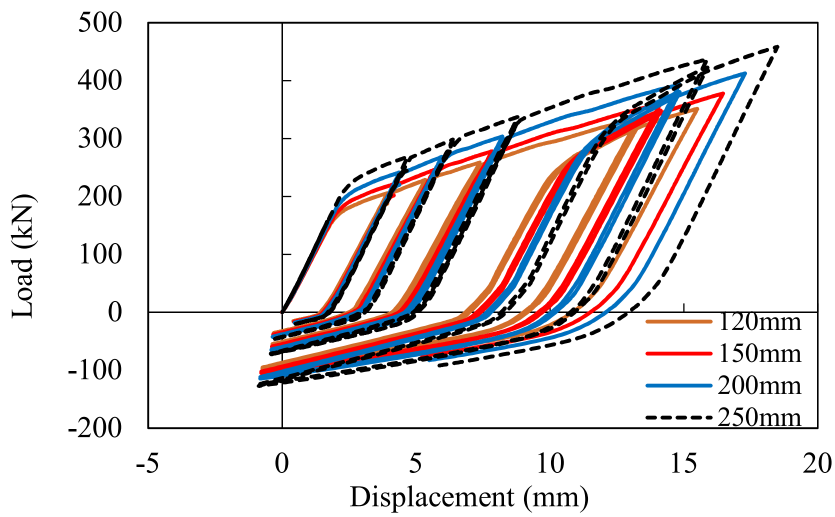

(b) Cyclic loading

Fig. 4.31 – Effect of the thickness of concrete slab

Table 4.1 – Details of S-1 and S-2

No.	Member	Dimensions
1	Steel column	SHS 300 x 300 x 10 mm
2	Concrete slab	3868 x 1600 mm
3	Endplates	270 x 610 x 12 mm
4	Equal angles	150 x 150 x 12 mm
5	Ajax blind bolts	M20 AJAX Grade 8 .8
6	Headed shear studs	19 x 100 mm
7	Primary steel beam	610UB101 x 1760 mm
8	Secondary steel beam	610UB101 x 626 mm
9	Longitudinal reinforcing	8 N12
10	Transverse reinforcing bars	19 N12

Table 4.2 – Stress-strain values for structural steel material

Element	σ_{us}	ε_{ps}	ε_{us}
Steel beam	1.28 σ_{ys}	10 ε_{ys}	30 ε_{ys}
Rebar	1.28 σ_{ys}	9 ε_{ys}	40 ε_{ys}
Profiled sheeting	_	20 ε_{ys}	_
Shear stud	_	25 ε_{ys}	_

Table 4.3 – Contact properties

Contact pair	Surfaces	Contact properties
A	Surface of blind bolt head and nut	Slave surface
	Corresponding surface of infilled concrete	Master surface
B	Surface of bolt nut and shank	Slave surface
	Inner surface of column tube and bolt hole	Master surface
C	Surface of bolt-nut attached to end-plate	Slave surface
	Outer surface of end-plate and bolt hole	Master surface
D	Outer surface of equal angle	Slave surface
	Inner surface of end plate	Master surface
E	Inner surface of equal angle	Master surface
	Outer surface of steel column	Slave surface
F	Inner surface of end plate	Slave surface
	Outer surface of steel column	Master surface
G	Surface of profiled sheeting	Master surface
	Top surface of steel beam flange	Slave surface
H	Inner surface of end-plate	Slave surface
	Outer surface of column tube	Master surface
I	Inner surface of column tube	Slave surface
	Surface of infilled concrete	Master surface

Table 4.4 – Contact types between different components

No.	Part instance 1	Part instance 2	Contact type
1	Bolt shank	Endplate hole	Surface to surface
2		Steel column hole	Surface to surface
3		Equal angles hole	Surface to surface
4	Concrete slab	Condek	Surface to surface
5		Reinforcement	Embedded constraint
6		Endplate	Surface to surface
7		Shear stud	Embedded constraint
8	Steel beam	Shear stud	Tie constraint
9		Endplate	Tie constraint
10		Condek	Surface to surface
11	Bolt	Steel hollow column	Surface to surface
12		Endplate	Surface to surface
13	Steel column	Concrete infill	Surface to surface
14		Concrete slab	Surface to surface
15		Equal angle	Surface to surface

Table 4.5 – Comparison between test results and predictions

Specimen	Moment resistance (kNm)			Initial stiffness (kNm/mrad)		
	Test	Predicted	Predicted/Test	Test	Predicted	Predicted/Test
S-1	594.88	588.5	0.98	99.74	95.93	0.96
S-2	601.64	616.9	1.02	99.25	100.02	1.01

Table 4.6 – Material related parameters selected for parametric studies

No.	Parameter	Value
1	Pretension force in blind bolts (%)	25, 50, 75, 100, 150
2	Compressive strength of concrete, f_c' (MPa)	25, 28, 32, 40, 50
3	Steel strength, f_{sy} (MPa)	250, 350, 450
4	Diameter of blind bolts (mm)	M16, M20, M24
5	Grade of blind bolt	8.8, 10.9, 12.9
6	Axial load on column (P_u)	0.2 P_u, 0.4 P_u, 0.6 P_u

Table 4.7 – Geometrical parameters selected for parametric studies

No.	Parameter	Value
1	Endplate thickness (mm)	8, 10, 12, 16, 20
2	Equal angle thickness (mm)	8, 10, 12, 16, 19
3	Reinforcement ratio (%)	N12, N16, N24, N28
4	Shear connection ratio (%)	35, 50, 100, 140
5	Slab depth (mm)	120, 150, 200, 250

CHAPTER 5

ANALYSIS OF BLIND-BOLTED COMPOSITE FRAMES

5.1. Introduction

Blind-bolted composite frames have received extensive appreciation due to significant benefits such as high moment capacity and ductility, easy fabrication and good seismic capacity and fire resistance as documented by various researchers such as Uy (2012), Ellobody and Young (2015) and Hicks and Pennington (2015).

In this research, the beam-to-column joints were innovatively designed in which one side blind bolts were used for connecting the steel beams to CFST column. The flexural performance of the beam-to-column joints have been investigated and discussed thoroughly in Chapters 3-4 through experiments and finite element models. These investigations were built on subassembly models that overlooked the global behaviour of structures. Therefore, frame analysis was performed where global assembly models were considered.

This chapter presents a simple two dimensional in-plane structural analysis of composite frames constructed with semi-rigid connections. Global models were developed for these frames using Abaqus software. Nonlinear material properties and large deformations were considered in the analysis to explore plastic behaviour of the connections under various types of loads. It is noteworthy, that the analyses were performed to establish a preliminary investigation and general understanding on the behaviour of low-rise semi-continuous unbraced frames that were exposed to various vertical and lateral design actions which mainly involved permanent and imposed actions, earthquake and wind actions. Results from the analysis were presented and discussed in detail to explore the flexural behaviour of these buildings under various circumstances. The results from this study contribute to provide useful guidelines for the design of these frames in future.

5.2. Frame analysis

5.2.1. General description

The frame models were constructed with three main components including the converted columns, converted beams and semi-rigid connections. The composite joint under consideration was a flush endplate joint designed under hogging moment and full shear connection in accordance with EN 1994-1-1 (2004). Four 610UB101 steel beams were connected to a 300×300 mm square hollow section column in a cruciform arrangement that represents the internal region of a composite frame. 12 mm thick equal angle sections were welded to the sides of CFST column with the help of the innovative one-side blind bolts. Four 12 mm thick flush endplates were welded to the steel beams and connected to the steel tubular columns with the help of M20 blind bolts. A 3868 mm×1600 mm×120 mm reinforced concrete slab was placed on the top. Semi-rigid connections were used to connect CFST columns with the composite beams. The details of the composite joint are presented in Chapter 3.

In the beginning, the selected column cross section was 400×400×8 mm with Grade 350. the beam section used was 460UB82.1 with Grade 350 while the thickness of concrete slab was 120mm with compressive strength of 40 MPa.

The research focussed on the engineering practice in Australia with moderate seismic actions. Therefore, low-rise frames of less than five stories were selected for the analysis. For simplicity, the frames were designed to keep the same numbers of bays in the orthogonal direction. Fig. 5.1 presents the elevation and plan view of a 3 bay by 3 storey frame model of a prototype building designated as an office building that is presented as the main case study herein. The floor plan of the building was 27 m × 27 m with three bays of 9 m length in each direction. The building consisted of three storeys with each being 4 m in height. The general details of the composite frame are presented in Table 5.1. The longer bay span makes it more demonstrative of the Australian building practice. The size of beams and columns were chosen that were commonly used in building practice.

It was observed that, even though the number of bays were kept same in both directions, the presence of continuous floor slab and secondary beams resulted in higher stiffness in out-of-plane direction as compared with the in-plane direction. Torsional behaviour or any out-of-plane effects can be considered to be insignificant. Hence the analysis can be simplified as a two-dimensional analysis considering in-plane direction as shown in Fig. 5.2. The actual values of wind and earthquake loads acting on the frame are shown in Fig. 5.3.

5.2.2. General analysis procedure

A flowchart of the frame analysis procedure is presented in Fig. 5.4. It can be broadly divided into three stages. Stage 1 comprised of different calculations that were pre-requisite for the analysis. It consisted of the calculations of design loads and load combinations according to the Australian Standards AS1170.0 (2002), AS/NZS 1170.2 (2011) and AS/NZS 1170.4 (2007). Initial stiffness and moment capacity of the joint were calculated and moment rotation models were developed. The composite beam and composite column were converted to an equivalent section of steel beam and steel column that were representative of similar cross-sectional properties as their composite counterpart. In second stage, the frame models were developed in Abaqus considering all geometrical and material nonlinearities. All the information calculated in Stage 1 was input into the software and the analysis was performed. The final stage involved interpretation of the results generated from the analysis and inspecting them against the limit state criteria from the Australian standards.

The design and analysis of the components ran in parallel as the moment distribution was affected by the stiffness and second moment of area. Hence, the component sizes were assumed at the beginning of the analysis. The results were checked against the design provisions specified in Australian standards and Eurocodes. If the results satisfied the requirements, they were accepted otherwise the frame was redesigned until the criteria were met. The analysis process involved hit and trial and was repeated unless a frame configuration was achieved that satisfied the limit states and did not involve overestimation of the member sizes.

5.3. Development of moment rotation model

5.3.1. Prediction of initial stiffness

An accurate analysis of the frame depends on the correct prediction of the initial stiffness of the connection. The analytical model developed by Thai and Uy (2016b) was used to calculate the stiffness coefficients of various components of the connection which are identified in **Chapter 2 "**Literature review" in Fig. 2.7. Fig. 2.8 presents the stiffness model for the flush endplate joint developed by Thai and Uy (2016b) that has two rows of bolt in tension and was used in this study for calculating the initial stiffness of the composite joint.

For a composite joint, the rotational stiffness should be calculated based on the flexibility of its basic joint components as expressed in Eq. (5.1). Each of these components is denoted by an elastic stiffness coefficient k_i, as stated in EN 1993-1-8 (2010). The specific stiffness of each joint components is highlighted in Fig. 2.8 as k_1, k_2, k_3, k_4, k_5, k_{10}, $k_{s,r}$, $k_{sc/Es}$. The initial stiffness of the joint can be calculated using the following mathematical equations

$$S_{ini} = \frac{Ez_{eq}^2}{\frac{1}{k_1} + \frac{1}{k_2} + \frac{1}{k_{eq}}} \tag{5.1}$$

where E is the Young's modulus of steel, k_{eq} is the equivalent stiffness coefficient and z_{eq} is the lever arm. k_1 and k_2 are infinite due to the presence of infill concrete. Therefore, Eq. (1) can be simplified as follows.

$$S_{ini} = \frac{Ez_{eq}^2}{\frac{1}{k_{eq}}} \tag{5.2}$$

The detailed calculation of initial stiffness is presented in **Appendix A.**

5.3.2. Prediction of design moment resistance, $M_{j,Rd}$

For a beam-to-column joint with a bolted end-plate connection, the design moment resistance can be calculated in accordance with EN 1993-1-8 (2010) as follows

$$M_{j,Rd} = \sum h_r F_{tr,Rd} \tag{5.3}$$

where, $F_{tr,Rd}$ is the effective design tension resistance of the bolt row r in consideration, h_r is the distance from bolt row to the center of compression and r is the number of bolt row. EN 1993-1-8 (2010) states that the effective design tension resistance $F_{tr,Rd}$ of a bolt row should be selected as the lowest value of the design tension resistance for an individual bolt row of the following components

- Column web in tension, $F_{t,wc,Rd}$
- Column flange in bending, $F_{t,fc,Rd}$
- Reinforcement in tension, $F_{t,r,Rd}$
- Endplate in bending, $F_{t,ep,Rd}$
- Beam web in tension, $F_{t,wb,Rd}$

Each of these components can be calculated in accordance with the procedure presented in EN 1993-1-8 (2010). The method for calculation is presented in detail in **Appendix B.**

5.3.3. Moment-rotation model

A design moment rotation curve should represent three major structural properties which are moment resistance, initial stiffness and rotation capacity. EN 1993-1-8 (2010) describes a joint in terms of a rotational spring that connects the center line of all the connecting members at a point of intersection as presented in Fig. 5.5.

The moment rotation curve can be broadly classified according to three major stages. The first stage is the elastic stage and its slope is equal to the initial stiffness of the joint that is presented in Eq. (5.1). The second stage is the inelastic stage and the third stage relates to the strain hardening behaviour. Ghobarah *et al.* (1996) and Azizinamini *et al.* (1987) proposed that there is a relationship between the elastic response and the strain-hardening response that can be termed as the stiffness in the strain-hardening stage $S_{j,pc}$. This stiffness can be calculated by multiplying the initial stiffness with a coefficient such as $\varphi S_{j,ini}$.. The coefficient φ has different values according to the type of the structure under consideration.

Consequently, a nonlinear analytical model was required to predict the inelastic response. The moment capacity was predicted using two different models as discussed by Wang *et al*. (2018). The method adopted follows the guidelines from EN 1993-1-8 (2010) to predict the moment-rotation behaviour in the elastic stage whereas the model developed by Yee and Melchers (1986) was used for the inelastic and strain hardening stage. The slope of the inelastic stage can be determined as follows

$$S_j = \frac{Ez^2}{\mu \sum_i \frac{1}{k_i}} \tag{5.4}$$

where, k_i is the stiffness coefficient for basic joint component, z is the lever arm, μ is the stiffness ratio, $S_{j,ini} / S_j$ and its value is considered as 1 for the calculation of initial stiffness. According to EN 1993-1-8 (2010) two thirds of the moment capacity defines the maximum limit for the elastic stage. After that the initial stiffness will be reduced by the factor μ defined as

$$\mu = \left(\frac{1.5 M_{j,Ed}}{M_{j,Rd}} \right)^{\Psi} \tag{5.5}$$

5.4. Component properties

The frame consisted of three major structural components that are composite beams, composite columns and semi-rigid joints.

5.4.1. Composite beams

Fig. 5.6 presents the representation of sagging and hogging moment regions which are two distinctive regions in a structure. The mid span regions are subjected to positive or sagging moments in which the concrete slab is in compression while steel is in tension. However, the force distribution of a joint subjected to hogging or negative moments is opposite to this scenario. Under hogging moments, concrete is considered as being cracked in tension and contributes very little to the strength while the compressive forces are primarily transferred through the beam. The concrete slab was presumed to be cracked and have no tensile strength in the hogging moment region. EN 1994-1-1 (2009) suggested the length of hogging moment region to span 15% of the beam length on each side of the internal support. It has been found from studies by Liew et al. (2001) to be sufficiently accurate for the elastic analysis of composite frames. Hence, this cracked length of $0.15L_b$ was adopted in this study to check the ultimate and serviceability limit states as highlighted in Fig. 5.6. Furthermore, the same length of hogging moment region was selected in studies by (Loh, 2004). As the composite section cannot be directly defined in Abaqus software (Abaqus 2012), therefore it was converted to an equivalent steel section that had the same stiffness and cross-sectional properties using modular ratio, α_m.

$$\alpha_m = \frac{E_s}{E_c} \tag{5.6}$$

Fig. 5.7 presents a general description of the cross-section conversion of composite beam to equivalent steel beam. The effective width of the composite slab was calculated separately for hogging and sagging regions based on the guidelines of EN 1994-1-1 as follows

$$b_{eff} = b_0 + \frac{0.5L_b}{8} + \frac{0.5L_b}{8} \tag{5.7}$$

$$b_{eff} = b_0 + \frac{0.7L_b}{8} + \frac{0.7L_b}{8} \tag{5.8}$$

where b_0 is distance between centers of outstand shear connectors. L_b is span of beams between columns. The effective width of concrete slab at hogging moments was 1125 mm whereas for sagging moment region it was 1575 mm. Moreover, EN 1998-1 (2004) proposes a different method to calculate effective width when considering seismic actions on the frames. According to that the effective width of concrete slab was calculated as 1800 mm for hogging and 1350 mm for sagging region. The cross-section area of concrete slab for sagging and hogging moment regions was calculated according to EN 1994-1-1 which was used to calculate the transformed cross-section area of the composite beam individually for both regions as follows.

$$A_0 = A_s + \frac{A_{ce}}{\alpha_m} \tag{5.9}$$

After that, the location of neutral axis and second moment of area of the converted composite beam for both regions was calculated. The details of the converted cross-section are presented in Table 5.2.

The composite section cannot be directly defined in Abaqus software (Abaqus 2012), therefore it was converted to an equivalent steel section that had the same stiffness and cross-sectional properties. Detailed calculations for the cross-section conversion are provided in **Appendix C**. As EN 1994-1-1 (2009) provides different equations to calculate the effective width for both hogging and sagging moment regions, therefore the conversion of sectional properties was performed discretely for both regions. The effects of creep and shrinkage of concrete was also considered for the long-term behaviour of composite beams.

The concrete slab was designed as 120 mm thick and nominal compressive strength of 40 N/mm^2. The yield stress for structural steel and reinforcing steel was taken as 350 Mpa and 500 MPa and ultimate strength was 430 Mpa and 600 Mpa respectively.

5.4.2. Composite columns

The width to thickness ratio of concrete filled steel tubular columns was kept less than 60 as it generally allows the full cross-section of steel to be effective according to Uy (1998). Just like composite beams, the CFST columns were also transformed into equivalent sections. According to EC4, the effective flexural stiffness of composite columns can be determined as follows.

$$(EI)_{eff} = K_0(E_a I_a + E_s I_s + K_e E_{cm} I_c) \tag{5.10}$$

where E_a and I_a are elastic modulus and second moment of area of steel tube respectively. E_s and I_s are elastic modulus and second moment of area of reinforcements respectively. E_{cm} and I_c are secant modulus and second moment of area of infilled concrete core respectively. K_o is a correction factor that is taken as 0.5. K_e is a calibration factor that is taken as 0.9 in accordance with EC4. Since there was no reinforcement present inside the CFST column, so its effect can be ignored. Eq. (5.10) can be rewritten as

$$(EI)_{eff} = k_0 (E_s I_s + k_e E_{cm} I_c) \tag{5.11}$$

As opposed to reality, the base columns were assumed to have fixed supports. This assumption of rigid base has also been made previously by Hensman and Nethercot (2001, 2002), Thai *et al*. (2016a) and Wang *et al*. (2018). Although a fully rigid connection is not achievable in reality, the degree of flexibility can be ignored if the base connections are designed properly.

5.4.3. Semi-rigid joints

In conventional analysis of frames, the behaviour of beam-to-column joints is considered as either rigid or pinned. However, in reality most connections used are semi-rigid in nature and experience moment capacities and rotational stiffnesses in the middle of the two extremes specified in EN 1993-1-8 (2010) and EN 1994-1-1 (2009) as illustrated in Fig. 5.8. The modern design codes such as EN 1993-1-8 (2010) and AISC-LRFD have formally recognized and accepted the consideration of semi-rigid behaviour in joints in order to reflect the actual situation. Thai *et al*. (2016a) and Aribert and Dinga (2002). Hence, the need arises to determine the key properties of the connection to be included in the frame analysis and design. Therefore, a proper finite element model was developed that involved semi rigid connections to connect beams to CFST columns in order to accurately simulate the behaviour of beam-to-column joints.

5.5. Design loads and load combinations

Four general types of loads were considered.to be acting on the frame which were dead loads (G), live loads (Q), wind loads (W) and earthquake loads (F_{eq}). These loads were calculated in accordance with AS/NZS 1170.0 (2002) . Table 5.3 summarises load combinations whereas the values of design loads calculated for a 3storey-by-3bay frame are presented in Table 5.4 . Both strength limit state and serviceability limit state were taken into consideration.

5.5.1. Dead load and live load

Dead loads consisted of the self-weight of the structural components such as concrete slab, steel beam and superimposed dead load of 1 kPa. Live load of 3 kPa was considered for an office building according to AS/NZS 1770.1 (2002) that was uniformly distributed on each floor. On the roofs, only dead load was considered to be acting.

5.5.2. Wind actions

The latest version of AS 1170.2 presents a generalized and more simplified procedure for the calculation of wind loading on building structures. The wind speed is calculated based on the annual probability of exceedance. The detailed calculations are described in **Appendix D.**

For wind loads, the critical design wind speed of 50-year design working life and 1/1000 years annual probability of exceedance was selected in the analysis according to AS/NZS 1770.2 (2011). The assumptions made for load calculations represent the maximum probable values that can be practically critical to the frame. Wind pressure was calculated that considered the combined effects of external and internal wind pressure acting on the frame and windward and leeward wall pressures were determined. These pressures were then converted to equivalent point loads acting on each of the floor as shown in Fig. 5.3.

5.5.3. Earthquake actions

Similarly, the earthquake actions were determined using AS/NZS 1170.4 (2007) based on a 50-year design period and 1/2500 annual probability of exceedance. Gibson and McCue (2001) illustrates that the prediction of earthquakes in Australia is quite uncertain and the standard event of 1 in 500 year is extremely minor and almost imposes no harm to properly designed structures. Hence, AS/NZS 1170.4 (2007) has extended the return period factor k_p *to* include events up to 1-in-2500 years by multiplying the site hazard factor by 1.8. Therefore, in order to avoid catastrophic failures to buildings and loss of lives, a higher earthquake loading level must be incorporated in the design of buildings and is also considered herein.

The total horizontal base shear was calculated initially which was later distributed as point loads with linearly increasing increments to each floor. The calculated earthquake design loads acting on each storey of the frame are presented in Table 5.4. the detailed procedure of calculating earthquake actions is outlined in **Appendix E**.

5.6. Sway deflection limit

In order to satisfy the serviceability requirement for an unbraced frame, a limit is imposed on the storey drift which is known as the horizontal displacement of a floor comparative to the floor underneath.

- AS1170.4 has enforced that limit on the inter-storey drift to be 1.5% for earthquake loading.
- In case of wind loading, this limit is specified as $h_s/150$, where h_s represents the storey height The EN 1993-1-1 (2005) and the British Standards Institution (1992, 2000) have proposed a more meticulous limit as $h_s/300$ in case of wind loading on the structures that corressponds to 0.333%. This value was used in this study as well
- AS/NZS 1170 suggested the mid span deflection limit of composite beams as $L_b/250$, where L_b represents the length of the beam.

5.7. Moment reversal

The reversal of moment in the connection region is likely to occur if the lateral loading applied to the structure is large enough to cause the connection moment to reverse. Originally the connection moment which is in negative bending having slab in tension is reversed to positive bending putting slab in compression. This method has been explained in detail by Liew *et al.* (2004). The connections were also checked for moment reversal in this study.

5.8. Development of frame model in Abaqus

5.8.1. General description

Abaqus software was used to accurately simulate the behaviour of all frames. The three main components of the frame that were precisely modelled included columns, beams and semi rigid connections. In addition to these, the proper selection of element type, adequate mesh size, load application and boundary conditions were the other significant parameters that were important to achieve accurate analysis results. A typical arrangement of a 3 bay by 3 storey frames in Abaqus is presented in Fig. 5.2.

5.8.2. Finite element type and mesh

Different element types were tried in order to find out the most suitable one to simulate the behaviour of the frame. From the Abaqus material library, two-node linear beam elements B31 was selected to model beams and columns instead of solid elements owing to the various benefits of using them in the analysis of frame structures. These are one-dimensional line elements in three-dimensional space that have stiffness affiliated with the deformation of the beam's axis. As the analysis aimed to investigate the global behaviour of the frame, minor details like the local stress distributions can be ignored. The beam elements were more feasible as they require lesser computational time and are easy to use. These elements were selected because they were preferred in global analysis models due to their computational proficiency. These elements were far more computationally efficient as compared with the solid elements since they had lesser degrees of freedoms. Hence, the speed of numerical simulation was increased.

Mesh convergence studies were conducted in order to find the most reasonable mesh that provided the most accurate results and also took lesser computational time. Based on these results, it was found that accurate results can be achieved when an approximate global size of 125 mm length of global seeds was used for both beams and columns. The finite element mesh of each beam contained approximately 74 nodes.

5.8.3. Loading and boundary conditions

The bottom surfaces of all concrete filled steel tubular columns were fixed against all degrees of freedoms. This assumption of rigid base was also made by Hensman and Nethercot (2002), Yao *et al*. (2009) and Wang *et al*. (2018). Although such degree of flexibility of a column base is hard to achieve in real practice as majority of the footings are not perfectly rigid in nature, this degree of flexibility becomes insignificant if the base connections are designed efficiently.

5.8.4. Material properties

The elastic-plastic material behaviour in Abaqus permits a multi-linear or bi-linear stress-strain curve to be used in the plastic option. This option was used to model the steel beam and steel column using a tri-linear elastic-plastic model as it is commonly used for structural steel. The first part of the tri-linear curve represents the elastic part up to the proportional limit followed by further yielding and strain hardening before fracture. The modulus of elasticity E was 2000,000 N/mm^2 and poisson's ratio was 0.3. The yield stress of steel material was taken as 350 N/mm^2 and ultimate stress was 430 N/mm^2 corresponding to a plastic strain of 0.1819. However, the cross-section conversion of composite beams and columns was based on the equivalence of stiffness that incorporated elastic material behaviour. Hence, the beams and columns remained in the elastic range.

For semi rigid joints, the material behaviour was input in the connector sections in the form of moment rotation models in order to include plastic behaviour. Among the advanced analysis techniques, the plastic hinge method is the most effective method of modelling beam-to-column semi-rigid joints. This element is superior to the conventionally used spring element and is also proposed by Liew *et al*. (2000) and Thai *et al.* (2016a). Therefore, the semi-rigid connections were modelled as a connector element type named as hinge in which the translations were restricted while the flexural rotations were allowed only. In order to incorporate the plastic behaviour of the composite joint, two sets of the moment rotation relationship data were assigned to the connector element. One represented hogging moment while the other represented sagging moment relationship.

5.8.5. Analysis technique

Newton's method also knows as Newton Raphson method was used in this study for analyzing the frame numerically. This method was named after Isaac Newton and Joseph Raphson. It is a very commonly used method that finds successively better approximations to the roots of a real valued function. It is used to solve non-linear equilibrium equations and is a potentially good tool to capture non-linear behaviour of the structures.

5.9. Results and discussions

Figs. 5.9-5.13 illustrates the frame results under various load combinations in strength limit state. The design action effects acting on all of the frame components as a result of each load combination were inspected carefully such that they were smaller than their corresponding design capacities. Hence this satisfied the ultimate limit states measures. The maximum vertical deformations of composite frame in serviceability limit state are presented in Fig. 5.14 whereas Fig. 5.15 presents the deflected shape of the frame under wind loading. From the results, the maximum value of deflection was 28.3 mm which was much smaller than deflection limit, $L_b/250$.

The selected column cross section was 300×300×10 mm with Grade 350. The beam selected was 610UB101 with Grade 350 while the thickness of concrete slab was 120 mm. The general details of these components are presented in Table 5.5. It was observed that the load combination 2 incorporating gravity loads alone were most critical to the frame in terms of producing maximum hogging moment as well as sagging bending moment. Load combinations 3 and 4 that represented the wind loading in Australia were observed to be more critical as compared to load combination 5 that represented earthquake loading in Australia.

The serviceability behaviour of the frame was also found to be reasonable. The maximum drift for each storey was found to be 23 mm for the top most storey, 18 mm for the middle storey and 11 mm for the following storey. It was also found that the sway displacement on the ground floor was the most critical. Limiting the drift of this floor would result in a satisfactory drift for all other floors too. The maximum long-term beam deflection due to creep and shrinkage was found to be satisfactory as well.

The frame analysis was then continued for a wide range of different storeys and different bay sizes as mentioned above. Tables 5.6 and 5.7 summarises the sagging moment and hogging moment envelopes under load combinations and the variation of sagging and hogging bending moments corresponding to the various load combinations in strength limit states is presented in Fig. 5.16 and 5.17.

The analysis results demonstrated that the maximum sagging and hogging moments occurred when LC2 was applied, while the minimum sagging and hogging moments appeared in LC3. Therefore, the moment-rotation relationship of the semi-rigid joint was extracted from Abaqus for LC2 which is presented in Fig. 5.18. It can be observed that the bolted flush endplate joints experienced plastic behaviour. The maximum value of hogging moment was found to be 216.6 kN.m. Moreover, it was observed that wind actions controlled the design rather than earthquake actions. The hogging moment at the interior support was found to span nearly 0.254 m on each side of the support that corresponds to 0.15 L_b. However, for wind and earthquake actions this value was found to be approximately 0.339 m on both sides which is equal to 0.2 L_b.

For the total range of frames, it was observed that the moment reversal did not occur at any of the interior supports when lateral loads of wind or earthquake were applied except for the tall and slender frames with 2 bays by 5 storey and 2 bays by 4 storey size. It was also observed that the maximum values of hogging and sagging moments always appeared in the exterior span on the ground floor. Therefore, it can be concluded that the beam-to-column joints do not have to be nesessarily designed for moment reversal provided that the structure is properly designed. Generally, tall slender frame design should be avoided and a greater number of ways tends to benefit the construction.

5.10. Summary of chapter

This chapter explained the behaviour and design of blind bolted composite frames with semi-rigid joints. Global models were created using Abaqus software to examine the flexural performance of frames under gravity and lateral loads of wind and earthquake. Two-dimensional finite element models were developed in which geometrical non-linearities and only in-plane deformations were considered. Beam elements were selected for simulating the beams and columns that helped to reduce the computational time and also improved the convergence. Moreover, the cross-section of composite beams and composite columns were converted to equivalent steel beam and steel column sections. In addition to that, the beam-to-column semi rigid joints were simulated using the connector elements which were capable of replicating the nonlinear behaviour. Moment-rotation relationships were assigned to the connector elements. Various design loads were considered in the analysis that included dead loads, live loads, wind loads and earthquake loads in accordance with the Australian standards. In order to determine the appropriate sizes of columns and beams, strength limit state and serviceability limit state criteria were utilised to authenticate the design.

The frame analysis was observed to be an easy and efficient procedure to design the composite frames that fulfilled the necessary requirements specified in the Australian Standards. The critical loading conditions were easily identified that affected the structural behaviour. The analysis results suggested that the load combination including dead loads and live loads affected the frame significantly in terms of bending moments. Moreover, wind actions were found to be more critical to the structures as compared with the earthquake actions. In addition, moment reversal did not occur at any of the interior supports due to lateral loads which implies that the connections do not necessarily need to be designed for moment reversal. The proposed analysis procedure provided useful information on the behaviour of these frames and similar types of frames and will be helpful for the design of similar structures in engineering practice.

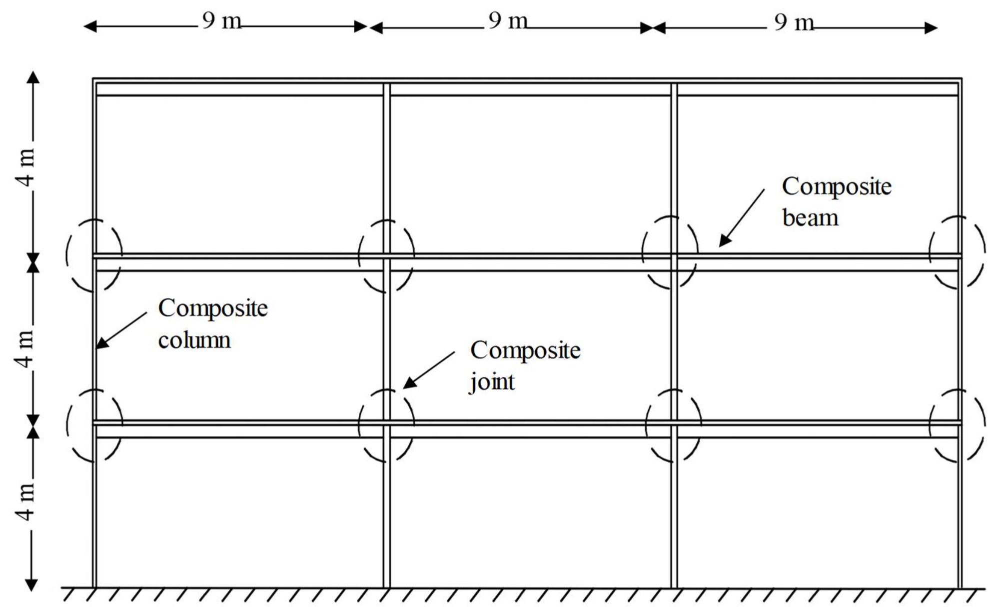

(a) Elevation view

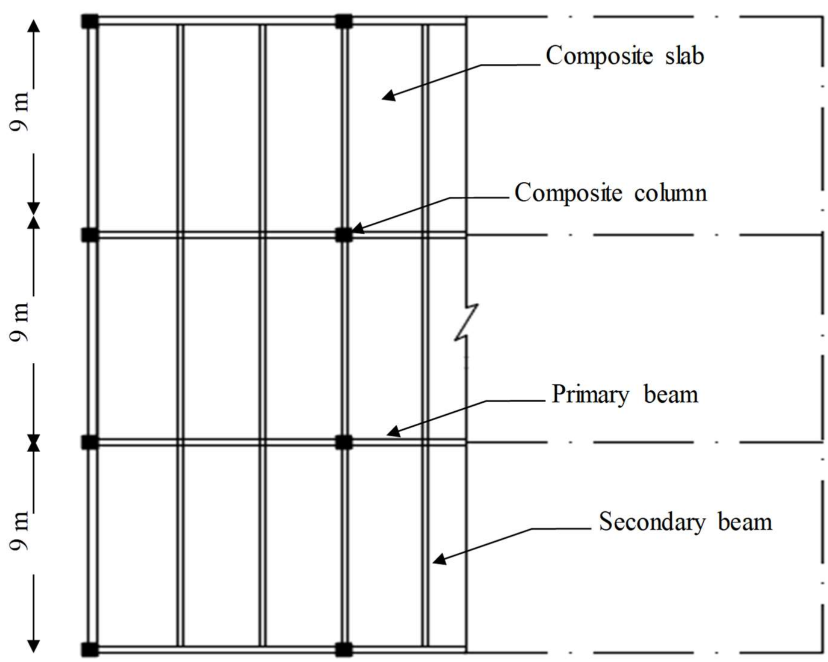

(b) Plan view

Fig. 5.1 – A composite frame with 3 bays and 3 stories (unit: m)

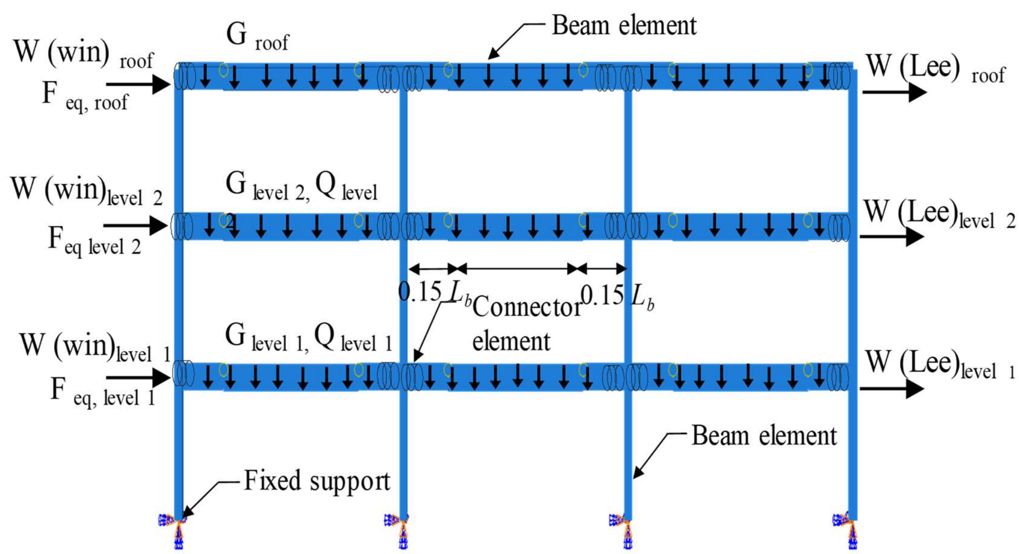

Fig. 5.2 – Finite element model displaying load actions

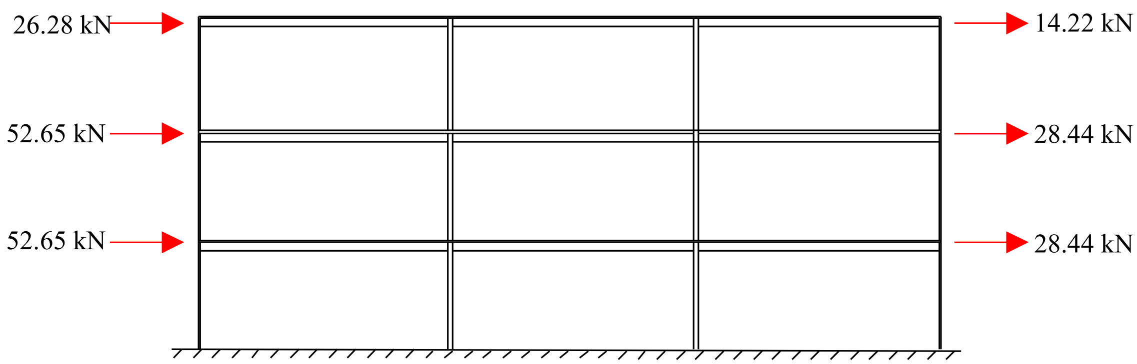

(a) Wind actions

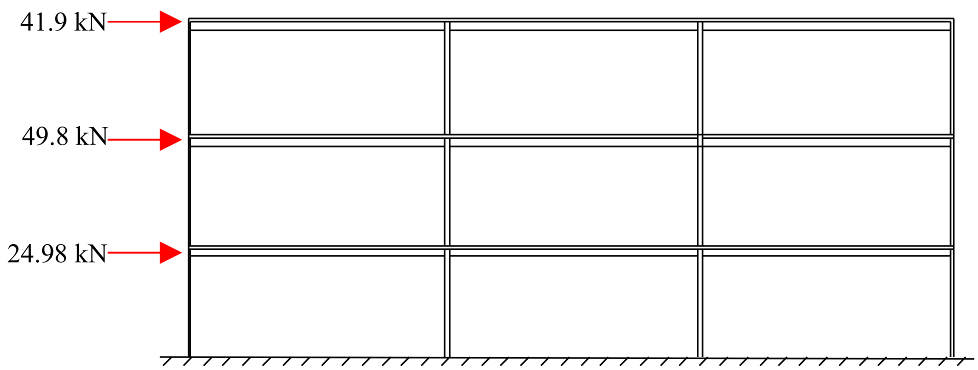

(b) Earthquake actions

Fig. 5.3 – Actual values of loads acting on the frame

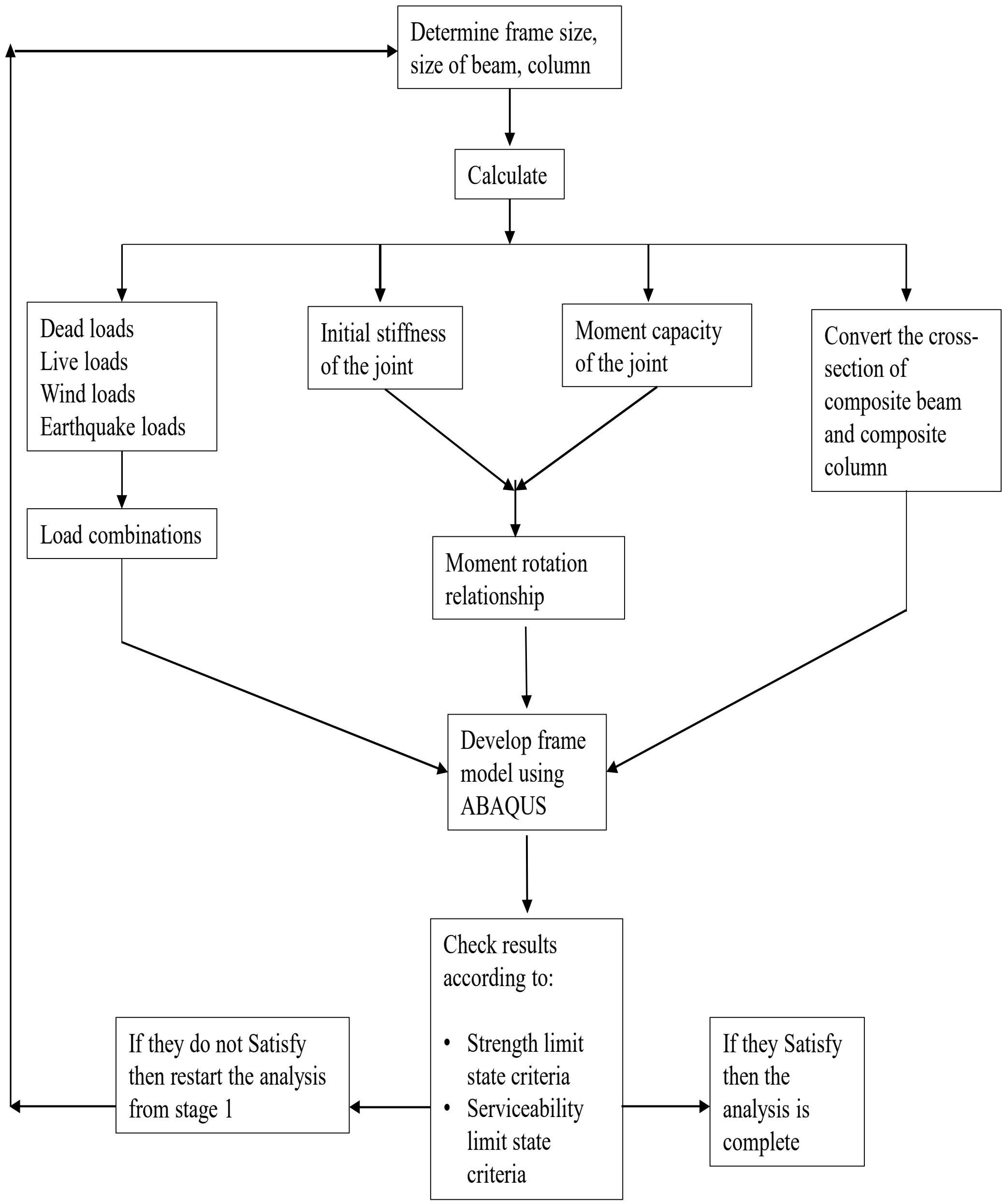

Fig. 5.4 – Flowchart of frame analysis

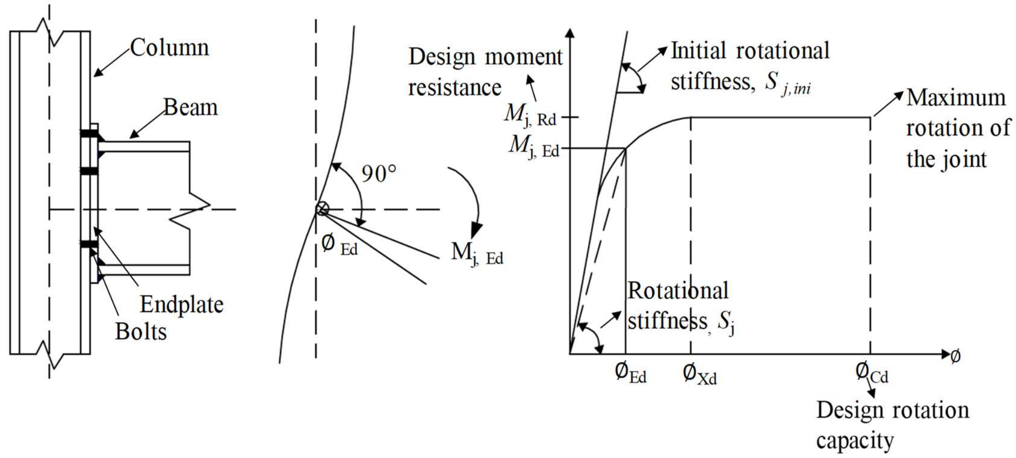

Fig. 5.5 – Design moment rotation characteristics of a joint (EN 1993-1-8, 2010)

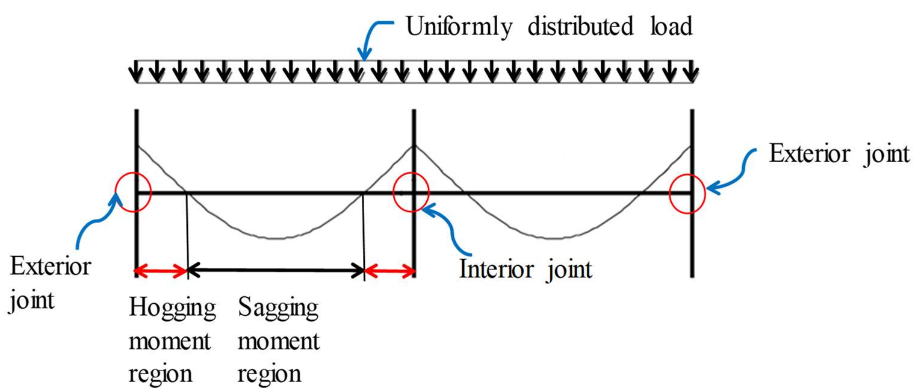

Fig. 5.6 – Sagging and hogging moment regions in a continuous or semi-continuous structure

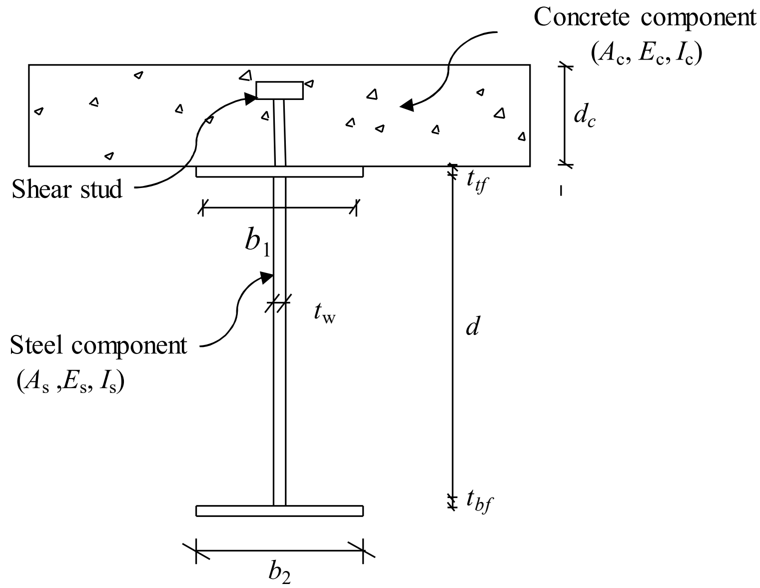

(a) Orignal section

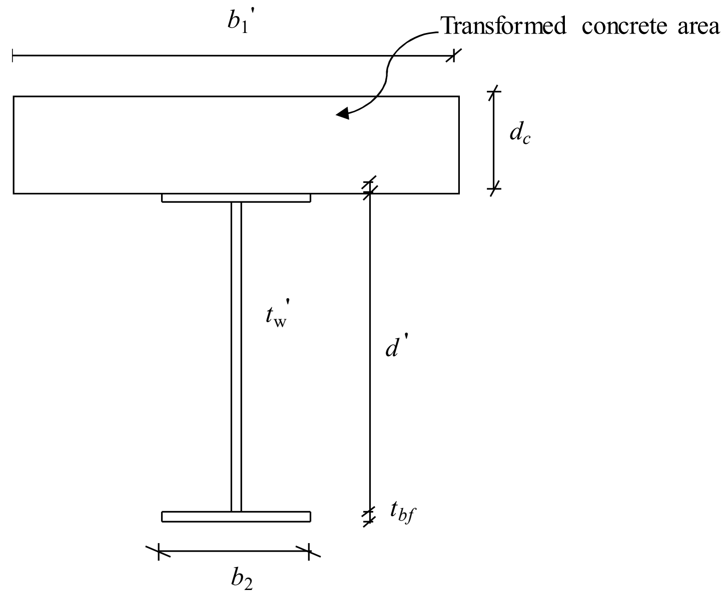

(b) Transformed section

Fig. 5.7 – Cross-section conversion of composite beam

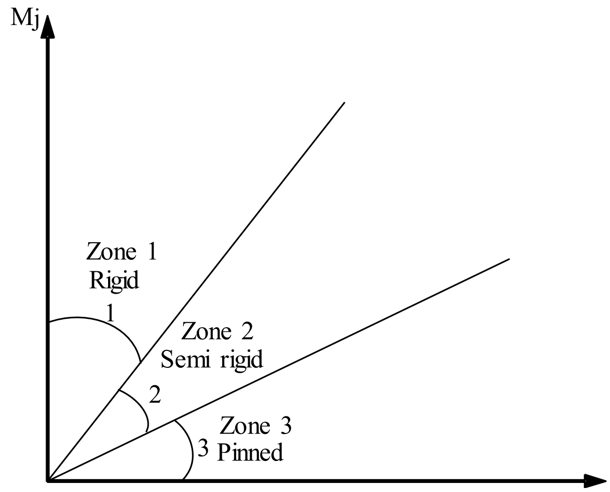

Fig. 5.8 – Classification of a joint ((EN 1993-1-8, 2010)

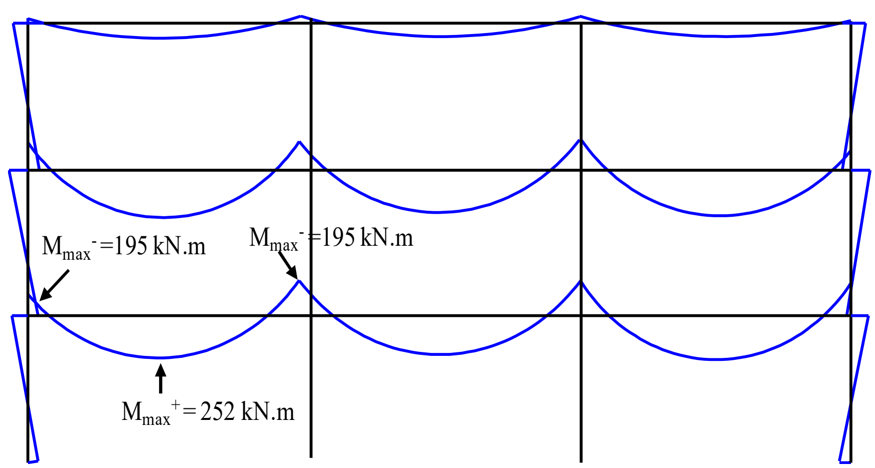

Fig. 5.9 – Bending moment diagrams for LC1

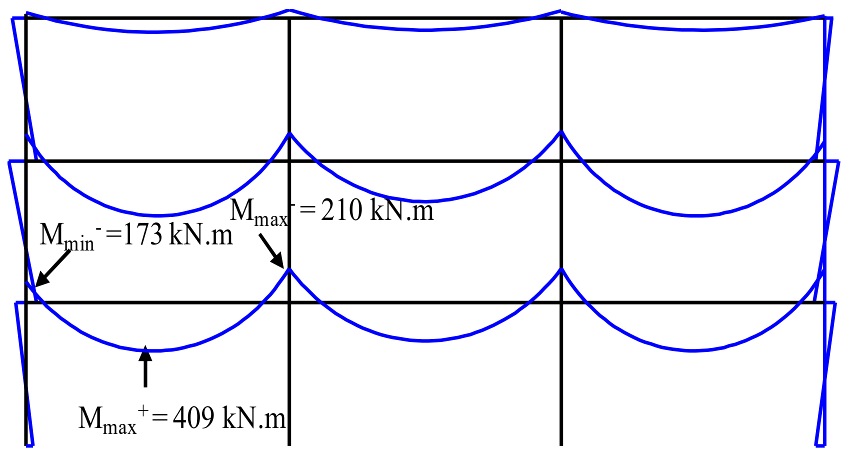

Fig. 5.10 – Bending moment diagrams for LC2

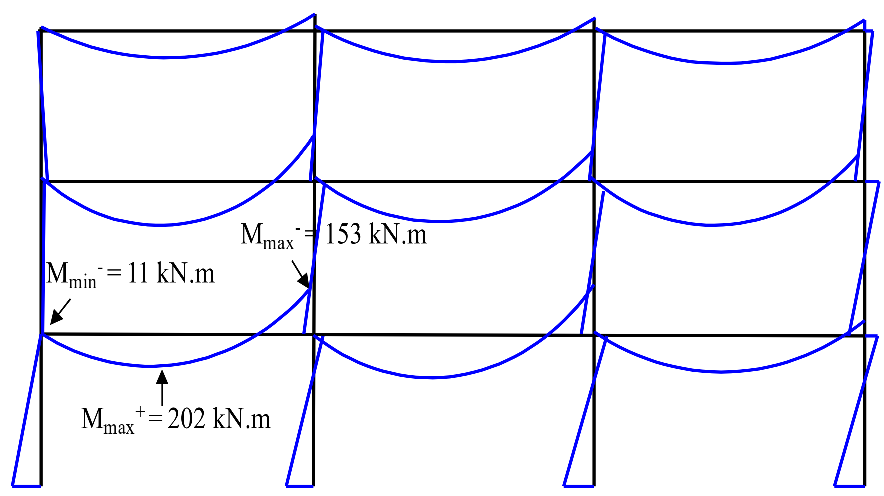

Fig. 5.11 – Bending moment diagrams for LC3

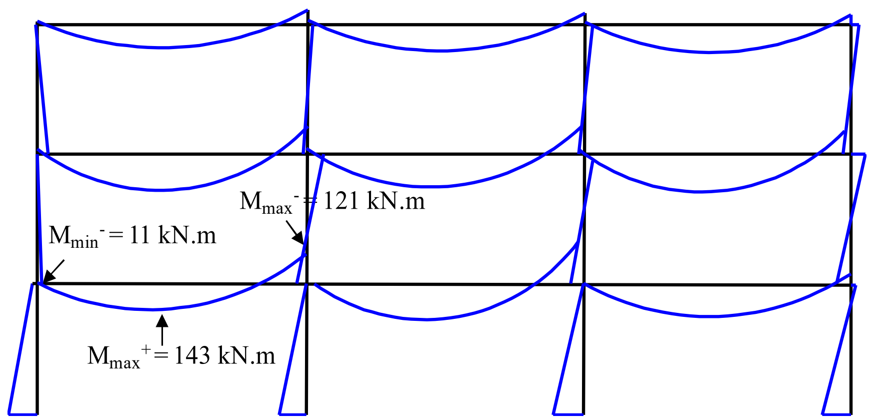

Fig. 5.12 – Bending moment diagrams for LC4

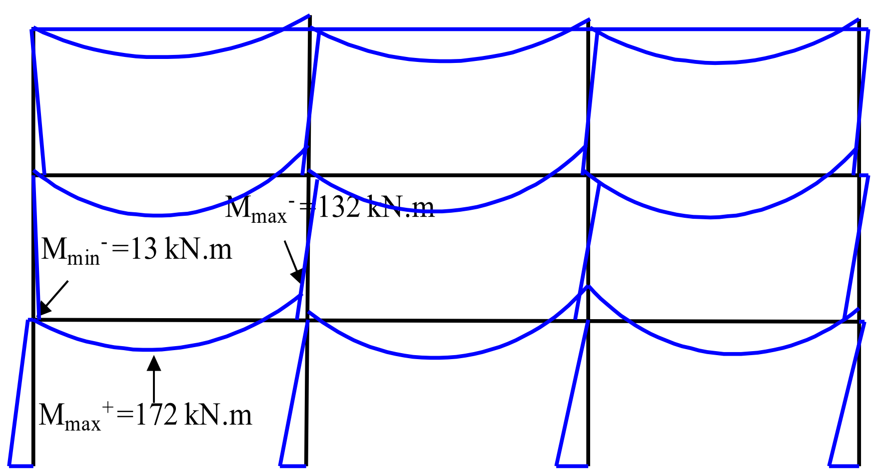

Fig. 5.13 – Bending moment diagram in strength limit state for LC5

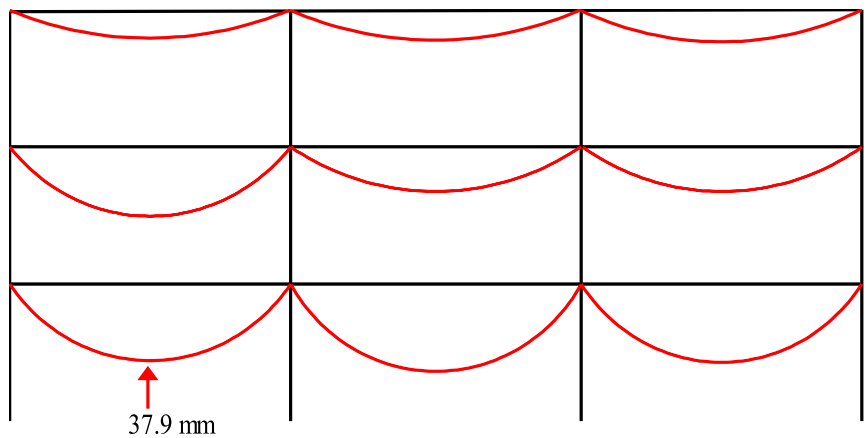

Fig. 5.14 – Maximum vertical deformations of composite frame in serviceability limit state

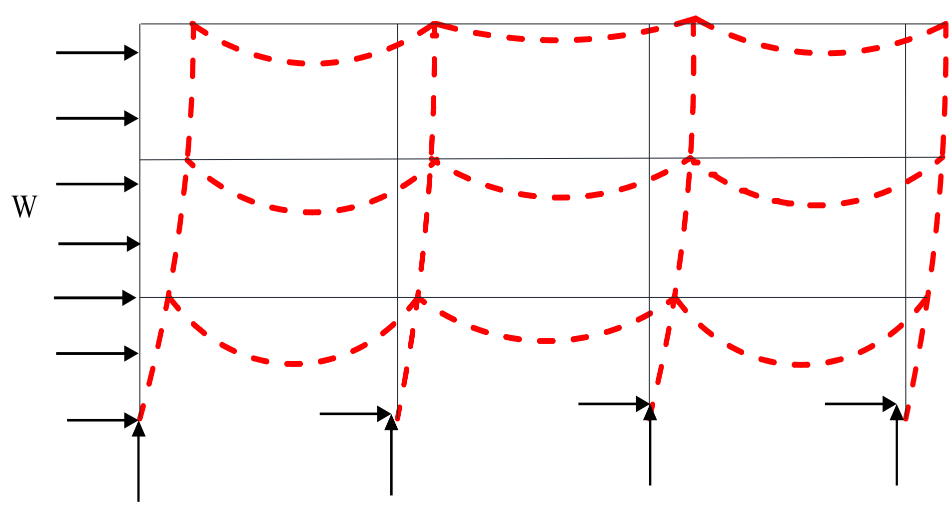

Fig. 5.15 – Displaced shape under wind loading

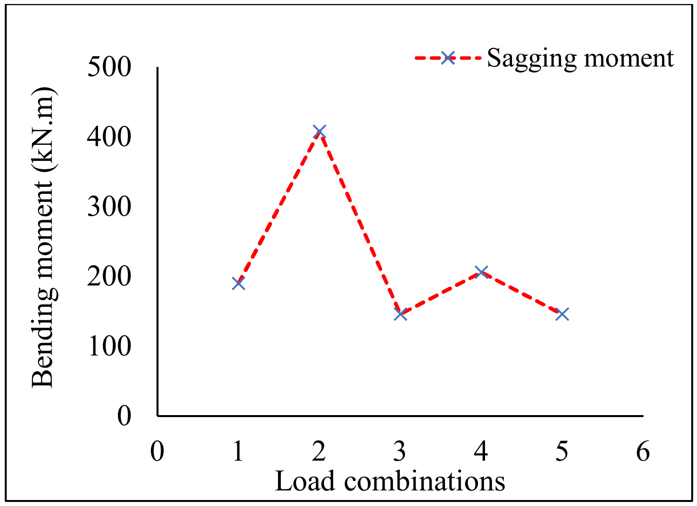

Fig. 5.16 – Maximum sagging moment of composite beams

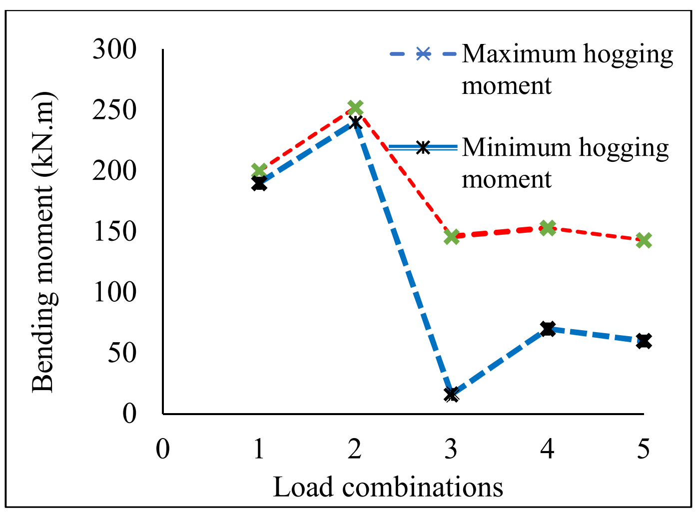

Fig. 5.17 – Hogging moment of composite joints

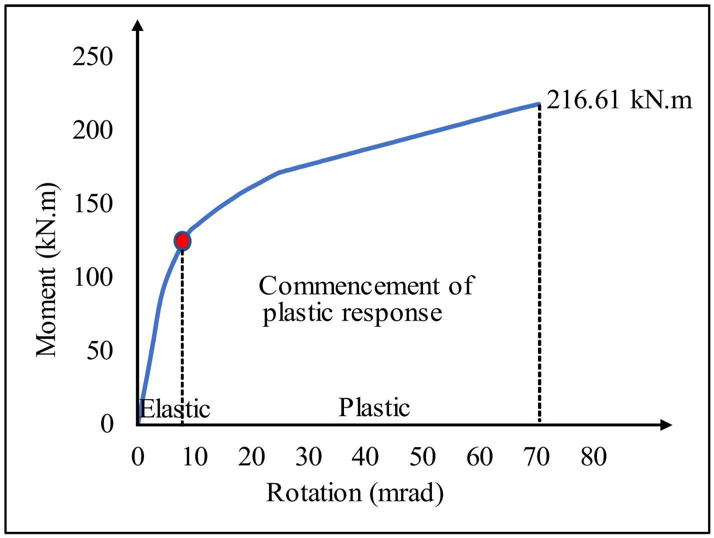

Fig. 5.18 – Moment-rotation relationship of semi-rigid composite joint

Table 5.1 – General details of composite frames considered

Feature	Range/Size
Number of storeys	2-5
Number of bays	2-4
Bay width	9 m x 9 m
Storey height	4 m

Table 5.2 – Details of the converted cross-section of composite beam to steel beam

Section	Details
Hogging moment region	b_3=290 mm, d_c=120 mm b_2=228 mm, t_{fb} =14.8 mm d'=587.2 mm, t_w =9.9 mm
Sagging moment region	b_3=350 mm, d_c=120 mm b_2=228 mm, t_{fb} =14.8 mm d'=587.2 mm, t_w =10.1 mm

Note: b_3 is the width of the converted cross-section, dc is the depth of concrete slab, b_2 is the width of bottom flange of steel beam, t_{tf} is the thickness of bottom flange, t_{fb} is the thickness of bottom flange, d' is the depth of the converted steel section, t_w is the thickness of beam web

Table 5.3 – Details of load combination

Number	Strength limit state	Number	Serviceability limit state
LC1	1.35G	LC6	W
LC2	1.2G+1.5Q	LC7	G+0.4Q+W
LC3	0.9G+W	LC8	G+0.7Q
LC4	1.2G+0.4Q+W	LC9	Feq
LC5	G+0.3Q +F_{eq}	LC10	G+0.4Q

Table 5.4 – Actual values of actions in frames

Storey	Dead load (kN/m)	Live load (kN/m)	Wind actions (kN)		Earthquake Actions (kN)
			Windward	Leeward	
First storey	19	13.5	52.65	28.44	24.9
Second storey	19	13.5	52.65	28.44	49.8
Third storey	10.3	0	26.28	14.22	41.9

Table 5.5 – General information of the frame components

Specimen	S-1
Steel column	300 × 300 × 10 mm, Grade 350, h_c=4000 mm, t_c=10 mm
Steel beam	610UB101 (602 × 228 ×14.8 × 10.6), Grade 350, d=602 mm, b_b=228 mm, t_w =10.6 mm, t_f =14.8 mm, A_b=13000 mm^2, E_b=2x10^5 Nmm^2, I_b=761x106 mm^4
Concrete slab	d=120 mm, b_{eff} =626 mm, A_c=75120 mm2 f_c=40 MPa, E_c=32,800 MPa

Table 5.6 – Sagging bending moment envelope in strength limit state

	Sagging bending moment (unit: kNm)		
	2 bays	3 bays	4 bays
2 storeys	399(9)	409(91)	402(97)
3 storeys	391(89)	409(89)	400(95)
4 storeys	387(87)1	407(89)	399(95)
5 storeys	383(83)	407(87)	397(91)

The values inside brackets represent minimum and outside brackets represents maximum sagging bending moments.

Table 5.7 – Hogging bending moment envelope in strength limit state

	Hogging bending moment (unit: kNm)		
	2 bays	3 bays	4 bays
2 storeys	255(33)	249(3)	250(31)
3 storeys	253(3)	240(11)	245(31)
4 storeys	210(-26)	235(5)	243(26)
5 storeys	203(-27)	249(3)	248(3)

The values inside brackets represents minimum and outside brackets represents maximum hogging bending moments.

CHAPTER 6

CONCLUSIONS

This thesis presents an investigation on a composite beam-to-column flush end plate connection developed using the novel blind bolting mechanism as an alternative to the conventional pin joints or rigid joints from the view point of economical design and simple joint detail. Firstly, the structural behaviour of the composite joints was investigated using experimental studies and finite element simulations. Subsequently, parametric studies were performed to identify the critical components that affected the load-displacement behaviour of these joints. Furthermore, the global behaviour of semi-rigid composite frames with the tested composite joints was studied by analytical method and numerical modelling.

Through the above comprehensive studies including experimental, numerical and analytical investigation, this thesis provided valuable knowledge on structural behaviour of the proposed beam-to-column flush end plate connection under static and cyclic loading scenarios. The conclusions derived through the experimental investigation, finite element modelling and frame analysis are presented as follows:

6.1. Experimental programme

The detailed description of the experimental programme is presented on Chapter 3. The following conclusions are drawn with respect to the structural behaviour of the beam-to-column joints tested under static and cyclic loading conditions.

1. Full scale tests were performed on typical blind bolted, beam-to-column flush endplate connections that demonstrated sufficient strength and stiffness for use within medium rise buildings

2. The test results demonstrated that these semi-rigid composite connections can perform satisfactorily in terms of yielding, maximum strength capacity and ultimate displacement.

3. The experimental results showed a significantly improved stiffness and ultimate strength when compared with the previous studies. No failure of blind bolts or shear studs was observed as in previous studies and also blind bolts performed very well for both loading scenarios which demonstrated improvement in the connection's performance.

4. According to EC3/EC4, the rotation capacity of the joint must be higher than 30 mrad in order to allow for plastic analysis and design. The test results confirmed that the beam-to-column composite joints offer satisfactory rotation capacities as specified by the EC3/EC4 design codes. Both connections behaved in a semi-rigid manner in terms of rigidity of the connections.

5. Fracture of reinforcement in the mid span of the concrete slab governed the ultimate strength of the joints in both specimens and both joints behaved in a ductile fashion.

6. The failure modes observed from the experiments comprised of reinforcing bar fracture and deformation of the flush end plates attached to the primary beams. No failure of shear connectors or blind bolts was observed. Also, both specimens demonstrated a very similar behaviour and exhibited similar failure modes despite of being subjected to different loading conditions.

6.2. Finite element modelling

The details of finite element model development, analysis results and parametric studies are explained in detail in Chapter 4. It was concluded that the FE models developed in this study are accurate and reliable to predict the global and local response of the composite beam-to-column joints with reasonable accuracy. Therefore, these models were considered satisfactory for performing parametric studies.

The parametric analysis suggested that the structural behaviour was largely affected by the end-plate thickness, reinforcement ratio, shear connection ratio, slab thickness and bolt diameter. On the other hand, thickness of equal angles, grade of steel, bolt diameter and shear connectors imposed little effects on the performance of these joints. With respect to the results of parametric study, several conclusions were drawn which are presented as follows.

1. The pretension force in the bolts did not appear to have a significant effect on the load capacity of the composite connection.

2. Compressive strength of concrete exhibited a strong influence on the initial stiffness and ultimate strength of the composite connection.

3. The grade of steel demonstrated a great contribution to the load capacity and also enhanced the ductility performance of the connection. However, the initial stiffness was not influenced by increase in the steel strength.

4. Increase in diameter of bolt had a significant effect on the strength and ductility of the composite connection up to M24 diameter. However, an increase in diameter above M24 did not appear to cause any further increase in the connection strength. The reason could be attributed to the fact that when the blind bolts are strong enough, the mode of failure is diverted to the cracking of concrete slab instead of blind bolt failure.

5. Increasing the grade of bolt slightly increased the ultimate capacity of the connection. However, the effect was not very significant.

6. The axial load had a very negligible effect on the load capacity of the connection and did not affect the stiffness and ductility of the connection.

7. A larger size of bolt led to a significant increase in the strength of the joint. Decrease in the diameter of blind bolts resulted in yielding of the bolts in the upper bolt row which resulted in failure of the joint.

8. Thickness of the flush endplates should not be too small so that the endplate fracture can be avoided. On the other hand, it should not be too thick so that brittle failure of bolts in the connection zone can also be avoided.

9. Thickness of endplate to bolt diameter ratio must be kept below 0.6. The 12 mm thick endplate seemed reasonable for the design of these connections.

10. A higher initial stiffness and load capacity can be achieved by adopting several options such as the thickness of flush end plate can be increased further from 12 mm to 19 mm. Similarly, N16 bars can be used instead of N12 bars to increase the strength further.

11. The use of equal angles on the sides of steel tubular column did not help to significantly enhance the performance of these connections. Therefore, some alternative method to increase the thickness of steel tubular column should be tested.

12. The increase in thickness of the concrete slab significantly increased the initial stiffness and ultimate load capacity of the joint. However, since the joint became highly stiff, it resulted in a reduction in ductility. Moreover, a thicker concrete slab reduced cracking of the concrete.

13. An increase in reinforcement ratio significantly increased the initial stiffness and load capacity of the connections. However, after a certain level it did not proved to be as beneficial in regards to further improvements in the beam-to-column connection's strength. After a certain limit, further increase in reinforcement area resulted in local buckling of the beam flange due to the development of compressive forces. A small value of reinforcement ratio led to limited strength and ductility. Therefore, an optimum value of reinforcement must be considered in the design.

14. Reduction in shear connection ratio resulted in a decrease in the load capacity and increased the deflection of the composite joints. It is suggested that the shear connection ratio should at least be 50% to avoid fracture of shear studs before reinforcing bar failure. It helped to prevent the failure of shear connectors and improved the ductility of these connections.

15. Five distinctive failure modes, i.e. longitudinal reinforcing bar fracture (RBF), blind bolt fracture (BF) of blind bolts in the top row, bolted shear connector failure (BSCF) of the shear connectors located on the primary beams, premature local buckling (LB) of bottom flange of the steel beam and plastic deformation of the flush end plate (FEPF) were observed in the parametric study conducted by using the FE models.

16. The parametric studies helped to deeply investigate the behaviour of these connections without going through the laborious and expensive experimental investigation.

6.3. Frame analysis

A range of moment resisting composite frames were designed and analysed in accordance with Australian standards and Eurocodes. Details of all necessary calculations have been presented in Chapter 5 following up with the development and analysis of the frame model using ABAQUS. Within the present scope of investigation, the following conclusions can be made.

1. Abaqus software is a convenient and efficient tool that can be effectively utilized for frame analysis and to perform parametric studies to further explore the behaviour of these frames under different loading scenarios.

2. The frame analysis is an effective procedure which helps to design composite frames that fulfil the requirements from standards.
3. Comparison of the predicted initial stiffness and moment capacity with the test results demonstrated that the moment rotation model was accurate and reliable to be adopted for further application.

4. The structure performed adequately when it was subjected to the applied gravity and lateral loads of wind and earthquake. This implied that the composite beam, column and connection capacities were likely to be sufficient.

5. Load combination incorporating gravity loads alone governed the design for all cases except 2x5 storey frame where earthquake loading governed and induced moment reversal at the beam-to-column connection.

6. From the results it can be observed that there will be a greater risk to high rise structures in terms of damage and loss of lives if there are more storeys than bays. Therefore, tall and slender structures should be avoided. Hence, a greater number of bays as compared to the stories can be advantageous.

7. The results from the analysis are helpful for understanding the complicated behaviour of blind bolted composite frames and can be applied to the design of these types of frames in engineering practice.

CHAPTER 7

RECOMMENDATIONS FOR FURTHER RESEARCH

It is recommended that further studies should be carried out in the following areas;

1. Further studies should be attempted to make changes on the column capacity, addition of stiffeners of various thicknesses and additional bolts. The possibility of using a viscoelastic material between the column surface and endplate can be studied as it might be beneficial to improve the flexibility of these connections under seismic loading conditions.

2. The thickness of concrete slab used in this study was 120 mm. From parametric studies results, it is recommended that the thickness of the concrete slab should be increased further in order to enhance the overall performance of these connections.

3. Recent experimental studies on similar connections demonstrated enhancements in the moment capacity and initial stiffness of these connections when circular columns were used instead of square CFST columns and when extended end plates instead of flush end plates were used. However, those specimens were subjected to static loading only. Following on these conclusions, it is

recommended that some alterations should be made to the design of the connections considered in this study such as, replacing the flush end plates with extended end plates and square CFST column with circular CFST column as it may help to enhance the strength of these connections when subjected to earthquake loads of higher return periods. Experimental studies must be performed in which these connections are subjected to cyclic loading conditions of 1-in-2500 years return period. Moreover, extensive parametric studies must be performed using extended stiffened endplate and round CFST column. The use of different types of end-plates and a greater number of bolts of smaller diameter versus smaller number of bolts of larger diameter must be explored to find the effect on the performance of these connections. These studies will be helpful to obtain an in-depth knowledge on the performance of these connections with the proposed alterations.

4. A significant similarity between the experimental and numerical results was found when the numerical results were compared with the experimental results. Therefore, it is suggested that finite element analysis is a very useful and powerful technique which provides a good prediction of the behaviour of structures just like experimental studies. Therefore, it is recommended to be used for further researches because of its accuracy, low cost and quicker results. However, it is highly recommended that the correct behaviour of materials should be input in order to obtain accurate output.

5. The structural frame designed in this study was subjected to the spectrum of critical wind and moderate earthquake forces in Australia for low-rise buildings

and this may not be relevant for high-rise buildings. Accordingly, experimental and analytical studies should be conducted on the behaviour of the composite beam-to-column joints when critical lateral loads are subjected with respect to high rise buildings.

6. The flexural response of these frames has been investigated in this research by analytical studies and numerical modelling. Experimental investigation should also be conducted in order to obtain more specific test data that accurately reflects the true flexural response of these frames. A two-dimensional frame analysis was performed in this study. It is recommended that the analysis should be extended to three dimensional studies. The eccentricity of loads and out-of-plane bending moments can be incorporated in the analysis. This will provide a closer reflection of the actual behaviour of these frames.

7. The cyclic loading in this research studies hogging bending moment condition only. However, the standard loading protocol considers both hogging and sagging bending moment. Moreover, the loading condition planned in this thesis is based on the fact that seismic effects in Australia are not very critical. Therefore, it is recommended that more experimental investigations must be undertaken that considers the composite beam-to-column joints under load reversal.

8. Furthermore, the current investigation considers semi-rigid connections only. Rigid and pinned connections should also be considered in future studies since

they are still broadly applied in the construction practice due to their unique behaviour.

9. In practical structural design, pattern loading needs to be considered to obtain the maximum design moment and deflection. It is recommended that the above effect is also investigated in the future.

APPENDIX A

DETERMINATION OF INITIAL STIFFNESS OF THE FLUSH END PLATE COMPOSITE JOINTS IN ACCORDANCE WITH THAI AND UY, (2016), EN 1993-1-8 AND EN 1994-1-1

The procedure to calculate the mechanical properties of composite flush endplate joints with blind bolts is illustrated as follows. The geometrical dimensions of the specimen are presented in Fig. 3.1 and summarized in Table A1.

A.1 GEOMETRICAL DIMENSIONS OF SPECIMEN, S-1

Steel column	L=9000 mm
	300 x 300 x 10 mm, Grade 350,
Secant modulus of concrete	
	h_c=1500 mm, t_c=10 mm
	610UB101 (602 x 228 x 14.8 x 10.6),
	Grade 350, d=602 mm, b=228 mm
Steel beam	t_w =10.6 mm, t_f =14.8 mm
	A_b=13000 mm2, E_b=2 x 10^5 Nmm^2
	I_b=761 x 10^6 mm^4

Concrete slab	d=120 mm, b_{eff} =626 mm A_c=75120 mm^2
Rebar	f_{sy}=500 MPa, f_{su}=600 MPa
Shear stud	Ø19x100 mm Shear span length=1695 mm k_{sc}=100 kN/mm

A.2 STIFFNESS COMPONENTS FOR COMPOSITE FLUSH END-PLATE CONNECTION

Fig. 2.8 represents the component model proposed by Thai and Uy (2016) for composite joint with two rows of bolts in tension. The stiffness components of the model are presented as follows.

- k_1_Stiffness coefficient of the column face in compression
- k_2_Stiffness coefficient of the column side walls in compression
- k_3_Stiffness coefficient of the column side walls in tension
- k_4_Stiffness coefficient of the column face in bending component
- k_5_Stiffness coefficient of the end-plate in bending component
- k_{10}_Stiffness coefficient of the bolts in tension

A.3 DETERMINATION OF k_1 AND k_2

Stiffness coefficient of the column face in compression is expressed as follows:

$k = \infty$ Eq. (1) in Thai and Uy, (2016)

Stiffness coefficient of the column side walls in compression is presented as follows:

$k = \infty$ Eq. (2) in Thai and Uy, (2016)

The stiffness coefficients k_1, and k_2 are assumed to be infinite due to the presence of concrete infill.

A.4 DETERMINATION OF k_3

Stiffness coefficient of the column side walls in tension is expressed as follows:

$k_3 = \xi t(1.1\bar{d} + 2.9t^{-0.4})$ Eq.19(b) in Thai and Uy, (2016)

$k_3 = 12.6$ mm

A.5 DETERMINATION OF k_4

Stiffness coefficient of the column face in bending component is represented as follows:

$$k_4 = t\bar{t}^2 \frac{5\bar{d} + (9 - 10\bar{g} - 278\bar{t}^2)\tan\bar{g}}{\bar{g}^3 - 1.5\bar{g}^2 + (0.464 + \bar{t})\bar{g} + 0.092 - \bar{t}}$$ Eq. 20(b) in Thai and Uy, (2016)

in which,

t = thickness of flush endplate

$\bar{t} = \frac{t}{h}$, thickness to width ratio

$\bar{g} = \frac{g}{h}$, bolt gauge-to-width ratio,

d = bolt diameter

$\bar{d} = \frac{d}{h}$, bolt diameter-to-width ratio

$k_4 = 1.395$ mm

A.6 DETERMINATION OF k_5

Stiffness coefficient of the endplate in bending is expressed as follows:

$$k_5 = 0.9 l_{eff} \left(\frac{t_p}{m}\right)^3$$ Table 6.1 in EN 1993-1-8

$k_5 = 1.944$ mm

A.7 DETERMINATION OF k_{10}

Stiffness coefficient of the bolts in tension is expressed as follows:

$$k_{10} = 1.6 \frac{A_b}{L_b}$$ Table 6.1 in EN 1993-1-8

$k_{10} = 10.05$ mm

A.8 DETERMINATION OF k_{eff}

The effective stiffness coefficient, k_{eff} of a bolt row can be expressed as:

$$k_{eff} = \frac{1}{\frac{1}{k_3} + \frac{1}{k_4} + \frac{1}{k_5} + \frac{1}{k_{10}}}$$

A.9 DETERMINATION OF $k_{s,red}$

Stiffness coefficient for the reinforcement representative of the slip of shear connection can be expressed as

$$\frac{1}{k_{s,red}} = \frac{k_{s,r}}{1 + \frac{E_s k_{s,r}}{k_{sc}}}$$

Here,

k_{sc} = stiffness of one shear connector

(Its value is considered as 100 kN/mm for a 19 mm diameter headed shear stud in case test results are not available)

$\mathrm{k_{s,red}} = 0.688$ mm

A.10 DETERMINATION OF $k_{s,r}$

Stiffness coefficient of the reinforcement is expressed as follows:

$$k_{s,r} = \frac{A_s}{h_c/2}$$ Table A.1 in EN 1994-1-1

Where,

A_s = area of steel

h_c = depth of steel tubular column

$k_{s,r} = 6.03$ mm

A.11 DETERMINATION OF k_{sc}

Stiffness coefficient of the shear connection is represented as follows:

$$k_{sc} = \frac{Nk_{sc}}{\nu - \frac{\nu - 1}{1 + \xi}\frac{h_s^2}{d_s}}$$ Section A.3 in EN 1994-1-1

$$\xi = \frac{E_b I_b}{E_s A_s d_s^2}$$

$$\nu = \sqrt{\frac{(1 + \xi) N k_{sc} l d_s^2}{E_b I_b}}$$

$k_{sc} = 321$ kN/mm

where,

$E_b I_b$ = bending stiffness of the steel beam

d_s = the distance between the centroid of the reinforcement and centroid of the steel beam

h = distance between centroid of beam flanges in tension and centroid of beam flanges in compression

h_s = the distance between longitudinal reinforcing bars in tension and centroid of beam flanges in compression.

N= number of shear connectors distributed over length 1 of the beam in hogging bending. This length is roughly assumed to be 15% of the total span

k_{sc}= Stiffness of one shear connector

A.11 DETERMINATION OF k_{eq}

The equivalent stiffness coefficient of the composite joint, k_{eq} can be expressed as

$$k_{eq} = \frac{K_{eff}h + K_{s,red}h_s}{z_{eq}}$$

$$k_{\mathrm{eq}} = 0.9629 \text{ mm}$$

$$z_{eq} = \frac{k_{eff}h^2 + k_{s,red}h_s^2}{k_{eff}h + k_{s,red}h_s}$$

$$z_{eq} = 716.811 \text{ mm}$$

A.12 DETERMINATION OF INITIAL STIFFNESS OF THE COMPOSITE JOINT, $S_{j,ini}$

Initial stiffness of the composite joint can be determined as follows:

$$S_{j,ini} = \frac{E\,Z^2{}_{eq}}{\Sigma \frac{1}{k_{eq}}}$$

where,

E= Young's modulus of structural steel

k_{eq}= equivalent stiffness

$S_{ini} = 98$ kNm/mrad

APPENDIX B

DETERMINATION OF DESIGN MOMENT RESISTANCE OF THE FLUSH END PLATE COMPOSITE JOINTS IN ACCORDANCE WITH EN 1993-1-8 (2010) AND EN 1994-1-1 (2004)

The procedure to calculate the moment capacity of the blind bolted composite flush endplate joints considered in this study is illustrated in this section. The design tension resistance for an individual bolt-row for some basic components should be considered which are as follows:

B.1 DESIGN TENSION RESISTANCE FOR THE BASIC COMPONENTS UNDER CONSIDERATION

- $F_{t,wc,Rd}$ _The columns web in tension,
- $F_{t,fc,Rd}$ _The column flange in bending,
- $F_{t,ep,Rd}$ _The end-plate in bending,
- $F_{t,wb,Rd}$ _The beam web in tension,
- $F_{t,Rf,Rd}$ _The reinforcement in tension,

The calculations for each of these components are as follows:

B.2 COLUMN WEB IN TENSION, $F_{t,wc,Rd}$

$F_{t,wc,Rd} = \dfrac{\omega b_{eff,t,wc} t_{wc} f_{y,wc}}{\gamma M_0}$ Clause 6.2.6.3 EN 1993-1-8

$\omega = 1$ Table 6.3 EN 1993-1-8

where,

ω= reduction factor that allows interaction with the shear in column web panel

e_1=end distance from the center of a fastener hole to the adjacent end of any part measured in the direction of loads transfer,

$e = 65mm$ Fig. 6.2 EN 1993-1-8

$e_1 = 24mm$

$m = 55mm$

$\Upsilon_{M0} = 1$ partial factor for resistance of cross-sections. $\Upsilon_{M0} = 1$ Clause 6.1 EN 1993-1-1

$b_{eff} = 301.25mm$ Table 6.4 EN 1993-1-8

$F_{t,wc,Rd}$=1863.2 kN

B.3 COLUMN FLANGE IN BENDING, $F_{t,fc,Rd}$

$$F_{t,fc,Rd} = \frac{b_{eff,b,fc} t_{fb} f_{\gamma,f_b}}{\gamma M_0}$$ Clause 6.2.6.4 EN 1993-1-8

$\sum l_{eff1} = 174.625mm$ (Mode 1)

$\sum l_{eff2} = 174.625mm$ (Mode 2)

$e_{min} = 75$, $t_{bp} = 12mm$, $M_{pl,1,Rd} = 10247.87Nmm$

$F_{t,fc,Rd} = 1350kN$

B.4 ENDPLATE IN BENDING, $F_{t,ep,Rd}$

Clause 6.2.6.5 EN 1993-1-8

$\sum l_{eff1} = 301.25mm$ (Mode 1)

$\sum l_{eff2} = 301.25mm$ (Mode 2)

where,

$t_p = 12mm$

$m = 55mm$

$m_2 = 76.2mm$

$M_{pl,2,Rd} = 5259.82kNmm$

$F_{t,ep,Rd} = 1350kN$

B.5 BEAM WEB IN TENSION, $F_{t,wb,Rd}$

$$F_{t,wb,Rd} = \frac{b_{eff,t,wbfy}}{\gamma_{M0}}$$ Clause 6.2.6.8 EN 1993-1-8

$\sum l_{eff1} = 302mm$ (Mode 1)

$\sum l_{eff2} = 302mm$ (Mode 2)

where,

$m = 55mm$

$m_2 = 76.2mm$

$M_{pl,1,Rd} = 3223.608kNmm$

$F_{t,Rd} = 675.288kN$

B.6 REINFORCEMENT IN TENSION, $F_{t,Rd}$

$F_{t,Rd}=A_s f_{sy}$

Table 6.2 EN 1994-1-1

where,

A_s= Area of the reinforcing bar

$F_{t,Rt} = 596kN$

The design moment resistance $M_{j,Rd}$ of a beam-to-column joint with a bolted-end plate connection can be determined as follows.

$$M_{j,Rd} = \sum_r h_r F_{tr,Rd}$$ Table 6.2 EN 1994-1-1

Where $F_{tr,Rd}$ is the effective design tension resistance of the bolt-row r, h_{r} is the distance from bolt-row in consideration to the centre of compression and *r* is the number of the bolt row.

The effective design tension force must be considered as the smallest value of the design tension resistance for an individual bolt-row of these components calculated above. Therefore,

$$M_{j,Rd} = 409.1kNm$$

APPENDIX C

CROSS-SECTION CONVERSION OF COMPOSITE BEAMS IN ACCORDANCE WITH EN 1994-1-1 AND EN 1998-1 (2004)

The calculation for cross-section conversion is based on steel beam 610UB101. Information regarding the geometrical parameters are denoted in Fig. 3.1. The effect of creep and shrinkage of concrete is ignored in this example.

C.1 GENERAL DETAILS OF THE COMPOSITE CROSS-SECTION

Length of composite beam	L=9000 mm
Secant modulus of concrete	E_{cm}=3.16×10^4 MPa
Depth of concrete slab	d_c=120 mm
Space between two shear connectors	b_0=0 mm
Width and thickness of top flange of beam	b_1=228 mm, t_{ft}=14.8 mm
Width and thickness of bottom flange of beam	b_2=228 mm, t_{fb}=14.8 mm
Depth and thickness of beam web	d_p=572 mm, t_w=10.6 mm

C.2 DETERMINATION OF EQUIVALENT CROSS-SECTION

The equivalent section can be computed as follows.

Cross-section area of steel beam

A_s=13000 mm^2

Location of neutral axis of steel beam

y_s=301 mm

Modulus ration of steel to concrete

α_E=5.96

Effective length of beam at hogging moment region

L_e=0.5L=4500 mm Clause 5.4.2.1 in EN 1994-1-1

Effective length of beam at sagging moment region

L_e=0.7L=6300 mm Clause 5.4.2.1 in EN 1994-1-1

Effective width of concrete slab at hogging moment region:

$$b_e = b_0 + \frac{L_e}{8} + \frac{L_e}{8} = 1125\text{mm}$$ Clause 5.4.1.2 in EN 1994-1-1

$$b_e = 1800\text{mm}$$ Clause 7.6.3 in EN 1998-1

Effective width of concrete slab at sagging moment region:

$$b_e = b_0 + \frac{L_e}{8} + \frac{L_e}{8} = 1575\text{mm}$$ Clause 5.4.1.2 in EN 1994-1-1

$b_e = 1350\mathrm{mm}$ Clause 7.6.3 in EN 1998-1

Converted cross-section area of composite beam at hogging moment region

$A_0 = A_s + \frac{A_{ce}}{\alpha_m} = 35651\mathrm{mm}^2$ (In accordance with EN 1994-1-1)

Converted cross-section area of composite beam at sagging moment region

$A_0 = A_s + \frac{A_{ce}}{\alpha_m} = 44710\mathrm{mm}^2$ (In accordance with EN 1994-1-1)

$A_0 = A_s + \frac{A_{ce}}{\alpha_m} = 40180\mathrm{mm}^2$ (In accordance with EN 1998-1)

Location of neutral axis of composite beam at hogging moment region

y_x=530 mm (In accordance with EN 1994-1-1)

y_x=567 mm (In accordance with EN 1998-1)

Location of neutral axis of composite beam at sagging moment region

y_x=557 mm (In accordance with EN 1994-1-1)

y_x=545 mm (In accordance with EN 1998-1)

Second moment of area of converted composite beam at hogging moment region

I_0=1.95×10^9 mm^4 (In accordance with EN 1994-1-1)

I_0=2.11×10^9 mm^4 (In accordance with EN 1998-1)

Second moment of area of converted composite beam at sagging moment region

I_0=2.07×10^9 mm^4 (In accordance with EN 1994-1-1)

I_0=2.01×10^9 mm^4 (In accordance with EN 1998-1)

C.3 GENERAL DETAILS OF THE CONVERTED EQUIVALENT CROSS-SECTION

Fig. 5.7 in Chapter 5 presents general details of the converted cross-section of the composite beam. The composite beam can be converted as follows.

At hogging moment region:

Width and depth of top flange	b_3=291 mm, d_c=120 mm (By EN 1994-1-1)
	b_3=381 mm, d_c=120 mm (By EN 1998-1)
Width and thickness of bottom flange	b_2=228 mm, t_{fb}=14.8 mm (By EN 1994-1-1)
	b_2=228 mm, t_{fb}=14.8 mm (By EN 1998-1)
Depth and thickness of beam web	d_{p1}=587.2 mm, t_w=10 mm (By EN 1994-1-1)
	d_{p1}=587.2 mm, t_w=9.9 mm (By EN 1998-1)

At sagging moment region:

Width and depth of top flange	b_3=350 mm, d_c=120 mm (By EN 1994-1-1)
	b_3=286.7 mm, d_c=120 mm (By EN 1998-1)
Width and thickness of bottom flange	b_2=288 mm, t_{fb}=14.8 mm (By EN 1994-1-1)

	b_2=288 mm, t_{fb}=14.8 mm (By EN 1998-1)
Depth and thickness of beam web	d_{p1}=587.2 mm, t_w=10.1 mm (By EN 1994-1-1)
	d_{p1}=587.2 mm, t_w=10.1 mm (By EN 1998-1)

APPENDIX D
DETERMINATION OF WIND ACTIONS ACCORDING TO AS/NZS 1170.2 (STANDARDS AUSTRALIA/STANDARDS NZ, 2002c)

All notations, clauses, tables, figures and supplements presented in this section are referenced from AS/NZS 1170.2 (Standards Australia/Standards New Zealand, 2002c) unless specified.

The procedure for calculating wind actions (*W*) on building structures involves the following steps:

- Calculation of site wind speed
- Calculation of design wind speed based on site wind speed
- Calculation of design wind pressures and distributed forces
- Calculation of wind actions

The necessary calculations for the determination of wind actions for a three-bay by three-storey frame are presented for an example as follows.

D.1 SITE WIND SPEED ($V_{sit,\beta}$)

$$V_{sit,\beta} = V_R M_d (M_{z,cat} M_s M_t)$$

Where,

V_R	Regional gust wind speed for annual probability of exceedance =46 m/s (in Region B that characterizes the most adverse circumstances in Australia for maximum cases, a 50-year design working life and 1/500 annual probability of exceedance is considered)	Clause 3.2
M_d	Wind directional multiplier	
	=0.95	Clause 3.3.2
$M_{z,cat}$	Terrain/height multiplier	
	=0.94 (assumed for buildings less than 20m in height, terrain category 2 and terrain roughness less than 3 m. This topography constitutes grasslands with 1.5 m to 5 m high, well-scattered obstacles and maximum 2 obstructions per hectare.	Clause 4.2.2
M_s	Shielding multiplier	
	=1.0 (the effect of shielding for a particular wind direction is ignored)	Clause 4.3.1
M_t	Topographic multiplier	
	=1.32 (assumed as the average for upwind slope)	Clause 4.4.2

Finally, $V_{sit,\beta} = 54.22$ m/s.

D.2 DESIGN WIND SPEED (*$V_{des,\theta}$*)

$V_{des,\theta}$ =54.22 m/s (assumed to be taken equal to $V_{sit,\beta}$. This value should not be lesser than 30 m/s for ultimate limit states design) Clause 2.3

D.3 DESIGN WIND PRESSURE (*p*)

$$p = (0.5\rho_{air})[V_{des,\theta}]^2 C_{fig} C_{dyn}$$

Where,

ρ_{air} Density of air, which is 1.2 kg/m³ Clause 2.4.1

C_{fig} Aerodynamic shape factor (for a confined building)

C_{dyn} Dynamic response factor

=1.0 (for buildings that are not largely sensitive to wind) Clause 6.1

For enclosed buildings, the aerodynamic shape of factor can be represented as:

$C_{fig,e} = C_{p,e} K_a K_{c,e} K_l K_p$ for external pressures

where,

$C_{p,e}$ External pressure coefficient

=0.7 (for windward wall, the wind speed is assumed to remain constant for buildings less than 25 m high, irrespective of Clause 5.4.1

height)

=-0.5 (for leeward wall, assuming the roof pitch to be smaller than 10 degrees) Clause 5.4.1

K_a Area reduction factor

=1.0 (supposing tributary area less than 10 m^2) Clause 5.4.2

$K_{c,e}$ Combination factor applied to external pressures

=0.9 (assuming 75% contribution of wind actions to an action effect) Clause 5.4.3

K_l Local pressure factor for cladding

=1.0 (no cladding is considered) Clause 5.4.4

K_p Permeable cladding reduction factor for roofs and side walls

=0.63 (assuming that the external surface consists of no permeable cladding) Clause 5.4.5

Similarly, for internal pressures,

$$C_{fig,i} = C_{p,i} K_{c,i}$$

$C_{p,i}$ Internal pressure coefficient

=-0.2 or 0.0 (assuming a building is completely sealed, choose whichever value is more severe for combined forces) Clause 5.3.4

$K_{c,i}$ Combination factor applied to internal pressures

=1.0 (assuming no effective surface for internal pressures) Clause 5.4.3

Since the length-to-width or width-to-depth ratio is less than 4, therefore the frictional drag forces can be neglected. Consequently, the aerodynamic shape of factor is considered as 0.83 for windward walls and 0.45 for leeward walls.

Ultimately, the design wind pressure exerted on windward walls is:

$$\rho = 0.5 \times 1.2 \times 54.222^2 \times 0.83 \times 1$$

$$\rho = 1.46 \text{ kPa}$$

The design wind pressure exerted on leeward walls is:

$$\rho = 0.5 \times 1.2 \times 54.222^2 \times 0.45 \times 1$$

$$\rho = 0.79 \text{ kPa}$$

D.4 DESIGN WIND ACTIONS (*F*)

$$F = \sum (p_z A_z)$$

Where,

p_z Design wind pressure normal to the surface at height z (kPa)

(considering uniform distribution of pressure with respect to height)

=1.46 kPa for windward walls

=0.79 kPa for leeward walls

A_z A reference area on which the pressure acts at height z(m^2)

=36 m^2 (for 1st storey)

(Considering a three-storey by three-bay frame)

=36 m^2 (for 2nd storey)

=18 m^2 (for 3rd storey)

Therefore, design wind actions for windward walls at each level can be 52.56 kN, 52.56 kN and 26.28 kN, respectively. Design wind actions for leeward walls at each level can be 28.44 kN, 28.44 kN and 14.22 kN, respectively.

APPENDIX E

DETERMINATION OF EARTHQUAKE LOADS IN ACCORDANCE WITH AS/NZS 1170.4 (STANDARDS AUSTRALIA, 1993)

All notations, clauses, tables, figures and supplements presented in this section are referenced from AS/NZS 1170.2 (Standards Australia/Standards New Zealand, 2002c) unless specified. The magnitude of earthquake actions changes with the building height. The forces acting at each level are calculated separately in order to simplify the calculation procedure. The necessary calculations for the determination of wind actions for a three-bay by three-storey frame are presented for an example as follows.

E. 1 IMPORTANCE LEVEL FOR STRUCTURES

In accordance with AS/NZS 1170.0, third importance level for structures is adopted based on 50-year design working life and 1/1000 annual probability of exceedance. It typically reflects the most adverse situations in Australia regarding earthquake design.

E.2 PROBABILITY FACTOR (k_p) AND HAZARD FACTOR (Z)

In Clause 3.1, the probability factor is taken as 1.8 given that the annual probability of exceedance is 1/2500.

Concerning hazard factor, a value of 0.12 is adopted since it covers the most regions of Australia including some major cities.

E.3 SITE SUB-SOIL CLASS

The site sub-soil is defined as Class D which represent deep or soft soil site.

E.4 EARTHQUAKE DESIGN CATEGORY (EDC)

For third importance level of structures, Class D site sub-soil, k_pZ is equal to 0.15

Where K_p is the probability factor and Z is the hazard factor.

E.5 EARTHQUAKE DESIGN CATEGORY II

The earth quake design category selected herein is EDC II that is suitable for building height less than 25 m. For structures with height less than 15 m, a simplified design method is recommended as follows.

$$F_i = K_s [k_p Z S_p / \mu] W_i$$

where

K_s Factor to account for floor

=1.8 (for the first floor) Clause 5.4.2.3

=3.6 (for the second floor)

=5.5 (for the roof)

S_p Structural performance factor

=0.77 Clause 6.5

μ Structural ductility factor

=2.0 Clause 6.5

W_i Seismic weight of structure or component at level i

$Wi = Gi + \sum \Psi_C Q_I$

Where, G represents the permanent actions at i^{th} level, $\boldsymbol{\Psi_c}$ represents the combination factor for earthquake-imposed actions and Q represents the imposed actions on the structure

Using the above formula, earthquake actions are calculated as 24.9 kN for the first storey, 49.8 kN for second storey and 41.9 kN for the third storey respectively.

REFERENCES

Abolmaali, A., Matthys, J.H., Farooqi, M. and Choi, Y. (2005), "Development of moment-rotation model equations for flush end-plate connections", *Journal of Constructional Steel Research*, 61(12), 1595-1612.

ABAQUS User Manual, (2014), Version 6.14. Providence, RI, USA: DS SIMULIA Corp.

AISC 2005, "Specifications for structural steel buildings", *American Institute of Steel construction*

AISC-LRFD (1994), "Manual of steel construction", load and resistance factor design, Second edition.

Anderson, D. and Najafi, A.A. (1994), "Performance of composite connections: major axis end plate joints", *Journal of Constructional Steel Research*, 31(1), 31-57.

ANSI/AISC 360-16. (2016), "Specification for structural steel buildings", Chicago.

AS 1012.9-2014. (2014a), "Methods of testing concrete. Method 9: Compressive strength tests—Concrete, mortar and grout specimens", Standards Australia International Ltd.

AS 1012.10-2000. (2014b), "Methods of testing concrete. Method 10: Methods of testing concrete Determination of indirect tensile strength of concrete cylinders ('Brazil' or splitting test)", Standards Australia International Ltd.

AS 4291.1-2000 (2000), “Mechanical properties of fasteners made of carbon steel and alloy steel Part 1: Bolts, screws and studs”. Standards Australia International Ltd.

AS/NZS 1170.0-2002. (2002), “Structural design actions. Part 0: general principles”, Australia.

AS/NZS 1170.1-2002. (2002), “Structural design actions. Part 1: permanent, imposed and other actions”, Standards Australia International Ltd.

AS/NZS 1170.2-2011. (2011), “Structural design actions. Part 2: wind actions”, Standards Australia International Ltd.

AS/NZS 1170.4-2007. (2007), “Structural design actions. Part 4: Earthquake actions in Australia”, Standards Australia International Ltd.

AS 1391-2007. (2007), “Metallic materials tensile testing at ambient temperature”, Standards Australia International Ltd.

AS 2327.1-2003. (2003), “Composite structures. Part 1: Simply supported beams”, Standards Australia International Ltd.

AS 4291.1-2000. (2000), “Mechanical properties of fasteners made of carbon steel and alloy steel. Part 1: Bolt, screws and studs.”, Standards Australia International Ltd.

Ali A., Kim, D. and CHO S., (2011), Experimental study of flush end plate beam-to-column composite joints with precast slabs and deconstructable bolted shear connectors, *Nuclear energy and Technology*, 45, 89-98.

Ali, A., Kim, D. and Cho, S. G. (2013), "Modelling of nonlinear cyclic load behaviour of I-shaped composite steel-concrete shear walls of nuclear power plants," *Nuclear Engineering and Technology*, 45(1), 89-98.

Ammerman, D.J. and Leon, R.T. (1990), "Unbraced frames with semi-rigid composite connections", *AISC Engineering Journal*, American Institute of Steel Construction, First Quarter, 12-21.

Ataei, A., Bradford M.A. (2013), Parametric studies of semi-rigid flush end plate joints with concrete-filled steel tubular columns, *Applied Mechanics and Materials*, 553, 588-593.

Ataei, A., Bradford M.A., Valipour H. (2015), Experimental study of flush end plate beam-to-CFST column composite joints with deconstructable bolted shear connectors, *Engineering Structures*, 99, 616-630.

Ataei, A., Bradford M.A., Liu, X. (2016a), Experimental study of flush end plate beam-to-column composite joints with precast slabs and deconstructable bolted shear connectors, *Structures*, 7, 43-58.

Ataei, A., Bradford M.A., Valipour H. (2016b), Finite element analysis of HSS semi-rigid composite joints with precast concrete slabs and demountable bolted shear connectors, *Finite Element in Analysis and Design*, 122, 16-38.

Aribert, J.M. and Dinga, O.N. (2002). "Modelling and experimental investigation of bolted flush end-plate composite beam-to-column joints", *Composite Construction in Steel and Concrete IV, Proceedings of the conference*, Banff, Alberta, Canada, ASCE, 711-724.

Azizinamini, A., Bradburn, J.H. and Radziminski, J.B. (1987), "Initial stiffness of semi-rigid steel beam-to-column connections", *Journal of Constructional Steel Research*, 8, 71-90.

Barnett, T.C., Tizani, W. & Nethercot, D.A. (2000), 'Blind bolted moment resisting connections to structural hollow sections', *Fourth International workshop on connections in Steel Structures*, Roanoke.

Bernuzzi, R., Zandonini, R. and Zanon, P. (1996), "Experimental analysis and modelling of semi-rigid steel joints under cyclic reversal loading", *Journal of Constructional Steel Research*, 38(2), 95-123.

Beavan, J., Fielding, E., Motagh, M., Samsonov, S., & Donnelly, N. (2011), "Fault Location and Slip Distribution of the 22 February 2011 Mw 6.2 Christchurch, New Zealand, Earthquake from Geodetic Data", Seismological Research Letters, 82, 789-799.

Birtel, V. and Mark, P. (2006)"Parameterized Finite Element Modelling of RC Beam Shear Failure," *Abaqus User's Conference*, 95-108.

Braconi, A., Elamary, A. and Salvatore, W. (2010), "Seismic behaviour of beam-to-column partial-strength joints for steel–concrete composite frames", *Journal of Constructional Steel Research*, 66(12), 1431-1444.

Brown, N. D. and Anderson, D. (2001), "Structural properties of composite major axis end plate connections", *Journal of constructional steel research*, 57(3), 327-349.

Broderick, B.M. and Thomson, A.W. (2002), "The response of flush end plate joints under earthquake loading", *Journal of Constructional Steel Research*, 58, 1161-1175.

Bursi, O.S. and Gramola, G. (1999). "Behaviour of composite substructures with full and partial shear connection under quasi-static cyclic and pseudo-dynamic displacements, *Materials and Structures*, 33, 154-163.

British Standards Institution (1992a). *Eurocode 3: Design of composite steel and concrete structures, Part 1., General rules and rules for buildings, DDENV 1993-1-1,* European Committee for Standardization (CEN).

British Standards Institution (1992b). *Eurocode 4: Design of steel and structures, Part 1.1, General rules and rules for buildings, DDENV 1994-1-1,* European Committee for Standardization (CEN).

British Standards Institution (2000). *BS 5950-1, Structural use of steel works in buildings, Part 1: Code of practice for design-rolled and welded sections,* British Standards Institution, London.

Carreira D.J., Chu K.H. (1985). Stress-strain relationship for plain concrete in compression. *ACI Structural Journal*, 82(6), 797–804.

Chandler, A.M., Lam, N.T.K. (2001), "Deterministic seismic hazard parameters and engineering risk implications for the Hong Kong region", *Journal of Asian Earth Sciences,* 20, 59-72.

Da Silva, L.S., Simoes, R.D. and Cruz, P.J. (2001), "Experimental behaviour of end-plate beam-to-column composite joints under monotonical loading", *Engineering Structures*, 23(11), 1383-1409.

Daniels, J.H. and Fisher, J.W. (1966), "Fatigue behaviour of continuous composite beams", Fritz Engineering Laboratory Report No. 324.1, Department of Civil Engineering, Lehigh University, Bethlehem, Pennsylvania.

Daniels, J.H. and Fisher, J.W. (1967), "Static behaviour of continuous composite beams", Fritz Engineering Laboratory Report No. 324.2, Department of Civil Engineering, Lehigh University, Bethlehem, Pennsylvania.

Díaz, C., Victoria, M., Martí, P. and Querin, O.M. (2011), "FE model of beam-to-column extended end-plate joints", *Journal of Constructional Steel Research*, 67(10), 1578-1590.

Egan, B., McCarthy, M.A., Gray, P.J. and Frizzell, R.M. (2012), "Modelling of a single bolt counter sunk composite joint using implicit and explicit finite element analysis", *Computational Material Science*, 64, 203-208.

Elghazouli, AY, Málaga, C., Castro, J.M. and Orton, A.H. (2009), “Experimental monotonic and cyclic behaviour of blind-bolted angle connections”, *Engineering Structures*, 31, 2540-53.

Ellobody, E. and Young, B. (2015), “Nonlinear analysis of composite castellated beams with profiled steel sheeting exposed to different fire conditions”, *Journal of Constructional Steel Research*, 113, 247-260.

EN 1993-1-1. (2005), “Eurocode 3: Design of steel structures. Part 1–1: General rules and rules for buildings”, Brussels, Belgium: European Committee for Standardization.

EN 1993-1-8. (2010), “Eurocode 3: Design of Steel Structures. Part 1-8: Design of Joints”, Brussels, Belgium: European Committee for Standardization.

EN 1994-1-1. (2004), “Eurocode 4: Design of Composite Steel and Concrete Structures. Part 1-1: General Rules and Rules for Buildings”, Brussels, Belgium: European Committee for Standardization.

EN 1998-1. (2004), “Eurocode 8: Design of structures for earthquake resistance. Part 1: General rules, seismic actions and rules for buildings”, Brussels, Belgium: European Committee for Standardization.

Erkmen R.E., Bradford M.A. (2009), Nonlinear elastic analysis of composite beams curved in-plan. *Engineering Structures*, 31: 1613-1624.

F. Aslani, B. Uy, Z. Tao and F. Mashiri, (2015), "Behaviour and design of composite columns incorporating compact high-strength steel plates," *Journal of Constructional Steel Research*, 107, 94-110.

Gaull, B.A., Michael-Leiba M. and Rynn J.M.W. (1990), “Probabilistic earthquake risk maps of Australia”. *Australian Journal of Earth Sciences*, 37, 169-187

Gomes, F., Jaspart, J.P. and Maquoi, R. (1996), "Moment capacity of beam-to-column minor-axis joints, Proceedings of the IABSE Colloquium on semi-rigid structural connection", *Journal of Constructional Steel Research*, 319-326.

Ghobarah, A., Mourad, S. and Korol, R.M. (1996), "Moment-rotation relationship of blind bolted connections for HSS columns", *Journal of Constructional Steel Research*, 40(1), 63-91.

Gibson, G. and McCue, K. (2001), "Seismological contributions to earthquake loading codes", *Proceedings of Earthquake codes in the real world, AEES Australian Earthquake Engineering Society*, Canberra, November 2001.

Goldsworthy, H.M. and Gardner, A.P. (2006), "Feasibility study for blind-bolted connections to concrete-filled circular steel tubular columns", *Structural Engineering and Mechanics*, 24(4), 463-478.

Hassan K., Tao Z., Mirza O. Song T.Y. and Han, L.H. (2014), "Finite element analysis of steel beam-CFST column joints with blind bolts" *The Australasian Structural Engineering 2014 Conference (ASEC 2014)*, 9-11 July 2014, Auckland, New Zealand (56)

Han, L.H., Wang, W.D., & Zhao, X.L. (2008), Behaviour of steel beam to concrete-filled SHS column frames: Finite element model and verifications. *Engineering Structures*, 30, 1647-58

Hensman, J. and Nethercot, D.A. (2001), "Numerical study of unbraced composite frames: generation of data to validate use of the wind moment method of design", *Journal of Constructional Steel Research*, 57, 791-809.

Hensman, J. and Nethercot, D.A. (2002), "Extending the wind moment method to composite frames", *Composite Construction in Steel and Concrete IV, Proceedings of the conference*, Banff, Alberta, Canada, ASCE, 676-685.

Hicks, S.J. and Pennington, A. (2015), “Partial factors for the design resistance of composite beams in bending”, *Journal of Constructional Steel Research*, 105(2), 74-85.

Jeyarajan S., Liew J. Y. R. and Koh C. G. (2015). Enhancing the robustness of steel-concrete composite buildings under column loss scenarios, *International Journal of Protective Structures*, 6 (3), 529-550

Jeyarajan S., Liew J. Y. R. and Koh C. G. (2016). Analysis of steel-concrete composite buildings, *International Journal of Protective Structures*, 6 (3), 529-550

J. M. Aribert and O. N. Dinga, (2000), "Modelling and experimental investigation of bolted flush end-plate composite beam-to-column joints," *Composite Construction in Steel and Concrete*, 4, 711-724.

Kataoka, M.N. and El Debs, A.L.H. (2014), “Parametric study of composite beam-column connections using 3D finite element modelling”, *Journal of Constructional Steel Research*, 102, 136-149.

Kim, B., Wright, H.D., Cairns R. and Bradford, M.A. (1999), “The numerical simulation of shear connection. In M.A. Bradford et al. (Eds.), *Mechanics of Structures and Materials*; Proceedings of 16th ACMSM, Sydney 8-10 December 1999. Rotterdam: Balkema.

Lam, N.T.K., Gaull, B.A., Wilson, J.L. (2007), “Calculation of earthquake actions on building structures in Australia”. *Electronic Journal of Structural Engineers* (EJSE), Special Issue: *Loading on Structures* 2007, 22-40.

Lee, S.S. and Moon, T.S. (2002), “Moment–rotation model of semi-rigid connections with angles”, *Engineering structures*, 24(2), 227-237.

Leon, R.T., Ammerman, D.J., Lin, J. and McCauley, R.D. (1987). "Semi-rigid composite steel frames", *AISC Engineering Journal*, American Institute of Steel Construction, Fourth Quarter, 147-155.

Li, T.Q., Nethercot, D.A. and Choo, B.S. (1996a), "Behaviour of flush end-plate composite connections with unbalanced moment and variable shear moment ratios—I. Experimental behaviour", *Journal of Constructional Steel Research*, 38(2), 125-164.

Li, T.Q., Nethercot, D.A. and Choo, B.S. (1996b), "Behaviour of flush end-plate composite connections with unbalanced moment and variable shear/moment ratios—II. Prediction of moment capacity", *Journal of Constructional Steel Research*, 38(2), 165-198.

Li, T.J., Li, Q., G., Lou B. G. and Chen, Z.L. (2012), "Experimental investigation on flush end-plate bolted composite connection in fire", *Journal of Constructional Steel Research*, 76, 121-132.

Li, D., Uy, B., Patel, V. and F. Aslani, (2017) "Analysis and design of demountable embedded steel column base connections," *Steel and Composite Structures*, 23(3), 303-315.

Liew, J.R., Teo, T.H., Shanmugam, N.E. and Yu, C.H. (2000), "Testing of steel–concrete composite connections and appraisal of results", *Journal of Constructional Steel Research*, 56(2), 117-150.

Liew, J.R., Teo, T.H. and Shanmugam, N.E. (2004a), "Composite joints subject to reversal of loading—Part 1: experimental study", *Journal of Constructional Steel Research*, 60(2), 221-246.

Liew, J.R., Teo, T.H. and Shanmugam, N.E. (2004b), “Composite joints subject to reversal of loading—Part 2: analytical assessments”, *Journal of Constructional Steel Research*, 60(2), 247-268.

Loh, H.Y. (2004), “The effects of Partial Shear Connection in Hogging Moment Regions of Composite Steel-Concrete Structures”, PhD diss., University of New South Wales.

Loh, H.Y., Uy, B. and Bradford, M.A. (2006 a), “The effects of partial shear connection in composite flush end plate joints - Part I – Experimental study”, *Journal of Constructional Steel Research*, 62(4), 391-412.

Loh, H.Y., Uy, B. and Bradford, M.A. (2006 b), “The effects of partial shear connection in composite flush end plate joints - Part II - Analytical study and design appraisal”, *Journal of Constructional Steel Research*, 62(4), 391-412.

L. H. Han, W. D. Wang and B. Uy, (2008) "Experimental behaviour of steel reduced beam section to concrete-filled circular hollow section connections," *Journal of Constructional Steel Research*, 64, 493-504.

Maenpaa, D. (2007), “Composite beam-column flush end plate connections subjected to low-probability, high consequence loading”, School of Engineering, Undergraduate honors thesis: University of Western Sydney.

McGuire, W. (1988), ‘Introduction’, *Journal of Constructional Steel Research*, 10, 1-35.

Mirza, O. and Uy, B. (2011), “Behaviour of composite beam–column flush end-plate connections subjected to low-probability, high-consequence loading”, *Engineering Structures*, 33(2), 647-662.

Mirza, O. and Uy, B. (2012), “Finite element modelling of beam-to-column flush end-plate connections using blind bolts”, *Tubular Structures XIV: Proceedings of the*

14th International Symposium on Tubular Structures, London, UK, 12-14 September 2012, 127-132.

Morris L.J. (1988), "Design Rules for Connection in the United Kingdom". In: W. F. Chen, (ed). steel beam-to-column building connections, USA: Elsevier Applied Science, 375-413.

Mourad. S. (1993), Behaviour of blind bolted moment connections for square HSS columns (PhD Thesis) Department of Civil Engineering, McMaster University Hamilton Ontario, Canada.

Nie, J.G., Tao, M.X., Cai, C.S. and Chen, G. (2011), "Modeling and investigation of elasto-plastic behavior of steel-concrete composite frame systems", *Journal of Constructional Steel Research*, 67(12), 1973-1984.

Nogueiro, P., Silva, L.S.D., Bento, R. and Simões, R. (2009), "Calibration of model parameters for the cyclic response of end-plate beam-to-column steel-concrete composite joints", *Steel and Composite Structures*, 9, 39-58.

Oktavianus, Y., Chang, H., Goldsworthy, H.M. and Gad, E.F. (2017), "Component model for pull-out behaviour of headed anchored blind bolt within concrete filled circular hollow section", *Engineering Structures*, 148, 210-224.

Pokharel, T., Goldsworthy, H.M. & Gad, E.F., (2014), "Displacement-Based Seismic Assessment of Moment Resisting Frames with Blind Bolted Connections", *Proceedings of the Australian Earthquake Engineering Society 2014 Conference*, Lorne, Australia

Paulay, T., and Priestley, M.J.N. (1990), "Seismic Design of Reinforced Concrete and Masonry Buildings", John Wiley and Sons Inc, New York.

Pathirana, S.W., Uy, B., Mirza, O. and Zhu, X. (2016), "Flexural behaviour of composite steel–concrete beams utilizing blind bolt shear connectors", *Engineering Structures*, 114, 181-194.

Salvatore, W, Bursi, OS, & Lucchesi, D. (2005), "Design, testing and analysis of high ductile partial-strength steel–concrete composite beam-to-column joints", *Journal of Computers and Structures*, 83, 2334-2352

Scawthorn, C. (2003), "Earthquakes", in Chen, W-F, & Scawthorn C (Ed.), *Earthquakes Engineering Handbook*, CRC Press, US, 1-66.

Shanmugam, NE, Lakshmi B, (2001), "State of the Art on Steel-Concrete Composite Columns", *Journal of Constructional Steel Research*, 1041-1080.

De Silvana, N, & El Debs, A , (2004), "An experimental study of connections between I-beam and concrete filled steel tubular columns", *Steel and Composite Structures*, 4, 303-15.

Song, T.Y., Tao, Z., Razzazzadeh, A., Han, L.H. and Zhou, K. (2017), "Fire performance of blind bolted composite beam to column joints", *Journal of Constructional Steel Research*, 132, 29-42.

Taranath BS (2005). Wind and Earthquake Resistant Buildings, 1st. ed. New York: Marcel Dekker, .262-75.

Tsonos, AG (2000), 'Effect of Vertical Hoops on the Behaviour of Reinforced Concrete Beam-to-Column Connection, *European Earthquake Engineering*, 14. 2, 13–26.

Tahmasebinia F, Ranzi G, Zona A (2012). A probabilistic three-dimensional finite element study on simply-supported composite floor beams. *Australian Journal of Structural Engineering*, 12, 251-262

Tahmasebinia F, Ranzi G, Zona A (2013). Probabilistic three-dimensional finite element study on composite beams with steel trapezoidal decking. *Journal of Constructional Steel Research*, 80, 394-411.

Tao, Z., Wang, B .and Q. Yu, (2013) "Finite element modelling of concrete-filled steel stub columns under axial compression," *Journal of Constructional Steel Research*, 89, 121-131

Tao, Z., Hassan, M.K., Song, T.Y. and Han, L.H. (2017), “Experimental study on blind bolted connections to concrete-filled stainless-steel columns”, *Journal of Constructional Steel Research*, 128, 825-838.

Tanlak, N., Sonmez, F. and Talay, E. (2011), “Detailed and simplified models of bolted joints under impact loading”, *Journal of Strain Analysis*, 46, 213-225.

Thai, H.T. and Uy, B. (2015). “Finite element modelling of blind bolted composite joints”, *Journal of Constructional Steel Research*, 112, 339-353.

Thai, H.T., Uy, B., Kang, W.H. and Hicks, S. (2016a), “System reliability evaluation of steel frames with semi-rigid connections”, *Journal of Constructional Steel Research*, 121, 29-39.

Thai, H.T. and Uy, B. (2016b), “Rotational stiffness and moment resistance of bolted endplate joints with hollow or CFST columns”, *Journal of Constructional Steel Research*, 126, 139-152.

Thai, H.T., Uy, B., Aslani, F. (2017), “Behaviour of bolted endplate composite joints to square and circular CFST columns”, *Journal of Constructional Steel Research*, 131, 68-82.

Tingley, D.D. and Davison, B. (2011), “Design for deconstruction and material reuse”, *Proceedings of the Institution of Civil Engineers-Energy*, 164(4), 195-204.

Tizani, W., Al-Mughairi, A., Owen, J.S. and Pitrakkos, T. (2013a), “Rotational stiffness of a blind-bolted connection to concrete-filled tubes using modified Hollo-bolt”, *Journal of Constructional Steel Research*, 80, 317-331.

Tizani, W., Wang, Z.Y., Hajirasouliha, I. (2013b), “Hysteretic performance of a new blind bolted connection to concrete filled columns under cyclic loading: An experimental investigation”, *Engineering Structures*, 46, 535-546.

Tizani, W., Rahman, N.A. and Pitrakkos, T. (2014), “Fatigue life of an anchored blind-bolt loaded in tension”, *Journal of Constructional Steel Research*, 93, 1-8.

T. Q. Li, D. A. Nethercot, and B. S. Choo, (1996), "Behaviour of flush end-plate composite connections with unbalanced moment and variable shear/moment ratios—I. Experimental behaviour," *Journal of Constructional Steel Research*, 38(2), 125-164.

Uy, B. and Liew, J.Y.R. (2003), “Composite steel–concrete structures”, In Chen, W.F., Liew, J.Y.R. (Eds.), Civil Engineering Handbook, CRC Press, Boca Raton.

Uy, B. (2012), “Applications, behaviour and design of composite steel-concrete structures”, *Advances in Structural Engineering*, 15(9), 1559-1571.

Uy, B., Patel, V., Li, D.X. and Aslani, F. (2017), “Behaviour and design of connections for demountable steel and composite structures”, *Structures*, 9, 1-12.

Vasdravellis, G., Uy, B, Tan, L. and Kirkland. B. (2012) “Behaviour and design of composite beams subjected to negative bending and compression”, *Journal of Constructional Steel Research*, 79, 34-47.

Wang, Hasegawa, A. and Shioi, Y. (2001), 'Study on Strength Evaluation Formula for Reinforced Concrete Filled Steel Tubular Structures', in First International Conference on Steel & composite Structures, Pusan, Korea, pp. 881-8.

Wang, J.F., Han, L.H. and Uy, B. (2009a), "Behaviour of flush end plate joints to concrete-filled steel tubular columns", *Journal of Constructional Steel Research*, 65(4), 925-939.

Wang, J.F., Han, L.H. and Uy, B. (2009b), "Hysteretic behaviour of flush end plate joints to concrete-filled steel tubular columns", *Journal of Constructional Steel Research*, 65(8-9), 1644-1663.

Wang, W.D., Han, L.H. and Zhao, X.L. (2009c), "Analytical behavior of frames with steel beams to concrete-filled steel tubular column", *Journal of Constructional Steel Research*, 65(3), 497-508.

Wang, Z.Y., Tizani, W. and Wang, Q.Y. (2010), "Strength and initial stiffness of a blind-bolt connection based on the T-stub model", *Engineering Structures*, 32(9), 2505-2517.

Wang, A. J. (2010), "Numerical studies on the structural behaviour of composite end-plate connections", *Canadian Journal of Civil Engineering*, 37(6), 907-921.

Wang, J. and Chen, L. (2012), "Experimental investigation of extended end plate joints to concrete-filled steel tubular columns", *Journal of Constructional Steel Research*, 79, 56-70.

Wang, J. and Guo, S. (2012), "Structural performance of blind bolted end plate joints to concrete-filled thin-walled steel tubular columns", *Thin-Walled Structures*, 60, 54-68.

Wang, J. and Spencer Jr, B.F. (2013), "Experimental and analytical behavior of blind bolted moment connections", *Journal of Constructional Steel Research*, 82, 33-47.

Wang, J., Zhang, L. and Spencer Jr, B.F. (2013), "Seismic response of extended end plate joints to concrete-filled steel tubular columns", *Engineering Structures*, 49, 876-892.

Wang, J.F., Zhang, H.J. and Jiang, Z. (2016a), "Seismic behaviour of blind bolted end plate composite joints to CFST columns", *Thin-Walled Structures*, 108, 256-269.

Wang, W., Fang, C., Qin, X., Chen, Y. and Li, L. (2016c), "Performance of practical beam-to-SHS column connections against progressive collapse", *Engineering Structures*, 106, 332-347.

Wang, J., Zhu, H.M., Uy, B. and Aslani, F. (2016b), "Behaviour of demountable steel and composite beam-to-column connections (Eds. Young, B. and Cai, Y.)", *Proceedings of the 8th International Conference on Steel and Aluminum Structures* (ICSAS 2016), 7-9 December 2016, Hong Kong, China.

Wang, J., Li, B., Wang, D. and Zhao, C. (2017a), "Cyclic testing of steel beam blind bolted to CFST column composite frames with SBTD concrete slabs", *Engineering Structures*, 148, 293-311.

Wang, J., Pan, X. and Peng, X. (2017b), "Pseudo-dynamic tests of assembly blind bolted composite frames to CFST columns", *Journal of Constructional Steel Research*, 139, 83-100.

Wang, J., Uy, B., Li, D. (2018a), "Behaviour and design of demountable beam-to-column composite bolted joints with extended end-plates", *Journal of Constructional Steel Research*, 144, 221-235.

Wang, J., Uy, B., Li, D. (2018b) "Analysis of demountable steel and composite frames with semi-rigid bolted joints", *Journal of Constructional Steel Research*, 144, 221-235.

Wilson, J.L., Lam, N.T.K. (2006), "Recent developments in the research and practice of earthquake engineering in Australia", *Proceedings of Earthquake Engineering in Australia*, Canberra, November, AEES.

Wu, L.Y, Chung, L.L., Tsai, S.F., Shen, T.J., and Huang, G.L. (2005), "Seismic behavior of bolted beam-to-column connections for concrete filled steel tube," *Journal of Constructional Steel Research*, 61(10), 1387-1410

Xiao, Y., Choo, B.S. and Nethercot, D.A. (1994). "Composite connections in steel and concrete. I. Experimental behaviour of composite beam-column connections", *Journal of Constructional Steel Research*, 31, 3-30.

Xiao, Y., Choo, B.S. and Nethercot, D.A. (1996), "Composite connections in steel and concrete. II. Moment capacity of end plate beam to column connections," *Journal of Constructional Steel Research*, 37(1), 63-90.

Xu, A.H., Chen, H., Shi, Y.J., Wang, Y.Q. (2005), 'Analysis of Structural Behaviour of Beam-to-Column Composite Joints in High-Rising Steel Structure', *Advances in Steel Structure*, (1), 881-6.

Vegte, G., Makino, Y. (2004), "Numerical simulation of bolted connections: the implicit versus the explicit approach", *Connections in steel structures*, 89-98.

Yeomans, N. (1998), 'Rectangular hollow section column connections using the Lindapter Hollo-bolt', in Tubular Structures VIII, *Proceedings of the 8th International Symposium on Tubular Structures*, Rotterdam

Yee, Y.L. and Melchers, R.E. (1986), "Moment-Rotation Curves for Bolted Connections", *Journal of Structural Engineering*, 112(3), 615-635.

Yao, H, Goldsworthy, H, & Gad, E (2008), 'Experimental and numerical investigation on the tensile behavior of Blind-Bolted T-stub connections to concrete-filled circular columns', *Journal of Structural Engineering*, 134,.198-208

Zhao, H. (2016), "Analysis of seismic behavior of composite frame structures", *Steel and Composite Structures*, 20(3), 719-729.

Zhao, H., Kunnath, S.K. and Yuan, Y. (2010), "Simplified nonlinear response simulation of composite steel–concrete beams and CFST columns", *Engineering Structures*, 32(9), 2825-2831.

Zhao, Z., Liang, B., Liu, H. and Li, Y. (2018), "Simplified numerical model for high-strength bolted connections", *Engineering Structures*, 164, 119-127.

Zhou, T., Jia, Y., Xu, M., Wang, X. and Chen, Z. (2015), "Experimental study on the seismic performance of L-shaped column composed of concrete-filled steel tubes frame structures", *Journal of Constructional Steel Research*, 114, 77-88.

Zona A and Ranzi G (2011). Finite element models for nonlinear analysis of steel–concrete composite beams with partial interaction in combined bending and shear. *Finite Elements in Analysis and Design*, 47, 98-118.